Geology of the Caballo Mountains, New Mexico

William R. Seager and Greg H. Mack

Memoir 49

New Mexico Bureau of Geology and Mineral Resources

2003

A division of

New Mexico Institute of Mining and Technology

Memoir 49

Geology of the Caballo Mountains, New Mexico

William R. Seager and Greg H. Mack
New Mexico State University, Las Cruces, New Mexico 88003

New Mexico Bureau of Geology and Mineral Resources
A Division of New Mexico Institute of Mining and Technology

Socorro 2003

Geology of the Caballo Mountains, New Mexico

The New Mexico Bureau of Geology and Mineral Resources
A Division of New Mexico Institute of Mining and Technology
801 Leroy Place
Socorro, NM 87801
(505) 835-5420
http://geoinfo.nmt.edu

Project Editor
Nancy Gilson

Layout
Nancy Gilson

Cartography
Tom Kaus
Leo Gabaldon
Nancy Gilson

Editorial Assistance
Elizabeth Campbell
Jeanne Deardorff
Gina D'Ambrosio
Jane A. Calvert Love
Susan Voss

Library of Congress Cataloging-in-Publication Data

Seager, William R.
Geology of the Caballo Mountains, New Mexico / by William R. Seager and Greg H. Mack.
p. cm. -- (Memoir ; 49)
Includes bibliographical references and index.
ISBN 1-883905-15-X
1. Geology--New Mexico--Caballo Mountains. 2. Geology, Structural--New Mexico--Caballo Mountains. I. Mack, Greg H. II. Title. III. Memoir (New Mexico. Bureau of Geology and Mineral Resources) ; 49.
QE143.S43 2003
557.89'67--dc21

2003006676

Published by authority of the State of New Mexico, NMSA 1953 Sec. 63-1-4
Printed in the United States of America
First Printing

COVER—Our cover painting of the Burbank Canyon area in the central Caballo Mountains is by William Seager. The southward view features the great eastward-tilted fault block of Precambrian and Paleozoic rocks that constitute the backbone of the range. Reddish rocks at the base of the mountains are Precambrian granite followed upward by lower Paleozoic limestone, dolomite, and sandstone, which form ledges and cliffs in middle slopes of the mountains. Pennsylvanian limestone caps the range and forms an easterly inclined dip slope. In the upper right part of the painting, the Red Hills fault block is separated from the high mountains by Apache graben.

Summary

The Caballo Mountains, just south of Truth or Consequences, rise to an elevation of 7,065 feet. Today they are flanked on the west side by Caballo Reservoir and on the east side by the Jornada del Muerto. An extraordinary geologic section is preserved here. Precambrian igneous and metamorphic rocks (granites and schists) provide a view of the Precambrian history of this part of the country, and an extraordinary thickness of sedimentary rocks (whose collective thickness is more than 3.5 miles) give us an unparalleled picture of the evolution of southern New Mexico.

Development of these mountains began with compression and uplift associated with the Laramide orogeny, at the end of the Mesozoic. Since then the complex geologic history of this part of New Mexico has included uplift, erosion, faulting, volcanic activity, continental deposition, and, finally, the development of the Rio Grande rift. That complex geologic history is well documented in this volume.

This memoir is the result of many years of study and field work on the part of the authors, who have drawn together in one place this comprehensive description of the region. The volume is heavily illustrated with photographs, maps, stratigraphic sections, and other graphics. It contains both an index and a glossary.

Table of Contents

TABLES

FIGURES

Preface

One of the most enduring studies of New Mexico geology is *Geology of the Caballo Mountains*, by V. C. Kelley and Caswell Silver in 1952. Their study provided a solid foundation of geologic data and interpretations, relied upon by several generations of geologists interested in the geomorphology, mineral deposits, oil potential, stratigraphy, structure, and regional tectonics of southern New Mexico. Not only geologists have benefited from *Geology of the Caballo Mountains*. Ranchers motivated by the search for water, part-time miners interested in the gold and other metal deposits in the range, and untold hundreds of others who find the Caballo Mountains a source of pleasure for hiking or other recreational activities find the book informative and understandable, providing them with an appreciation of the history of the mountains and surrounding region that is not often found in technical books. *Geology of the Caballo Mountains* has deservedly become one of the most influential classics in New Mexico geology.

The present study of the Caballo Mountains began in 1980 as previously unmapped sections of the range were mapped in preparation for publication of *Geology of the Northwest Quarter of the Las Cruces 1° x 2° Sheet* (Seager et al., 1982). Throughout the more than twenty years that we have studied the geology of the Caballos, we have had four main goals in mind. Perhaps most important was to map, subdivide, date, and interpret the Cenozoic strata that crop out widely on both the eastern and western flanks of the range. Undifferentiated by Kelley and Silver (1952), we believed these rocks could provide insights into the timing and character of Laramide deformation, evolution of the Caballo uplift and adjacent basins, and history of the Rio Grande, and they could also help identify the most recently active, potentially dangerous faults in the area. Second, because Kelley and Silver (1952) emphasized lower Paleozoic stratigraphy and late Tertiary structure, we tried to focus on more detailed studies of upper Paleozoic, Cretaceous, and Cenozoic stratigraphy, as well as Laramide structure. The more we learned about late Cenozoic stratigraphy, the more important late Cenozoic structure became. Eventually the integration of the two became a third goal. Finally, we hoped to apply our understanding of local Caballo geology toward a broader interpretation of the Mesozoic and Cenozoic evolution of south-central New Mexico. We paid only cursory attention to some of the mineral deposits in the area, and did not attempt evaluation of either the petroleum or ground-water resources.

To help accomplish our goals, we made geologic maps of most of the range at a scale of 1:24,000, using USGS 7½-min. topographic quadrangle maps as bases. Such maps were not available to Kelley and Silver (1952). The geologic maps covered by this report include the following quadrangles, all of which are either published by the New Mexico Bureau of Mines (Geology) and Mineral Resources or are in press: Rincon (Seager and Hawley, 1973); Garfield (Seager and Mack, 1991); McLeod Tank (Seager and Mack, 1998); Alivio (Seager, in press); Caballo and Apache Gap (Seager and Mack, in press a); Cutter and Upham (Seager and Mack, in press b); Hatch (Seager et al., in press); and Engle (Mack and Seager, in press). Together with the unpublished map by Mason (1976) covering the northern Caballo Mountains (mostly Palomas Gap quadrangle) and the published map by Lozinsky (1986) of the Elephant Butte area, these maps provide nearly complete coverage of the Caballo Mountains and adjacent areas at a scale of 1:24,000.

This book is based on the geologic maps and their companion cross sections. It is intended to supplement the maps and sections by providing descriptions, interpretations, and summaries of the rocks and structures portrayed on the maps. By using the maps and text together, we hope the reader will appreciate the extraordinarily complete geologic story the Caballo Mountains offer.

We suggest the Caballo Mountains as a stratigraphic and structural reference area for persons interested in the geologic history of southern New Mexico. The mountains contain excellent outcrops of the most complete stratigraphic sequence in southern New Mexico, and arguably within the entire state. Except for Triassic and Jurassic, every period of the Phanerozoic is represented by sedimentary and/or volcanic rocks, which collectively attain a thickness of more than 5.6 km (3.5 mi). Proterozoic metamorphic and plutonic rocks are also represented. Major Laramide contractile and late Tertiary extensional structures are well exposed, and their genetic relationship to syntectonic sedimentary deposits are clear. Access to all of the rocks and structures is relatively easy owing to a good network of secondary roads and because of the mountains' status as mostly public land. The Caballo Mountains probably are unique in New Mexico in terms of the relatively complete geologic history that their rocks reveal. Realizing the Caballos can serve as a geologic reference area for a much broader region, we have sought to be as complete and detailed in our account of the geology as the rocks, structures, and concepts justify.

—William R. Seager
G. H. Mack
Las Cruces, New Mexico
2002

Abstract

Located east of the Rio Grande between Truth or Consequences and Hatch, New Mexico, the Caballo Mountains are one of the major uplifts in the southern Rio Grande rift. In terms of the relatively complete geologic history that their rocks reveal, the mountains may be unique in New Mexico. In addition to Precambrian metamorphic and plutonic rocks, every period of the Phanerozoic, except Triassic and Jurassic, is represented by outcrops of sedimentary rocks, which collectively are more than 5.6 km (3.5 mi) thick.

Oldest Precambrian rocks include Proterozoic amphibolite, schist, and gneiss, whose protoliths suggest deposition in a continental rift. Amphibolite-grade metamorphism and isoclinal folding accompanied closure of the rift, and this was followed by emplacement of epizonal anorogenic plutons, one of which is 1.3 Ga. Small alkalic plutons of possible Late Cambrian age intruded the Proterozoic terrane, followed by interregional erosional beveling of the basement rocks.

Throughout the early and middle Paleozoic, southern New Mexico was a tropical epicratonal shelf, alternately flooded by shallow marine seas and exposed to erosion. Totaling only 425 m (1,394 ft) thick, four stratigraphic sequences consist mostly of limestone and dolomite, each sequence bounded by an interregional or regional unconformity. Major cycles of epeirogenic uplift and subsidence and/or eustatic sea level changes are seemingly recorded by each stratigraphic sequence. Onset of mountain building associated with the Ancestral Rocky Mountains is indicated by local doming of lower and middle Paleozoic rocks during the latest Mississippian or earliest Pennsylvanian regional regression.

Upper Paleozoic strata include a mixed assemblage of marine and non-marine rocks that reflect depositional environments controlled by both Ancestral Rocky Mountain uplifts and basins. Pennsylvanian strata are mostly marine limestone and shale, as much as 570 m (1,870 ft) thick, deposited on the western margin of the Orogrande Basin, whereas Lower and middle Permian strata include fluvial red beds overlain by eolian sandstone, lagoonal gypsum and tidal-flat to marine limestone and dolomite as much as 700 m (2,296 ft) thick. Both Pennsylvanian and Permian strata thicken eastward into the Orogrande Basin; pebble clasts of Desmoinesian and Missourian limestone within Upper Pennsylvanian and Lower Permian conglomeratic beds suggest periodic subaerial erosion of the western flank of the basin.

There is no rock record of Late Permian through Early Cretaceous events in the Caballo Mountains. However, in Early Cretaceous time, the Caballo area was apparently located on the northeastern flank of a rift shoulder that bordered the Chihuahua trough/Bisbee Basin in southwestern New Mexico. The rift shoulder was onlapped and buried in Late Cretaceous time by nearly 1,000 m (3,280 ft) of marine and non-marine siliciclastic sediment and thin coal seams, part of the Western Interior foreland basin deposits that stretched from southern New Mexico to Alberta. By latest Cretaceous (Campanian–Maastrichtian) time, a volcanic arc extended from southwestern New Mexico into the Caballo area.

Earliest contractional stresses of the Laramide orogeny began in Maastrichtian time, producing broad uplift and erosion of volcanic arc rocks and deposition of mostly fluvial volcaniclastic sediment in an incipient intermontane basin. Laramide stresses intensified during the Paleocene and Eocene, producing the northwest-trending, northeast-verging Rio Grande uplift. With as much as 2.0 km (1.2 mi) of relief, the basement-cored uplift was rapidly eroded down to Precambrian rocks, the detritus being swept into the complementary Love Ranch Basin to the north and Potrillo Basin to the south. By middle to late Eocene time alluvial-fan, fluvial, and playa deposits had filled the Love Ranch Basin and onlapped and buried the uplift.

As Laramide uplift and basins were leveled, an Andean-type continental arc was reestablished in southwestern New Mexico. Alluvial aprons from andesitic volcanic centers spread across the Caballo area, accumulating to more than 600 m (1,968 ft) thick. Beginning in latest Eocene and earliest Oligocene, basalt-rhyolite volcanism commenced in south-central New Mexico, accompanied by the development of the broad, shallow Goodsight–Cedar Hills Basin, indications that an extensional stress regime had replaced the volcanic arc. The basin was filled in part by outflow sheets from cauldrons in southwestern New Mexico, as well as by siliciclastic rocks derived from uplifted basin margins, from erosion of volcanic topography, and from reworking of tephra. Increasing extensional strain is suggested by outpourings of huge volumes of upper Oligocene plateau basaltic andesite, fed by northwest-trending dike systems, as well as by central vents. In latest Oligocene time, syneruption alluvial aprons (Thurman Formation) sloped southward from the Mt. Withington cauldron and perhaps Nogal Canyon cauldron to the Caballo area, where distal parts of the apron interfingered with plateau basaltic andesite. More than 500 m (1,640 ft) thick adjacent to major Caballo faults, the clastic aprons may have been deposited in incipient grabens.

Strong uplift of the southern Caballo and Red House fault blocks began in latest

Oligocene or early Miocene time, continuing through the Miocene. The location of the uplifts and trend of the boundary faults was probably controlled by a northeast-southwest extensional stress field and by the position of northwesterly trending Laramide thrust faults. Uplift of segments of the Caballo block by negative inversion of Laramide thrust faults can be documented locally. Corresponding to the uplift was deposition of as much as 1,000 m (3,280 ft) of alluvial fan, playa, and lacustrine sediments in complementary half grabens, the ancestral Hatch–Rincon and Palomas Basins. In latest Miocene or early Pliocene time faulting stepped basinward, narrowing the half grabens, forming the outline of the modern Hatch–Rincon and Palomas Basins, and creating a series of intrabasin uplifts and grabens. On the eastern flank of the range, the Jornada Draw fault was initiated to help accommodate the growing structural relief between the rising Caballo block and downwarping Jornada del Muerto. Eruption of small volumes of alkalic basalt accompanied the latest Miocene–Pliocene rifting, particularly in the Cutter Sag accommodation zone. Throughout its extensional history, a favored mode of block faulting in the Caballo Mountains area was drape folding, which eventually led to the formation of several faulted, extensional domes and synclines.

Approximately 5 Ma ago the Ancestral Rio Grande entered the Palomas and Hatch–Rincon Basins, its position within the basins controlled by basin symmetry. By 0.78 Ma the river began to alternately incise and backfill the basins, creating a stepped sequence of terraces along valley and tributary walls. Probably driven by climatic changes related to glaciation in the northern hemisphere, the cycles of erosion and backfilling dominated the basins during middle to late Pleistocene and Holocene time. Recurrent faulting along the western margin of the Mud Springs–northern Caballo–Red Hills fault blocks has continued throughout the Pleistocene into the Holocene, at times probably triggering landslides in the Caballo Mountains.

Mineral resources in the Caballo Mountains were exploited largely between 1883 and 1952, but only small tonnages of modest value were ever shipped. Among the most valuable commodities produced were copper, gold, and fluorspar, although vanadium drew the most attention.

Good exposures and access, together with the nearly complete geologic rock record, suggest that the Caballo Mountains could be used as a geologic reference area for a large part of southern New Mexico. The descriptions of rock units and structures, as well as interpretations of environments of deposition and history, may have broad applicablity and prove useful in interpreting the geology of other ranges in the southern part of the state. Furthermore, folds of extensional origin, which elsewhere in the world form important buried oil traps, are exposed in outcrop, providing complex analogs for subsurface structures.

Introduction

Location, physical features, and access

The Caballo Mountains are located on the eastern side of the Rio Grande and Caballo Reservoir between the towns of Truth or Consequences and Hatch in south-central New Mexico (Figs. 1, 2). Approximately 50 km (31 mi) in length, the northerly trending range stretches from northern Doña Ana County well into central Sierra County. Although the high granite and limestone ridge that forms the backbone of the range is less than 5 km (3.1 mi) wide, lower foothills on both sides of the ridge expand the width of the range locally to 10 km (6.2 mi) or more. The highest part of the range, Timber Mountain, is 2,306 m (7,565 ft) above sea level, approximately 1,036 m (3,400 ft) above Caballo Reservoir located along its western base, and nearly 1,000 m (3,280 ft) above the floor of the Jornada del Muerto desert to the east. Local relief is commonly 600 m (1,968 ft) or more along the precipitous western escarpment of the range (Fig. 3), substantially less along the eastern flank, which is distinguished by a series of east-sloping cuestas (Fig. 4) or hogbacks and low-dipping pediment surfaces. Comparatively low foothills along the southwestern flank of the range are outlying fault blocks with names like Derry Hills, Red House Mountain, Red Hills, and Apache Valley.

Although large parts of the Caballo Mountains can be entered only by foot or horseback, a fairly good system of roads provides modest access to various parts of the range (Fig. 2). These roads connect with five interchanges on I–25 or with NM–51, a paved highway between Engle and Truth or Consequences. The eastern flank of the range may be entered either from the Upham interchange on I–25 located east of Rincon or from NM–51. The Upham interchange is connected to Engle by a maintained gravel road that follows the railroad spur from Rincon to Engle along the western side of the Jornada del Muerto. From this road several jeep or improved gravel roads penetrate the mountains, one of which ascends Timber Mountain to a communications facility. At the Rincon exit on I–25 a short dirt road climbs the Rincon Hills, and at the Hatch exit another dirt road leads to Palm Park and Red House Mountain. Access to the Derry Hills, Nakaye Mountain, and Apache Valley is afforded by an improved gravel road connecting with I–25 at the Garfield interchange, but this road is steep and rough as it ascends Nakaye Mountain. The Red Hills, Apache Valley, and the western slope of the Caballo Mountains are accessible by a network of dirt roads that join I–25 at the Caballo–Percha dam exit, whereas the northern part of the range may be entered from NM–51 east of the Rio Grande in Truth or Consequences. Although a few of the secondary roads throughout the mountains are periodically graded, most are not maintained. All may be impassable or nearly so after heavy rains.

Most of the land in the Caballo Mountains is administered by the Bureau of Land Management or, along the river, by the Elephant Butte Irrigation District. Small mining ventures, recreation, and cattle grazing are the main uses of the land. Several cattle ranches are located within or adjacent to the mountains, and many of the roads within the range are maintained by ranchers and lead to water tanks.

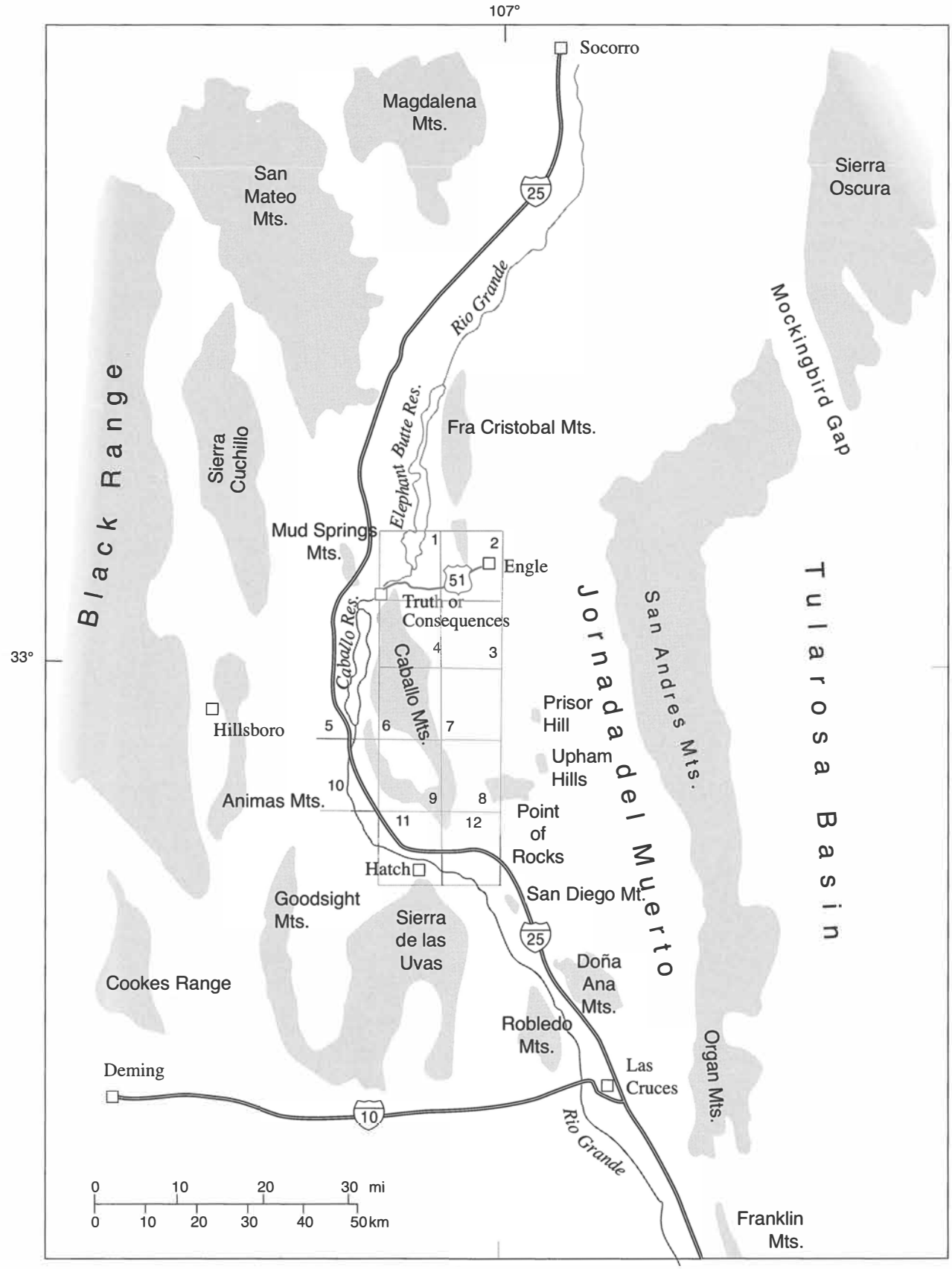

FIGURE 1—Location map, south-central New Mexico. Numbered quadrangles referred to in text are: **1**—Elephant Butte (Lozinsky 1986); **2**—Engle (Mack and Seager, in press); **3**—Cutter (Seager and Mack, in press b); **4**—Caballo Peak (Mason, 1976); **5**—Caballo (Seager and Mack, in press a); **6**—Apache Gap (Seager and Mack, in press a); **7**—Upham (Seager and Mack, in press b); **8**—Alivio (Seager, in press); **9**—McLeod Tank (Seager and Mack, 1998); **10**—Garfield (Seager and Mack, 1991); **11**—Hatch (Seager et al., in press); and **12**—Rincon (Seager and Hawley, 1973).

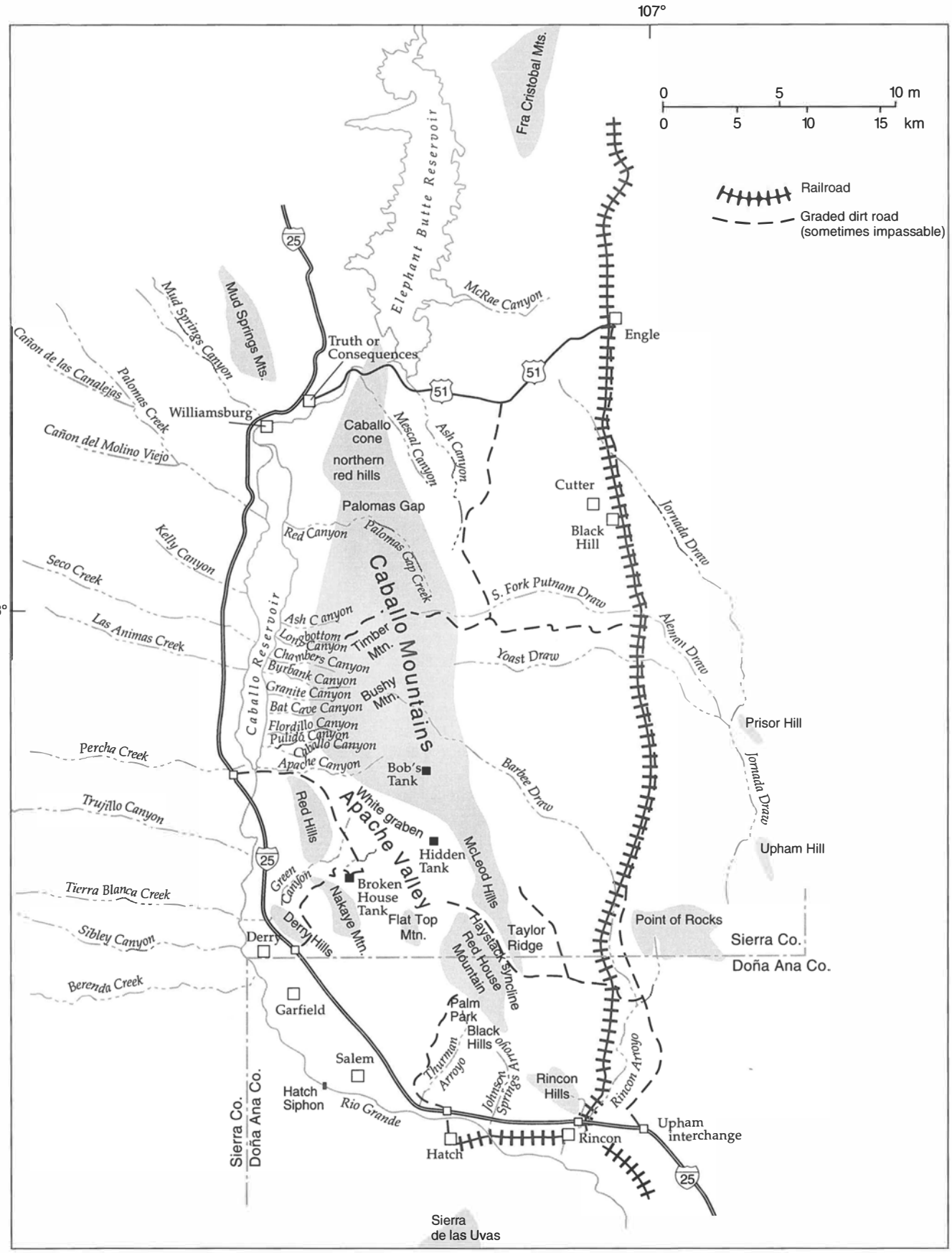

FIGURE 2—Location map, Caballo Mountains.

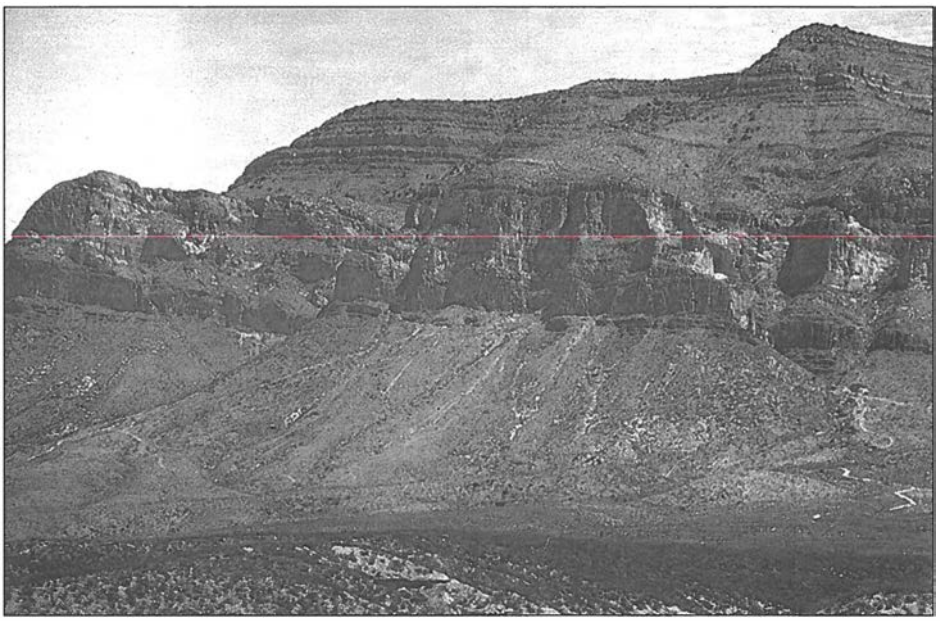

FIGURE 3—Western footwall escarpment of Caballo Mountains between Apache and Burbank Canyons.

Previous work

Since the middle 1800s when the first sketches of the Caballo Mountains and comments on their geology were published (Antisell, 1856; Shumard, 1859), many geologists have penned accounts of various aspects of the geology, and numerous theses have been completed, mostly at New Mexico universities. For a comprehensive listing and comments on work completed before 1952, the interested reader should consult Kelley and Silver (1952). Especially important early contributions include those of Herrick (1898) and Keyes (1905), who described the geology as well as ore deposits; Gordon and Graton (1906) and Lee and Girty (1909) on Paleozoic rocks; Lindgren et al. (1910), who referred extensively to the geology; Darton (1922), author of the first published geologic map of the range; Johnston (1928) and Rothrock et al. (1946) on fluorspar deposits; Harley (1934) on vanadium and gold deposits together with much geologic data; and Thompson (1942), who identified and named the Derryan Series from the Derry Hills. In 1951, Doyle mapped the northern part of the range as part of his M.S. research. As we acknowledged in the preface, the first detailed geologic map of the entire range and comprehensive account of the geology was published in 1952 by Kelley and Silver.

Between 1952 and 1982, topical geologic studies in the range were scattered and sporadic, and few new geologic maps were completed, probably because of the excellence of Kelley and Silver's map. Bushnell (1953) mapped the McRae Canyon area in conjunction with his study of Cretaceous rocks, and Mason (1976) produced an excellent map of the Caballo Peak (Palomas Gap) quadrangle at a scale of 1:24,000. Studies by Condie and Budding (1979) focused on Precambrian rocks, and McAnulty (1978) described fluorite deposits. King (1973) studied fusulinids in Middle to Lower Pennsylvanian strata in the Derry Hills, and Melvin (1963) described Cretaceous rocks south of NM–51 in the Mescal Canyon area.

Since 1982 geologic studies in the Caballo area accelerated, beginning with the republication of Kelley and Silvers' (1952) map on a topographic base, in color but at a smaller scale, 1:125,000 (Seager et al., 1982). Most importantly Cenozoic formations on the new map were differentiated, and additional structures were identified in the southern part of the range. Lozinsky (1986) mapped the Elephant Butte area at a scale of 1:24,000, followed by Seager and Mack's (1991, 1998) maps of the Garfield and McLeod Tank quadrangles. Other studies were more topical. McLemore (1986) and Bauer and Lozinsky (1986) published maps and interpretations of basement rocks in the Red Hills and Burbank Canyon areas, respectively. Lozinsky and Hawley (1986a, b) named and described the Palomas Formation in the Palomas Basin, and Foley et al. (1988), Machette (1987), and Machette et al. (1998) studied the piedmont scarp along the western base of the mountains. Pennsylvanian rocks were investigated by Kalesky (1988), Singleton (1990), and Thompson (1991); Cretaceous rocks by Wallin (1983); and Rio Grande rift deposits, including the Bell Top and Thurman Formations, were the subject of reports by Nightengale (1993), Kieling (1993), Boryta and McIntosh (1994), and Kieling (1994). In 1986 Clemons and Osburn provided an overview of the geology of the Truth or Consequences area, including the Caballo Mountains, and Mack et al., 1998c, published a review of the stratigraphy of south-central New Mexico, which also included the Caballo Mountains.

Another group of studies, published mostly during the 1990s, has resulted from our studies of the Caballo Mountains in recent years. Among these are papers on the Laramide evolution of

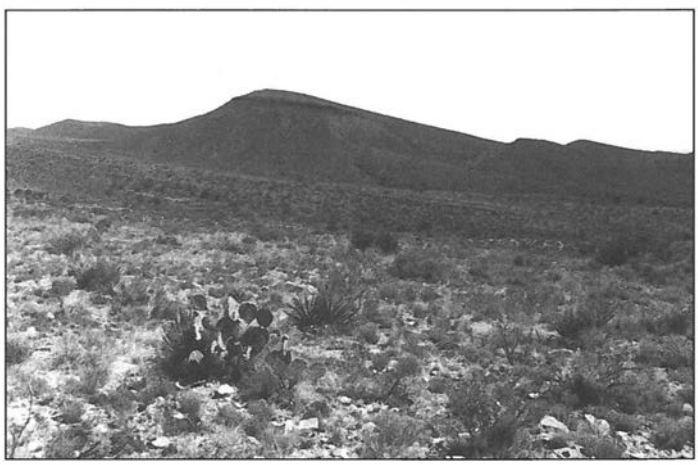

FIGURE 4—Cuestas of dark Abo Formation above Bar B Formation on eastern dip slope of Caballo Mountains. View looks northeast.

south-central New Mexico (Seager, 1983; Seager et al., 1986; Seager and Mack, 1986; Seager et al., 1997); the evolution of the southern Rio Grande rift (Mack et al., 1994a,b,c); the ancestral Rio Grande and basin tectonics (Mack and Seager, 1990; Mack and James, 1993; Leeder et al., 1996a,b; Mack and Leeder, 1999; Mack et al., 2002); the Jornada Draw fault (Seager and Mack, 1995); transfer zones (Mack and Seager, 1995); the age and correlation of the Camp Rice and Palomas Formations (Mack et al., 1993, 1996, 1998c); Camp Rice and Palomas paleosols and paleoclimate (Mack and James, 1992; Mack et al., 1994d; Mack et al., 2002); the Permian Abo and Yeso Formations (Mack et al., 1995, in press; Mack and Suguio, 1991; Mack and Dinterman, 2002); and Cretaceous paleosols (Mack, 1992; Buck and Mack, 1995), paleobotany (Upchurch and Mack, 1998), and dinosaurs (Lucas et al., 1998).

Plan of the book

The book has been divided into ten sections. The first, Precambrian/Cambrian(?) basement rocks is followed by seven that correspond to a major change in tectonic setting of southern New Mexico during the Phanerozoic. The first setting is a shallow-marine, tropical platform on which lower Paleozoic strata were deposited. Upper Paleozoic rocks are related to or immediately followed the formation of Ancestral Rocky Mountains basins and uplifts. Upper Cretaceous rocks are foreland basin deposits that accumulated within and along the western margin of the Western Interior Seaway, followed by the establishment of a continental volcanic arc in southwestern New Mexico. The contractional Laramide orogeny in southern New Mexico is recorded in some detail by uppermost Cretaceous and lower Tertiary rocks. Finally, middle and upper Cenozoic rocks document the transition from continental volcanic arc to a regional extensional regime that culminated in the modern fault block mountains and basins of the Rio Grande rift. After a discussion of Precambrian rocks, the rocks and structures associated with each tectonic setting are described, from earliest to most recent, each accompanied by an account of the tectonic setting or tectonic evolution they record. This is followed by a chapter on landslides, and the last chapter summarizes the coal and mineral deposits in the area.

Acknowledgments

We are grateful to the New Mexico Bureau of Geology and Mineral Resources, particularly to Frank E. Kottlowski (deceased) and Charles E. Chapin, past directors, for their support of our geologic studies in the Caballo Mountains area. We thank D. D. Seager for her considerable effort in preparations of this report. We thank Frank Kottlowski and Steve Cather for their careful and helpful reviews of the manuscript, and William McIntosh for providing radiometric dates for several stratigraphic units in advance of their publication. Finally, we are grateful to Nancy Gilson, whose careful and thorough editing helped improve the clarity and content of each page of the text and figures.

Basement rocks

Basement rocks include metamorphic and plutonic rocks of probable Early to Middle Proterozoic age, as well as a suite of small alkalic intrusives that may be as young as Late Cambrian. They crop out along the base of the larger fault blocks in the Caballo Mountains, generally confined between the range-boundary fault and the nonconformity with Paleozoic rocks (Fig. 5). Outcrops in the Red Hills and along the western base of the Caballo block are particularly extensive, covering approximately 6 km^2 (2.3 mi^2) and more than 40 km^2 (15 mi^2) respectively. Small outcrops were also mapped on the western flank of Red House Mountain and on the southern margin of the Nakaye horst.

Precambrian rocks

At least four silicic plutons, separated by screens or septa of metamorphic rocks, comprise the Early to Middle Proterozoic suite of rocks (Fig. 5). Only a single radiometric date from these rocks has been published. Using the Rb–Sr whole-rock method, Muehlberger et al. (1966) determined an age of 1,304 ± 72 Ma (recalculated, using new decay constant) for the Caballo granite in the southern part of the range. Unfortunately, the exact location of the dated sample was not given by Muehlberger et al. (1966).

Precambrian outcrops north of 33°N were not mapped or studied during this investigation. They were mapped and described by Doyle (1951), Kelley and Silver (1952), and in some detail by Mason (1976) and Condie and Budding (1979). However, only Mason (1976) and Condie and Budding (1979) differentiated between various basement rock units on their maps. According to Mason (1976), approximately 80% of the basement in the northern Caballo Mountains consists of pink to red gneissic granite or granite. The remainder is a suite of metamorphic rocks, including biotite-hornblende gneiss and schist, mica schist, greenstone, and minor quartzite and metasiltstone, all metamorphosed in the amphibolite facies. The metamorphic rocks occur as small pod-shaped bodies enclosed by gneissic granite. General trends of metamorphic foliation are N22°W, N3°W, and N28°W. Small granite dikes cut only metamorphic rocks, but narrow pegmatite dikes less than 100 m (328 ft) in length cut both metamorphic and granitic rocks.

South of 33°N Precambrian metamorphic rocks, as well as different plutons, are delineated on the maps of Bauer and Lozinsky (1986), as well as our own. Four plutons—Longbottom granodiorite, granite dikes, Caballo granite, and unnamed granite/gneissic granite—are distinguished on our maps of the Caballo, Apache Gap, Garfield, and McLeod Tank quadrangles. Locally, we also mapped small bodies of red syenite. We made no detailed petrographic study of any of the basement rocks, although six thin sections of basement rocks were examined. The following summary is drawn partly from the descriptions of Bauer and Lozinsky (1986) and partly from our own field observations.

Metamorphic rocks

Although the Caballo granite contains numerous small pods of metamorphic rocks, the largest tract is located between Burbank and Longbottom Canyons. Approximately 8 km^2 (3 mi^2) in extent, the metamorphic sequence appears to form septa between an unnamed pluton on the north, the Longbottom granodiorite in the center, and the Caballo granite to the south. The foliation strikes nearly east-west, swinging to a northeasterly strike along the northern margin of the Longbottom granodiorite. In general, dips are steep toward the south but there are many exceptions. The presence of amphibole and fibrous sillimanite indicates amphibolite grade metamorphism, with the sillimanite implying a pre- or syn-kinematic temperature of at least 500°C (Bauer and Lozinsky, 1986).

Three groups of metamorphic rocks are conspicuous in outcrop: amphibolite, felsic gneisses, and schistose quartz-feldspar rocks. Fifty percent or more of the metamorphic sequence consists of weakly to strongly foliated amphibolite, including horn-

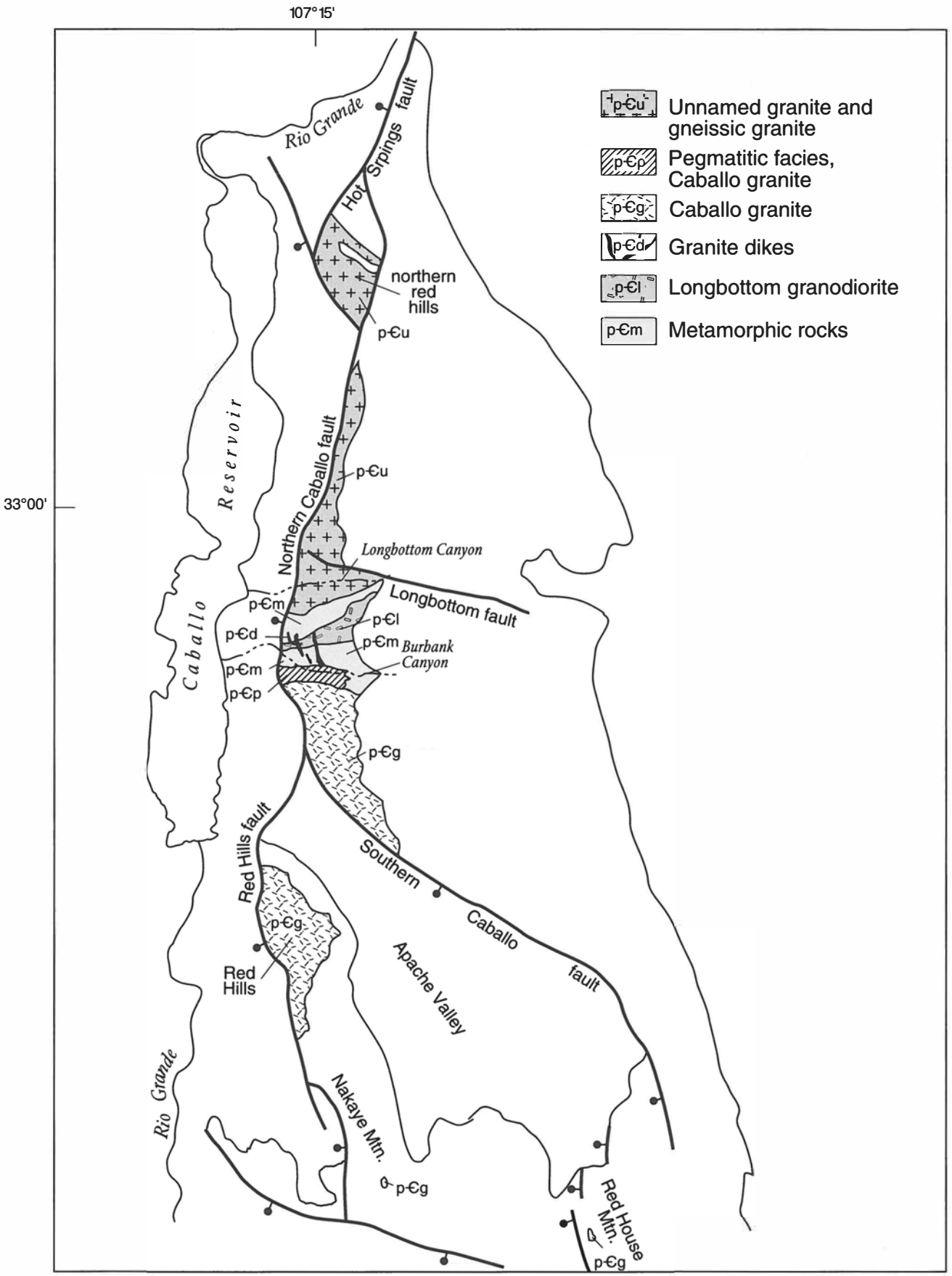

FIGURE 5—Index map of Precambrian rocks in the Caballo Mountains.

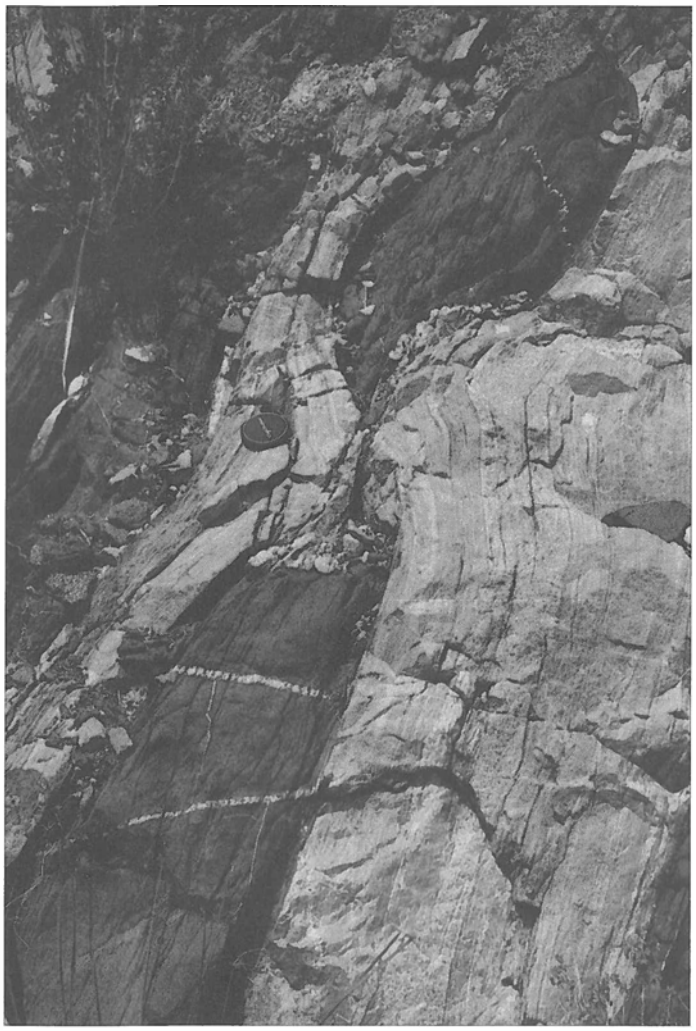

FIGURE 6—Boudinage of amphibolite layers in gneiss north of Burbank Canyon.

FIGURE 7—Near-isoclinal fold in quartz-feldspar-mica schist north of Burbank Canyon. Width of fold is approximately 50 cm (20 in). Fold hinge trends easterly and plunges east.

blende-biotite gneiss and biotite-hornblende schist. As much as 40% of the amphibolite is plagioclase, and garnet is locally present. Many amphibolites exhibit strong lineation, formed by smeared biotite and aligned hornblende, within the foliation planes. The lineation is approximately horizontal in most outcrops. Commonly 20–30 m (66–98 ft) wide, the amphibolite bodies are very discontinuous along strike, rarely extending more than a few hundred meters (1,500 ft) before pinching out within the enclosing, more felsic schists and gneisses. At outcrop-scale, boudinage of amphibolite layers is clear (Fig. 6), suggesting that this process also accounts for pod or lens shape of larger amphibolite masses. Protoliths of the amphibolite are interpreted to be a series of mafic, probably mostly basaltic, flows, dikes, or sills (Bauer and Lozinsky, 1986).

The amphibolite is interlayered on a grand scale with a variety of more felsic gneisses and schistose rocks. Gneisses are most abundant in the northern two-thirds of the metamorphic tract. They range from coarsely banded and coarse-grained to finely banded and finer grained. The transition between the two can often be observed in outcrops or even in hand specimens, where strong attenuation results in finely laminated, finer-grained gneisses. According to Bauer and Lozinsky (1986), the gneisses generally consist of quartz, sericitized plagioclase, microcline, biotite, and lesser amounts of chlorite, sillimanite, and fibrolite. One fine-grained, finely banded, distinctively red gneiss, approximately 50 m (164 ft) in width, can be traced for 3 km (1.8 mi), the width of the Precambrian outcrop belt. This gneiss, together with similar red gneisses located south of Longbottom Canyon, are mappable marker beds and probably represent a distinctive protolith. Most of the gneisses exhibit small open to closed folds, whose axial surfaces are parallel to regional foliation, according to Bauer and Lozinsky (1986). Small veins, pods, and narrow dikes of granite, usually ptygmatically folded, are locally common, suggesting a small degree of partial melting of the gneisses. Bauer and Lozinsky (1986) indicated the felsic gneiss probably was originally felsic volcanic rocks and/or hypabyssal silicic intrusives that were either coeval with or somewhat younger than the mafic rocks.

Schistose rocks are an important component of the metamorphic sequence in the septa between the Caballo and Longbottom plutons. Mica schists, quartzo-feldspathic schists, and gneisses with spaced or discontinuous zones of schistosity are interlayered with amphibolite. Both muscovite and biotite form the schistose layers. The most common lithology consists of alternating layers of quartz-feldspar aggregates, often weakly gneissic in texture, separated by bands of mica schist. The quartz-feldspar layers range from 1 to 100 cm (0.4 to 40 in) in width, the schistose layers 1–30 cm (0.4–12 in) in width. Outcrop-scale folds within such layers are nearly isoclinal, with axial surfaces and limbs nearly parallel to regional foliation (Fig. 7). Although no map-scale folds were observed, it is likely that much of the repetition of amphibolite, felsic gneiss, and schistose rocks is due to near isoclinal folding along hinges that trend approximately east-west. Protoliths of these schistose rocks probably include a variety of pelitic sedimentary rocks, including shales and argillaceous lithic and/or feldspathic sandstones that were interbedded with or intruded by the mafic and felsic igneous rocks.

Plutonic rocks

Four siliceous plutons have invaded metamorphic rocks in the Caballo Mountains. Largely separated by septa of metamorphic rocks, there are nonetheless sufficient crosscutting relationships to establish the order of emplacement of all but one of the plutons. Longbottom granodiorite was intruded first, followed by northwest-trending granite dikes and the Caballo granite. The relative age of an unnamed pink granite in the Longbottom Canyon area is not known.

Longbottom granodiorite

Longbottom granodiorite was named by Bauer and Lozinsky (1986) for Longbottom Canyon, although almost all of the pluton crops out within the south fork of Chambers Canyon (Fig. 8). The intrusion invaded the central part of the metamorphic sequence

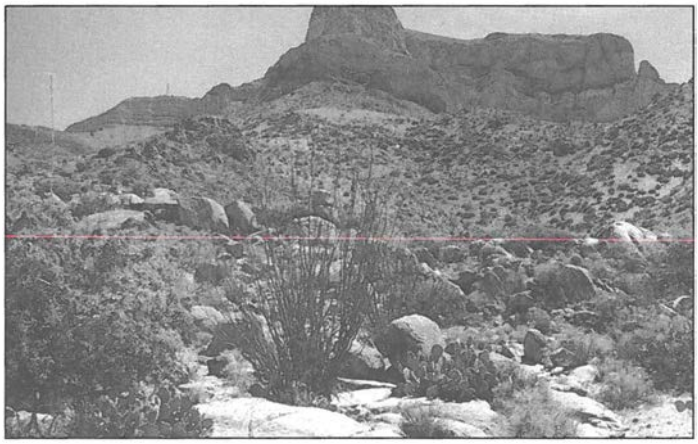

FIGURE 8—Spheroidally weathered outcrops of Longbottom granodiorite in south fork of Chambers Canyon. Lower Paleozoic strata form cliffs in center of photo, whereas Pennsylvanian rocks cap Timber Mountain at upper left.

and is essentially concordant with metamorphic foliation. We regard all contacts as sharp, although Bauer and Lozinsky (1986) described them as gradational. Only 0.3 km (0.2 mi) wide at its junction with the Caballo fault, the pluton widens eastward to 1.8 km (1.1 mi) at the unconformity with Paleozoic rocks. Foliation in the metamorphic rocks on the northern flank of the intrusion bend in response to thickening of the pluton, suggesting forceful intrusion. At the margins of the granodiorite numerous apophyses invade the metamorphic rocks, mostly concordantly, but locally discordantly, so that the northern margin in particular has a ragged pattern in plan view. The pluton also contains many xenoliths of metamorphic rock, a few as long as 300 m (984 ft), but mostly 20 m (66 ft) or less. The smaller xenoliths have sharp, angular margins; foliation within them is truncated by the granodiorite (Fig. 9). A flow-foliation formed by aligned feldspar phenocrysts is common along the contacts with wallrock and the larger xenoliths, but the interior parts of the pluton lack foliation. Equigranular granite dikes trending northwest cut the granodiorite.

The most conspicuous aspect of the Longbottom granodiorite is the crowded assemblage of euhedral phenocrysts of microcline and plagioclase. As much as 3 cm (1.2 in) long, the phenocrysts are set in a coarse-grained matrix of equigranular quartz, plagioclase, microcline, biotite, and sphene (Bauer and Lozinsky, 1986). In general, the granodiorite is gray on fresh surfaces and weathers tan, but locally it is red, mostly as a result of reddening of the phenocrysts, suggestive of potassium metasomatism and/or hematitization.

Granite dikes

Six granite dikes transect both metamorphic rocks and the Longbottom granodiorite. They terminate against the Caballo granite and are cut by pegmatite dikes associated with the margin of the Caballo granite. The dikes trend approximately N40°W and are as much as 10 m (33 ft) wide. The longest is more than 1 km (0.6 mi) in length. Consisting primarily of equigranular aggregates of quartz and feldspar, the granites display an aplitic texture, although they may be quite coarse grained. Some of the dikes apparently occupy faults of small displacement, and at least one dike is offset laterally by an east-trending fault. None of the dikes are foliated, nor are they deformed by ductile deformation.

Caballo granite

The Caballo granite is the largest pluton in the Precambrian terrane, and its full extent is probably batholithic in proportion. It can be traced discontinuously southward from Burbank Canyon for 19 km (12 mi) and includes most of the granitic rocks in the

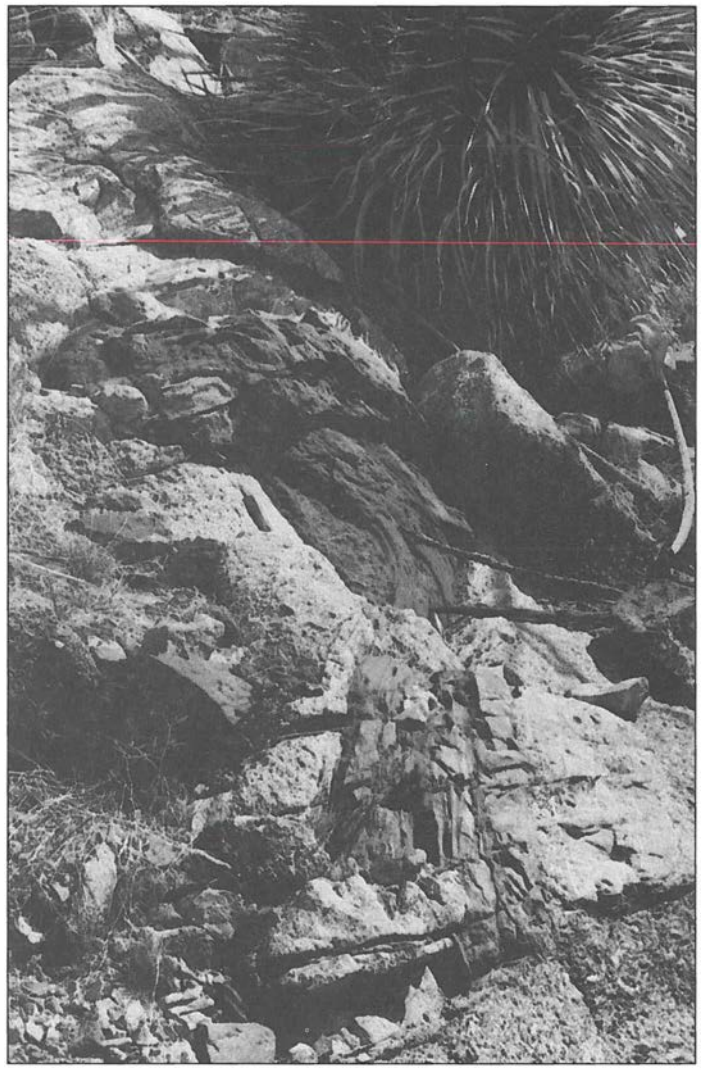

FIGURE 9—Xenolith of amphibolite in Longbottom granodiorite. Note sharp contacts of granodiorite cutting foliation in amphibolite. Exposures are in south fork of Chambers Canyon.

Red Hills as well as those in the western slopes of Red House Mountain. The northern margin of the Caballo granite is distinguished by an easterly trending zone of common pegmatite sheets, collectively nearly 0.5 km (0.3 mi) wide, centered on Burbank Canyon. The sheets intrude rocks of the metamorphic complex, particularly amphibolite, the spacing between sheets increasing northward into the metamorphic series as the thickness of sheets decreases. Although the pegmatites generally follow the strike of metamorphic foliation, some are discordant with depth, whereas others are prevailingly concordant. One of the outermost dikes in the system transects a northwest-trending granite/aplite dike, indicating that the pegmatite/Caballo granite is younger.

South of the marginal pegmatite complex, the Caballo granite consists of pink to orange, coarse-grained, equigranular granite. According to Bauer and Lozinsky (1986), quartz, microcline, plagioclase, microperthite, and chlorite are the principal minerals, but McLemore (1986) also reports accessory amounts of muscovite/sericite, biotite, iron oxides, and zircon. Homogenous over large areas, the Caballo granite also contains local areas of well-developed foliation (Bauer and Lozinsky, 1986; McLemore, 1986). Pod-shaped xenoliths of amphibolite occur sparingly within the granite. A few aplite and pegmatite dikes and quartz veins are also present, but they do not exceed a meter in width

or a few meters in length. The 1,304 ± 72 Ma age of the Caballo granite obtained by Muehlberger et al. (1966) indicates a Middle Proterozoic age.

Unnamed granite and gneissic granite

The northern boundary of the metamorphic rock sequence is marked by the intrusive contact of another pink, coarse-grained, equigranular granite. Located approximately 0.5 km (0.3 mi) south of Longbottom Canyon, the contact is prevailingly concordant but locally cuts across metamorphic foliation. No pegmatites are present along the contact. The granite, which has not been named, can be traced northward across both Longbottom Canyon and the Longbottom fault to near latitude 33°N, where it is replaced, at least in part, by tan, gneissic granite. Small bodies of red syenite, lenses of amphibolite, and irregular zones of porphyritic granitic rock, which may be Longbottom granodiorite, are also present within the pink granite.

There is little general agreement among Condie and Budding (1979), Bauer and Lozinsky (1986), and ourselves as to the relative age and correlation of the pink granite. Condie and Budding (1979) considered it to be part of the Caballo granite, making the metamorphic sequence a roof pendant within that pluton. However, they also show the granite terminating against the Longbottom fault, north of which a separate syenite and red granite pluton extends to the Palomas Gap area. Bauer and Lozinsky (1986) also believed the pink granite to be Caballo granite, but they show it extending north of the Longbottom fault, in spite of being transected by the fault. We propose that the unnamed pink granite represents a separate pluton, distinct from the Caballo granite, and that the metamorphic sequence is a septa, rather than a roof pendant, that separates the unnamed pink granite from the Longbottom granodiorite and Caballo granite. If the metamorphic sequence were a roof pendant within the Caballo granite, the pegmatite facies should be developed on its northern margin as well as its southern. The fact that the pink granite along the northern margin of the metamorphic terrane lacks pegmatites suggests that it is not Caballo granite, but rather a separate pluton. The relationship between the pink granite and tan gneissic granite near 33°N is not known, but the small bodies of red syenite are similar to those in the Red Hills, thought to be of Late Cambrian age by McLemore (1986).

Tectonic setting

Metamorphic protoliths in the Caballo Mountains are interpreted to be a suite of bimodal mafic and felsic volcanic and/or hypabyssal intrusives together with lithic or feldspathic sandstones and shales. The association is typical of continental rifts (Condie and Budding, 1979), and Condie (1982) favored continental-margin, back-arc basins as the specific site of rifting. According to Condie and Budding (1979), mafic magmas are derived from rising mantle plumes beneath the rifted terrane, whereas felsic magmatism is generated by partial melting of the lower crust where it has been invaded by basaltic mantle melts.

Following emplacement of sedimentary and volcanic and/or hypabyssal igneous rocks within the rift system, regional metamorphism at amphibolite grade created the metamorphic sequence now exposed. Metamorphism was accompanied by at least two episodes of severe contractional strain as recorded by structures in gneisses and schistose rocks. The earliest deformation produced compositional layering and schistosity that was subsequently folded to form east-trending, nearly isoclinal folds, whose limbs and axial surfaces are parallel to the dominant foliation present in outcrops. Bauer and Lozinsky (1986) suggest that a third minor deformational event produced non-penetrative crenulation folds in amphibolites.

Clearly this contractional orogeny closed and severely deformed the pre-existing rift system. Condie (1982) suggested that back-arc rift basins may be closed as a result of an Andean-type orogeny, whereas Grambling et al. (1988) and Bowring and Karlstrom (1990) emphasize the compressional deformation and metamorphism associated with assembly of tectonostratigraphic terranes along the southwest margin of the North American continent. Although the exact tectonic setting of the contractional orogeny may be debated, its results are clear. Isoclinal folding of the rift fill must have thickened the crust substantially, and at the mid- to lower-crustal level represented by the metamorphic rocks, temperatures approached the ternary eutectic melting point.

Regional metamorphism and contractional deformation was followed by emplacement of four siliceous plutons during the Middle Proterozoic. Several lines of evidence suggest that the suite of plutons is post-orogenic, that is, substantially younger than the regional metamorphic event, and was emplaced at fairly shallow levels in the crust. The evidence includes (1) numerous angular xenoliths, whose foliation is truncated by the igneous rocks; (2) sharp contacts everywhere between igneous and metamorphic rocks; (3) lack of penetrative foliation within any pluton, although foliation produced by flow alignment of phenocrysts is common along the margins of the Longbottom granodiorite, and schlieren are present locally in the Caballo granite; and (4) forcible rather than passive intrusion of the Longbottom granodiorite.

If the four Precambrian plutons are shallow, epizonal intrusives, they are frozen against metamorphic rocks that formed at a much deeper level. This implies that uplift and sufficiently deep erosion is required to bring the metamorphic rocks into the upper crust before being intruded by plutons. The uplift may have been an isostatic response to thickening of the crust by isoclinal folding and heating during metamorphism. In view of the potentially long period of time that may be required to juxtapose epizonal plutons against mid- or lower-crustal rocks, it seems likely that the tectonic setting of the plutons is different from and unrelated to the preceding contractional regime. The silicic, epizonal plutons do not appear to represent continental arc magmatism (Anderson, 1983; Bauer and Lozinsky, 1986), but rather are likely to be part of a belt of anorogenic granites emplaced between 1.0 and 1.5 Ga (Anderson, 1983). They probably were emplaced during a new extensional regime which, according to Anderson (1983), extended in a broad belt from the southwestern USA northeastward to the Great Lakes region.

Unfortunately, none of the events recorded by the Precambrian rocks in the Caballo Mountains have been dated, with the exception of the 1.3 Ga date for emplacement of the anorogenic Caballo granite. Based on dates of similar suites of rock exposed elsewhere in New Mexico, Condie and Budding (1979) suggested that Precambrian rocks in southern New Mexico may span the interval between 1.7 and 1.3 Ga, nearly the length of the Phanerozoic. Clearly, there is little data to constrain the length of each Precambrian event or the span of time between them. Hundreds of millions of years may separate emplacement of the anorogenic granites from the preceding contractional orogeny, for example. It seems likely that Precambrian rocks actually represent only a small fraction of the 400 Ma interval represented by the oldest and youngest rocks.

Late Cambrian(?) plutons

More than 25 bodies of red microcline syenite, quartz syenite, and alkalic granite intrude the Caballo granite in the Red Hills (McLemore, 1986), and several have invaded the unnamed granite and gneissic granite north of Longbottom Canyon. Although undated, McLemore (1986) speculated that the syenitic rocks may be latest Cambrian in age, based on lithologic similarities with dated alkalic and carbonatite intrusives within basement rocks elsewhere in New Mexico. Typically small, the plutons range from flat-lying, tabular bodies a few meters to a few hundred meters long and as much as a few meters wide to small,

near vertical pipes. Pervasive hematitization and chloritic alteration have obscured original textures. Unusually high K_2O/Na_2O ratios, together with replacement textures, mineralogy, and locally gradational contacts suggest the syenites are a result of potassium metasomatism (McLemore, 1986).

Because of the evidence for potassium metasomatism, McLemore (1986) envisioned two possible modes of emplacement for the syenites. Syenitic magmas may have invaded the Caballo granite and were subsequently metasomatized by late magmatic or post-magmatic fluids. Alternatively, potassium-rich fluids, derived from a deeper alkalic magma, may have altered the granite to syenite along fractures. In any case, an extensional tectonic setting seems to be required for these alkalic rocks (Loring and Armstrong, 1980; McLemore, 1987a,b; Evans and Clemons, 1988). McMillan and McLemore (1999) suggested that these and other alkalic rocks of similar ages throughout New Mexico define a New Mexico aulacogen.

Although Boyd and Wolfe (1953) claimed that red syenite in the Red Hills area intrudes the Bliss Formation, we are convinced that the syenite is nonconformably beneath the Bliss everywhere. In view of the Late Cambrian age of the Bliss, it is difficult to understand the Late Cambrian to Ordovician ages reported for the alkalic rocks in southern New Mexico where the Bliss is also present (Evans and Clemons, 1988). If the radiometric ages are correct, they imply that alkalic plutons were emplaced, uplifted, and exposed to erosion in a very short period of time in the Late Cambrian. No sediments related to such uplift and erosion are known, nor are there sediments related to an aulacogen or any other kind of Cambrian extensional basin. What is clear is that by Late Cambrian time, basement rocks across southern New Mexico presented a nearly featureless surface, locally surmounted by low hills (Kottlowski et al., 1973) and scoured by shallow channels (F. E. Kottlowski, personal comm., 2000) across which the first Paleozoic sea transgressed.

Lower and middle Paleozoic shelf deposits

Throughout early and medial Paleozoic time, southern New Mexico was an epicratonal shelf region, alternatively exposed to erosion and flooded by shallow, tropical seas. In the Caballo Mountains area, a thickness of only 400 m (1,312 ft) or so of sedimentary rock, mostly limestone and dolomite (Fig. 10), records these transgressions and regressions over a time span of nearly 190 m.y. The low sediment accumulation rates confirm the stability of the shelf and its slow rate of subsidence. The sedimentary deposits include the Bliss, El Paso, and Montoya Formations of Late Cambrian and Ordovician age; the Fusselman Dolomite of Silurian age; the Percha Shale of Devonian age; and the Lake Valley Formation of Mississippian age.

Bliss Formation

The basal Paleozoic stratigraphic unit in the Caballo Mountains and elsewhere in southern New Mexico and west Texas is the Bliss Formation, named by Richardson (1904) for exposures in the Franklin Mountains near El Paso, Texas. The Bliss Formation forms an easily recognizable dark band between the reddish slopes of Precambrian rocks and the steep, gray cliffs of Ordovician carbonate rocks on the footwall scarps of the Caballo Mountains and Red Hills (Fig. 11). The Bliss is also locally exposed on Red House and Nakaye Mountains. Although the Bliss was measured at Burbank Canyon, the north end of the Red Hills, and at Nakaye Mountain, there is so little difference in the details of the three sections that only the Burbank Canyon section is shown in Figure 12.

Based on a sparse invertebrate fauna, the Bliss Formation in south-central New Mexico has been interpreted to span the Cambrian–Ordovician boundary (Flower, 1953, 1969). Taylor and Repetski (1995) recently collected a suite of trilobite and conodont fossils from the Bliss at Cable Canyon in the Caballo Mountains (now called Flordillo Canyon on USGS 7½-min Caballo and Apache Gap quadrangles). This new fossil assemblage demonstrates that the lower half of the Bliss corresponds to the Trempealeauan stage of the uppermost Cambrian, whereas the upper half of the formation belongs in the Skullrockian stage of the lowermost Ordovician.

The Bliss Formation thins northward from about 73 m (239 ft) in the Franklin Mountains near El Paso, Texas, to a pinchout in the northern Fra Cristobal Mountains (McCleary, 1960; Mack et al., 1998a). The overall northward thinning is primarily depositional in origin, although the pinchout in the Fra Cristobal Mountains may in part be due to erosion associated with the sub-Pennsylvanian unconformity. In the Caballo Mountains, the Bliss is between 30 and 40 m (98 and 131 ft) thick. The Bliss unconformably overlies Precambrian (Upper Proterozoic) crystalline basement with only a few meters of relief apparent on the unconformity at any one outcrop. The gradational upper contact with the El Paso Formation is generally picked at either the last appearance of thick, > 1 m (> 3.3 ft), beds of sandstone or at the base of the steep cliff composed primarily of limestone.

Description

The Bliss Formation in the Caballo Mountains consists of five rock types (Fig. 12). Present in the lower third of the formation are medium to thick beds of brown to tan, granular to pebbly, coarse to very coarse, arkosic sandstone. Locally, the basal few centimeters of the Bliss contain a conglomerate composed of pebbles of quartz, as well as metamorphic and granitic rocks. The coarse sandstone beds commonly display numerous *Skolithos* burrows up to 20 cm (8.1 in) long (Fig. 13), and locally have horizontal laminae, trough crossbeds, and fragments of phosphatic shells. Also present in the lower part of the formation is a bed ranging from 0.5 to 2 m (1.6 to 6.6 ft) thick of maroon oolitic ironstone first described by Kelley (1949, 1951). The coarsest iron oolites, up to granule size, are at the base of the bed and gradationally overlie the upper coarse sandstone. The upper part of the bed consists of massive, bioturbated, fine sand-size iron oolites.

One of the most common rock types in the Bliss Formation is green, micaceous, very fine sandstone to coarse siltstone. The green color is imparted by an abundance of finely disseminated, peloidal glauconite. Bioturbation is common and consists of a variety of horizontal and subvertical burrows that largely disrupt the original depositional layering. Whitish fragments of phosphatic brachiopods are locally abundant. In the upper part of the formation, glauconitic very fine sandstones are interbedded on the scale of 5–50 cm (2–20 in) with ledge-forming sandstones and limestones. The ledge-forming sandstones are maroon and exhibit horizontal laminae, hummocky stratification, and ripple cross laminae. A few beds have large symmetrical ripples in beds 10–30 cm (4–12 in) thick (Fig. 14). The large ripples have amplitudes of 5 cm (2 in), wavelengths of 35 cm (14 in), and complex internal laminae indicative of wave oscillation processes. Horizontal and subvertical burrows are also common on bedding planes of the ledge-forming sandstones. The brown to gray limestones have a thickness distribution similar to that the of ledge-forming, fine sandstones and contain echinoderm columnals and fragments of brachiopods and trilobites, as well as peloidal glauconite and medium sand-size detrital quartz grains. Commonly recrystallized to coarse calcite, the limestones

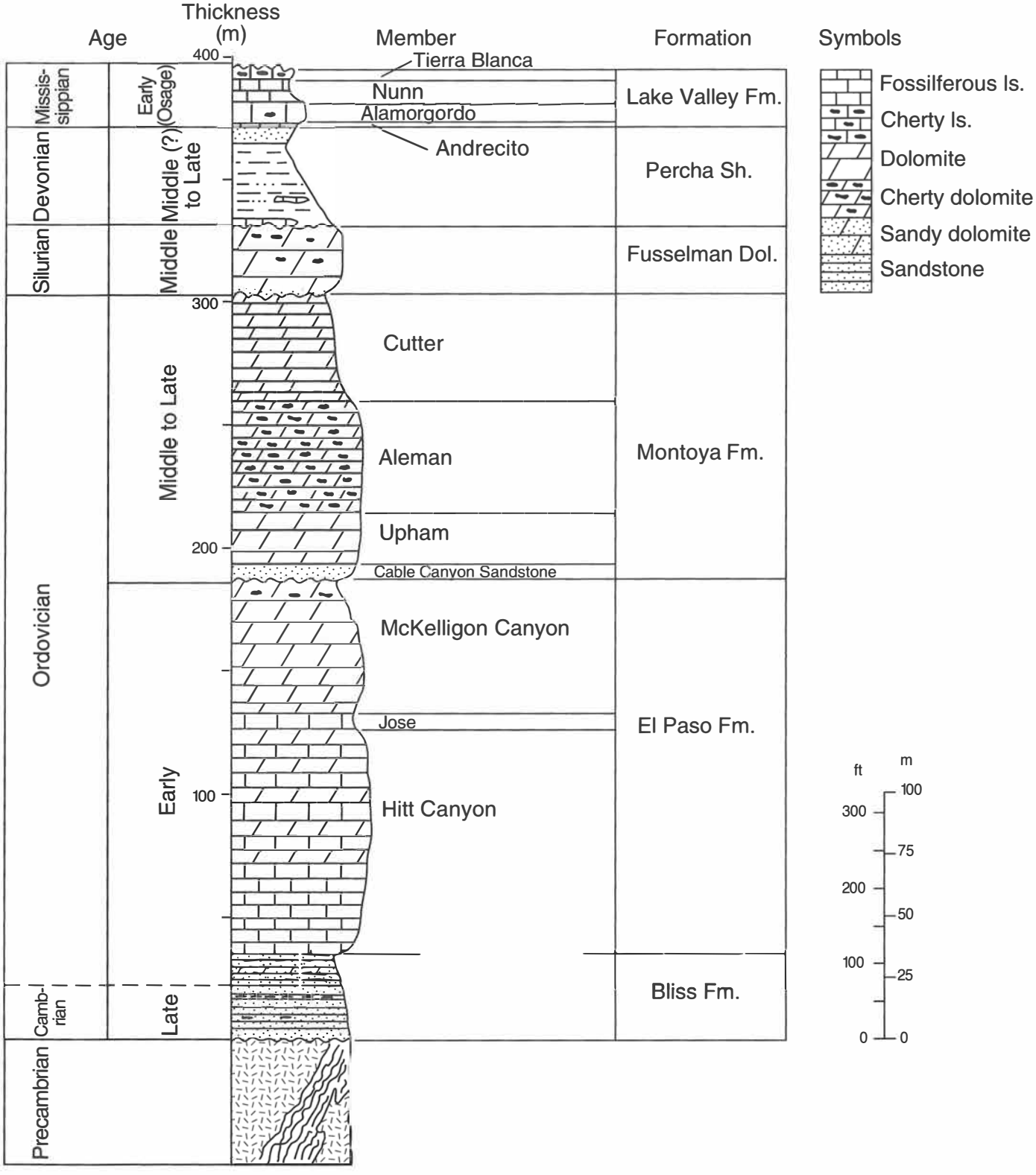

FIGURE 10—Stratigraphic column of lower and middle Paleozoic rocks.

also contain scattered dolomite rhombs and hematite. Like the ledge-forming sandstones, the limestones display hummocky stratification, ripple cross laminae, and large wave oscillation ripples, and the upper few centimeters of many of the limestone beds are disrupted by bioturbation.

Depositional environments

The Bliss Formation was deposited during the Cambrian–Ordovician transgression that affected most of North America (Raatz, 2002). Hayes and Cone (1975) demonstrated that the basal unit in the transgressive sequence becomes younger eastward from southwestern Arizona, across southern New Mexico, and into west Texas, implying that the sea transgressed eastward. However, northward depositional thinning of the Bliss in New Mexico also argues for a northward component of transgression as well (Kottlowski, 1963, 1965). Most previous workers concluded that the Bliss is shallow-marine to shoreline in origin, although considerable variation exists in the details of the depositional models (cf. Lewis, 1962; Kottlowski, 1963; Hoffman, 1976; Thompson and Potter, 1981; Ottensman, 1983; Chafetz et al., 1986; Stageman, 1987).

In the Caballo Mountains, the basal few tens of centimeters of the Bliss are interpreted to be a transgressive lag, formed by reworking of the Precambrian surface by rising sea level. The granules and pebbles of granite, metamorphic rocks, and quartz represent the coarse fraction that could not be moved seaward by storms. Above the lag are two beds of crossbedded, *Skolithos*-bearing, medium- to coarse-grained sandstones interpreted to represent upper shoreface or foreshore environments deposited in upward-shallowing cycles. Each bed is overlain by finer-grained facies produced by a deepening event.

The remainder of the Bliss is composed of numerous interbeds of glauconitic, very fine sandstone; ledge-forming, hematitic, very fine sandstone; and limestone, which represent alternating quiet-water and storm deposition. The only variation in this pattern at Burbank Canyon is the interval between 17 and 20 m (5 and 66 ft) from the base in which limestones are absent. The glauconitic, very fine sandstones represent slow deposition from suspension on a shallow-marine shelf. This interpretation is supported by the fine grain size, the abundance of horizontal burrows, and pervasive glauconite, which is generally interpreted to accumulate during episodes of reduced sediment influx and slow sedimentation (cf. Van Houten and Purucker, 1984). In contrast, the presence of hummocky stratification in the hematitic sandstones and limestones and of intraclasts and fossil hash in the limestones indicate they are storm deposits (cf. Cheel and Leckie, 1993). In many cases, hummocky stratification is overlain by wave oscillation ripples, and bed tops display numerous horizontal burrows, reflecting reworking of the top of the storm bed during the waning stage of the storm (wave oscillation ripples) and subsequent fair weather (bioturbation). There is no evidence in the three sections measured in this study for sub-aerial exposure, stromatolites, or limestone deposition other than by storms. Consequently, there is no indication of the upward-shallowing cycles described by Chafetz et al. (1986) for the Bliss near Silver City. The one exception might be a bed of whitish medium sandstone directly above the green, glauconitic, very fine sandstone marker bed (Fig. 15). The light colored sandstone has prominent wave oscillation ripples expressed on the bed top and as ripple cross laminae, and may represent deposition in the lower shoreface. The presence of both siliciclastic and carbonate storm deposits may be a response to fluctuations in the amount of detrital sediment brought to the shoreline and redistributed by storms.

A detailed study of the origin of the iron oolites in the Bliss Formation is beyond the scope of this study. However, it is instructive to consider how features of the iron oolites in the Bliss relate to the current controversy on the origin of these enigmatic

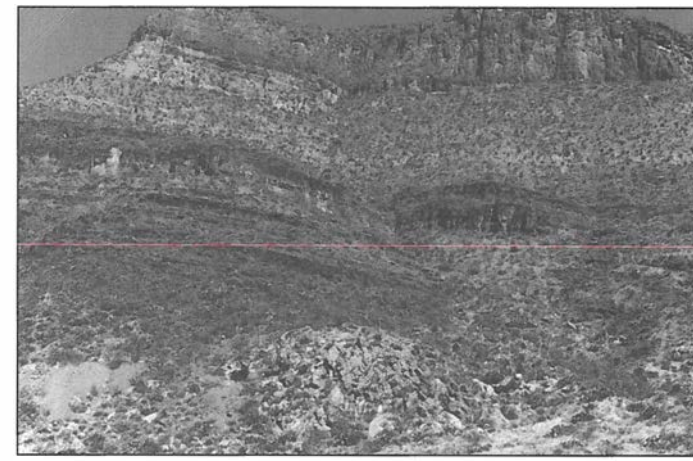

FIGURE 11—Dark, thinly bedded Bliss Formation (Cambrian–Ordovician) near the base of the cliff on the north side of Longbottom Canyon.

deposits. Most Phanerozoic iron oolites are thought to be marine in origin, and the prevailing idea is that the ooids are primary precipitates, rather than diagenetic replacements of originally non-ferruginous ooids (Young, 1989). The most common mineral in iron oolites is berthierine, an iron-rich serpentine, which may diagenetically alter to chamosite of the chlorite group (Young, 1989). Goethite is present in some oolitic ironstones, and may be primary or an alteration of berthierine (Gehring, 1989). Three models are invoked for the origin of Phanerozoic iron oolites: (1) marine reworking of iron ooids or pisoids originally produced in soils (Siehl and Thein, 1989), (2) formation of iron ooids in marine environments characterized by low sediment supply, active reworking of the sediment, and a contribution of ferruginous weathering products (Van Houten and Purucker, 1984), and (3) an exhalative origin, in which dissolved iron is supplied to the sea floor from the subsurface via faults, fissures, and/or vents (Kimberley, 1994).

The iron oolite bed in the Bliss Formation appears to conform to many of the criteria described in the models listed above, particularly the first two. The Bliss iron oolite is presumably marine, because of the gradational lower contact with *Skolithos*-bearing sandstones and extensive bioturbation in the upper part of the bed, although no marine fossils have been found in the oolite bed itself. Slow sediment accumulation rate and/or reworking of previously deposited sediment during formation of the Bliss iron oolites is suggested by its stratigraphic position above upper shoreface/foreshore sandstone and beneath deeper water facies, marking either a lowstand or rising sea level. Tropical weathering in the equatorial setting of New Mexico in latest Cambrian time could have supplied pedogenic iron to the sea, or produced an iron-rich regolith that was subsequently reworked by transgression. Reworking of an iron-rich regolith would be particularly pertinent if, as suggested by Flower (1969), there is an unconformity in the Bliss that corresponds to the stratigraphic position of the iron oolite. However, iron oolites are not present everywhere in the Bliss in southwestern New Mexico, which would probably be expected if the sea transgressed a regional iron-rich regolith. Moreover, it is not clear whether tropical weathering in the absence of vascular land plants, as would have been the case in the latest Cambrian, would have formed soil products similar to those forming today. There are few data at this time from the Bliss Formation pertinent to the exhalative model of iron oolite formation. There is no evidence for vents, fissures, or faults that could have acted as conduits for the iron-rich fluids to invade the sea floor. However, the fact that iron oolites in the Bliss are restricted to an east-west band across southwestern New Mexico may argue for a linear localization of

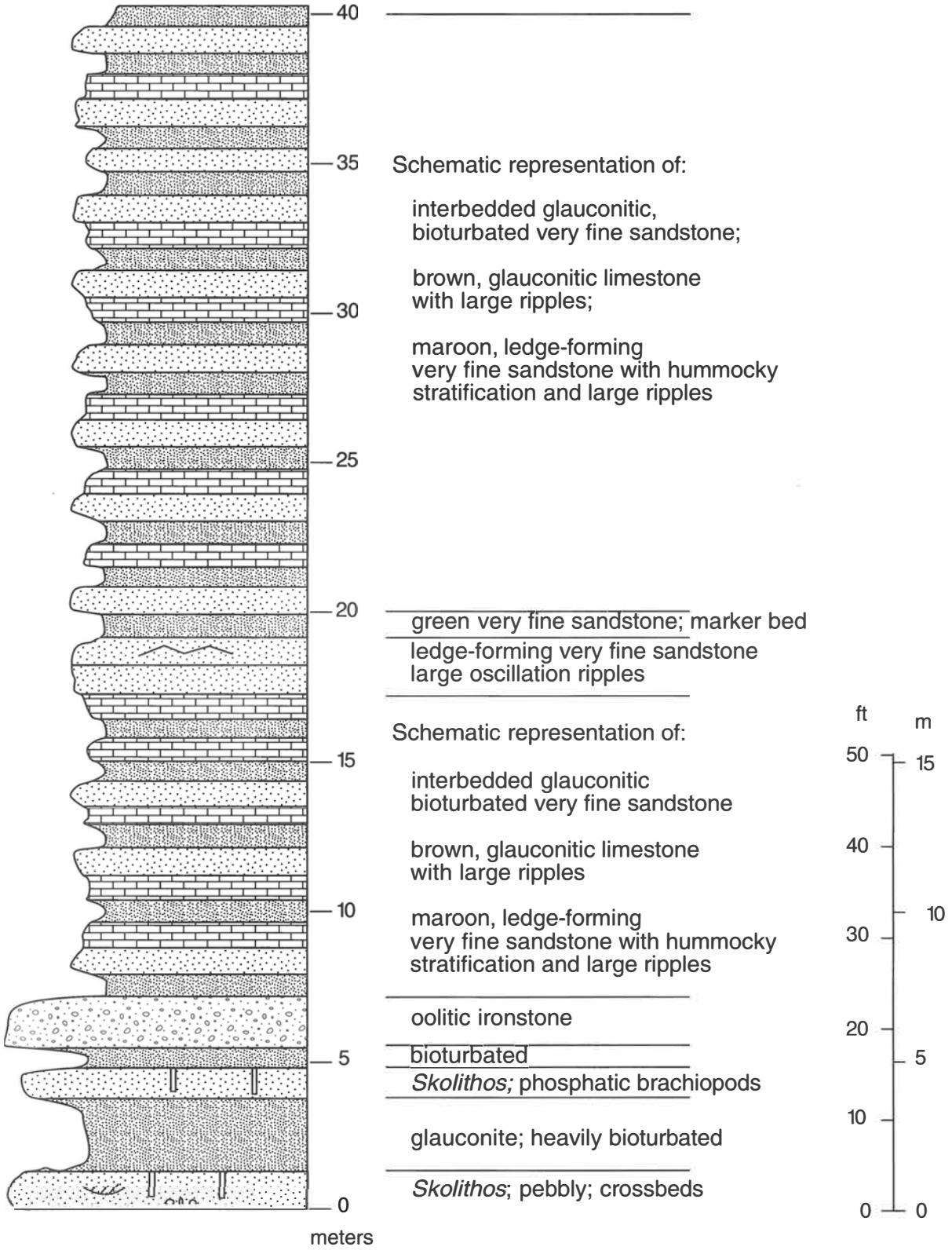

FIGURE 12—Measured section of the Bliss Formation (Cambrian–Ordovician) at Burbank Canyon (SE¼ sec. 34 T15S R4W). Upper 32 m (105 ft) is a schematic representation of the fine-scale interbedding of rock types.

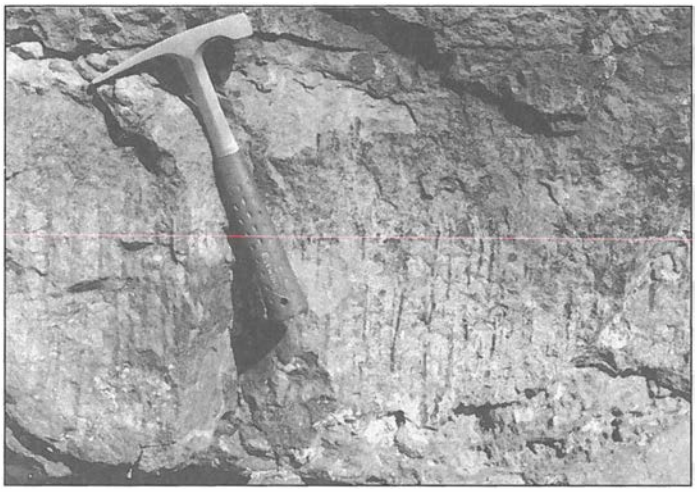

FIGURE 13—*Skolithos* burrows in the basal sandstones of the Bliss Formation (Cambrian–Ordovician) at Burbank Canyon. Hammer is 25 cm (9.8 in) long.

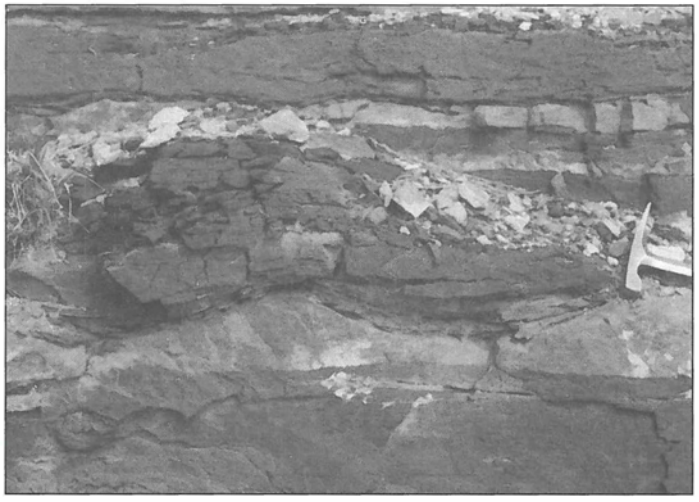

FIGURE 14—Large-scale wave oscillation ripples in the Bliss Formation (Cambrian–Ordovician) at Burbank Canyon (SE ¼ sec. 34 T15S R4W). Hammer is 25 cm (9.8 in) long.

the conditions necessary for the formation of the iron oolites.

It should be clear from this discussion that none of the models for the formation of iron oolites can be ruled out at this time. Clearly, more work needs to be done on the iron oolites of the Bliss Formation before their origin can be determined.

El Paso Formation

Named by Richardson (1904) for outcrops in the southern Franklin Mountains, the El Paso Formation has become a well-known formation exposed in many of the mountain ranges of southern New Mexico. In the Caballo Mountains, the formation is well displayed at Red House and Nakaye Mountains and in the Red Hills, but the most accessible outcrops are in Burbank and Trujillo Canyons, which drain the western escarpment of the main Caballo fault block. The formation consists of limestone, dolomitic limestone, and dolomite that weathers to ledgy slopes and high, cave-pocked cliffs (Fig. 16).

The El Paso Formation is Early Ordovician in age (Darton, 1917; Kottlowski et al., 1956; Hayes and Cone, 1975). The basal contact with the Bliss Formation is gradational and marked by several meters of intertonguing, dark purplish-black Bliss sandstone with tan, sandy dolomite of the El Paso. For mapping purposes, the contact in such sections was picked at the highest Bliss sandstone or the base of El Paso limestone cliffs. Locally, as at the measured section in the McLeod Tank quadrangle, the contact is sharp, separating dark Bliss sandstone below from ledgy, sandy dolomite above. The upper contact of the El Paso Formation is a sharp disconformity that is overlain by the brown-weathering, coarse-grained Cable Canyon Sandstone Member of the Montoya Formation or, locally in the Red Hills, by basal sandstones of the Pennsylvanian Red House Formation.

From a thickness of about 460 m (1,509 ft) in the Franklin Mountains, the El Paso thins northward to an east-west trending zero line that passes through the northern Fra Cristobal Range (Kottlowski, 1963, 1965; Greenwood et al., 1977; Clemons, 1991). In the Caballo Mountains, the El Paso Formation is 152 m (499 ft) thick at Nakaye Mountain, thinning northward to 119 m (390 ft) near Palomas Gap (Mason, 1976). According to Clemons (1991), northward thinning is a combination of pre-Montoya erosion and depositional thinning, but the northern pinchout may also

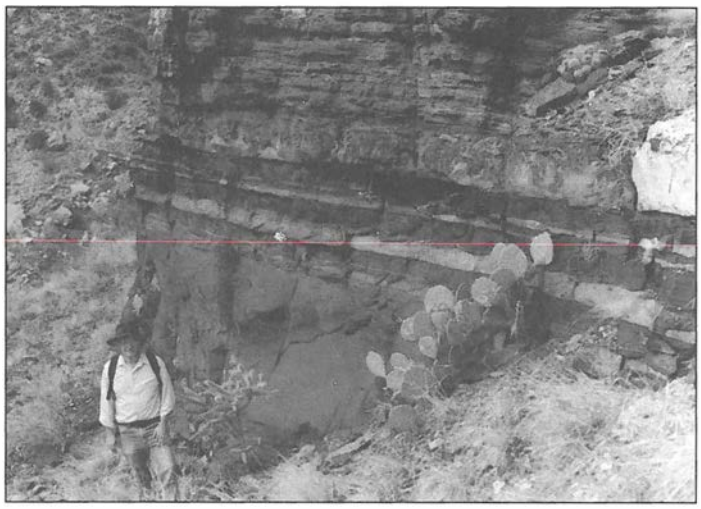

FIGURE 15—Green, glauconitc very fine sandstone (dark) interbedded with medium to coarse sandstone (light) containing wave oscillation ripples, hummocky stratification, and/or crossbeds in the Bliss Formation (Cambrian–Ordovician) at Burbank Canyon.

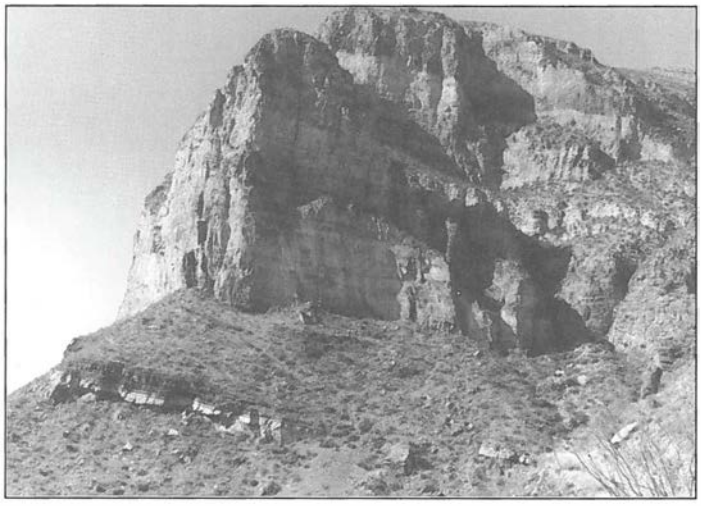

FIGURE 16—Cliff face on the north side of Burbank Canyon. Layered rocks in the lower part belong to the Cambrian–Ordovician Bliss Formation, which overlies Precambrian crystalline basement. Prominent middle cliff is the Lower Ordovician El Paso Formation, and dark band in the middle of the upper cliff is the base of the Upper Ordovician Montoya Formation (Cable Canyon Sandstone Member).

be a product of erosional truncation in Late Mississippian or Early Pennsylvanian time.

The El Paso Formation has been the subject of considerable disagreement concerning stratigraphic nomenclature. Kelley and Silver (1952) designated the El Paso in the Caballo Mountains as a group, subdividing it into lower Sierrite and upper Bat Cave Formations. Group status was subsequently applied to the El Paso elsewhere in southern New Mexico and far west Texas, but there is disagreement about formational names (Flower, 1965; 1969; LeMone, 1969; Lucia, 1968; Harbour, 1972; Hayes and Cone, 1975). Most recently, Clemons (1991) noted that most geologic maps at the scale of 1:24,000 show the El Paso as a single map unit, and, thus, it deserves formational status. Clemons favored subdividing the El Paso into four members, modified from Hayes and Cone (1975): in ascending order, Hitt Canyon, Jose, McKelligon, and Padre. All except the Padre Member, are present in the Caballo Mountains. The following descriptions are based on outcrops at the southern end of Nakaye Mountain.

Description

The Hitt Canyon Member consists of approximately 91 m (299 ft) of light-brown, medium-bedded, dolomitic limestone. The basal few meters of the member contain fine sand and silt, but the siliciclastic component appears to decrease rapidly upsection. The limestone is strongly bioturbated, and dolomite commonly occupies burrows. Occasionally, wavy laminae, which may be hummocky stratification, are visible despite the pervasive bioturbation. Discrete beds of medium-grained dolomite occur from 31 to 37 m (102 to 121 ft) and from 66 to 68 m (217 to 223 ft) above the base of the member. The most common rock types are fossiliferous wackestone and packstone that contain whole and broken fossils of trilobites and echinoderms, as well as gastropods, cephalopod siphuncles, sponges, and *Nuia* (Clemons, 1984, 1991). Other rock types include intraclast grainstone, fossiliferous grainstone, and one bed of stromatolitic boundstone 75 m (246 ft) above the base of the member.

The Jose Member, approximately 7 m (23 ft) thick, is a conspicuous dark-colored unit characterized by the presence of oolitic grainstone and packstone. The Jose also contains bioturbated, fossiliferous packstone.

Approximately 54 m (177 ft) thick, the McKelligon Member consists mostly of light-tan, fine-grained dolomite. However, the basal 6 m (20 ft) is similar in lithology to the Hitt Canyon Member and consists of light-gray, bioturbated, fossiliferous packstone and intraclast grainstone. Fifteen meters (49 ft) below the top of the member is a prominent 3 m (9.8 ft) thick silicified zone, and above that a 0.2 m (0.7 ft) thick stromatolite bed is found 12 m (39.4 ft) from the top.

Depositional environments

The El Paso Formation was deposited on a shallow-marine cratonic platform during the latter stage of the Cambrian–Ordovician transgression of North America (Clemons, 1991; Raatz, 2002). A delicate balance between the rates of subsidence, sea-level changes, and carbonate production resulted in a monotonous succession of facies in the Hitt Canyon Member and precluded small-scale shoaling cycles that are common in other carbonate cratonic and shelf sequences (cf. James, 1984). Abundance of micrite, diverse fauna, and pervasive bioturbation suggest that the bulk of the sediment was deposited below normal wave base in a well-oxygenated, open-marine environment. The shallow platform was periodically subjected to storms, which produced intraclast grainstones that locally exhibit graded bedding and which produced fossiliferous grainstones with hummocky stratification. Bioturbation of the storm deposits during subsequent fair-weather periods may have destroyed some or all of the original storm-related stratification.

Shoaling is indicated by the appearance of stromatolites near the top of the Hitt Canyon Member and by oolitic grainstone in the Jose Member (Clemons, 1991). These shallow-water horizons can be traced throughout southern New Mexico and west Texas, indicating a regional drop in relative sea level. It is unclear, however, whether the regional shoaling is due to a eustatic sea-level fall or to an increase in the rate of carbonate production with respect to subsidence and sea-level rise.

Normal, open-marine sedimentation resumed during deposition of the lower part of the McKelligon Member. Unfortunately, dolomitization of the remainder of the McKelligon Member inhibits interpretation of depositional environments.

Montoya Formation

The Montoya Formation was named by Richardson (1908) for outcrops in the southern Franklin Mountains near El Paso. Excellent exposures in the Caballo Mountains are widespread in the western escarpment of the main Caballo fault block, but the most easily accessible outcrops are located in the western slopes and canyons of Nakaye Mountain. The formation consists largely of cherty dolomite and dolomite that weathers to rugged cliffs and ledgy slopes.

Late Middle to Late Ordovician in age, but not latest Ordovician, (Flower, 1969; Hayes and Cone, 1975; Pope, 2002), the Montoya Formation disconformably overlies the El Paso Formation and is disconformably overlain by the Fusselman Dolomite or by Pennsylvanian rocks. The lower contact is marked by the change from light-colored dolomite of the McKelligon Member of the El Paso Formation to dark-brown weathering, cliff-forming Cable Canyon Sandstone at the base of the Montoya. The upper contact is also sharp, located at the top of light-colored, thin-bedded Cutter Member of the Montoya, above which a dark, massive cliff of Fusselman Dolomite or ledgy Pennsylvanian shale and limestone prevail.

From a maximum thickness of approximately 152 m (499 ft) in northern Chihuahua, Mexico, the Montoya Formation thins irregularly northward to a zero line north of the Fra Cristobal Range (Greenwood et al., 1977). In the Caballo Mountains, the formation ranges generally from 116 to 126 m (381 to 413 ft) thick in the central and southern part of the range to 100 m (328 ft) near Truth or Consequences (Kelley and Silver, 1952). However, in the Red Hills area, the formation was entirely removed by Late Mississippian or Early Pennsylvanian erosion, an erosional event that probably also contributed to the northward thinning of the Montoya north of the Percha and Fusselman pinchout near Burbank Canyon. Pre-Fusselman and pre-Percha erosion has also affected upper Montoya beds, both regionally and locally.

Although Richardson (1908) defined the Montoya as a formation, Kelley and Silver (1952) raised it to group status and defined four formations in the Caballo Mountains: Cable Canyon, Upham, Aleman, and Cutter, in ascending order. Although these units are widely recognized across south-central New Mexico, the Montoya is generally shown on geologic maps as a single unit. Consequently, the Montoya is herein regarded as a formation with four members.

Description

Kelley and Silver (1952) named the Cable Canyon Sandstone Member for exposures near the Sierrite mine near the head of what they informally referred to as Cable Canyon, but which is officially known as Flordillo Canyon. The Cable Canyon Sandstone Member consists of dark-brown, massive- to thick-bedded, ledge-forming quartz sandstone 6–11 m (20–36 ft) thick. Grain size of the sandstone is distinctly bimodal, consisting of well-rounded, very coarse sand and a few granules in a matrix of fine sand. Grain size appears to be homogeneous throughout the section, although in the southernmost Red Hills, the Cable Canyon

coarsens upward (Seager and Mack, 1991). Trough crossbeds in sets from 8 to 20 cm (3.1 to 7.9 in) are common, and burrowing is pervasive, locally destroying the crossbeds. The burrows are predominantly vertical. Crossbed paleocurrent orientations are bimodal, with a principal direction of N14°W (n = 10) and a secondary direction of S30°W (n = 5). No body fossils were found in the outcrops, but a piece of float contains a fragment of a solitary coral.

The Upham Member overlies the Cable Canyon Member along a sharp, but presumably conformable, contact. The Upham is composed of cliff-forming, dark-gray, massive- to thick-bedded, medium-grained dolomite 8–24 m (26–79 ft) thick. The basal meter contains scattered fine and coarse quartz grains. Silicified solitary corals, echinoderm columnals, and brachiopods exist throughout the member, but are most common in the upper 6 m (20 ft). The basal 15 m (49 ft) are heavily bioturbated. A few chert nodules appear in the upper 6 m (20 ft) as well.

The Aleman Member gradationally overlies the Upham Member and is approximately 46 m (151 ft) thick throughout the range. It is characterized by cliff-forming, fine-grained, medium-gray to dark-gray dolomite that contains numerous elongate black or gray chert nodules. The nodules parallel bedding and impart a ribbon-like structure to the dolomite. Locally near the base, the chert exists as laterally continuous beds. Six meters (20 ft) above the base of the member is a 1 m (3.3 ft) thick local zone of dolomite with several thin, 1 cm (0.4 in), layers and lenses of silicified whole brachiopods. The middle and upper portions of the member also contain zones of breccia and indistinct thin, wavy laminae.

The contact between the Aleman and overlying Cutter Member is sharp and is marked by the disappearance of chert nodules and by the change from cliff-forming dolomite to dolomite that weathers to a ledgy slope. The Cutter consists of 15–44 m (49–144 ft) of light-tan, cream, and light-gray, medium-bedded, fine-grained dolomite, locally laminated. Several thin, 1.5 m (4.9 ft) beds of bioturbated, fossiliferous wackestone, containing brachiopods and bryozoa, are present near the base. Mudstone, usually poorly exposed, that contains whole bryozoans and brachiopods was noted near the base of the section in a prospect adit on Nakaye Mountain. Light- and dark-gray mottling, some of which is due to bioturbation or brecciation, is locally present in beds approximately 29 m (95 ft) above the base of the member.

Depositional environments

Deposition of the Montoya Formation resulted from transgression of Middle to Late Ordovician shallow seas onto eroded El Paso strata (Raatz, 2002). Thickness variations in the Cable Canyon Sandstone probably reflect paleotopography on the erosion surface (Kottlowski, 1963). Bruno and Chafetz (1988) suggested that the Cable Canyon was deposited as shallow-marine sand ridges similar to those on the modern North Sea and Atlantic continental shelves (Swift and Field, 1981). Marine fauna, extensive bioturbation, and crossbeds are cited as evidence for this model (Bruno and Chafetz, 1988). The combination of crossbeds and extensive bioturbation suggests fluctuating energy. In contrast, upper shoreface sands commonly are crossbedded but display few burrows, whereas lower shoreface sands are heavily bioturbated but are not crossbedded (cf. Howard and Reineck, 1981). Bruno and Chafetz (1988) further suggested that seaward transport of detritus was accomplished by tidal currents, an interpretation that is consistent with bipolar paleocurrents observed in this study.

Pope (2002) interpreted the depositional environments of the carbonate-bearing members of the Montoya Formation throughout west Texas and southwestern New Mexico, including outcrops in the Caballo Mountains. He interpreted the Upham as having been deposited on a shallow, open-marine ramp characterized by warm water. He also showed that many of the bedded cherts in the lower Aleman contain high concentrations of sponge spicules and were deposited, along with interbedded fine-grained dolomites, in deep, probably cool, marine waters. Most fossiliferous beds in the Aleman represent shallow, open-marine environments. Although a few fossiliferous beds in the Cutter Member were deposited in lagoonal or open-marine environments, most of the member is interpreted as intertidal or supratidal in origin, with the fine laminae related to cyanobacterial mats. Geochemical analyses by Pope (2002) demonstrated that finely disseminated phosphate (1–5 wt%) is present in much of the Montoya. The phosphatic and cherty nature of the Montoya is interpreted by Pope (2002) to indicate upwelling along the southern passive margin of North America, perhaps influenced by Late Ordovician glaciation.

Fusselman Dolomite

The Fusselman Dolomite was named by Richardson (1908, 1909) for outcrops in the southern Franklin Mountains. Exposed in many of the ranges of southwestern New Mexico, the Fusselman also crops out in the Caballo Mountains, particularly in the escarpment south of Burbank Canyon, in Red House Mountain, and in the footwall of the Garfield fault. Accessible good exposures also are present at both the northern and southern ends of Nakaye Mountain.

The Fusselman comprises the only Silurian rocks in southern New Mexico. Although the Fusselman includes both Early and Middle Silurian strata at its type section (Richardson, 1909), only Middle Silurian beds are present farther north, including the Caballo Mountains (Kottlowski et al., 1956; Kottlowski, 1963). A sharp, disconformable surface of low relief separates the cliffy, dark-colored Fusselman from light-colored Cutter dolomite below. The upper contact with overlying Percha Shale is also a disconformity, usually identified by the silicified beds and undulating, channeled surfaces at the top of the Fusselman. North of Burbank Canyon and throughout the Red Hills area, the Fusselman is missing, having been removed by Early Devonian and/or Late Mississippian or Early Pennsylvanian erosion.

Regionally the Fusselman thins northward from 450 m (1,476 ft) thick in the Florida Mountains (Clemons and Brown, 1983) and 300 m (984 ft) in the Franklin Mountains to a zero edge that extends westward from Alamogordo to the central Caballo Mountains (Greenwood et al., 1977). Northward thinning reflects a combination of post-Fusselman (Early Devonian) erosion and depositional onlap (Kottlowski, 1963). With the exception of the Red Hills area noted above, the Fusselman Dolomite is 26–30 m (85–98 ft) thick throughout the southernmost Caballo Mountains. However, the formation thins rapidly northward to a pinchout exposed in the escarpment south of Burbank Canyon.

Description

Locally the base of the Fusselman Dolomite is marked by crossbedded sandy dolomite a few meters thick. Trough and planar crossbeds up to 40 cm (15.7 in) thick are present, as are fragments of solitary corals and echinoderm columnals. Crossbeds consist of siliclastic grains as well as local grainstones and dolomite grains. Above this the Fusselman is composed of dark-gray, medium-bedded, fine-grained dolomite with numerous dark chert nodules. The long axes of nodules commonly are parallel to bedding. The uppermost 2 m (6.6 ft) of the formation is generally silicified, containing silica and calcite-lined vugs.

Depositional environments

The Fusselman Dolomite was deposited during an Early to Middle Silurian transgression onto the southern margin of the North American craton. The crossbedded dolomite and siliciclastics at the base of the formation indicate relatively strong currents, but this facies is rare in the Fusselman through the remain-

der of southern New Mexico. Dolomitization has destroyed many or all of the original sedimentary textures and structures of most of the Fusselman, making interpretation of the depositional environment difficult. Kottlowski and Pray (1967) suggest that the Fusselman was deposited in a shallow-marine environment with some horizons deposited in the intertidal and supratidal zones. There is no evidence in this study to amplify on this model. The silicified beds at the top of the formation may be related to karst development before Devonian deposition (Kottlowski, 1963).

Percha Shale

The sequence of shaley strata above the Fusselman Dolomite in the Caballo Mountains is designated the Percha Shale. Named by Gordon and Graton (1907) for exposures near Percha Creek along the eastern flank of the Black Range, the unit is another widespread formation in south-central New Mexico. In the central and southern Caballo Mountains, the formation forms a distinctive slope, usually covered by thick colluvium, which contrasts strongly with underlying cliffs of dolomite and overlying cliffs of well-bedded Mississippian or Pennsylvanian limestone. Because it consists largely of soft, non-resistant shale, good exposures are uncommon. Satisfactory outcrops accessible with pickup or four-wheel drive are present on the southeastern slopes of Red House Mountain and in the hills west of Taylor Ridge.

Although Flower (1959) showed the Percha Formation to be latest Devonian in age, the formation may also contain Middle Devonian rocks in the Caballo area. This possibility is open because Kottlowski et al. (1956) recognized both Middle and Upper Devonian rock units in the San Andres range that are in the same stratigraphic position as the Percha of the Caballo Mountains. Whether part of the Percha in the Caballo Mountains is also Middle Devonian is unknown; tentatively, we accept the Late Devonian age for all of the Percha Shale in the Caballo area.

The Percha Shale unconformably overlies the Silurian Fusselman Dolomite. At southeasternmost outcrops in the range, the Percha is probably nearly conformable with the overlying Mississippian Lake Valley Formation, but elsewhere it is disconformably succeeded by the Pennsylvanian Red House Formation. The Percha–Lake Valley contact lacks evidence of substantial erosion and was chosen at the boundary between tan or pink, massive siltstone beds at the top of the Percha and thin, nodular limestone at the base of a prominent Lake Valley limestone cliff. In contrast, the Percha–Red House contact is strikingly disconformable, distinguished by the abrupt change from black, fissile shale to thin- or medium-bedded, burrowed, cherty limestone.

The Percha Shale is as much as 71 m (233 ft) thick where it is preserved beneath Mississippian strata in the southern Caballo Mountains. Northward, the formation thins rapidly and pinches out just south of Burbank Canyon, although it is present farther north in the Mud Springs Mountains (Maxwell and Oakman, 1990). South of Burbank Canyon the Percha is also locally absent or very thin in the Red Hills–Nakaye Mountain area. Both regional and local, irregular thinning of Percha strata resulted from Late Mississippian or Early Pennsylvanian erosion.

Description

Fissile, olive-gray to dark-gray shale or claystone comprise most of the Percha Formation. It weathers to a distinctive float consisting of green or dark gray chips. The lower 10–12 m (33–39 ft) of shale are particularly dark colored and organic rich, whereas higher shale beds may locally contain a scarce brachiopod fauna, particularly *Lingula* sp. Interbedded within the shale/claystone are thin siltstone or fine sandstone beds as well as limestone units. Siltstone units are as much as 2 m (6.6 ft) thick. Tan, micaceous, and thin-bedded to flaggy, they often contain horizontal burrows on bedding planes and asymmetrical, ripple cross-laminae in their upper parts. Limestone beds are far less common than siltstone/sandstone. Locally, thin, <1 m (<3.3 ft), beds of buff-weathering limestone occur at or near the base of the formation in the escarpment below Timber Mountain. Elsewhere thin lenses of limestone are interbedded with the shale. The thickest of these, about 2 m (6.6 ft) thick, crops out on the southeastern flank of Red House Mountain. This ledge-forming, fossiliferous grainstone displays small-scale trough crossbeds and ripple laminae. At Red House Mountain, the limestone appears to pinch out within a distance of 100 m (328 ft).

At southernmost exposures, uppermost Percha shale/claystone beds grade upward into approximately 5 m (16 ft) of tan to pale-red siltstone or very fine sandstone that often forms bold outcrops or cliffs beneath Mississippian limestone cliffs. Although Seager and Hawley (1973) originally assigned these rocks to the Caballero Formation in the Rincon Hills, we consider them to be part of the Percha Shale. The lower half of the siltstone-sandstone unit is medium bedded and heavily bioturbated and contains a few light-colored, silicified echinoderm columnals and gastropods. The upper half is thin bedded and displays ripple cross-laminae and horizontal and vertical burrows. Horizontal burrows are either sinuous or Y-shaped, the latter reaching a length of 12 cm (4.7 in) and a width of 7 mm (0.3 in). Two thin, 10 and 14 cm (3.9 and 4.3 in), beds near the top of the siltstone/sandstone unit display hummocky stratification that passes upward into ripples and burrows.

Depositional environments

The Percha Shale in south-central New Mexico was deposited in a cratonic sea that transgressed an erosional surface produced sometime between Late Silurian and Late Devonian time (Kottlowski, 1965; Raatz, 2002). Shale, the bulk of the formation, represents deposition in quiet water below normal wave base. The basal dark shale reflects stagnant, poorly oxygenated bottom waters. Organic-rich, dark shales similar to the basal Percha are commonly found near the base of transgressive sequences as a result of high organic productivity, poor circulation, and temperature stratification of the water (Schlanger and Jenkyns, 1976; Hallam and Bradshaw, 1979; Heckel, 1980). Olive-gray claystone in the upper part of the formation was deposited in contact with more highly oxygenated bottom water that periodically supported a benthic brachiopod fauna. Crossbedded limestone within the olive-gray claystone attest to locally strong current activity and may be analogous to hydrodynamic mounds that form on slight topographic highs in Florida Bay (Ball, 1967).

An increase in grain size and the presence of ripples suggest increased current activity during deposition of the siltstone/sandstone intervals, particularly during deposition of the upper sandstone/siltstone unit. However, extensive bioturbation and the predominance of horizontal grazing burrows indicate a relatively low stress environment, perhaps at or just below normal wave base. Deposition between normal and storm wave base is further suggested by the presence of hummocky stratification (Dott and Bourgeois, 1982).

The source of siliciclastic detritus of the Percha can be interpreted from regional lithofacies relationships (Kottlowski, 1963, 1965). A northward increase in the relative abundance of silt and sand suggests a source area in that direction, perhaps from the Transcontinental Arch. A sandy lithofacies is also present in southeastern Arizona, suggesting that detritus may have entered New Mexico from the southwest as well.

Lake Valley Formation

Mississippian strata in the Caballo Mountains belong to the Lake Valley Formation, whose type section is in the Lake Valley mining district of southwestern Sierra County (Cope, 1881, 1882; Keyes, 1904). Although the formation has been widely recognized in the ranges of south-central New Mexico, outcrops in the

Caballo Mountains are restricted to Red House Mountain in the southeastern part of the range. The formation can readily be spotted by the Alamogordo Member of the formation, which forms a blue-gray limestone cliff above the Percha slope. Accessible, although somewhat faulted, outcrops of the formation are present adjacent to Palm Park, whereas a more complete, less faulted, but less accessible section may be visited on the southeastern slopes of Red House Mountain in SE¼ NE¼ sec. 3 T18S R3W. Consisting entirely of limestone or cherty limestone, the formation weathers to cliffs, saddles, and ledgy slopes. To the south of the Caballo Mountains, the Lake Valley Formation is underlain by the Mississippian Caballero Formation (Kinderhookian) and is overlain by the Rancheria and Helms Formations (Meramecian and Chesterian; Lauden and Bowsher, 1949).

Known for its abundant, well-preserved invertebrate fauna, the Lake Valley Formation has been the subject of numerous paleontological studies. Among these, the most recent study by Kues (1986) provides a comprehensive list of fauna from the type section. All workers agree that the Lake Valley fauna is Osagean (Early Mississippian) in age (Kottlowski, 1963; Lane, 1974; Armstrong et al., 1979; Lane and DeKeyser, 1980; Lane and Ormiston, 1982; Kues, 1986). In the Caballo region, the Lake Valley is seemingly conformable with the underlying Percha Shale, although a minor disconformity may separate them. The transition between the two formations is distinguished by a change from pale-red or tan siltstone/sandstone at the top of the Percha to nodular, gray limestone at the base of Lake Valley limestone cliffs. The disconformable contact with overlying Pennsylvanian Red House Formation is often, although not always, identified by variable thicknesses of chert breccia at the base of the Red House, derived from underlying Mississippian units. The erosion surface is one of substantial relief, probably a paleokarst surface.

Owing to Late Mississippian or Early Pennsylvanian erosion, the thickness of the Lake Valley Formation varies considerably. Entirely removed from the western and northern parts of the Caballo area, the maximum preserved thickness is 24.7 m (81 ft) at Red House Mountain. This compares with thicknesses of 67 m (220 ft) at the type section to the west and 19–123 m (62–403 ft) in the San Andres Mountains to the east (Kottlowski et al., 1956).

Laudon and Bowsher (1949) subdivided the Lake Valley Formation into six members, which in ascending order are: Andrecito, Alamogordo, Nunn, Tierra Blanca, Arcente, and Doña Ana. The latter two members crop out only in the Sacramento and southern San Andres Mountains. The remaining four members are more widespread. Although Kelley and Silver (1952) recognized only the Alamogordo and Nunn Members in the southern Caballo Mountains, a stratigraphic section found in this study on the southeast flank of Red House Mountain (SE ¼ NE ¼ sec. 3 T18S R3W) contains the lower four members, totaling 24.7 m (81 ft) thick.

Description

The Andrecito Member is represented by 0.7 m (2.3 ft) of gray and tan mottled, nodular dolomitic limestone that forms a recess between ledges of sandstone at the top of the Percha Formation and limestone of the Alamogordo Member. Both upper and lower contacts are sharp. The Andrecito is present in all outcrops of the Lake Valley Formation in the southern Caballo Mountains.

The Alamogordo Member is 9 m (30 ft) thick and forms a cliff of medium-bedded, gray to bluish-gray limestone. Planar, parallel bedding is a distinctive trait that makes the Alamogordo easy to recognize from a distance. The Alamogordo consists of bioturbated fossiliferous packstone and wackestone composed of echinoderm columnals, brachiopods, and solitary corals. Some fossils are silicified and stand in relief on a weathered surface. Another distinctive characteristic of the Alamogordo Member is the presence of banded chert nodules, which are parallel to bedding and attain lengths up to 1 m (3.3 ft). The nodules display white and gray banding, either as solid gray core surrounded by a single white rim 0.5–1 cm (0.2–0.4 in) thick or as gray and white bands alternating on a scale of 1–5 mm (0.04–0.2 in) throughout the nodule. The Alamogordo Member has a very irregular thickness distribution in the southern Caballo Mountains, but in general thins northward.

The Alamogordo Member is overlain by 9 m (30 ft) of the Nunn Member, which consists of thin- to medium-bedded, locally wavy bedded, light-gray argillaceous packstone. The Nunn Member weathers into irregular slabs and forms gentle slopes. Numerous well-preserved fossils of echinoderms, brachiopods, solitary corals, and bryozoa can be found in float blocks or on bedding planes. Bioturbation is common, and a few light-colored chert nodules appear in the upper part of the member.

The uppermost member of the Lake Valley Formation exposed in the McLeod Tank quadrangle is the Tierra Blanca Member, which consists of 6 m (20 ft) of medium-bedded gray limestone. The Tierra Blanca Member is distinguished from the Nunn Member by the presence of many large white to pink chert nodules oriented parallel to bedding. The dominant rock type is fossiliferous grainstone, consisting of echinoderm columnals, brachiopods, and solitary corals, many of which are silicified. The upper meter of the member is pink to tan as a result of partial dolomitization. The Tierra Blanca Member crops out in a limited area in Red House Mountain, having been largely removed by Late Mississippian or Early Pennsylvanian erosion.

Depositional environments

Following an interval of little or no erosion in latest Devonian time, marine transgression in Early Mississippian advanced northward across New Mexico. The sedimentary record of this transgression in south-central New Mexico is the Caballero Formation, not present in the Caballo Mountains, and the Lake Valley Formation (Armstrong et al., 1979, 1980).

Deposition of the Lake Valley Formation in the vicinity of Caballo Mountains took place on a shallow-marine ramp, which was situated between a deeper-water starved basin to the south and carbonate tidal flats to the north (Meyers, 1978; Lane and DeKeyser, 1980; Raatz, 2002). The abundance of marine invertebrate fossils, particularly filter feeders, suggests a well-oxygenated, warm, shallow sea of normal salinity. The change from grainstones in the Andrecito Member to wackestones and packstones in the Alamogordo Member reflects a decrease in current energy, probably due to deepening of the water. A subsequent shoaling cycle is suggested by very fossiliferous packstones of the Nunn Member and grainstones of the Tierra Blanca Member.

Based on outcrops in the San Andres and Sacramento Mountains, east and southeast of the Caballo Mountains, Bachtel and Dorobek (1998) interpreted Mississippian stratigraphy in terms of four progradational sequences, sensu stricto Vail et al. (1977), of which only the lower two are represented in the Caballo Mountains. The lowest sequence boundary is developed south of the Caballo Mountains and is represented by the unconformable contact between the Caballero Formation and Devonian strata. Following transgressive onlap by the Caballero Formation, the Andrecito Member of the Lake Valley Formation prograded southward. The second sequence boundary is marked by the sharp and locally angular contact between the Andrecito and Alamogordo Members, the latter of which defines the transgressive systems tract. Upward-shoaling and southward progradation is represented by deposition of the overlying Nunn and Tierra Blanca Members.

The diagenetic history of the Lake Valley Formation in south-central New Mexico has been well documented by Meyers (1974, 1978) and by Meyers and Lohman (1978). Their work includes the types and origin of cements, the compaction history, and the

origin of chert. They recognized three types of calcite cement: cloudy cement of probable marine origin; clear cement of phreatic, meteoric origin; and cement with microdolomite inclusions that formed by mixing of marine and meteoric waters. Distinct zones in the latter two cements are defined on the basis of iron content, determined by cathodoluminescence.

Meyers (1980) and Meyers and Hill (1983) have also demonstrated that chemical and mechanical compaction was responsible for significant reduction in intergranular porosity. Pressure solution was the dominant mechanism of compaction, and was associated with the most poorly cemented rocks near the zone of ground-water recharge. Chert nodules developed early in the diagenetic history of the Lake Valley Formation before intense compaction and contemporaneously with calcite cementation (Meyers, 1977). The source of silica for the nodules appears to have been the dissolution of sponge spicules in contact with phreatic, meteoric ground water (Meyers, 1977; Meyers and James, 1978).

Early to middle Paleozoic paleogeography

During the early and middle Paleozoic, southern New Mexico was located near the western margin of Laurentia, a landmass that included present-day Greenland and Scotland as well as North America (Scotese, 1997). Owing to the orientation of Laurentia, the equator passed northeastward through the state, positioning southern New Mexico somewhat to the south of the equator. The southern part of the state was part of a broad epicontinental platform that extended from Arizona to central Texas (Cloud and Barnes, 1948); it sloped southward (modern direction) at very low angles from the Transcontinental Arch. A persistently emergent area, the Transcontinental Arch extended from central New Mexico northeastward (modern direction) through the midcontinent region (Ross, 1976), controlling patterns of sedimentation throughout the early and middle Paleozoic. The southern New Mexico platform was alternately flooded by shallow tropical seas and exposed to erosion.

Sloss's (1963) concept of cratonic stratigraphic sequences may be applied to the lower and middle Paleozoic rocks of southern New Mexico (Raatz, 2002). The transgressive Cambrian–Ordovician Bliss and El Paso Formations comprise part of Sloss's Sauk sequence, whereas the overlying Tippecanoe sequence includes the Ordovician Montoya Formation and Silurian Fusselman Dolomite. Sloss's (1963) Kaskaskia sequence is represented by the Devonian Percha Shale and Mississippian Lake Valley Formation. Like Sloss's sequences, each sequence in southern New Mexico is bounded by an unconformity of interregional extent, although the Montoya and Fusselman Formations are separated by an intra-sequence unconformity. The broad implication of stratigraphic sequences and their associated unconformities is that they are the products of very widespread and long-lasting flooding events on craton margins or interiors. Causes of such transgressions (and regressions) include epeirogenic subsidence and uplift and global (eustatic) sea-level changes. A debate continues over the relative importance of the two mechanisms, largely because it is difficult to distinguish between their signals in the sedimentary record (e.g. Sloss and Speed, 1974; Sleep, 1976).

Vail et al. (1977) identified global cycles of relative sea-level change through the Phanerozoic. In southern New Mexico, the age of transgressive lower Paleozoic formations correlates well with times of Vail et al. (1977) cycles of global sea-level rise, whereas the bounding unconformities correspond to intervals of relative sea-level fall (Raatz, 2002). For example, the Bliss–El Paso, Montoya, and Fusselman Formations represent transgressive units deposited during global sea-level rises in the Late Cambrian and Ordovician, Middle to Late Ordovician, and Early to Middle Silurian. The unconformities between these units represent low stands of sea level during Early Ordovician, end of Ordovician, and Late Silurian. Consequently, based on the Vail et al. (1977) global sea-level curves, the interpretation that the lower Paleozoic succession in southern New Mexico was controlled by and is a record of eustatic changes in sea level is convincing. More recent studies, however, have shown that epeirogenic movements on the continents also result in widespread and long-lasting flooding events.

The work of Bond (1978), Algeo and Seslavinsky (1995), Sahagian (1987), and Bond and Kominz (1991) has permitted a quantitative separation of eustatic and epeirogenic sea-level changes and has also shown the importance of epeirogenic in large-scale subsidence and flooding of cratonic margins and interiors. A mechanism for long-time scale, widespread subsidence of continental margins and interiors was recently proposed by Pysklywec and Mitrovica (1998). These authors showed by modeling experiments that large-scale subsidence of the lithosphere would result from the interaction of descending slabs and plumes with a phase transition at 660 km (410 mi) depth. Their results are certainly applicable to active continental margins and continental interiors and may also be applicable to the southern New Mexico platform during the lower to middle Paleozoic.

The debate over the relative importance of global versus epeirogenic sea-level changes continues, and in southern New Mexico it still is not clear whether one or both of these processes controlled the development of the lower and middle Paleozoic stratigraphic sequences. In any event, sea-level fall at the end of the Mississippian resulted in the erosional beveling of all previously deposited strata. In the Caballo Mountains area sea-level fall was accompanied by structural doming of Mississippian and older strata, deformation that may be viewed as a precursor to the more severe mountain building events that were to follow in the Pennsylvanian and Permian Periods throughout New Mexico.

Middle Mississippian–Early Pennsylvanian unconformity

The unconformity at the base of the Pennsylvanian System in the Caballo Mountains truncates older rock units ranging from Lake Valley Formation deep into the El Paso Formation. The Red House subcrop map (Fig. 17) suggests irregular erosion of a broad, northerly trending, domal uplift centered on the northern Red Hills area where the El Paso Formation was exposed before deposition of the Red House Formation. Above chert-bearing members of the Lake Valley Formation, chert breccia is associated with the unconformity and is interpreted to be related to karst topography. Elsewhere, the unconformity is a relatively planar surface free of chert breccia, but is locally distinguished by shallow channels filled with siliciclastic detritus.

Although the deformation and erosion clearly took place between middle Mississippian (Meramec) and earliest Pennsylvanian (Morrow?–Atoka ?) time, the precise age of the unconformity is uncertain. Elsewhere in southern New Mexico, important unconformities of middle Mississippian (post-Osage, pre-Meramec) age and latest Mississippian–Early Pennsylvanian (post-Chester, pre-Atoka) age have been identified (Meyers, 1974; Armstrong et al., 1979, 1980; Harbour, 1972; Seager, 1981). The unconformity in the Caballo area may represent either of these or both. For example, both may be represented if the karst topography above the Lake Valley Formation is a remnant of the older erosion surface, whereas the more extensive, truncating, karst-free parts of the unconformity represent Late Mississippian–Early Pennsylvanian erosion. Based on regional relationships depicted by Kottlowski (1975), we prefer the interpretation that the basal Pennsylvanian unconformity is essentially Late Mississippian–earliest Pennsylvanian in age throughout southern New Mexico, including the Caballo Mountains.

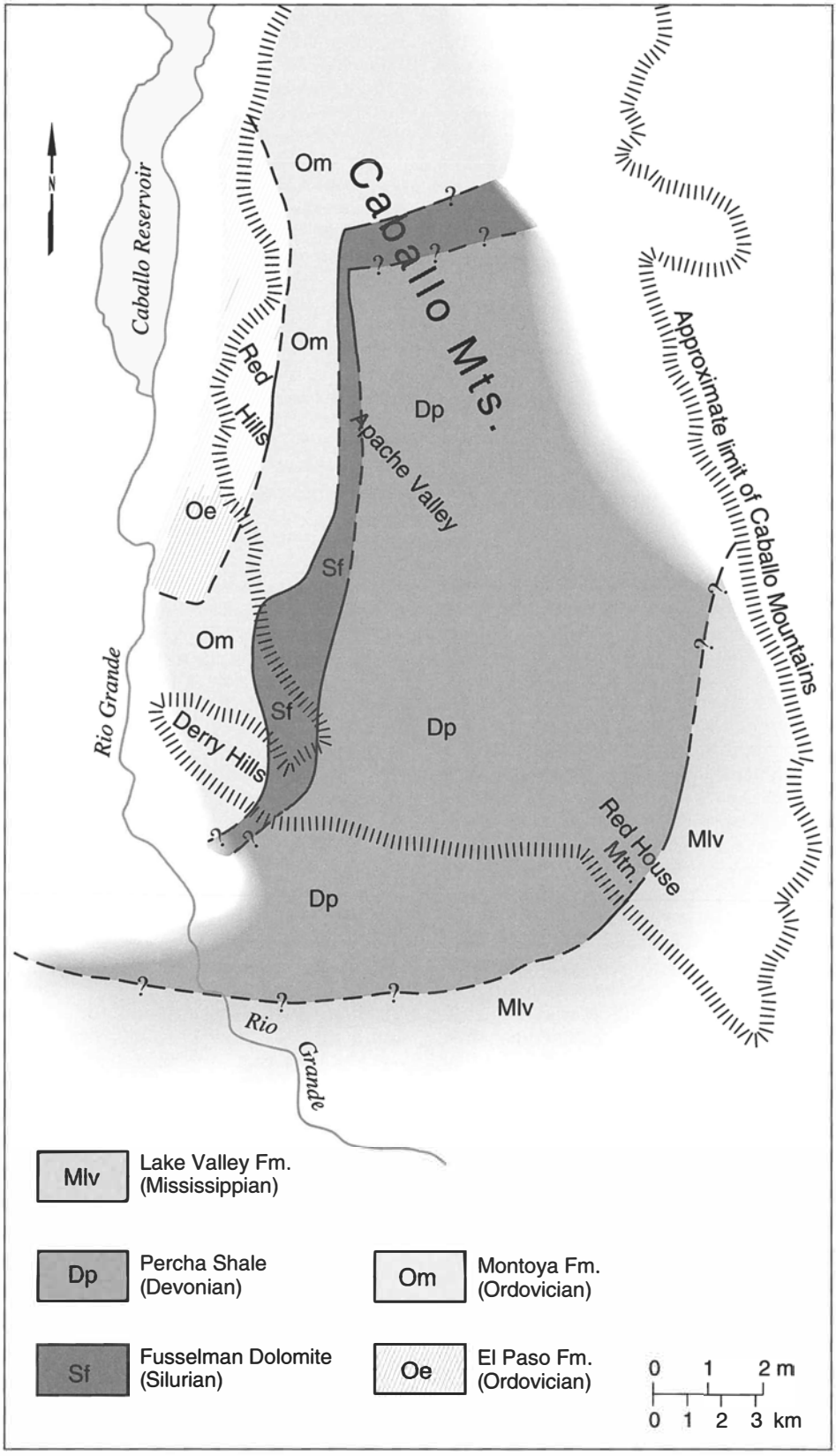

FIGURE 17—Pennsylvanian subcrop map in Caballo Mountains area.

Permian–Pennsylvanian Ancestral Rocky Mountains

Most of the state of New Mexico and large parts of adjacent states were affected by a major mountain building event in the Pennsylvanian and Permian Periods referred to as the Ancestral Rocky Mountains (Kluth and Coney, 1981; Kluth, 1986; Ye et al., 1996). This deformational event was characterized by a series of discontinuous, north- to northwest-trending uplifts, many of them cored by Precambrian crystalline basement. The uplifts were separated by rapidly subsiding intermontane basins, in which were deposited a variety of mixed marine and non-marine siliciclastic, carbonate, and evaporite rocks. The combined thickness of these strata is generally in excess of all previously deposited Paleozoic rocks. Permian–Pennsylvanian strata are unique within the Paleozoic stratigraphic succession in southern New Mexico by recording the first appearance of widespread conglomerates as well as non-marine depositional environments. In the Caballo Mountains and vicinity, Permian–Pennsylvanian strata are represented by the Pennsylvanian Red House, Nakaye, and Bar B Formations, which belong to the Magdalena Group, and by the Permian Abo and Yeso Formations. All were deposited on the western flank of the Orogrande Basin (Pray, 1959; Kottlowski, 1960; Jordan, 1975).

Magdalena Group

The Pennsylvanian System in southern New Mexico is generally referred to as the Magdalena Group, which was first defined by Gordon (1907) in the Magdalena mining district of Socorro County, New Mexico. Thompson (1942) subdivided Pennsylvanian rocks in southern New Mexico into eight groups and 15 formations, many of them with their type section in and near the Caballo Mountains. Although many of Thompson's subdivisions are locally mappable, Kelley and Silver (1952) chose instead to divide the Magdalena Group in the Caballo Mountains into three mappable formations, which in ascending order are the Red House, Nakaye, and Bar B. These three formations were measured as part of this study in a continuous exposure between Green Canyon and Red Hill Tank (SW¼ sec. 10 and NW¼ sec. 15 T17S R4W). In addition, Kalesky (1988) measured nine sections of the Red House Formation, Singleton (1990) measured five sections of the Bar B Formation, and Soreghan (1992a) measured one section of the uppermost Nakaye and Bar B Formations.

Kues (2001) recently proposed revision of Pennsylvanian rock-stratigraphic terminology in New Mexico. He recommended: (1) abandonment of the Magdalena as a formal stratigraphic name; (2) elevation of the Madera Formation of northern New Mexico to group status, treating its existing members as formations; and (3) extension of Madera Group terminology into southern New Mexico, including the Caballo Mountains. In this report we have maintained the original stratigraphic terminology of Kelley and Silver (1952), because these names appear on geologic maps and in the literature.

Studies of fusulinids by Thompson (1942, 1948) and King (1973) indicate that the base of the Red House Formation in the Derry Hills is Atokan in age. However, analyses of brachiopods by Sutherland and Manger (1984) and foraminifera by Groves (1986) and Clopine (1992) in the same Derry Hills section suggest that the base of the Red House may span the Morrowan–Atokan boundary. The Atokan–Desmoinesian boundary is very close to or coincident with the Red House–Nakaye contact (Kottlowski, 1960). Fusulinid biostratigraphy by Soreghan (1992a) defined 75 m (246 ft) of Missourian and 109 m (358 ft) of Virgilian strata in the Bar B Formation in the McLeod Hills. A study of fusulinids in the Derry Hills and McLeod Hills by Thompson (1991) suggests that the Bar B–Nakaye contact is mid-Desmoinesian. Thompson (1991) also determined that the Bar B in the McLeod Hills consists of approximately 70 m (230 ft) of Missourian strata, 30 m (98 ft) of Virgilian strata, and 115 m (377 ft) of lowermost Permian (Wolfcampian) strata, whereas the Bar B in the Derry Hills has 35 m (115 ft) of Desmoinesian, 54.5 m (179 ft) of Missourian, no Virgilian, and 3.5 m (11.5 ft) of Wolfcampian strata. These data indicate a significant but obscure unconformity within the Bar B Formation in the Derry Hills.

The Magdalena Group has a disconformable lower contact and a conformable upper contact. The Red House Formation in the Caballo Mountains disconformably overlies rocks ranging in age from the Mississippian Lake Valley Formation to the Ordovician El Paso Formation. The Red House Formation is primarily a slope former and stands in sharp contrast to the stair-stepped cliffs of the overlying Nakaye Formation. The contact between the Red House and Nakaye Formations was chosen at the base of a prominent cliff of thick, > 4 m (>13 ft), limestone with dark, ribbony chert nodules. At the site of the measured section, the contact was easily delineated, although there are several thin beds of cherty limestone below the contact. It is conceivable, however, that in other exposures the natural topographic break between the Red House and Nakaye Formations could be at a stratigraphically different level than the one selected for the measured section.

The contact between the Nakaye and Bar B Formations is placed at the base of a distinctive micrite limestone, whose light-tan color on the weathered surface and thin, platy bedding contrast markedly with the gray, medium- to thick-bedded, blocky limestones of the Nakaye Formation. Above this contact, shale occupies a greater proportion of the section.

The upper contact of the Bar B Formation with overlying red beds of the Abo Formation was placed by Kelley and Silver (1952) at the top of the uppermost marine limestone. Unfortunately, there are several limestone beds near the contact that are unfossiliferous or contain small, unidentifiable allochems that could be fossils, making the criterion of Kelley and Silver (1952) difficult to apply. Although we generally chose the top of the highest limestone bed as the Bar B–Abo contact, a prominent limestone bed occurs within the Abo in the Derry Hills area. In some places in southern New Mexico, the transition between the Magdalena Group and Abo Formation is characterized by as much as 100 m (328 ft) of interbedded conglomerate, red shale, dolomite, and limestone known as the Bursum Formation (Kottlowski, 1963). The Bursum spans the Virgilian–Wolfcampian boundary and may become younger southward (Kottlowski, 1963). Although the Bursum was not selected as a map unit in this study, it is clear that the upper 50–100 m (164–328 ft) of conglomerate, red shale, and dolomite in the Bar B Formation are correlative with the Bursum, particularly since Thompson (1991) established a Wolfcampian age for this part of the formation in the McLeod Hills.

Thickness of the three formations of the Magdalena Group vary considerably within the Caballo Mountains and vicinity. Kalesky (1988) demonstrated that the Red House Formation varies from 35 to 86 m (115 to 282 ft) thick, generally increasing to the east and north. Similarly, the Nakaye Formation increases in thickness from 140 m (459 ft) at the Derry Hills to 200 m (656 ft) in the McLeod Hills. The Bar B Formation shows a similar trend, increasing from 93 m (305 ft) at the Derry Hills to 206 m (676 ft) in the McLeod Hills, according to Singleton (1990). However, our measured sections indicate the Bar B Formation is approximately 280 m (918 ft) thick on the eastern flank of the range. The difference in thickness determined by Singleton (1990) and ourselves is probably a result of different choices in upper and lower contacts. The eastward thickening of the Magdalena Group continues into Hembrillo Canyon in the San Andres Mountains, where it is 933 m (3,060 ft) thick (Kottlowski et al., 1956).

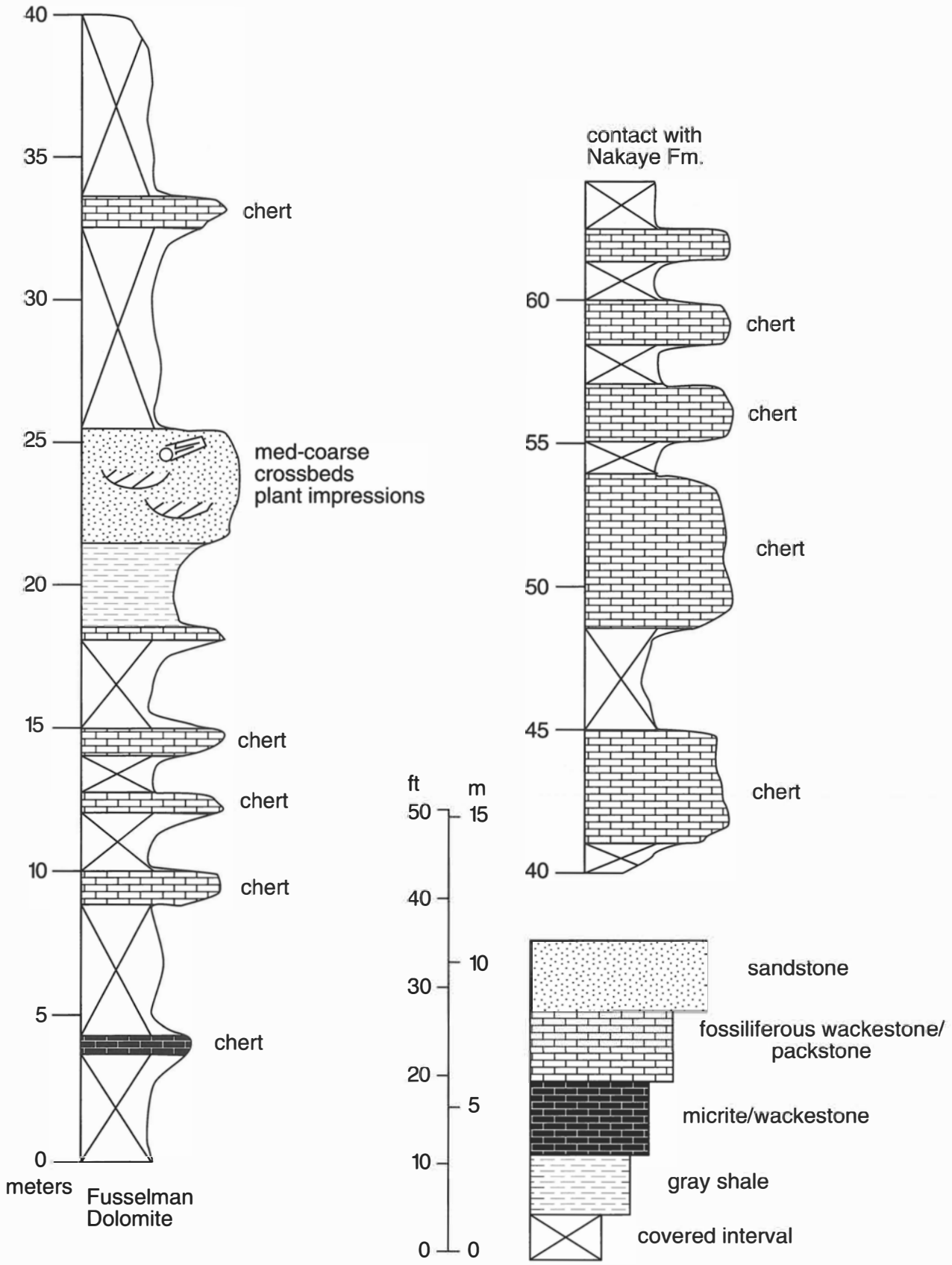

FIGURE 18—Measured section of the Red House Formation of the Magdalena Group (Pennsylvanian) between Green Canyon and Red Hill Tank (SW¼ sec. 10 T17S R4W). Upper part of sandstone at 25 m (82 ft) contains twig impressions.

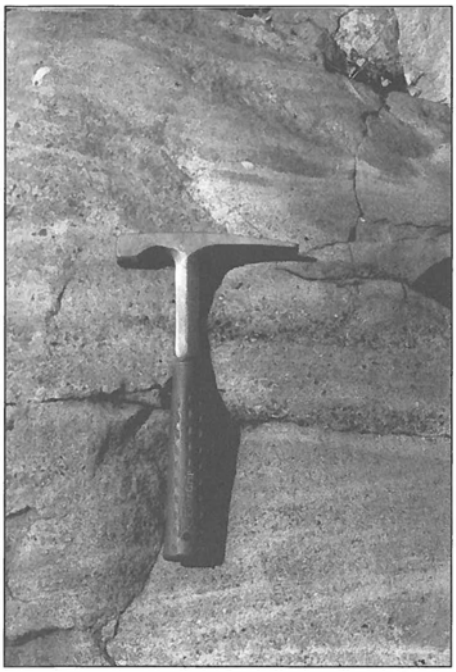

FIGURE 19—Crossbedded, granular, medium- to coarse-grained sandstone near the middle of the Red House Formation (Pennsylvanian) at Nakaye Mountain. Hammer is 25 cm (9.8 in) long.

FIGURE 20—Characteristic stair-step bedding of the Nakaye Formation (Pennsylvanian) at the north end of the Red Hills.

Red House Formation

Description

The Red House Formation consists primarily of fossiliferous packstone and gray or green shale, the latter commonly manifested as covered intervals (Fig. 18). The fossiliferous packstones are gray or mottled gray and tan, and range from 1 to 7 m (3.3 to 23 ft) thick. Bioturbation within the packstones is common and the body fossils consist of brachiopods, echinoderm columnals, bryozoans, corals, ostracods, and foraminifera, including fusulinids. Gray or black chert is also common, but not as abundant as in the overlying Nakaye Formation. Less common types of limestones in the Red House Formation are poorly fossiliferous wackestone and bioclastic-intraclastic grainstone.

Many sections of the Red House Formation in the Caballo Mountains have a basal sandstone and/or chert-pebble conglomerate up to 3 m (9.8 ft) thick (Kalesky, 1988), although this was not observed at the measured section (Fig. 18). Another prominent sandstone or calcareous siltstone is present in the middle of the formation and was used by Kalesky (1988) as a marker horizon. The middle sandstone coarsens upward from medium sand to coarse sand, granules, or pebbles, and displays trough and planar crossbeds, vertical burrows, symmetrical ripple marks, and plant impressions (Fig. 19). Paleocurrents at the measured section and elsewhere in the range (Kalesky, 1988) are unimodal to the southeast. The least common siliciclastic facies is thin (few cm) red siltstone that overlies gray shale or limestone.

Depositional environments

The Red House Formation in the Caballo Mountains was largely deposited on a shallow-marine shelf. Shallow, normal marine conditions are suggested by the diverse invertebrate fauna, particularly the abundance of filter feeders, in the fossiliferous limestones. Occasionally the environment shoaled enough to produce grainstones, but this was rare. However, more restricted marine conditions are suggested by the poorly fossiliferous wackestones and black shale, the latter being deposited on a poorly oxygenated sea floor. During rare retreats of the sea the region was sub-aerially exposed, resulting in deposition of thin, red siltstones (Kalesky, 1988).

The lateral discontinuity of the basal sandstone/conglomerate implies it was deposited in paleovalleys, either by fluvial backfilling during transgression or in a paralic environment. The middle sandstone is interpreted by Kalesky (1988) to represent offshore marine bars, because of a sharp basal contact, upward coarsening, and numerous erosional discontinuities between the crossbeds. Thickening of the middle sandstone to the northwest suggests derivation from that direction, and southeast-directed paleocurrents may reflect the dominant direction of geostrophic storm currents (Kalesky, 1988).

Nakaye Formation

Description

The Nakaye Formation is characterized by ledges of limestone 1–15 m (3.3–49 ft) thick separated by thinner covered slopes, imparting a distinctive stair-step topographic profile (Figs. 20, 21). Locally in steep gullies, the covered intervals can be seen to consist of gray shale. The most common limestones are gray, bioturbated, fossiliferous packstones, which contain whole and broken brachiopods, bryozoans, echinoderm columnals, fusulinids and other foraminifera, corals, gastropods, and phylloid algae (Fig. 22). In some beds the replacement of burrows by dolomite result in gray and tan mottling. Dark-gray or black chert is very common in the fossiliferous limestones. Gray grainstones are less common and are composed either of intraclasts and bioclasts or ooids (Fig. 21).

Depositional environments

Open-marine deposition of limestone was the dominant process for the Nakaye Formation. Deposition below normal wave base in warm, well-oxygenated marine water is indicated by the abundance of bioturbated packstones with a diverse, filter-feeding marine fauna. Rarely, higher energy periods due to storms or shoaling are indicated by the bioclastic and oolitic grainstones. Because of poor exposure, there is little evidence on the origin of the gray shales. They most probably represent deeper, less oxygenated water than that which deposited the fossiliferous packstones. Alternatively, the gray shales may represent deposits in bays or lagoons.

Bar B Formation

Description

The Bar B Formation consists of interbedded limestone, dolomite, shale, and conglomerate. Shale generally exists as covered intervals and is far more common in the Bar B Formation than in the underlying Nakaye Formation. The shale is dark gray, but locally displays a purplish-gray color. A few of the shales in the upper

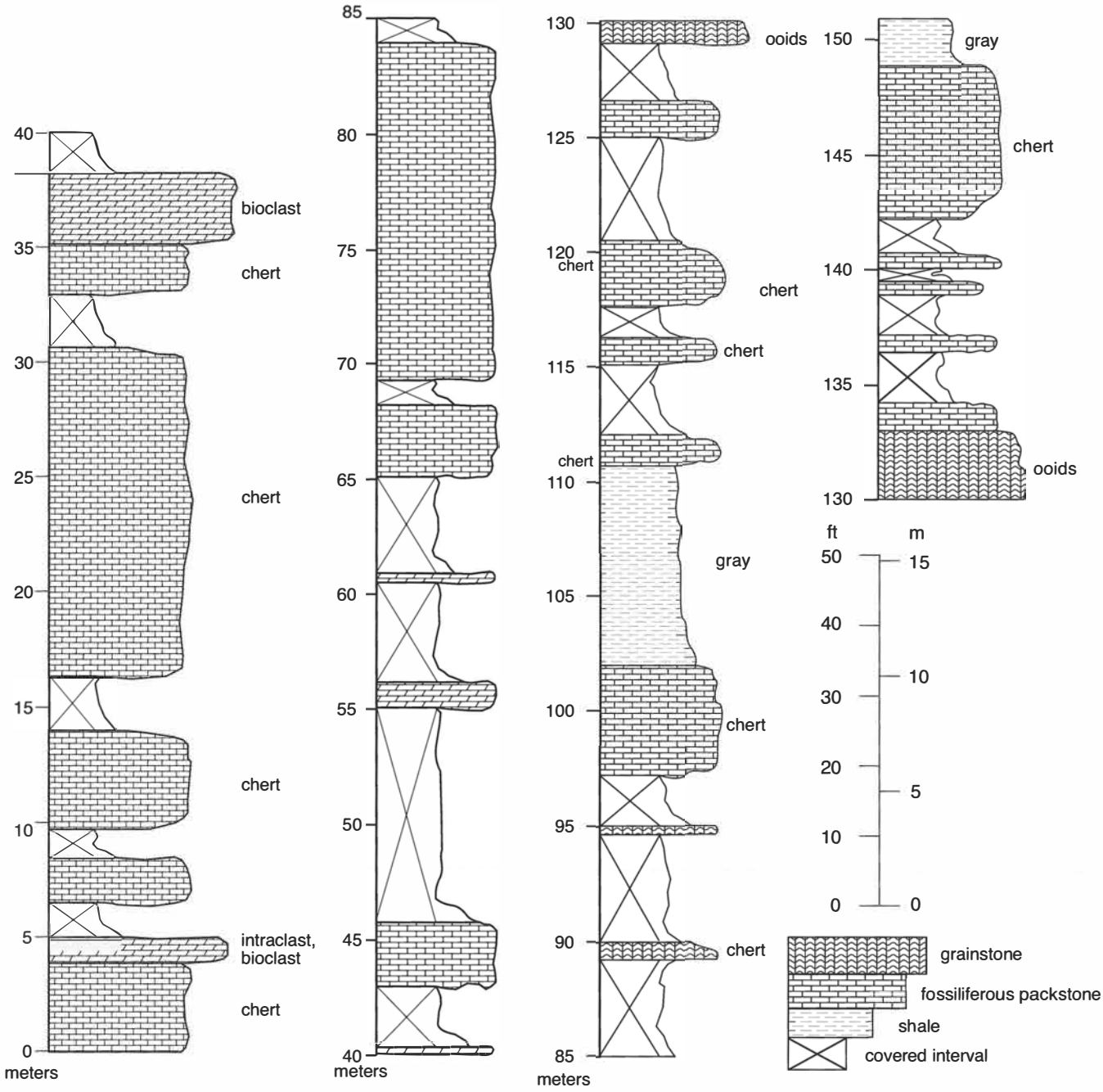

FIGURE 21—Measured section of the Nakaye Formation (Pennsylvanian) between Green Canyon and Red Hill Tank (NW¼ sec. 15 T17S R4W).

part of the formation in the McLeod Hills are red and have calcic nodules. Limestone beds form gray and tan ledges ranging from 1 to 5 m (3.3 to 16 ft) thick. Over half of the limestones are tan-weathering or tan and gray mottled micrites or dolomicrites with few or no allochems, although ostracods or gastropods may be locally present. Bed tops of some of the dolomicrites are brecciated with red shale or siltstone between the clasts. In addition, the Bar B has gray and gray and tan mottled, fossiliferous packstones and grainstones similar to those in the Nakaye Formation. Tan dolomites less than 1 m (3.3 ft) thick are most common in the upper part of the formation in the McLeod Hills.

Conglomerates are generally present in the uppermost part of the Bar B Formation. Only one conglomerate is present at the measured section (Fig. 23), but there are three in the Derry Hills and a dozen in the McLeod Hills (Singleton, 1990). The conglomerates range in thickness from 0.5 to 3 m (1.6 to 9.8 ft) and are composed of pebbles and small cobbles of limestone, dolomite, and chert. The matrix is sandy and may contain marine fossils, including fusulinids (Thompson, 1991). Fusulinids in the clasts suggest they were derived from Desmoinesian and Missourian limestones (Thompson, 1991).

Depositional environments

A change to more restricted marine conditions occurred during deposition of the Bar B Formation, as indicated by the abundance of dark-gray shales and dolomicrites. Moreover, red shales and brecciation of the dolomicrites suggest periodic sub-aerial exposure, and some of the dolomites in the eastern part of the range contain wavy laminae and fenestral fabric indicative of deposition in an intertidal or supratidal setting. However, open-

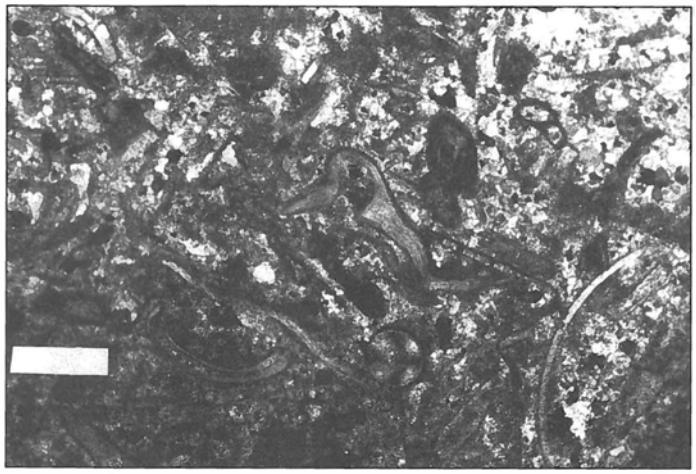

FIGURE 22—Photomicrograph of partially recrystallized, fossiliferous packstone of the Nakaye Formation (Pennsylvanian). Bar scale is 0.25 mm (0.1 in) long.

marine deposition is also indicated by fossiliferous packstones and grainstones.

In her regional study of Missourian and Virgilian strata of the Pedregosa and Orogrande Basins, Soreghan (1992a, 1994) recognized 24 upward-shoaling cycles in each of seven stratigraphic sections, including one in the Caballo Mountains. She argued that this cyclicity is glacial-eustatic in origin, because (1) several cycles are capped by emergence features that indicate base-level dropped sufficiently to force sea level to fall below the level of subtidal sediment, (2) the number of cycles are the same within and between the basins, which argues for a regional control, and (3) the apparent cycle frequency, determined by dividing the number of cycles by the duration of the Missourian and Virgilian ages, is approximately 400 kyrs/cycle, which is consistent with the longer-term orbital eccentricity Milankovitch cycle. Because Gondwanan continental glaciation occurred from Late Mississippian through most of the Permian (Crowell, 1978; Caputo and Crowell, 1985; Frakes et al., 1992, p. 38), it is likely that glacial eustacy affected sedimentation throughout the entire Magdalena Group, not just within the Bar B Formation.

Limestone-clast conglomerates in the upper part of the Bar B Formation have important implications for Late Pennsylvanian and Early Permian tectonism in the vicinity of the Caballo Mountains. Singleton (1990) and Lawton et al. (2002) demonstrated that Virgilian and Early Permian conglomerates are concentrated in the vicinity of the Caballo Mountains and are associated with unconformities within the Magdalena Group. They believe that the Bar B conglomerates were locally derived and that uplift occurred along the western margin of the Orogrande Basin, although the origin of the uplift is not known.

Abo Formation

Named by Lee and Girty (1909) for exposures in Abo Canyon in the Manzano Mountains, red beds of the Abo Formation constitute the most distinctive map unit in south-central New Mexico. The Abo Formation interfingers southward with limestones and gray shales of the Hueco Formation and pinches out as a map unit south of Las Cruces (Kottlowski, 1963, 1965; Jordan, 1975; Mack and James, 1986). The Abo Formation is well exposed near the Derry Hills, in Apache graben, and along the eastern flank of the range (Fig. 4).

The Abo Formation is considered to be Wolfcampian (Early Permian) in age, based on vertebrate fossils (Langston, 1953; Romer, 1960; Berman and Reisz, 1980) and because of the interfingering of the Abo with fusulinid-bearing limestones of the Hueco Formation (Thompson, 1954). In the Robledo Mountains near Las Cruces, the Abo Tongue of the Hueco Formation is late Wolfcampian in age (Kues, 1995; Kietzke and Lucas, 1995; Kozur and LeMone, 1995). However, plant fossils collected north of the Caballo Mountains suggest the Abo is both Wolfcampian and early Leonardian in age (Read and Mamay, 1964; Hunt, 1983). Vertebrate and plant fossils are sparse in the Abo and have not been studied in the detail required to provide convincing regional correlations.

In the Caballo Mountains, the conformable contact between the Abo Formation and underlying Bar B Formation is generally placed at the top of the highest limestone bed in the Bar B Formation, although locally in the Derry Hills area, thin limestone beds are present in the basal parts of typical Abo red beds. The conformable contact between the Abo and overlying Yeso Formation is marked by the change from brick-red shale and siltstone of the Abo to orange and light-green sandstone of the Meseta Blanca Sandstone Member of the Yeso Formation. Thickening eastward within the Caballo Mountains, the Abo Formation is 141 m (463 ft) thick in Apache graben (NE¼ sec. 1 T17S R4W) and 305 m (1,000 ft) thick at Bob's Tank (NW¼ sec. 28 T16S R3W).

Description

The Abo Formation in the Caballo Mountains is composed of four rock types, although all four are not necessarily present at each exposure (Fig. 24). The most abundant rock type is red shale/mudstone, which generally forms covered slopes, but can be observed in steep gullies and cut banks of major arroyos. The red mudstone has a blocky texture and commonly displays slickensides and meter-scale, concave-upward fractures (Fig. 25). Calcic nodules 1–6 cm (0.5–2.4 in) in diameter or thin, < 1 m (< 3.3 ft), subhorizontal sheets of carbonate are also present in some beds (Fig. 26). A minor amount of the shale is green or displays green and red mottling.

Also common in the Abo Formation are ledges of red, brown, or tan siltstone or very fine sandstone (Fig. 27). A majority of the beds are thin, <1m (<3.3 ft), and have symmetrical ripple cross laminae or horizontal laminae in the lower part, whereas the upper part may have dessication cracks, burrows, root traces, plant impressions, vertebrate and insect tracks, and calcic nodules. A few thin, <1 m (<3.3 ft), siltstone beds, particularly in the upper part of the formation, are massive in appearance with the exception of a few burrows in the upper few centimeters. The thickest siltstone beds, which range from 3 to 7 m (10 to 23 ft), exist as broad sheets (width/depth >15) or narrow ribbons. In addition to the structures listed above, the thickest beds may have small-scale trough crossbeds (Fig. 28) and low-angle erosion surfaces mantled by rip-up-clast pebble conglomerate. The sheet sandstone/siltstones also commonly display lateral accretion sets.

Much less common than red shale and siltstone are thin, < 0.5 m (< 1.6 ft), beds of rip-up-clast conglomerate, which are most common in the lower part of the formation. The conglomerates are composed entirely of granule- and pebble-sized intraformational clasts of shale, siltstone, and carbonate. The conglomerates occupy broad, shallow channels and are usually devoid of sedimentary structures, although small-scale trough crossbeds are locally present.

The least common rock type in the Abo Formation is limestone or dolostone. The thickest, 2 m (6.6 ft), is exposed in the Derry Hills and consists of micrite with a few scattered ostracods. The other limestones and dolostones are about 0.5 m (1.6 ft) thick and pinch out laterally within a few tens of meters. Unfossiliferous, these thinner limestones and dolostones commonly are brecciated, especially in the upper part.

Depositional environments

The Abo Formation in the Caballo Mountains was deposited on a broad alluvial plain traversed by high sinuosity streams. The

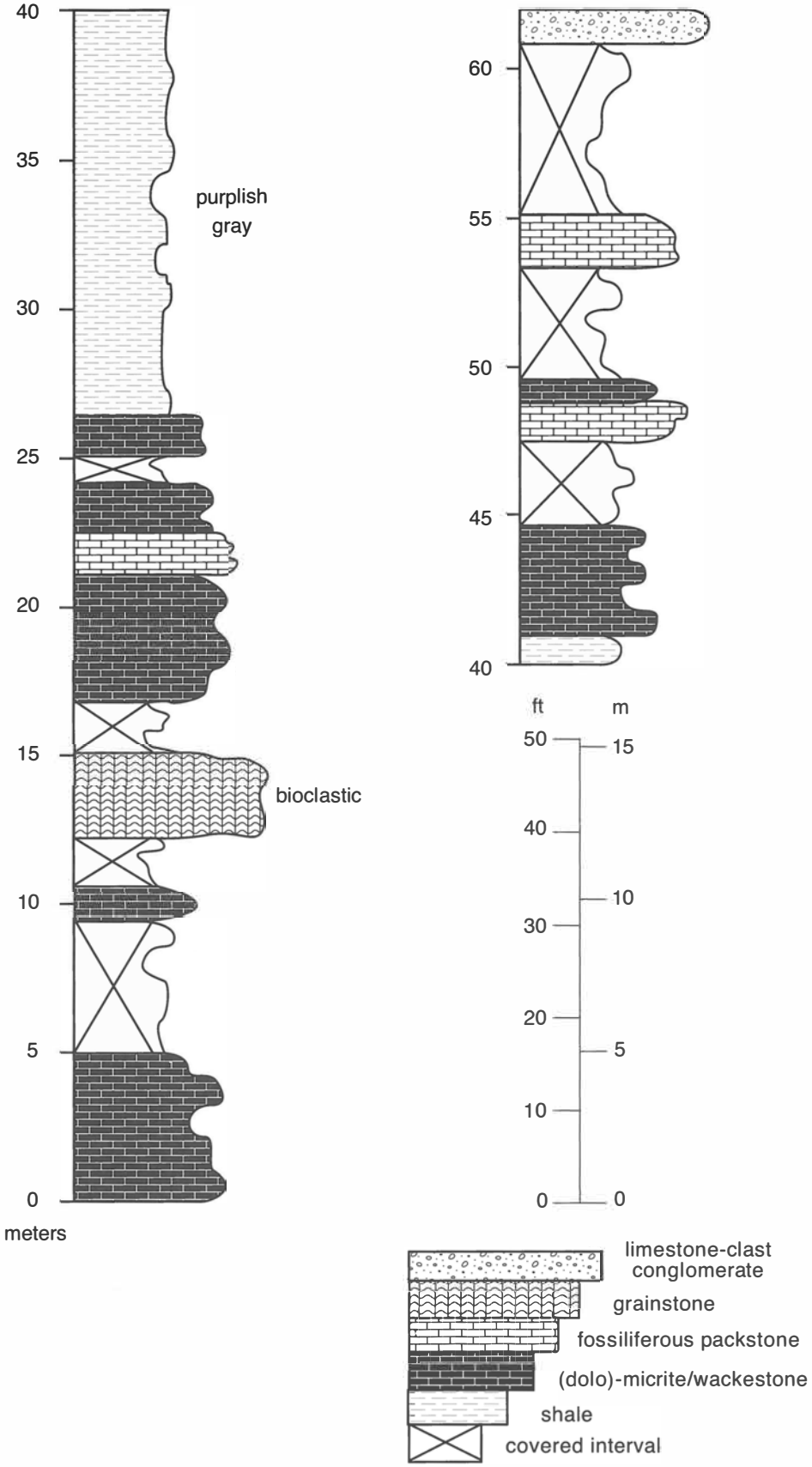

FIGURE 23—Measured section of the Bar B Formation (Pennsylvanian) between Green Canyon and Red Hill Tank (NW¼ sec. 15 T17S R4W).

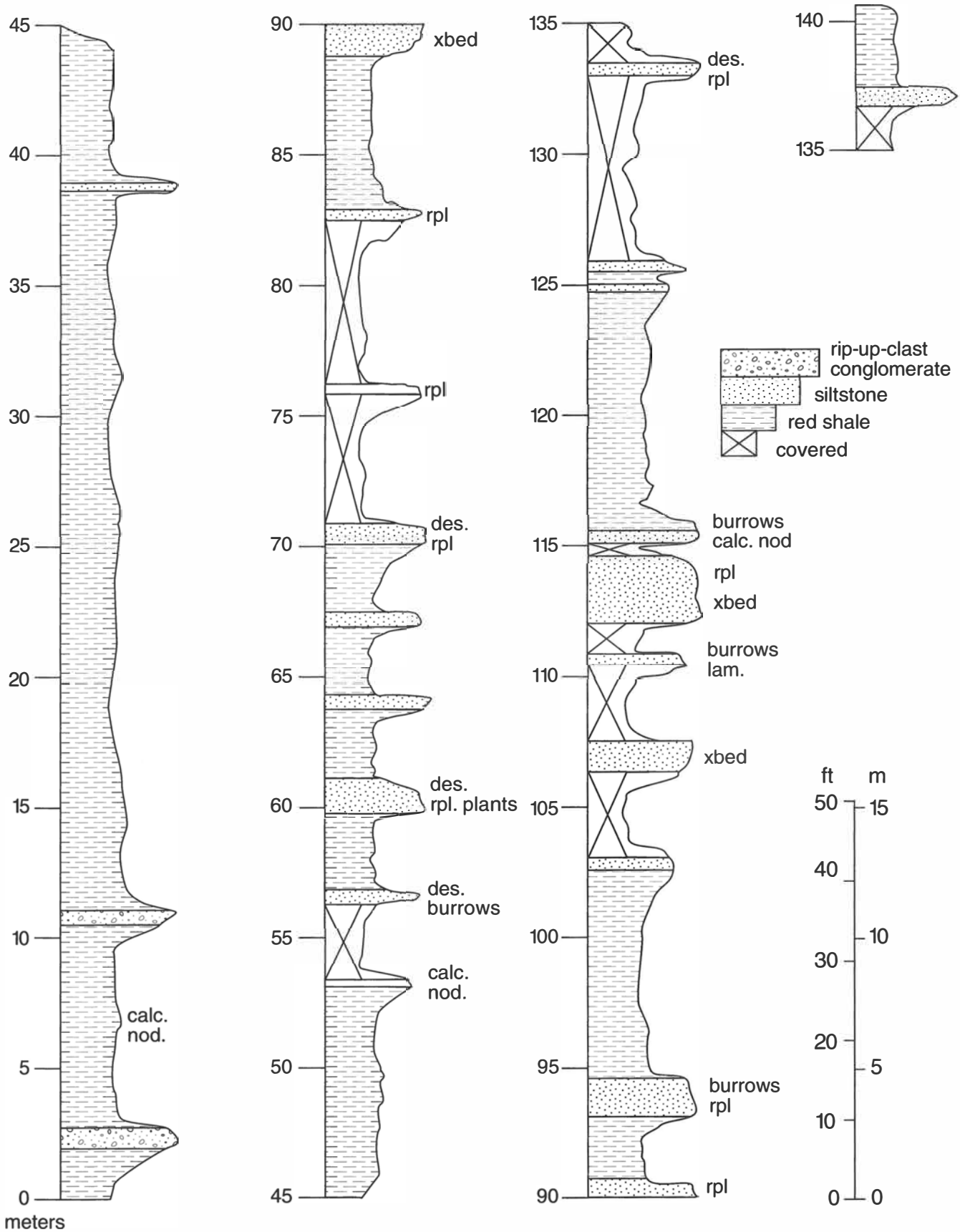

FIGURE 24—Measured section of the Abo Formation (Permian) northwest of Hidden Tank (SW¼ sec. 31 T16S R3W). calc. nod. = calcic nodules; rpl = ripples; xbed = crossbeds; des. = desiccation cracks; lam. = laminae.

FIGURE 25—Low-angle, concave-upward fractures referred to as wedge-shaped peds in floodplain red mudstone of the Permian Abo Formation near Bob's Tank on the eastern side of the range. Wedge-shaped peds are soil features produced by shrinking and swelling of expandable clays. Hammer is 25 cm (9.8 in) long.

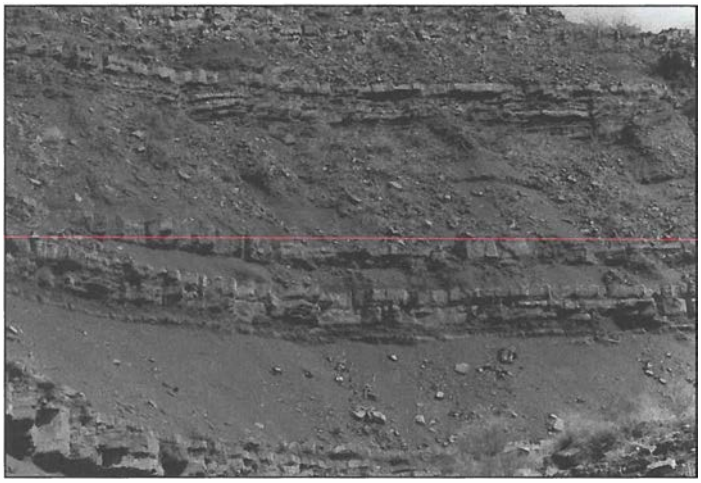

FIGURE 27—Ledges of thin-bedded siltstone deposited as crevasse splays interbedded with slope-forming floodplain red mudstones of the Permian Abo Formation near Bob's Tank in the eastern part of the range.

FIGURE 26—Calcic nodules and tubules in blocky red floodplain mudstone of the Permian Abo Formation near Bob's Tank in the eastern side of the range. Hammer is 25 cm (9.8 in) long.

FIGURE 28—Three-meter- (20-ft-) thick siltstone channel in the Permian Abo Formation displaying a lateral accretion set that resulted from point bar deposition. View is to the north at Yoast Draw. Channel flowed south and point bar grew westward.

Abo fluvial system was characterized by widely dispersed silt-bed or very fine sand-bed rivers, broad, well-oxidized floodplains, and evidence in both the channel and floodplain strata for marked seasonality of paleoclimate. These characteristics were strongly influenced by the overall dry and megamonsoonal climate postulated for Pangea in Early Permian time (Parrish et al., 1982; Crowley et al., 1989; Kutzbach and Gallimore, 1989).

The larger trunk streams deposited siltstone to very fine sandstone sheets from 3 to 7 m (9.8 to 23 ft) thick and hundreds of meters wide. These ledge-forming intervals hold up the Abo ridges, but overall are few in number in any given measured section. Both single story and multistory channels are present with the erosional base of the stories locally mantled by a thin, < 0.5 m (< 1.6 ft), lag of rip-up-clast conglomerate. The larger channels exhibit lateral accretion sets that dip either to the east or west and indicate paleoflow of the sinuous channels to the south, the direction of regional paleoslope (Figs. 28, 29; Mack et al., 1995, in press). The most abundant sedimentary structures in the channels are asymmetrical ripple cross-laminae, although trough crossbeds and horizontal laminae are present in some cases. The fact that flume studies show that ripples are stable over a very large range of velocity/shear stress for silt-sized sediment may explain, in part, the abundance of ripple cross-laminae in the Abo channels (cf. Harms et al., 1975). In many cases the upper surfaces of the lateral accretion sets are modified by bioturbation, root traces, desiccation cracks, and/or calcic nodules, suggesting that lateral growth of the point bar was periodically interrupted by sub-aerial exposure. Moreover, a few of the large channels may have been influenced by tidal currents, as suggested by mud drapes and an abundance of vertical burrows resembling those of *Skolithos* (Mack et al., 1995, in press).

In addition to the laterally accreting, sinuous channels, the Abo alluvial plain also contained symmetrical, ribbon channels that infilled vertically. These channels may represent straight to slightly sinuous tributaries of the major trunk streams and/or channels created by the initial stage of avulsion of a major sinuous channel (Mack et al., 1995, in press).

The least common type of Abo channel consists of broad shallow channels infilled with rip-up-clast pebble conglomerate. Generally less than 0.5 m (1.6 ft), thick and traceable for only a few tens of meters laterally, these channels were probably isolated on the floodplain and were not connected to larger, more perennial streams.

FIGURE 29—Siltstone channel of the Abo Formation infilled with a lateral accretion set. View is to the east, near Bob's Tank in the eastern part of the range.

Sedimentation on the floodplain of the Abo fluvial system was primarily by deposition of mud from suspension, but also included crevasse splays, carbonate-precipitating lakes, and eolian processes. Overbank deposits of red shale and mudstone dominate the Abo sections. The mudstone has a blocky texture and commonly displays slickensides and concave-upward fractures interpreted to be wedge-shaped peds (cf. Gustavson, 1991). The latter two features are indicative of vertic soils, in which the dominant process is shrinking and swelling of expandable clays, a process enhanced by strongly seasonal precipitation. Some Abo mudstones also contain calcic nodules and tubules from 2 to 6 cm (0.8 to 2.4 in) in diameter, which are interpreted to be pedogenic, because (1) the calcite is microcrystalline, similar to that of modern soil carbonate, (2) the tubules are oriented perpendicular to bedding and commonly taper downward, indicative of rhizoliths (Klappa, 1980), and (3) the parent sediment displays other pedogenic features, such as peds, root traces, and clay coats (argillans) lining peds, voids, and planes (Sherry, 1990; Mack et al., 1995, in press). The majority of calcic paleosols in the Abo consist of discrete nodules and tubules and correspond to stage II morphology calcic soils, although locally massive beds up to a meter thick may represent stage III morphology (cf. Gile et al., 1966). Carbonate is also present within the red mudstone as subhorizontal sheets or ribbons with sharp upper and lower boundaries, which may represent shallow ground water calcrete (cf. Pimental et al., 1996). Locally, the floodplain shale and mudstone is mottled red and green, suggesting alternating oxidizing and reducing conditions related to a fluctuating water table. The abundance of overbank shale and mudstone in the Abo Formation implies that the floodplains were stable for long periods of time between incursions by major trunk streams.

Interbedded with floodplain shale are thin, 0.3–1 m (1–3.3 ft), laterally extensive beds of ledge-forming red siltstone interpreted to have been deposited as crevasse splays. The lower part of these beds displays ripple cross-laminae and horizontal laminae, while the upper part is modified by desiccation cracks, root traces, burrows, and/or calcic nodules. The crevasse-splay beds may exist singly, or in vertical packages of two to five beds separated by a few centimeters or tens of centimeters of shale. Because the beds commonly thicken upward, the stacked crevasse-splays are interpreted to represent progradation of crevasse-splay wedges into low areas of the floodplain (Fig. 27).

The Abo floodplains were intermittently occupied, particularly during deposition of the lower part of the formation, by shallow, carbonate-precipitating lakes, represented by thin limestones and dolostones. These lakes periodically desiccated, resulting in brecciation and the addition of red silt and clay to the matrix. The inability to correlate the lacustrine limestones between closely spaced sections suggests they were small in size.

The uppermost part of the Abo Formation locally contains thin, < 1 m (< 3.3 ft), siltstone beds that lack any evidence of current-generated sedimentary structures, although the tops of the beds may be heavily bioturbated. These beds resemble the loessites described in Permian–Pennsylvanian red beds in the Eagle Basin of northwestern Colorado (Johnson, 1989). Preservation of eolian silt on the floodplain during the end of Abo deposition was a precursor to widespread eolian sedimentation of the basal member of the overlying Yeso Formation. Moreover, Soreghan (1992b) suggests that marine siltstones in the Permian–Pennsylvanian Pedregosa Basin of southeastern Arizona and southwestern New Mexico represent eolian dust that spread southward from the dune fields of the Colorado Plateau. Perhaps the predominance of silt-sized bedload in the Abo channels is related to fluvial reworking of eolian silt, initially deposited on the floodplain or that mantled catchments in the Ancestral Rocky Mountains (Mack et al., in press).

Yeso Formation

The Permian Yeso Formation was named by Lee and Girty (1909) for exposures at Mesa del Yeso, located about 19 km (12 mi) northeast of Socorro, New Mexico. Based on exposures near Rhodes Pass in the San Andres Mountains, Wilpolt and Wanek (1951) divided the Yeso into four members. Four members are also recognizable in the Caballo Mountains, but only the basal Meseta Blanca Sandstone Member is similar enough to the rocks in Rhodes Canyon to warrant use of the names of Wilpolt and Wanek (1951). The other three members of the Yeso Formation in the Caballo Mountains are, in ascending order, red siltstone-dolomite, limestone, and sandstone-limestone members (Mack and Suguio, 1991). The lower two members are mapped as a single unit (lower Yeso), as are the upper two members (upper Yeso). The Meseta Blanca Sandstone Member was measured near Broken House Tank in the McLeod Tank quadrangle, whereas the other three members were measured near Hidden Tank in the McLeod Tank quadrangle, and along the eastern flank of the range in the northeasternmost part of the McLeod Tank quadrangle and eastern part of the Apache Gap quadrangle (Fig. 2).

The Yeso Formation is Leonardian in age (Kottlowski, 1963) and is probably coeval to parts of the Colina and Epitaph Formations of southwestern New Mexico and southeastern Arizona and to the Schnebly Hill Formation in northeastern Arizona (Blakey, 1990; Soreghan, 1992a, 1994). In the Caballo Mountains, the conformable contact between the Yeso and underlying Abo Formations is placed at the change from brick-red shale and siltstone of the Abo to orange and green siltstones and sandstones of the Yeso. The Yeso Formation is unconformably overlain by the Cretaceous Dakota Sandstone, although there are places within the range where the Yeso and Upper Cretaceous rocks were completely removed by Laramide erosion.

Kelley and Silver (1952) mapped the limestone and sandstone-limestone members of this report as the San Andres Formation. In the northern Caballo Mountains, Lozinsky (1986) restricted the Yeso Formation to the Meseta Blanca Sandstone Member of this report and designated overlying limestones, dolomites, and sandstones as the San Andres Formation. These interpretations require dramatic thickness and lithologic variations in the Yeso between the San Andres and Caballo Mountains and between the Fra Cristobal and Caballo Mountains, or a significant unconformity between the Yeso and San Andres Formations. Because the Yeso described in this report is similar in thickness and rock types to the Yeso in the San Andres Mountains, we argue that the San Andres Formation is not present in the Caballo Mountains, and that those strata previously mapped as San Andres belong to the Yeso Formation.

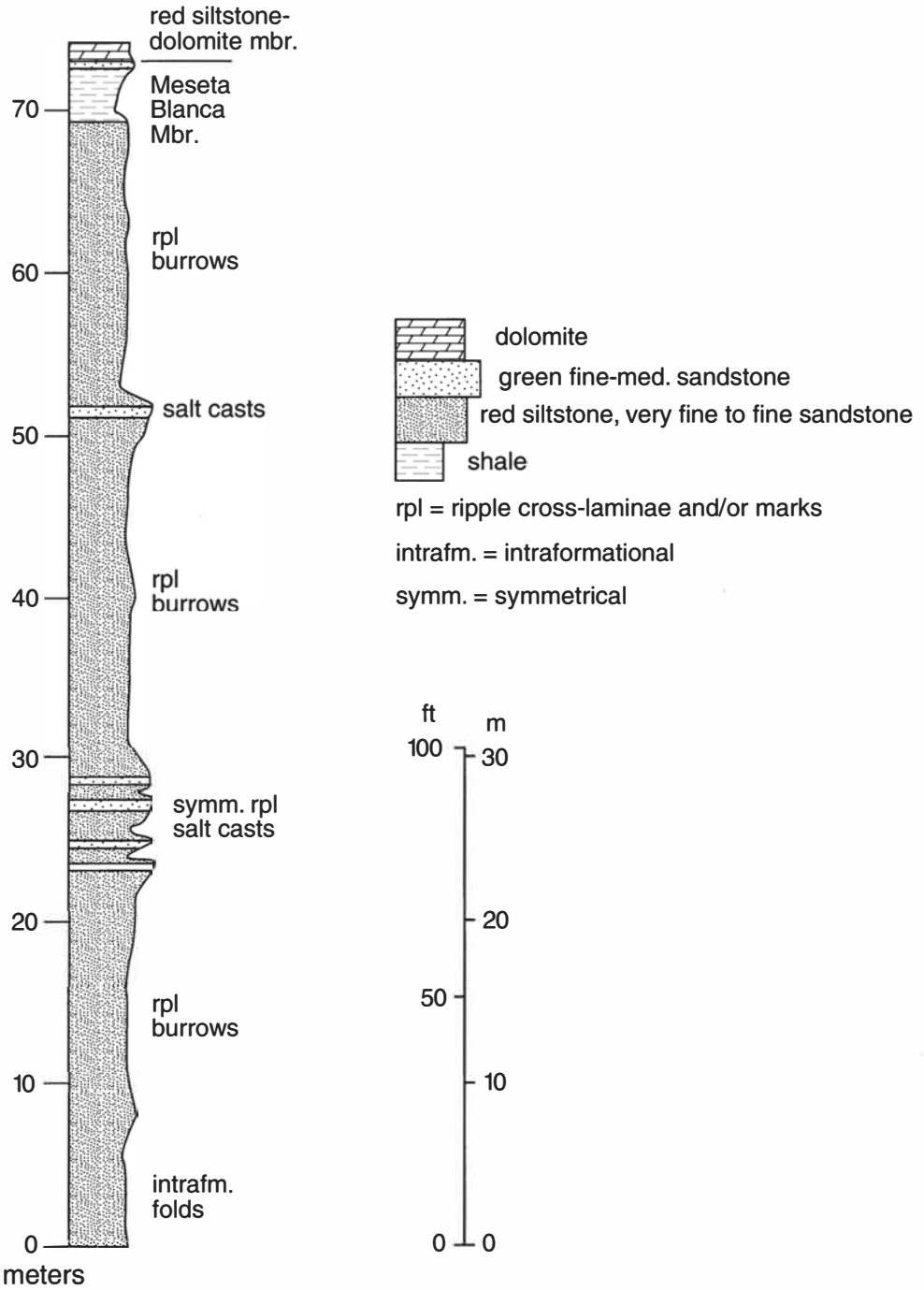

FIGURE 30—Measured section of the Meseta Blanca Sandstone Member of the Yeso Formation (Permian) near Broken House Tank (NW¼ sec. 14 T17S R4W).

In the Caballo Mountains the Yeso Formation thickens eastward from 214 m to 396 m (702 to 1,300 ft). About a third of the thickness difference is due to the fact that there is 61 m (200 ft) more of the upper member preserved beneath the Dakota along the eastern margin of the range than at Hidden Tank. The remainder of the thickness difference is in the red siltstone-dolomite member, which is almost three times thicker along the eastern flank of the range than at Hidden Tank as a result of very thick intervals of gypsum. The Meseta Blanca Sandstone, 72 m (236 ft), and limestone members, 24–28 m (79–92 ft), show little or no variation in thickness throughout the range.

Meseta Blanca Sandstone Member

Description

The Meseta Blanca Sandstone Member consists primarily of orange, very fine to fine-grained, well sorted sandstone, although a few beds of medium-grained sandstone and siltstone are also present (Fig. 30). From a distance, the Meseta Blanca Sandstone Member has alternating ledges and recessed intervals, the latter of which were initially assumed to be underlain by shale or mudstone. However, upon closer inspection, most of the recessed intervals were found to be composed of bioturbated sandstone with the same grain size as the ledgy beds above and below. Shale/mudstone is rare and is restricted to the uppermost part of the section. The orange sandstones display millimeter- to

FIGURE 31—Wind ripples in the Meseta Blanca Sandstone Member of the Yeso Formation (Permian) near Broken House Tank. Hammer is 25 cm (9.8 in) long.

centimeter-scale horizontal or low-angle laminae that result from climbing, low-amplitude asymmetrical ripples (Fig. 31). Locally, the laminae are partially destroyed by bioturbation and desiccation cracks. Crossbeds in sets up to 30 cm (11.8 in) thick are rare. In addition, there are several distinctive beds of white to light-green, fine-grained sandstone with symmetrical ripple marks, salt casts, and burrows. Soft-sediment deformation in the form of small-scale disrupted laminae is also present, and a 2 m (6.5 ft) thick bed of sandstone near the base of the member has large intraformational folds truncated by the overlying bed.

Depositional environments

The most diagnostic features of the Meseta Blanca Sandstone Member in the Caballo Mountains are the fine grain size, excellent sorting, and the predominance of climbing, low-amplitude ripples, suggesting deposition as an eolian sand sheet (Mack and Suguio, 1991; Mack and Dinterman, 2002). Fryberger et al. (1979) described a modern eolian sand sheet located southwest (upwind) of the dune field that makes up Great Sand Dunes National Monument, Colorado. Deposition on the modern sand sheet is by subcritically-climbing, low-amplitude eolian ripples, resulting in horizontal and low-angle laminae that may or may not display ripple foresets. This type of structure has been described elsewhere in modern eolian dune fields (Hunter, 1977), has been produced experimentally (Fryberger and Schenk, 1981), and is identical to the ripple laminae in the Meseta Blanca Sandstone Member. Zones of heavy bioturbation, which are common in the Meseta Blanca Sandstone Member, are also described in the eolian sand sheet near Great Sand Dunes National Monument, as well as in other modern eolian dunes (Ahlbrandt et al., 1978; Fryberger et al., 1979).

The light green, rippled sandstone beds with salt casts in the Meseta Blanca Sandstone Member are interpreted by Mack and Dinterman (2002) as deposits of coastal salinas.

Red siltstone-dolomite member

Description

The contact between the Meseta Blanca Sandstone Member and the red siltstone-dolomite member is placed at the base of the first thick, > 1 m (3.3 ft), carbonate bed, usually a dolomite. The upper contact is at the base of cliff-forming dark-gray limestones of the limestone member. The red siltstone-dolomite member consists of interbeds of four rock types: dolomite, limestone, siltstone to very fine sandstone, and gypsum (Figs. 32, 33). Dolomite is thin- to medium-bedded, light gray to tan, and fine grained. Thin horizontal laminae to wavy laminae, some of which may be stromatolites, are common in the dolomite, as are spar-filled vugs ranging in diameter from less than a millimeter to several centimeters. Brecciation, desiccation cracks, and gypsum pseudomorphs are locally present in the dolomite, although a few beds display no internal structures. Limestones are gray, thin- to medium-bedded, fossiliferous and peloidal wackestones and packstones. Fossils are generally small and difficult to identify in hand specimen, although thin sections reveal ostracods, foraminifera, brachiopods, gastropods, and pelecypods. Several of the limestone beds are recrystallized to coarse, sparry calcite.

Siltstones or very fine grained sandstones are commonly red to orange, although some are white or green. They exhibit low-amplitude ripple cross-laminae and bioturbation similar to that in the Meseta Blanca Sandstone Member, and some siltstones/sandstones contain salt casts and gypsum cement. Locally, the siltstones and sandstones are intercalated on the scale of 10–20 cm (4–8 in) with dolomite.

Approximately one-half of the measured section of the red siltstone-dolomite member along the eastern flank of the range is composed of gypsum (Fig. 32). It is also likely that the covered intervals are underlain by gypsum, an interpretation supported by the presence of a gypsiferous crust in the soil. Gypsum beds are sugary to alabaster and consist of millimeter- to centimeter-scale light and dark bands. No gypsum beds were observed in outcrop at Hidden Tank, although a limestone collapse breccia probably resulted from dissolution of underlying gypsum (Fig. 33).

Depositional environments

The red siltstone-dolomite member was deposited in upward-shallowing cycles that ranged from shallow-marine or lagoonal, to tidal flat, to eolian (Mack and Dinterman, 2002). A modern analog to the environments of the red siltstone-dolomite member occur along the western coast of the Persian Gulf (cf. Kendall and Skipwith, 1969). A shallow-marine origin for the limestones is indicated by abundant micrite and the presence of a normal-marine fauna. A tidal-flat origin for the dolomites is suggested by stromatolites, spar-filled vugs that resemble fenestral fabric, brecciation, gypsum pseudomorphs, desiccation cracks, and the lack of fossils (cf. Logan et al., 1964; Shinn, 1968). Dolomitization probably occurred within a few thousand years after deposition of a micrite host as a result of reflux of hypersaline ground water, a process occurring along many modern arid carbonate shorelines (cf. Shinn et al., 1965; Deffeyes et al., 1965; Illing et al., 1965). The dolomitic tidal flat was periodically invaded by an eolian sand sheet, corresponding to the siltstones and very fine sandstones containing low-amplitude eolian ripples. The presence of shallow, hypersaline ground waters within the siltstones/sandstones is indicated by salt casts and gypsum cement. The fine, horizontal laminae in the gypsum beds suggest deposition in hypersaline lagoons or on a shallow saline marine platform (saltern), an interpretation made by Hunter and Ingersoll (1981) for gypsum of the Yeso Formation located north of the Caballo Mountains. Supratidal gypsum, in contrast, is commonly nodular and has a distinctive chicken-wire fabric that is not present in the red siltstone-dolomite member. Massive dolomites may also be lagoonal in origin. The numerous upward-shallowing cycles may reflect glacial-eustatic fluctuations in sea level, although Gondwanan glaciers were much less widespread by late Early Permian time (Frakes et al., 1992).

Limestone member

Description

The limestone member conformably overlies the red siltstone-dolomite member and is conformably overlain by the sandstone-limestone member. The limestone member holds up low ridges and is composed of dark-gray, thin- to medium-bedded, fossiliferous packstone (Fig. 33). Fossils include brachiopods, bryozoa, gastropods, pelecypods, corals, and a variety of foraminifera (Fig. 34). Some fossils are silicified and a few dark-gray chert nodules are present.

Depositional environments

Open-marine conditions prevailed during deposition of the

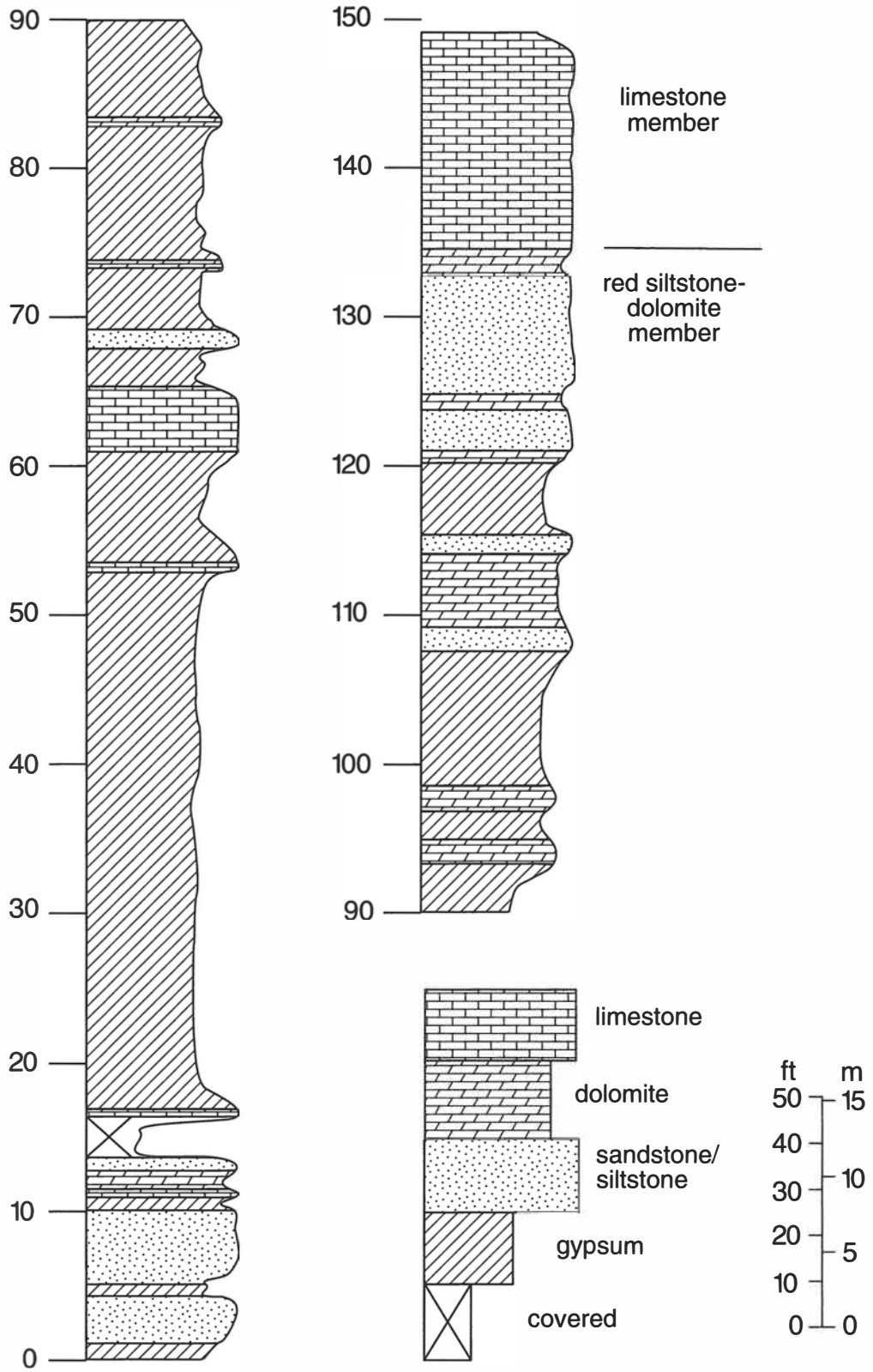

FIGURE 32—Measured section of the red siltstone-dolomite and limestone members of the Yeso Formation (Permian) along the eastern flank of the range (NE¼ sec. 7 T16S R3W).

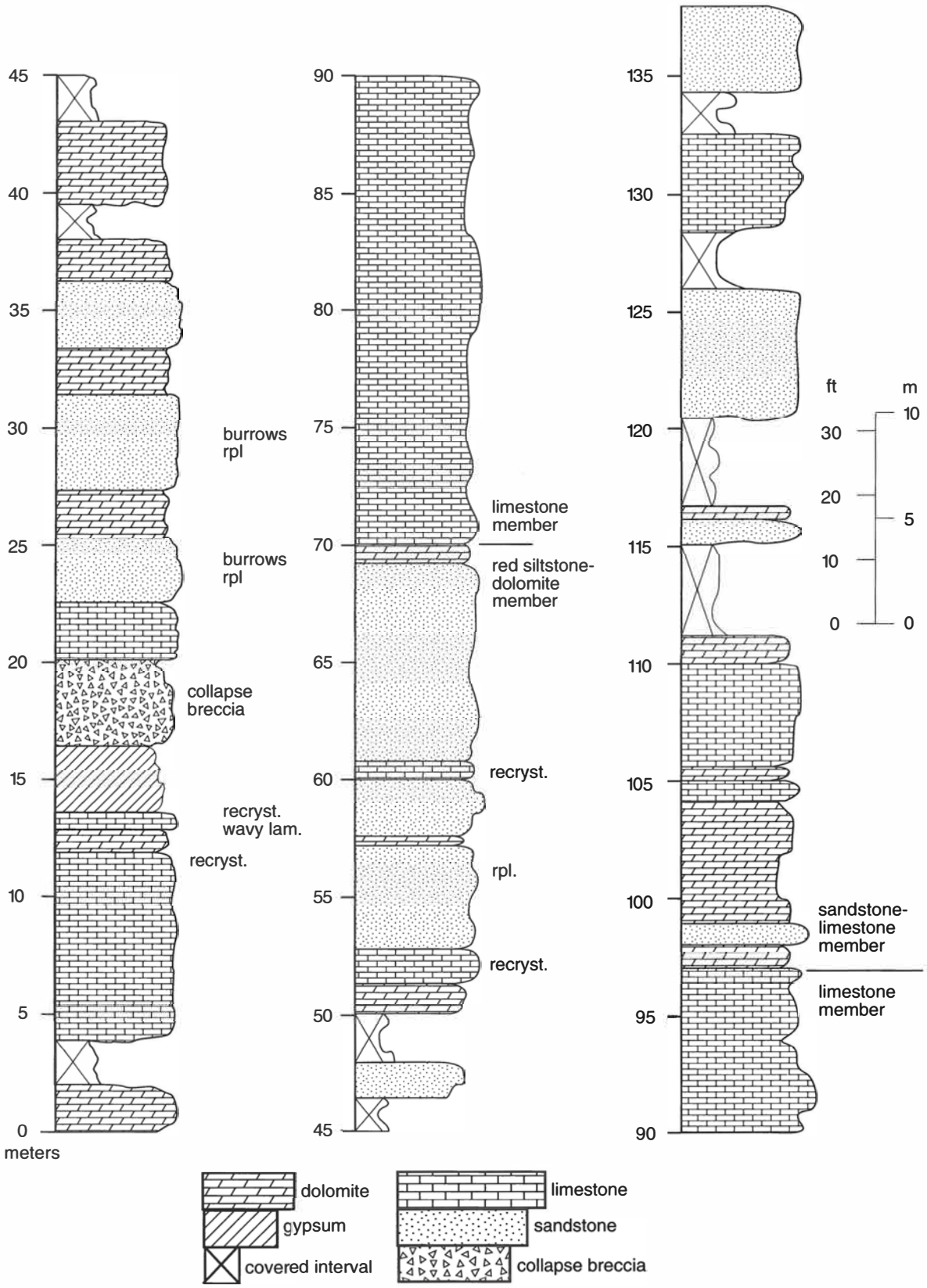

FIGURE 33—Measured section of the red siltstone-dolomite, limestone, and sandstone-limestone members of the Yeso Formation (Permian) near Hidden Tank in Apache Valley (SE¼ sec. 6 T17S R3W). rpl = ripples; recryst. = recrystallized; lam. = laminae.

limestone member. The diverse marine fauna, the presence of filter feeders, and micrite matrix argue for a shallow, low-energy marine environment characterized by warm, well oxygenated water of normal salinity. Mack and Dinterman (2002) suggested that the limestone member may correlate with other prominent Yeso limestones in northern New Mexico and may represent the time of maximum transgression during Yeso deposition.

Sandstone-limestone member

Description and depositional environments

The conformable contact between the limestone member and sandstone-limestone member is placed at the base of the first sandstone or tan dolomite. At Hidden Tank the sandstone-limestone member is 40 m (131 ft) thick, whereas an additional 61 m (200 ft) is exposed along the eastern flank of the range (Figs. 33, 35). This difference in thickness is related to the depth of erosion beneath the Cretaceous Dakota Sandstone. Rock types in the sandstone-limestone member are the same as in the red siltstone-dolomite member, although the sandstone-limestone member also contains oolitic and fossiliferous grainstones. Like the red siltstone-dolomite member, the sandstone-limestone member is also interpreted to represent upward-shallowing cycles of shallow-marine to lagoonal, tidal flat, and eolian facies. The return to the upward-shallowing cycles following open-marine deposition of the limestone member suggests an overall regression (Mack and Suguio, 1991).

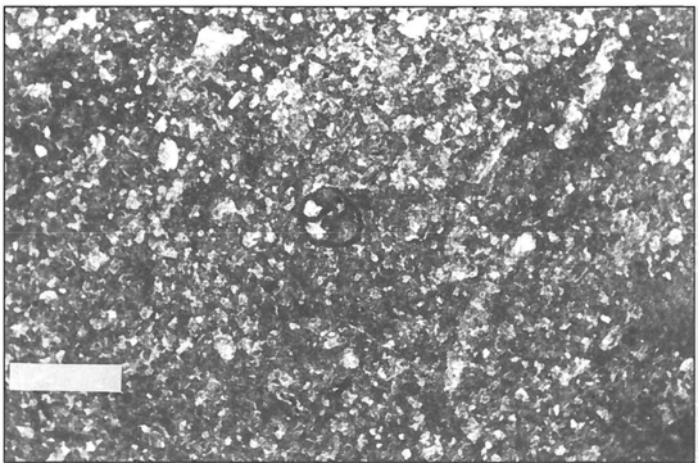

FIGURE 34—Photomicrograph of foraminiferal wackestone of the limestone member of the Yeso Formation (Permian). Bar scale is 0.25 mm (0.1 in) long.

Permian–Pennsylvanian Ancestral Rocky Mountains

During Pennsylvanian and Early Permian time, the formerly stable craton of New Mexico and adjacent states experienced a major deformational event referred to as the Ancestral Rocky Mountains. Deformation was characterized by a series of discontinuous block uplifts separated by intermontane basins. In southern New Mexico, the principal uplift was the Pedernal Mountains, which trended north and was cored by Precambrian crystalline basement (Fig. 36). Adjacent to the Pedernal Mountains were the Delaware Basin to the east and the Orogrande Basin to the west. Other tectonic elements in southern New Mexico and adjacent areas included the Florida and Diablo platforms and the Pedregosa Basin (Fig. 36).

The eastern margin of the Orogrande Basin is generally considered the "active" margin, because of more rapid subsidence and a greater influx of siliciclastic detritus, including coarse conglomerates (Otte, 1959; Jordan, 1975; Wilson and Jordan, 1988). The Caballo Mountains are positioned on the "inactive" side of the basin, characterized by thinner, carbonate-rich strata, especially in the Pennsylvanian. However, doming of the rocks beneath the Pennsylvanian Red House Formation, the presence of unconformities within the Magdalena Group, and locally derived conglomerates in the Pennsylvanian section in the Caballo Mountains argues for at least mild tectonism along the western flank of the Orogrande Basin (Lawton et al., 2002).

Initial subsidence of the Orogrande Basin may have begun as early as middle Mississippian, and the time of maximum subsidence is generally considered to have been in the Virgilian (Jordan, 1975; Wilson and Jordan, 1988; Singleton, 1990; Raatz, 2002). By the time of deposition of the middle to late Wolfcampian Abo Formation, the influence of the major tectonic elements in southwestern New Mexico was much less pronounced. The Abo–Hueco facies transition, which marked the position of the shoreline, trends northeast across southwestern New Mexico and seems little affected by the Florida platform and Pedregosa Basin. Most of the siliciclastic sediment in the Abo Formation, with the exception of that in the Sacramento Mountains, appears to have been derived from the north rather than from the Pedernal Mountains (Jordan, 1975; Mack and James, 1986). However, the Orogrande Basin was still subsiding in an asymmetrical fashion during Abo deposition, as indicated by eastward thickening (Singleton, 1990; Mack et al., in press b) and a prominent northward embayment of the Abo–Hueco transitional zone (Doña Ana bight of Mack et al., 1995). Moreover, conglomerates in the lower part of the Abo in the Sacramento Mountains indicate that locally high relief persisted in the Pedernal Mountains (Speer, 1983). However, the Pedernal Mountains were completely worn down and onlapped during deposition of the Leonardian Yeso Formation (Kottlowski, 1963; Mack and Dinterman, in press).

A variety of tectonic models have been proposed to explain the origin of the Ancestral Rocky Mountains. A popular model relates deformation in the continental interior of the Ancestral Rocky Mountains to collision between North America and northern Gondwana along the Ouachita–Marathon convergent margin (Hills, 1970; Kluth and Coney, 1981; Kluth, 1986; Budnick, 1986; Ross and Ross, 1986; Soegaard and Caldwell, 1990). This model proposes that the uplifts and basins may have experienced compression, transtension, and/or transpression, because of changes in stress regime as the collision migrated westward through time and because of reactivation of pre-existing basement fractures (e.g. Stevenson and Baars, 1986; Budnick, 1986; Soegaard and Caldwell, 1990). The presence of syndepositional folds and unconformities along the eastern margin of the Orogrande Basin (Pray, 1959) are consistent with a compressional or transpressional regime. The evidence for tectonic activity along the western margin of the basin and a rhombic basin form indicated by Virgilian isopachs suggested to Lawton et al. (2002) that the Orogrande Basin may have had a transpressional, strike-slip origin.

Alternatively, Ye et al. (1996) emphasized the similarity between the style and scale of deformation of the Ancestral Rocky Mountains and the Laramide Rocky Mountains and modern Sierra Pampeanas broken foreland of Argentina. They suggest that deformation in the Ancestral Rocky Mountains resulted from northeastward, low-angle subduction along the southwestern margin of North America. There is little evidence to support such a plate-tectonic setting in Permian–Pennsylvanian time.

Finally, Goldstein (1984) points out the signficance of regional subsidence, manifested by similar subsidence histories of the basins of the Ancestral Rocky Mountains and by mid to Late Permian subsidence of the uplifts themselves. Goldstein (1984) proposed north-directed, low-angle subduction of an oceanic plate beneath the southern margin of North America, which ultimately resulted in regional isostatic subsidence. Once again, there is little evidence to support this plate-tectonic configuration.

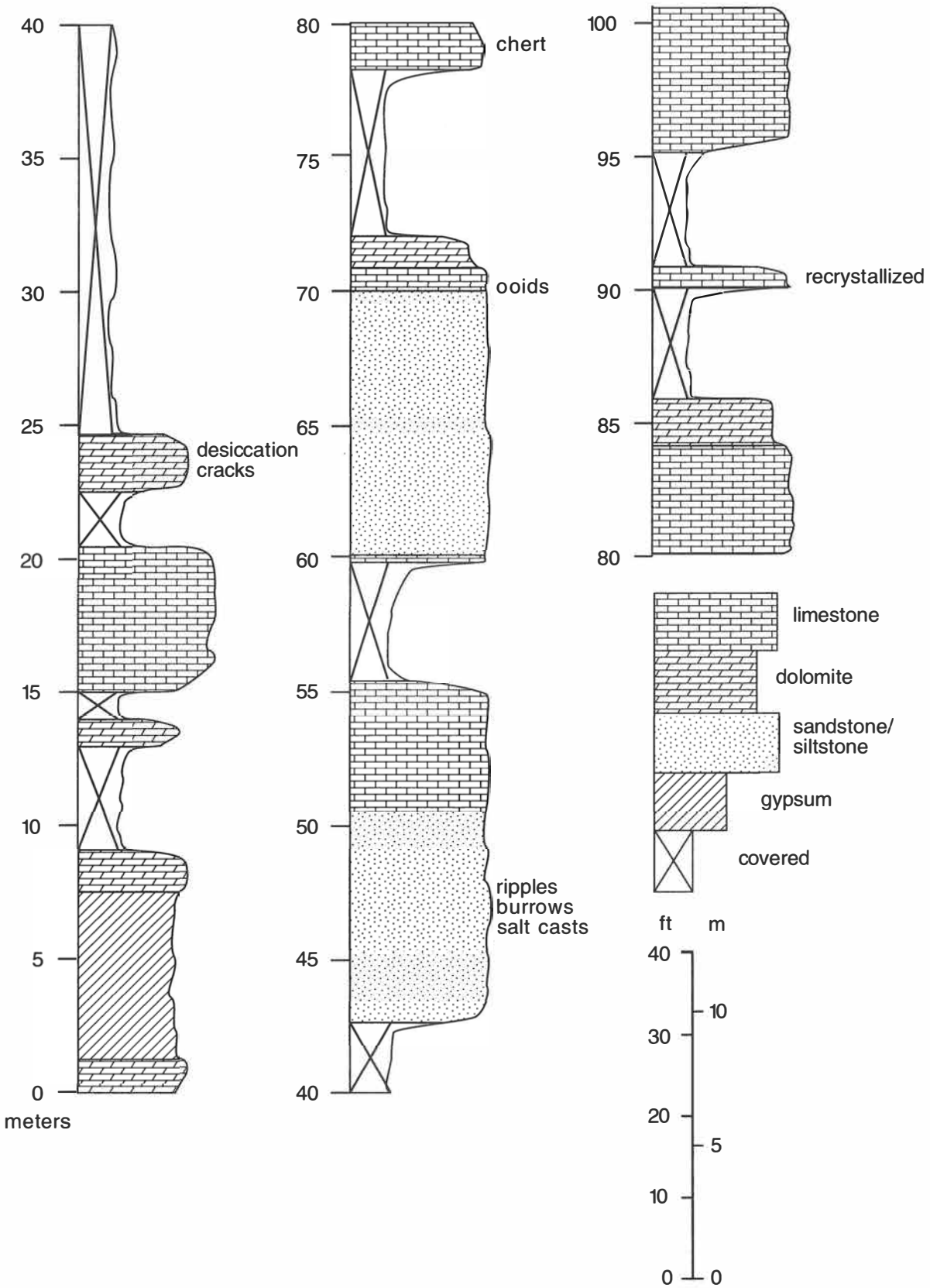

FIGURE 35—Measured section of the sandstone-limestone member of the Yeso Formation (Permian) along the eastern flank of the range (SE¼ sec. 34 and SW¼ sec. 35 T16S R3W).

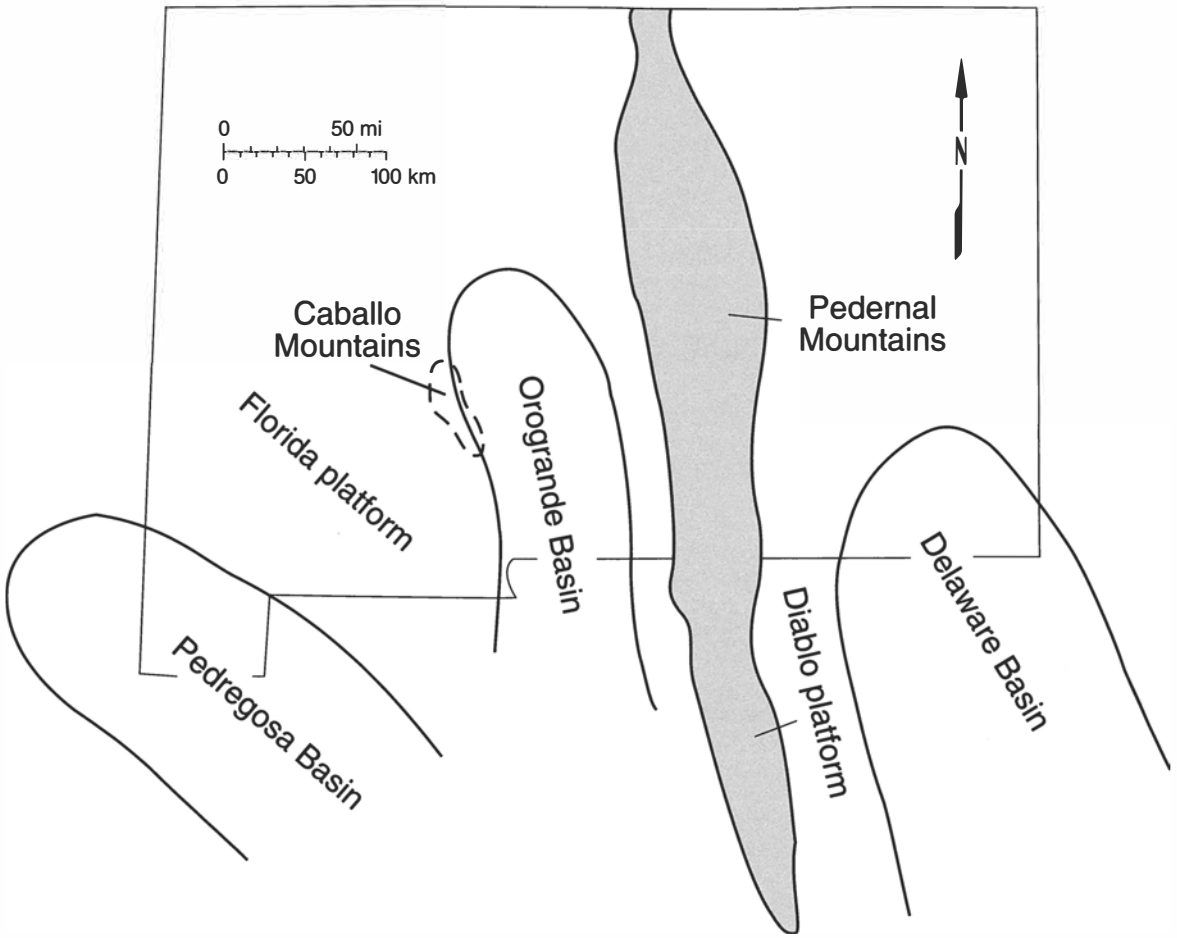

FIGURE 36—Major tectonic elements of the Permian–Pennsylvanian Ancestral Rocky Mountains in southern New Mexico.

Basal Cretaceous unconformity

In southwestern New Mexico and southeastern Arizona, a thick sequence of Lower Cretaceous and locally Upper Jurassic sedimentary rocks was deposited in a west-northwest-trending rift basin known as the Chihuahua trough in New Mexico and as the Bisbee Basin in Arizona (Kottlowski, 1965; Greenwood et al., 1977; Bilodeau, 1982; Dickinson et al., 1986; Mack, 1987; Lawton, 2002). The northern margin of the basin was an uplifted rift shoulder that supplied terrigenous sediment to the basin; Lower Cretaceous deposits are either thin or absent on this rift shoulder. The area of the present Caballo Mountains, as well as adjacent ranges, were located on the rift shoulder throughout Early Cretaceous time. Sites of erosion during the Early and middle Cretaceous, the rift shoulders were not onlapped and buried until Late Cretaceous time.

Based on Upper Cretaceous subcrop patterns, Dickinson et al., (1986) suggest that the rift shoulder was tilted gently northward. This idea is well demonstrated in south-central and southwestern New Mexico where progressively younger Paleozoic stratigraphic units unconformably underlie Cretaceous sandstone in a northeasterly direction. Southwest of Silver City Upper Cretaceous sandstone overlies Precambrian rocks along the inferred highest part of the rift shoulder. Farther east, in the Cookes Range, basal Cretaceous sandstone (including both Upper and Lower Cretaceous units) overlie Abo and Pennsylvanian strata. Farther north in the Caballo and southern San Andres Mountains, the Dakota Sandstone was deposited on Yeso beds, and still farther north in the Fra Cristobal and northern San Andres Mountains, San Andres Limestone is present beneath the Dakota Sandstone. Thus, the base of the Upper Cretaceous section is an important angular unconformity of regional extent. It was created by erosional beveling of gently north-tilted sedimentary formations that comprised the rift shoulder. However, the angular discordance is small, probably less than 1°, accounting for the disconformable appearance of the unconformity at outcrop scale. The Upper Cretaceous rocks, which onlapped and buried the rift shoulder, are thick and well exposed in the Caballo Mountains.

Upper Cretaceous foreland basin deposits

Upper Cretaceous foreland basin strata totaling almost 1,000 m (3,280 ft) thick are exposed in the northern and northeastern part of the Caballo Mountains. Included in this sequence are the Dakota, Rio Salado Tongue of the Mancos, Tres Hermanos, D-Cross Tongue of the Mancos, Gallup, and Crevasse Canyon Formations (Fig. 37). The section at Mescal Canyon in the Elephant Butte quadrangle represents the most complete, best exposed, easily accessible exposure of Upper Cretaceous strata in southern New Mexico. In addition, Upper Cretaceous rocks are widely but not well exposed in the Engle, Palomas Gap, Cutter, Upham, and Apache Gap quadrangles. Within these quadrangles, the best exposure is in Putnam Draw in the northwestern part of the Upham and northeastern part of the Apache Gap quadrangles. The McRae Formation is also Cretaceous in age, but was deposited in a Laramide basin and will thus be discussed in the context of the Laramide orogeny.

Dakota Sandstone

Since it was first named by Meek and Hayden (1861) for exposures in northwestern Nebraska, the Dakota has become one of the most widely used stratigraphic units in the central and southern Rocky Mountains and Great Plains. Partly as a consequence of its widespread use, there is considerable variability in stratigraphic nomenclature with designations of Group, Series, Stage, Formation, and Sandstone. In this report, the Dakota Sandstone is given formation status, because it is mappable at the scale of 1:24,000. Throughout south-central New Mexico, the Dakota Sandstone is poorly fossiliferous and is considered to be middle Cenomanian in age based on its conformable contact with the overlying Mancos Shale (Hook, 1983). In the Caballo Mountains, the Dakota unconformably overlies the sandstone-limestone member of the Yeso Formation.

The Dakota Sandstone is well exposed at three locations in the Caballo Mountains, including Putnam Draw in the northeastern part of the Apache Gap quadrangle (NW¼ sec. 22 T15S R3W), at Mescal Canyon in the southeastern part of the Elephant Butte quadrangle (NW¼ sec. 36 T13S R4W), and at Hidden Tank in the McLeod Tank quadrangle (NW¼ sec. 5 T17S R3W); measured sections from the latter two areas are shown in Figure 38. At the two measured sections, the Dakota Sandstone is approximately 30 m (98 ft) thick. However, variability in thickness of the Dakota in and adjacent to the Caballo Mountains is common, a result of variable relief on the pre-Dakota unconformity. This concept is well illustrated by comparing the thickness of the Dakota at Hidden Tank with an exposure 6 km (3.7 mi) to the northeast in the northeasternmost part of the McLeod Tank quadrangle. At the latter site, the Dakota is only 2 m (6.6 ft) thick, and 61 m (200 ft) more of the underlying Yeso Formation is preserved there than at Hidden Tank where the Dakota is 30 m (98 ft) thick. Similarly, Bauer (1989), using geophysical logs, has documented that the Dakota in the Jornada del Muerto Basin, east of the Caballo Mountains, varies in thickness from 42 to 106 m (138 to 348 ft).

Description

The basal meter or less of the Dakota generally consists of conglomerate composed of quartz and sandstone pebbles. The conglomerate is overlain by 6–8 m (20–26 ft) of medium-grained quartz sandstone containing trough and planar crossbeds and horizontal laminae. Impressions of tree trunks and stems are locally present. At Putnam Draw, this lower sandstone displays lateral accretions sets (Fig. 39). The middle part of the Dakota at the two measured sections is dominated by gray, blocky shale, but also has thin, <1.5 m (< 4.9 ft), light-colored, ledge-forming, very fine to fine-grained sandstones. The thin sandstones exhibit asymmetrical ripple cross-laminae and root traces. At Hidden Tank, the shale-rich part of the section is overlain by another thick, trough-crossbedded, fine- to medium-grained sandstone and a quartz-pebble conglomerate.

At Mescal Canyon, the uppermost gray shale is heavily bioturbated, has a few fragments of oyster shells, and has limonite stains presumably related to alteration of pyrite. Overlying the bioturbated shale are thin-bedded, fine-grained sandstones displaying ripple cross-laminae, flaser bedding, and burrows. These two intervals are not evident at Hidden Tank.

An upper ledge-forming sandstone is present at both measured sections and throughout the range and is characterized by fine- to medium-grain size, wavy bedding, trough crossbeds, and abundant *Ophiomorpha* burrows (Fig. 40). The sandstone is overlain by a thin, < 1 m (< 3.3 ft), granule-pebble conglomerate or granular-pebbly, medium-grained sandstone displaying numerous burrows and an occasional shark tooth and shell fragments. The conglomerate is immediately overlain by the Mancos Shale.

Depositional environments

The Dakota Sandstone in south-central New Mexico represents the lower part of a transgressive sequence that continues upward into the middle of the Rio Salado Tongue of the Mancos Shale (Molenaar, 1983a; Hook, 1983). The lower and middle parts of the formation are interpreted to be fluvial in origin and can be subdivided into channel and floodplain facies. Channel sandstones and conglomerates constitute single and multistory sheets that range from 6 to 8 m (20 to 26 ft) thick. The dominant bedforms in the channels were three-dimensional dunes, resulting in trough crossbeds. Lateral accretion sets were only observed in one sand body, although the lack of laterally persistent, suitably oriented outcrops probably inhibits their recognition. Crossbed paleocurrent data collected in this study and by Bauer (1989) indicate eastward to northeastward paleoflow, directions consistent with the interpretation of Molenaar (1983a) that the Cenomanian shoreline in New Mexico had a north-northwest trend and faced seaward to the east-northeast. Floodplain strata are as abundant as channel sandstones/conglomerates and consist of overbank shale and thin, crevasse-splay sandstones. Thickness variations in the Dakota are primarily restricted to the fluvial part of the section, suggesting the rivers backfilled paleovalleys cut into the Yeso Formation (Bauer, 1989).

The stratigraphically lowest evidence of marine influence in the Dakota at the Mescal Canyon measured section is bioturbated shale and sandstone. The abundance of burrows and scattered oyster shells in the lower shale suggest deposition in a lagoon or estuary, while the overlying rippled and bioturbated sandstones resemble tidal-flat deposits (Mack et al., 1998b). The uppermost ledge-forming sandstone is present throughout the range and has clear evidence of marine influence in the form of *Ophiomorpha* burrows. This sandstone appears to be too heavily bioturbated to represent an upper shoreface or foreshore sandstone (cf. Howard and Reineck, 1981). Instead, wavy bedding, which locally represents reactivation surfaces on crossbeds, and lateral accretion sets described by Bauer (1989) suggest deposition as a flood-tidal delta (Bauer, 1989, Mack et al., 1998b). The uppermost conglomerate is a transgressive lag, which mantles an erosion surface, called a ravinement, which is cut by rising sea level (Swift, 1968). The transgressive lag preserves sediment too coarse to be distributed seaward by storms during the transgressive event. The ravinement tends to erode areas landward of the shoreface, but may preserve some paralic sediment beneath the unconformity, as it apparently has done in the Dakota Sandstone in the Caballo Mountains (cf. Demarest and Kraft, 1987).

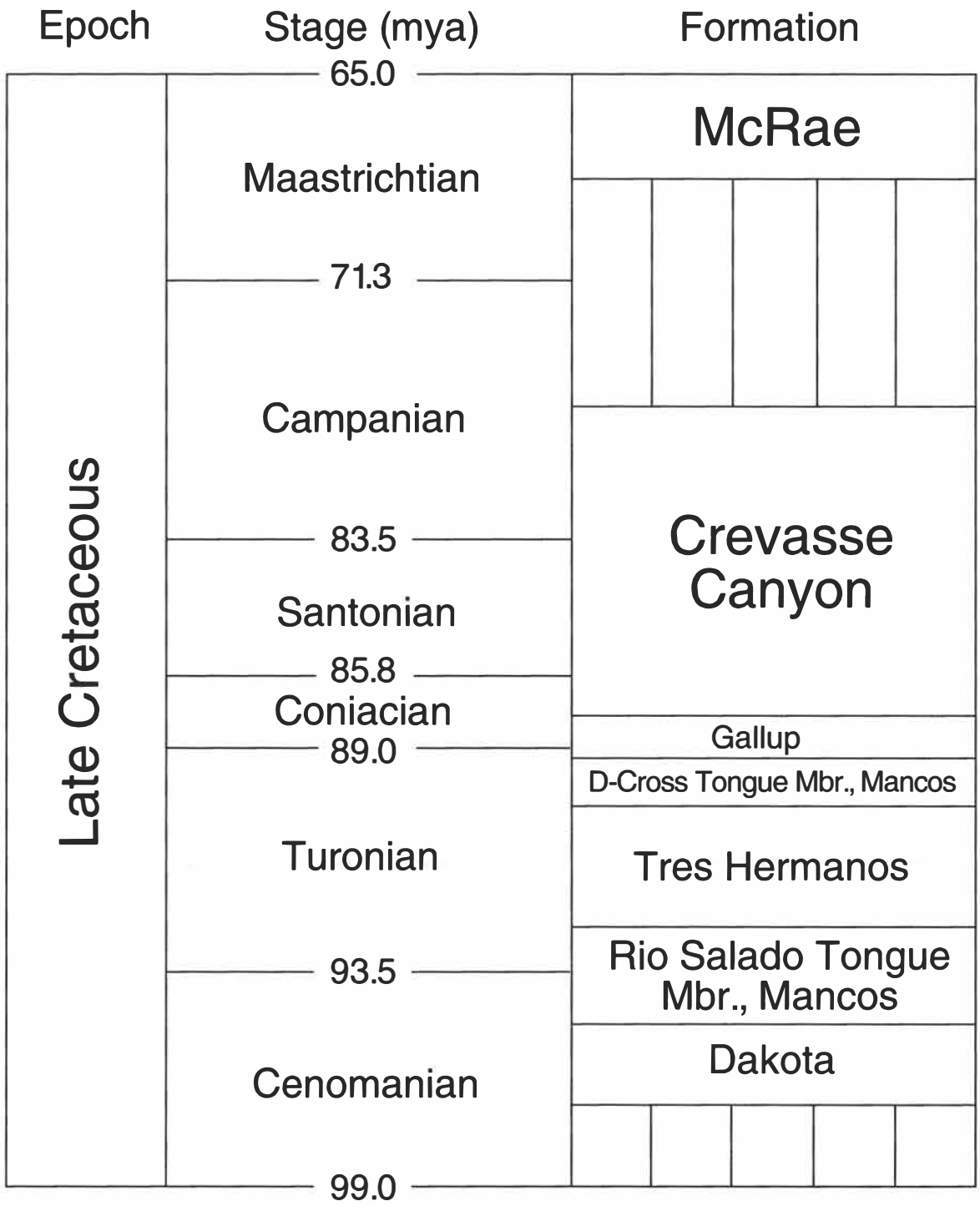

FIGURE 37—Upper Cretaceous correlation chart for the Caballo Mountains and vicinity (Palmer and Geissman, 1999).

Rio Salado Tongue of the Mancos Shale

The Mancos Shale was named by Cross (1899) for exposures near the town of Mancos in southwestern Colorado, and has been applied extensively throughout New Mexico. The Mancos has been extended as far south as the southern San Andres Mountains, the Burro Mountains, Cooke's Range, and the Silver City area (Seager, 1981; Molenaar, 1983a; Mack et al., 1998b). In south-central New Mexico, the Mancos is divided into a lower Rio Salado Tongue and an upper D-Cross Tongue, separated by the Tres Hermanos Formation (Hook and Cobban, 1981; Molenaar, 1983a; Hook, 1983; Hook et al., 1983). The Rio Salado Tongue is late Cenomanian to early Turonian in age (Hook, 1983).

The Rio Salado Tongue of the Mancos Shale is best exposed in Mescal Canyon in the Elephant Butte quadrangle (S½ sec. 36 T13S R4W), where it is approximately 120 m (394 ft) thick. It is also well exposed near Hidden Tank and Mine Tank in the McLeod Tank quadrangle, and in Putnam Draw in the northeastern part of the Apache Gap quadrangle. The Rio Salado Tongue conformably overlies the Dakota Sandstone and is conformably overlain by the Tres Hermanos Formation. The latter contact is placed at the base of a thick, > 3 m (>10 ft), ledge-form-

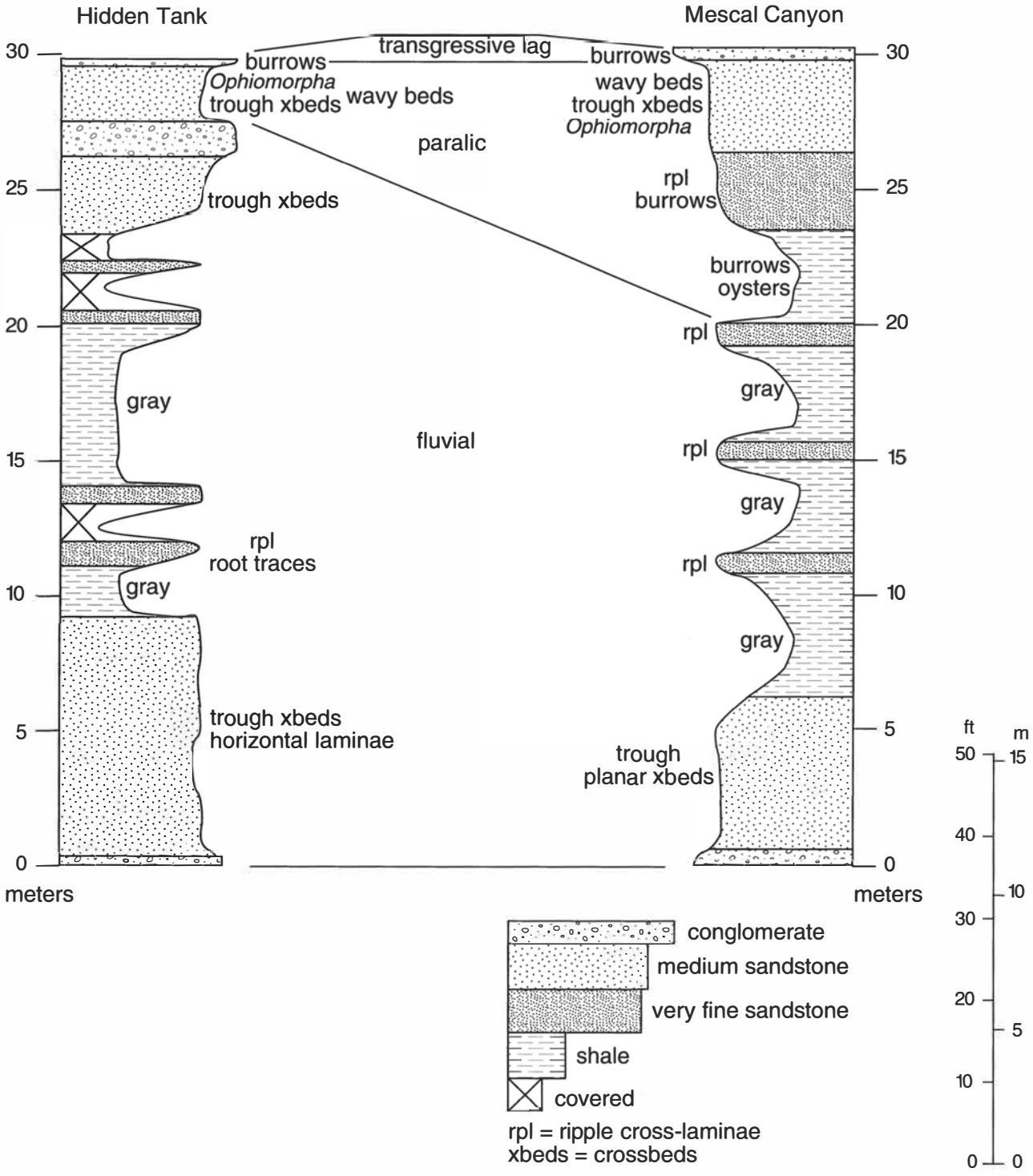

FIGURE 38—Measured sections of the Upper Cretaceous Dakota Sandstone at Mescal Canyon (NW¼ sec. 36 T13S R4W) and Hidden Tank (NW¼ sec. 5 T17S R3W).

ing sandstone referred to as the Atarque Sandstone Member of the Tres Hermanos Formation (Wallin, 1983; Mack et al., 1998b).

Description

The Rio Salado Tongue of the Mancos Shale consists of gray shale and tan siltstone to very fine grained sandstone interbedded on the scale of a few centimeters to a few meters. The shale is dark gray, fissile, and sparsely fossiliferous. The ledge-forming sandstone/siltstone beds have sharp upper and lower contacts, as well as horizontal laminae, symmetrical ripple cross-laminae and ripple marks, hummocky stratification, horizontal burrows, and a few fossils. The relative abundance of shale is greatest in the middle of the Rio Salado Tongue (Fig. 41). Fossils primarily include bivalves, gastropods, and ammonites, although Lucas and Anderson (1998) described the occurrence of the coral *Archohelia dartoni* Wells from Mescal Canyon. Also present in the lower third of the Rio Salado Tongue are up to five yellowish bentonites 3–15 cm (1.2–5.9 inches) thick (Fig. 42). These ben-

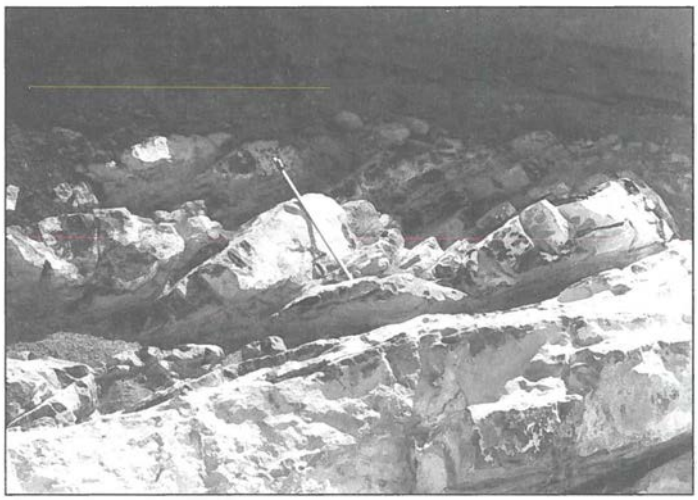

FIGURE 39—Lateral accretion set resulting from point-bar deposition in the basal part of the Dakota Sandstone (Upper Cretaceous) in Putnam Draw. Jacob's staff is 1.5 m (4.9 ft) long.

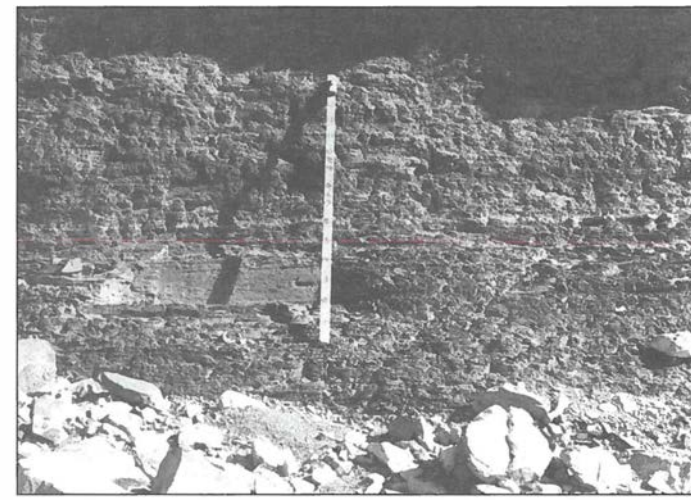

FIGURE 41—Thinly bedded, gray shale and siltstone near the middle of the Rio Salado Tongue of the Mancos Shale (Upper Cretaceous) in Putnam Draw. Jacob's staff is 1.5 m (4.9 ft) long.

FIGURE 40—*Ophiomorpha* burrows in the upper sandstone of the Dakota Sandstone (Upper Cretaceous) in Mescal Canyon.

FIGURE 42—Two light-colored bentonites in the Rio Salado Tongue of the Mancos Shale (Upper Cretaceous) in Mescal Canyon.

tonites are well exposed near the mouth of Mescal Canyon and in Putnam Draw, and have also been observed by us south of the Chino mine in Grant County.

Depositional environments

The Rio Salado Tongue of the Mancos Shale was deposited in the Western Interior Seaway during the latter part of the T1 transgression and early part of the R1 regression of Molenaar (1983a). The turn-around point, or time of maximum water depth, appears to be in the middle of the formation, which is dominated by shale. In sequence stratigraphic terminology (cf. Van Wagoner et al., 1990), the lower part of the Rio Salado Tongue is part of a transgressive systems tract that begins with the Dakota Sandstone, and the upper part of the Rio Salado Tongue is the base of a highstand systems tract (Mack et al., 1998b).

Deposition of silt and clay from suspension below normal wave base produced the gray shales, whereas sharp basal contacts and hummocky stratification suggest the thin beds of siltstone or very fine sandstone are storm deposits. However, a few beds of very fine sandstone display graded beds at the base and horizontal laminae above, which may represent the basal part of the Bouma sequence produced by turbidity flows.

Benthic fauna in the Rio Salado Tongue is dominated by bivalves and is under represented in normal-marine filter feeders (Kauffman, 1975). The restricted fauna may be due to either poorly oxygenated bottom waters or abnormal salinity. Frush and Eicher (1975) suggested that low oxygen levels may have been produced during times when an oxygen-minimum layer, which results from decay of particulate organic matter as it descends through the water column, expanded sufficiently to intersect the floor of the seaway. In contrast, Kauffman (1975) argued that there is no evidence of widespread reducing conditions, and that a more likely cause for the restricted fauna was periodic influx of meteoric water by rivers. Subsequent studies of basinal facies of the Western Interior Seaway supported Kauffman (1975), and emphasized the role of climatic cycles, perhaps related to Milankovitch orbital perturbations (Pratt, 1984; Barron et al., 1985; Laferriere et al., 1987).

Tres Hermanos Formation

Originally defined by Herrick (1900) for exposures in central New Mexico, the Tres Hermanos Formation occupies a conformable stratigraphic position between the Rio Salado and D-Cross Tongues of the Mancos Shale (Hook et al., 1983). The Tres Hermanos Formation is divided into three members, which in ascending order are the Atarque Sandstone, Carthage, and Fite

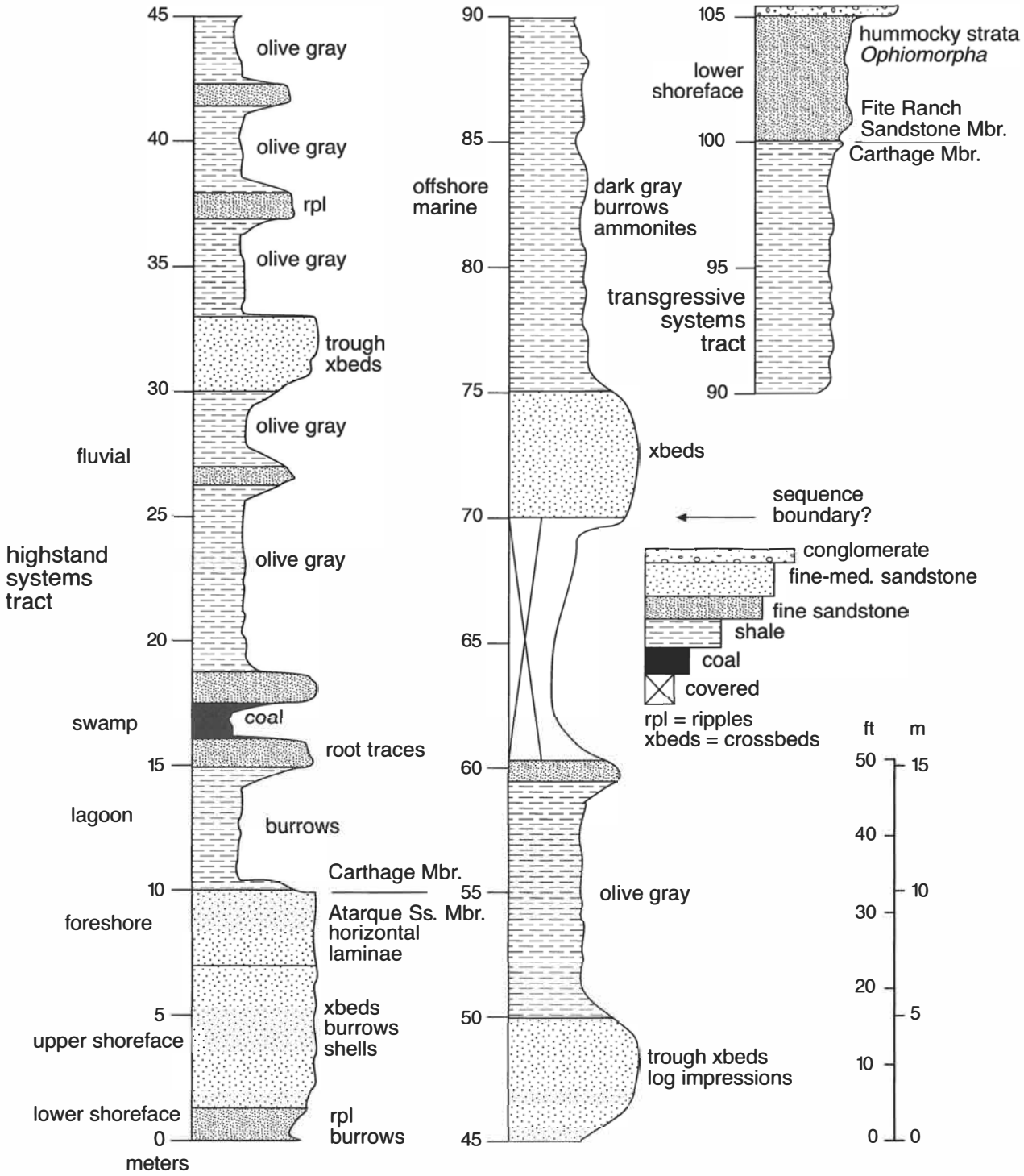

FIGURE 43—Measured section of the Tres Hermanos Formation (Upper Cretaceous) in Mescal Canyon (S½ sec. 36 T13S R4W).

anch Sandstone (Hook et al., 1983). The stratigraphic nomenlature of the Tres Hermanos Formation was first applied to Mescal Canyon in the Caballo Mountains by Wallin (1983) and Molenaar (1983a), and the best outcrops of the formation are in Mescal Canyon (S½ sec. 36 T13S R4W). The formation is also xposed in Putnam Draw (NE¼ sec. 22 and NW¼ sec. 23 T15S 3W), although structural complications prevent measurement f a complete section. The lower part of the Tres Hermanos ormation is also exposed at Hidden Tank (NE¼ sec. 5 T17S 3W). In south-central New Mexico, the Tres Hermanos Formation ranges in age from late early Turonian to earliest late Turonian (Hook et al., 1983; Hook, 1983). In Mescal Canyon, the Tres Hermanos Formation is 105 m (344 ft) thick, and includes 10 m (33 ft) of the Atarque Member, 90 m (295 ft) of the Carthage Member, and 5 m (16 ft) of the Fite Ranch Member (Fig. 43).

Description

The Atarque Sandstone Member is composed of 10 m (33 ft) of ridge-forming tan sandstone that coarsens upward. The Atarque displays a vertical change in primary sedimentary structures

from symmetrical ripple marks, to trough crossbeds, to horizontal laminae. The degree of bioturbation decreases upsection, as well as changing from predominantly horizontal to predominantly vertical burrows (Fig. 43).

The base of the Carthage Member consists of heavily bioturbated dark-gray shale, overlain by thin sandstones with root traces and a thin coal (Fig. 43). The bulk of the Carthage Member, however, is composed of ledge-forming, tan to brown, fine- to medium-grained sandstone 1–5 m (3.3–16 ft) thick, separated by thicker intervals of olive-gray mudstone and thin, < 1 m (< 3.3 ft), fine-grained sandstones. The thicker sandstones contain trough crossbeds, as well as a few asymmetrical ripple cross-laminae, mudstone rip-up clasts, and wood impressions. Crossbed paleocurrents measured by Wallin (1983) indicate paleoflow to the northeast. Olive-gray mudstones have a blocky fabric and locally display fine root traces, while the thin sandstone interbeds commonly have burrows and root traces and less commonly have asymmetrical ripple cross-laminae. The uppermost shale in the Carthage Member at Mescal Canyon is dark gray and contains interbeds of gray, very fine grained, heavily bioturbated sandstone. Several ammonites have been collected in this study from the upper dark shale.

The upper 5 m (16 ft) of the Tres Hermanos Formation consists of light-colored fine-grained sandstones assigned to the Fite Ranch Sandstone Member (Wallin, 1983; Mack et al., 1998a). Hummocky stratification and *Ophiomorpha* burrows are common in the Fite Ranch Sandstone Member, and the upper 0.5 m (1.6 ft) consists of dark-brown, calcareous, granular, medium-grained sandstone with shell fragments and shark teeth (Fig. 44).

Depositional environments

The Tres Hermanos Formation represents the upper part of the R1 regression and the lower part of the T2 transgression of Molenaar (1983a). In sequence stratigraphic terminology, the R1 regression is a highstand systems tract, and the T2 transgression is a transgressive systems tract (cf. Van Wagoner et al., 1990). The Atarque Sandstone and basal Carthage Members at Mescal Canyon are interpreted to represent progradation of a barrier island system. The Atarque Sandstone Member displays a vertical stacking of lower shoreface (bioturbated sandstone with wave oscillation ripples), to upper shoreface (crossbedded sandstone with shell hash and vertical burrows), to foreshore (horizontally laminated sandstone with vertical burrows; cf. Howard and Reineck, 1981). Overlying the foreshore sandstone, and constituting the base of the Carthage Member, are heavily bioturbated shale, interpreted to be lagoonal, and rooted sandstones and coal, deposited in a coastal swamp. The overlying thick sandstones of the Carthage Member were deposited in fluvial channels that flowed northeastward, whereas mudstones and interbedded thin sandstones represent overbank and crevasse-splay environments, respectively.

Onset of the T2 transgression begins with gray, bioturbated, and fossiliferous shale and sandstones at the top of the Carthage Member and continues into lower shoreface deposits of the Fite Ranch Sandstone Member. These beds constitute a lowstand systems tract and imply that somewhere below them is a sequence boundary, although because it is within non-marine rocks, its exact position is not known (Fig. 43; Mack et al., 1998b). The uppermost brown, granular sandstone of the Fite Ranch Sandstone Member is a transgressive lag that defines the flooding surface that separates the Tres Hermanos Formation from deeper-water sediment of the D-Cross Tongue of the Mancos Shale.

D-Cross Tongue of the Mancos Shale

At Mescal Canyon and Putnam Draw, the Tres Hermanos Formation is conformably overlain by the D-Cross Tongue of the Mancos Shale. Throughout south-central New Mexico, the D-Cross Tongue is late Turonian in age, although it probably becomes younger toward the south and southwest (Dane and Bachman, 1957; Molenaar, 1983a; Hook, 1983; Wallin, 1983; Cobban and Hook, 1989). At Mescal Canyon the D-Cross is approximately 50 m (164 ft) thick, whereas at Putnam Draw it is only about 20 m (66 ft) thick. Dark shale of the D-Cross immediately overlies a dark-brown granular sandstone of the Fite Ranch Sandstone Member, and grades upward into the Gallup Sandstone by the progressive addition of sandstone beds.

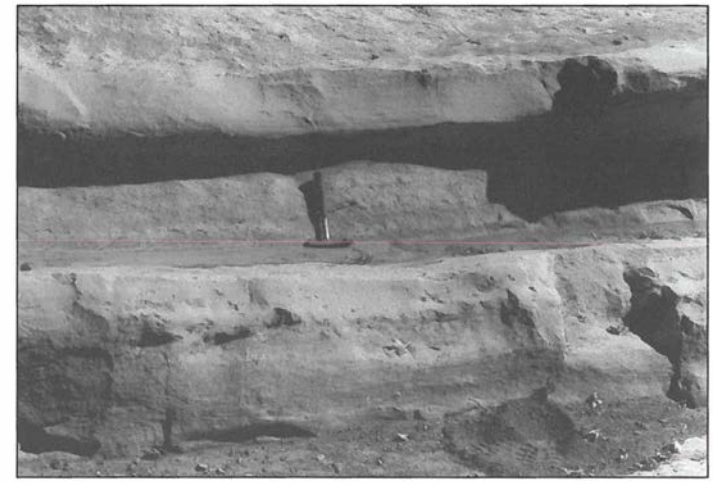

FIGURE 44—Medium-bedded, fine-grained sandstones of the Fite Ranch Sandstone Member of the Tres Hermanos Formation (Upper Cretaceous) exhibiting hummocky stratification and bioturbation in Mescal Canyon. Hammer is 25 cm (9.8 inches) long.

Description and depositional environments

The D-Cross Tongue consists primarily of dark-gray, fissile shale that locally contains dark-brown, calcareous concretions. An ammonite was taken from one of the concretions. In the upper and lower parts of the formation are several thin, < 1 m (< 3.3 ft), fine-grained sandstones with horizontal burrows and scattered shell fragments.

The D-Cross Tongue was deposited in prodelta to delta front environments, and constitutes the upper part of the T2 transgression and the lower part of the R2 regression of Molenaar (1983a). The turn-around point, or time of maximum water depth, between the T2 transgression and R2 regression appears to be near the middle of the formation, where the shale to sandstone ratio is the highest. In the context of sequence stratigraphy, the lower part of the D-Cross belongs to a transgressive systems tract, while the upper part initiates a highstand systems tract that continues into the base of the Gallup Sandstone (Mack et al., 1998b).

Gallup Sandstone

In the Caballo Mountains, the D-Cross Tongue of the Mancos Shale is conformably overlain by the Gallup Sandstone, whose type section is a few kilometers east of Gallup, New Mexico (Sears, 1925; Molenaar, 1983b). In the Caballo Mountains, the Gallup Sandstone is best exposed in Mescal Canyon (Fig. 45), whereas only the lower part is well exposed in Putnam Draw. The Gallup is absent at Hidden Tank, because of Laramide erosion. The Gallup Sandstone has also been described in the Love Ranch area of the southern San Andres Mountains, which constitutes the southernmost exposure of the formation (Seager, 1981). Throughout south-central New Mexico, the Gallup Sandstone is time transgressive, ranging in age from early late Turonian to early Coniacian and becoming younger to the east-northeast (Molenaar, 1983a,b; Cobban and Hook, 1989). At Mescal Canyon, the Gallup is 40 m (131 ft) thick, whereas at

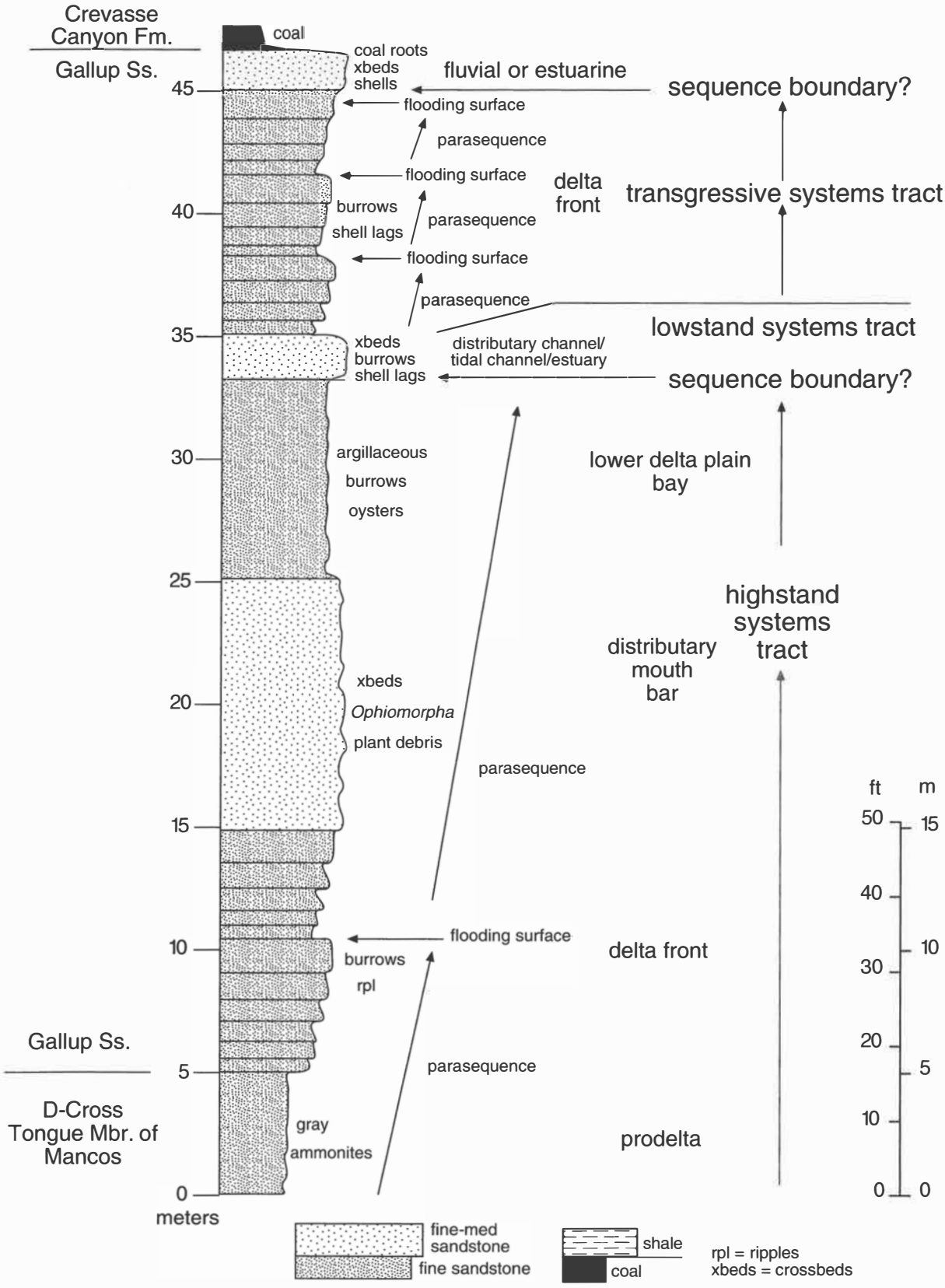

FIGURE 45—Measured section of the Gallup Sandstone (Upper Cretaceous) in Mescal Canyon (S½ sec. 36 T13S R4W).

Putnam Draw it is 33 m (108 ft) thick. The upper contact with the Crevasse Canyon Formation is conformable and is placed at the base of a thin coal at Mescal Canyon (Fig. 45).

Description

The Gallup Sandstone in the Caballo Mountains is divisible into three parts, each of which is well exposed at Mescal Canyon (Fig. 45). The lower part is characterized by a systematic upsection increase in the number and thickness of beds of fine sandstone at the expense of intercalated gray, silty shales. By the top of the lower part, shale beds are absent, and the prevalent rock type is tan to light-brown, thin- to medium-bedded, very fine to fine-grained sandstone. Sedimentary structures include horizontal laminae, hummocky stratification, ripple cross-laminae, and numerous horizontal and a few vertical burrows. At Mescal Canyon, this part of the Gallup is arranged into two cycles characterized by the upward thickening of beds. The contact between the upward-thickening cycles is occupied by a zone of dark-brown, calcareous concretions containing shell fragments.

The middle of the Gallup Sandstone is characterized by a 10 m (33 ft) thick sandstone that makes a prominent ridge or cliff (Fig. 46). The light-colored sandstone is fine to medium grained and thick bedded or massive. Bioturbation is less common than in underlying sandstones, although the upper bed surface is locally covered by a dense network of *Ophiomorpha* burrows (Fig. 47). Crossbeds, horizontal laminae, and ripple cross-laminae are rare in the middle sandstone. A distinctive feature is the presence of dark, finely macerated plant debris.

The upper part of the Gallup Sandstone begins with a dark-gray, argillaceous sandstone containing numerous burrows and whole oyster shells. Truncating the oyster-bearing sandstone is a sandstone channel containing a shell lag at the base, trough crossbeds, and a few vertical burrows near the top. The sandstone channel is overlain by gray, thin-bedded, heavily bioturbated very fine to fine-grained sandstones similar in appearance to those in the lower part of the formation. Several thin, < 20 cm (< 7.9 in), sandstone beds with sharp erosional bases and numerous shell fragments are present within this interval. The uppermost bed in the Gallup is a sandstone that exhibits channel morphology and has trough crossbeds and a few bivalve shell fragments. The upper part of this sandstone is darkened by coaly root traces and is overlain by a thin coal that marks the base of the Crevasse Canyon Formation (Mack, 1992).

Depositional environments

The Gallup Sandstone in the Caballo Mountains was deposited by a small delta during the R2 regression of Molenaar (1983a). The upper part of the D-Cross Tongue and lower and middle parts of the Gallup are interpreted to represent deposition in prodelta, delta front, and distributary mouth bar environments, respectively. A deltaic model for the Gallup is supported by (1) the greater thickness of the Gallup compared to the barrier island sandstones of the Atarque Sandstone Member of the Tres Hermanos Formation; (2) the absence of a systematic vertical change in sedimentary structures diagnostic of prograding beaches and barrier islands; and (3) the abundance of fine macerated plant debris, which is characteristic of many modern delta front and distributary mouth bar sands (Coleman and Prior, 1980). The oyster-bearing sandstones above the distributary mouth bar sandstone are interpreted to represent brackish bays on the lower delta plain. The upper part of the formation consists primarily of delta front sandstones identical to those at the base of the formation, overlain and underlain by channel sandstones that may represent distributary channels, tidal channels, or estuaries (Fig. 45).

The vertical juxtaposition of facies in the Gallup Sandstone has interesting implications in the context of sequence stratigraphy

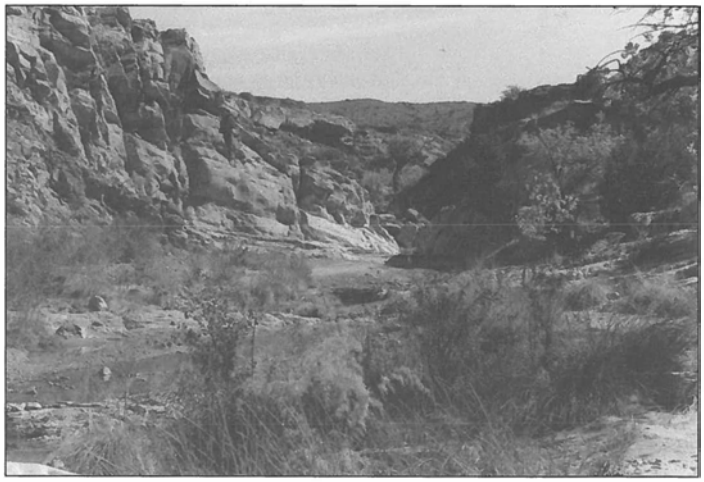

FIGURE 46—View to the southeast of thick sandstone ledges in the middle part of the Gallup Sandstone (Upper Cretaceous) in Mescal Canyon.

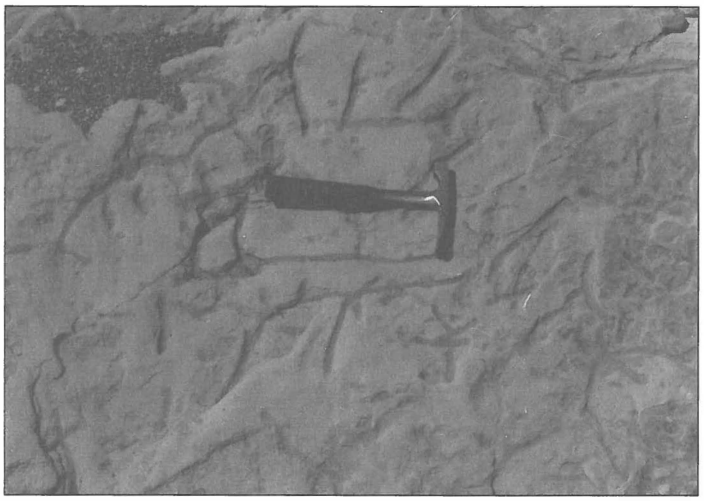

FIGURE 47—Bedding plane view of top of middle sandstone of the Gallup Sandstone (Upper Cretaceous) showing numerous *Ophiomorpha* burrows. Hammer is 25 cm (9.8 inches) long.

(Fig. 45; Mack et al., 1998b). The interval from the upper D-Cross through the oyster-bearing sandstones of the Gallup constitutes a prograding delta deposited as a highstand systems tract during the R2 regression of Molenaar (1983a; Fig. 45). The part of the highstand systems tract illustrated in Figure 45 is composed of two parasequences, defining a progradational parasequence set (cf. Van Wagoner et al., 1990). The lower parasequence consists of prodelta shales and the lower upward-thickening cycle of delta-front sandstones, whereas the upper parasequence includes the upper interval of delta-front sandstones, the distributary mouth bar sandstone, and the oyster-bearing sandstones deposited in bays on the lower delta plain. The flooding surface separating the parasequences is marked by the dark-brown, calcareous concretions with shell fragments. Conforming to the definition of a progradational parasequence set, the upper parasequence has more landward facies than the lower parasequence (cf. Van Wagoner et al., 1990).

The presence of delta-front sandstones above the oyster-bearing sandstones of the lower delta plain indicates a substantial rise in sea level and deposition of a transgressive system tract, which is composed of an aggradational parasequence set consisting of three parasequences entirely within delta-front sandstones and capped by shell-rich lags marking the flooding surfaces. An important consequence of the upper transgressive sys-

FIGURE 48—In situ petrified Angiosperm stump in the Crevasse Canyon Formation (Upper Cretaceous). Hammer is 25 cm (9.8 inches) long.

tem tract is that the channel sandstone directly above the oyster-bearing sandstone and beneath the upper delta-front sandstones may mark a sequence boundary and represents deposition in a tidal channel or estuary in a lowstand systems tract. Similarly, the channel sandstone at the top of the Gallup represents a significant landward shift of facies and may mark a second sequence boundary. In order to test these ideas, the Gallup will have to be examined and correlated on a regional scale in both the surface and subsurface.

Crevasse Canyon Formation

The Crevasse Canyon Formation was defined by Allen and Balk (1954) for largely non-marine sedimentary rocks above the Gallup Sandstone and beneath the Point Lookout Sandstone. Wallin (1983) and Molenaar (1983a) applied the name Crevasse Canyon Formation to non-marine rocks above the Gallup Sandstone in Mescal Canyon in the Elephant Butte quadrangle, despite the fact that the Point Lookout Sandstone is not present. Wallin (1983) further subdivided the Crevasse Canyon Formation in Mescal Canyon into a lower coal-bearing member, middle barren member, and upper Ash Canyon member. We were unable to consistently distinguish between the coal-bearing and barren members in the Cutter, Upham, and Engle quadrangles. Consequently, we divided the Crevasse Canyon Formation into only two members, a lower member consisting of interbedded brown and olive mudstone and sandstone, and the Ash Canyon member, composed primarily of light-colored sandstone.

No age-diagnostic body fossils have been found in the Crevasse Canyon Formation in the Caballo Mountains. However, pollen was recovered from a single shale in the lower member east of Mescal Canyon and sent to Arthur Sweet of the Canadian Geological Survey, National Resources Canada, for identification. This sample contains *Labrapollis* sp., *Pseudoplicapollis cuneata*, and *Aquilapollenites*, indicating a probable early Campanian age. The pollen data, plus the conformable contact with the Gallup Sandstone, suggest that the Crevasse Canyon Formation in the Caballo Mountains spans part of the Coniacian, the Santonian, and at least the lower part of the Campanian. The Crevasse Canyon Formation is unconformably overlain by the McRae Formation. The thickness of the Crevasse Canyon Formation in the Caballo Mountains is approximately 671 m (2,200 ft), including 305 m (1,000 ft) of lower member and 366 m (1,200 ft) of Ash Canyon member.

Despite a broad outcrop area in the Cutter, Upham, Apache Gap, Palomas Gap, Elephant Butte, and Engle quadrangles, the lower member of the Crevasse Canyon Formation is not well exposed. The best outcrops of both sandstone and mudstone are confined to deep arroyos. Sandstones of the Ash Canyon member are better exposed than those of the lower member and form low hogbacks, cuestas, and mesas. Mudstones of the Ash Canyon member are generally only exposed in deep arroyos. The contact between the Ash Canyon member and lower member is mutually intertonguing. Prominent beds of Ash Canyon sandstone can locally be found as low as the middle part of the lower member. More commonly, one to three Ash Canyon tongues, each about 9–15 m (30–48 ft) thick, exist in the upper 60–90 m (197–295 ft) of the lower member. An attempt was made to map these tongues separately, at least where they form prominent outcrops, and to place the Ash Canyon–lower member contact above these tongues at the base of a nearly continuous section of sandstone. This strategy was not always successful, and locally the basal contact of the Ash Canyon member may actually represent the base of Ash Canyon tongues tens of meters below the mapped contact elsewhere.

Description

The lower member of the Crevasse Canyon Formation consists of ledge-forming sandstones interbedded with slope-forming intervals of mudstone and thin sandstones. The ledge-forming sandstones are gray, tan, or greenish brown, fine to medium grained, and exhibit sharp erosional lower contacts and gradational upper contacts characterized by thin interbeds of sandstone and mudstone. Sheetlike to lenticular in shape, the sandstones range from 2 to 8 m (6.6 to 26 ft) thick. Trough crossbedding is the most common sedimentary structure, but horizontal laminae with parting lineation, asymmetrical ripple cross-laminae, and thin horizons of mudstone rip-up clasts are also present. Several sandstone beds contain large, 2 m (6.6 ft), diameter, dark-brown, calcareous to ferruginous concretions.

Poorly exposed mudstone interbedded with thin, < 1 m (< 3.3 ft), sandstones separate the ledge-forming sandstones of the lower member. Mudstones are gray to olive gray and commonly display a blocky texture and fine root traces. The interbedded thin sandstones are dark brown, olive brown, or tan, fine to very fine grained, and either exhibit horizontal laminae and asymmetrical ripple cross-laminae or have pervasive root traces and burrows that obliterate most primary sedimentary structures. Leaf and stem fossils are present in some of the thin sandstones, although they are not common.

The Ash Canyon member contains a higher percentage of sandstone and less mudstone than the lower member. In addition, the sandstones are lighter colored, thicker, and coarser grained than those of the lower member. Ash Canyon sandstones are as much as 15 m (49 ft) thick and commonly are medium to coarse grained with thin beds or lenses of quartz and chert pebbles. A sparkly appearance is diagnostic of Ash Canyon sandstones, probably related to crystal faces on quartz cement. Like sandstones in the lower member, Ash Canyon sandstones display trough crossbeds, horizontal laminae, and ripple cross-laminae. Mudstones and interbedded thin sandstones are also present in the Ash Canyon member, although they are less abundant than in the lower member. Several in situ petrified Angiosperm stumps are present in the Ash Canyon member in the northern part of the Upham quadrangle (Fig. 48).

Depositional environments

Both the lower and Ash Canyon members of the Crevasse Canyon Formation are fluvial in origin. The main difference between the members is that the Ash Canyon channel sandstones are multistory sheets, whereas channels in the lower member tend to be single story sheets and ribbons. Crossbed paleocurrent data collected by Wallin (1983) indicate paleoflow to the northeast, a direction consistent with the inferred north-

west-trending shorelines of the Western Interior Seaway in New Mexico (Molenaar, 1983a). Paleosols are common in the overbank mudstones. The most mature paleosols consist of a thin, gray A horizon, a light-colored E horizon, and a thick, olive-gray, argillic B horizon, indicative of well drained soils in a relatively humid climate (Mack, 1992). Rarely, the paleosols are carbonaceous or coaly, suggesting waterlogged soils associated with a high water table. Thin sandstones interbedded with the overbank mudstones are interpreted to have been deposited as crevasse splays.

Cretaceous Western Interior foreland basin

Cretaceous sedimentary rocks in the Rocky Mountains of the USA and Canada are generally interpreted to have been deposited in a foreland basin that was complementary to the Sevier fold and thrust belt (Jordan, 1981; Lawton, 1985, 1994; Heller et al., 1986; DeCelles and Currie, 1996). The basin subsided in response to emplacement of thrust sheets generated in a back-arc setting. Although sedimentation was primarily influenced by erosion of sediment from the fold and thrust belt, relative sea-level changes in the Western Interior Seaway also locally influenced basin architecture, particularly in the distal parts of the basin. The widespread nature of some of the transgressions suggests a significant eustatic component.

Despite similarities in the basic stratigraphy, Upper Cretaceous sedimentary rocks in New Mexico display several differences compared to coeval rocks farther north that suggest along-strike variations in the nature of the foreland basin. Unlike farther north, Upper Cretaceous sedimentary rocks in New Mexico are thin and do not thicken dramatically southwestward toward the presumed source (cf. McGookey et al., 1972). Moreover, no thrust faults of the appropriate age have been recognized southwest of the exposures of Upper Cretaceous rocks in New Mexico in the area that was presumably the source of the detritus. Instead, Cretaceous sedimentary rocks in the Burro Mountains of southwestern New Mexico unconformably overlie Precambrian crystalline basement, which was exposed along the northern shoulder (Mogollon–Burro massif of Lawton, 1994) of the extensional Bisbee Basin/Chihuahua trough. These data suggest that thrust loading may not have been the driving force for subsidence in the New Mexico part of the Cretaceous foreland basin, although it is not yet clear what caused this part of the basin to subside.

Even though a tectonic model for the New Mexico part of the Cretaceous foreland basin remains elusive, provenance of the sandstones provides evidence for the rocks exposed in the source area. Sandstones of the Tres Hermanos, Gallup, and Crevasse Canyon Formations are lithofeldspathic and were derived from a mixture of volcanic, sedimentary, and low-grade metamorphic source rocks (Table 1). Volcanic rock fragments are the most common lithic grains and are composed of plagioclase laths and a few mafic minerals or, less commonly, of plagioclase and quartz. These lithic grains indicate andesitic to dacitic source rocks. In addition, the Ash Canyon member of the Crevasse Canyon Formation also contains volcanic-lithic grains composed of a microcrystalline mosaic of quartz and potassium feldspar, which appear to have been derived from volcanic rocks of silicic composition. Other lithic grains include chert and pelitic rock fragments, indicative of a sedimentary provenance, and a few foliated quartz-mica rock fragments derived from low-grade metamorphic rocks. The principal feldspar is plagioclase, which is consistent with derivation from intermediate to silicic volcanic rocks. Potassium feldspar is relatively uncommon. Also present, but not common, are feldspar grains with a distinctive checkerboard twinning. Because these grains are not stained by sodium cobaltinitrite, they are probably albitized potassium feldspars (cf. Middleton, 1972; Johansen, 1986). The abundance of grains derived from andesitic volcanic rocks suggests that the continental-margin arc may have been a significant contributor of sand to the foreland basin in New Mexico, a provenance that was rare in the foreland basin farther north. Alternatively, the volcanic source rocks may have resulted from uplift of Bisbee Basin or arc-related volcanics in southern Arizona, an idea more fully developed by Cumella (1983) in his study of Upper Cretaceous rocks of the San Juan Basin.

TABLE 1—Detrital modes of medium or fine- to medium-grained sandstones of the Crevasse Canyon and McRae Formations, based on 300 points per sample for the Crevasse Canyon and 200 points per sample for the McRae. **MXQ** = monocrystalline quartz; **PXQ** = polycrystalline quartz; **KSP** = potassium feldspar; **PLG** = plagioclase feldspar; **CHT** = chert; **PRF** = pelitic rock fragment; **MRF** = metamorphic rock fragment; **VRF** = volcanic rock fragment; **QFF** = quartzo-feldspathic rock fragment; **ACC** = accessory minerals.

			MXQ	PXQ	KSP	PLG	CHT	PRF	MRF	VRF	QFF	ACC
	lower	UK-24	34.3	10.0	4.5	23.5	4.3	1.7	1.3	19.0	1.3	0.0
	member	UK-25	35.7	5.0	6.7	19.3	9.7	1.3	1.7	17.7	3.0	0.0
Crevasse		UK-26	41.3	8.0	6.7	19.3	7.0	2.0	2.0	12.7	1.0	0.0
Canyon		UK-27	29.0	5.3	5.7	22.0	12.7	2.0	2.3	19.7	1.3	0.0
Formation												
	upper	UK-30	55.3	7.6	5.3	9.3	11.7	1.0	1.7	6.7	1.3	0.0
	member	UK-31	52.0	5.0	8.0	8.7	15.3	2.3	0.3	7.7	0.7	0.0
		UK-32	66.7	9.3	5.0	4.0	11.3	0.0	0.3	2.3	1.3	0.0
		UK-33	53.7	11.0	6.3	3.0	16.0	0.7	2.3	5.7	1.7	0.0
		UK-34	64.0	11.0	3.3	3.0	15.0	0.0	1.3	1.3	1.0	0.0
	Jose	Kmj-1	19.0	5.5	0.0	35.5	9.5	1.0	0.5	29.0	0.0	0.0
	Creek	Kmj-4	5.5	0.0	0.0	23.0	1.0	0.0	0.0	70.0	0.0	0.5
	Member	Kmj-5	18.5	1.0	0.0	39.0	8.0	0.0	0.0	33.0	0.0	0.0
		Kmj-12	1.0	0.0	0.0	51.0	2.0	0.0	0.0	45.0	0.0	1.0
McRae		Kmj-14	0.0	0.0	0.0	38.0	0.0	0.0	0.0	62.0	0.0	0.0
Formation												
	Hall	Kmh-1	0.0	0.0	0.0	31.0	0.0	0.0	0.0	69.0	0.0	0.0
	Lake	Kmh-6	1.0	0.0	0.0	31.0	0.0	0.0	0.0	68.0	0.0	0.0
	Member	Kmh-8	0.0	0.0	0.0	60.0	0.0	0.0	0.0	40.0	0.0	0.0
		Kmh-13	8.0	1.0	0.0	52.5	1.5	0.0	0.0	37.0	0.0	0.0

Upper Cretaceous volcanic arc rocks

The large size of volcanic boulders within the McRae and basal Love Ranch Formations as well as transport direction indicators suggest that a series of volcanic rocks covered much of the Caballo Mountains area in Late Cretaceous (Campanian–Maastrichtian) time. Although these rocks were completely eroded from the Caballo area during the Laramide orogeny, remnants of the volcanic field, as well as Upper Cretaceous intrusive rocks, are present in the Animas Mountains along the western margin of the Black Range. Dated 68–75 Ma (Hedlund, 1977; Kelley and Chapin, 1997), these volcanic rocks and intrusives are associated with an apparently collapsed stratovolcano located east-northeast of Hillsboro, that may have been a source for at least some of the volcanic series in the Caballo area.

Description

From a detailed study of clasts in the McRae and lower Love Ranch Formations, Chapman-Fahey (1996) reconstructed the general character of the volcanic field. Dacite, trachydacite, and trachyandesite were the most common lavas and/or intrusive rocks, most of which were aphanitic-porphyritic in texture. Lesser amounts of rhyolite, rhyolite tuff, and breccia were also present within the field. Silica content ranged from 56% to 77%. The clasts in the McRae Formation are similar chemically and petrographically to the outcropping Upper Cretaceous igneous rocks in the Animas Mountains area, but clasts in the Love Ranch Formation are different and their origin is unknown.

Mode of emplacement and tectonic setting

The volcanic series was emplaced as lava flows and/or hypabyssal intrusives and probably lahar deposits across the Caballo area. Sources may have been the igneous centers in the Animas Mountains, or, more likely, centers closer to the Caballo area, now buried beneath the Palomas Basin. Trace element signatures for the clasts in the McRae and Love Ranch Formations are consistent with a continental arc tectonic setting (Chapman-Fahey, 1996), making these rocks the northeastern limit in New Mexico of an Upper Cretaceous volcanic arc extending southwesterly into the bootheel region of New Mexico. Trace element patterns also suggest a systematic "unroofing" of the volcanic sequence, probably in response to Laramide uplift and erosion, which closely followed emplacement of the volcanic rocks.

Laramide orogeny

During latest Cretaceous and early Tertiary time, the western interior of the USA, including southern New Mexico, experienced compressional deformation referred to as the Laramide orogeny. The Cretaceous foreland basin was segmented by a series of basement-cored block uplifts separated by continental intermontane basins. In the Caballo Mountains and vicinity, Laramide basin-fill rocks belong to the McRae Formation (Maastrichtian–Paleocene?) and the Love Ranch Formation (Paleocene (?)–Eocene). The stratigraphy and sedimentology of these formations are described below, followed by a discussion of the structural and sedimentologic evolution of the Laramide Rio Grande uplift and complementary Love Ranch Basin in and around the Caballo Mountains.

McRae Formation

The McRae Formation was named by Kelley and Silver (1952) for exposures in the Elephant Butte quadrangle near Fort McRae, which is usually submerged beneath Elephant Butte Reservoir. Bushnell (1953, 1955) divided the McRae into two members, the lower Jose Creek and upper Hall Lake. The members were used as map units by many workers, including Lozinsky (1986) in the Elephant Butte quadrangle, by Mack and Seager (in press) in the Engle quadrangle, and by Seager and Mack (in press b) in the Cutter and Upham quadrangles.

The McRae Formation is considered to be latest Cretaceous (late Maastrichtian) in age, based on the presence of a Lancian dinosaur fauna (Lozinsky et al., 1984; Wolberg et al., 1986), including a jaw fragment assigned to *Tyrannosaurus rex* (Gillette et al., 1986) and a horn and skull fragments from *Torosaurus* (Lucas et al., 1998). Dinosaur bones have been found in both members of the McRae Formation, indicating that all of the Jose Creek Member and at least part of the Hall Lake Member are Maastrichtian in age. However, Lozinsky et al. (1984) and Wolberg et al. (1986) suggest the Hall Lake Member may cross the Cretaceous–Tertiary boundary. If so, this boundary has not yet been identified in the Hall Lake Member.

The Jose Creek Member of the McRae Formation unconformably overlies the Ash Canyon member of the Crevasse Canyon Formation and can be distinguished from it by darker color, more feldspathic sandstones, and overall coarser grain size. The Jose Creek Member is thickest in the Cutter Sag area east of Elephant Butte Reservoir and thins southward to a feather edge along the east-central flank of the Caballo Mountains. Near Kettle Top Butte in the Elephant Butte quadrangle, the Jose Creek Member is 170 m (558 ft) thick, whereas a few kilometers to the south in the Engle quadrangle it thins to 109 m (358 ft) (Fig. 49). Farther south, just north of Aleman Draw, the Jose Creek Member is 61 m (200 ft) thick, thinning southward to 30 m (98 ft) along the western edge of the Upham quadrangle.

The Hall Lake Member conformably overlies the Jose Creek Member throughout most of its outcrop area and is unconformably overlain by the Love Ranch Formation or by the Palomas Formation. The contact between the Jose Creek and Hall Lake Members is placed at the first appearance of deep-purple and red mudstone or sandstone or at the base of a thick quartzite-cobble and boulder conglomerate. A complete stratigraphic section of the Hall Lake Member is not present due to structural complications, and the maximum exposed thickness in the Engle quadrangle is approximately 235 m (771 ft). Bushnell (1953, 1955) suggested that the Hall Lake Member may be as much as 880 m (2,886 ft) thick, but this seems excessive. In the Elephant Butte quadrangle there does not appear to be more than 400 m (1,312 ft) of the Hall Lake Member exposed. Like the Jose Creek Member, the Hall Lake Member thins southward. The Hall Lake Member is estimated to be 183 m (600 ft) thick at Aleman Draw where it overlies the Jose Creek Member. Farther south at Yoast Draw the Hall Lake Member thins to less than 15 m (49 ft), where it overlies the Crevasse Canyon Formation with angular unconformity, the Jose Creek Member having pinched out between the two drainages.

Jose Creek Member

The Jose Creek Member consists of brown to greenish-gray conglomeratic sandstone and conglomerate, interbedded olive-gray mudstone and brown fine-grained sandstone, and tan to purple volcanic ash (Fig. 49). Conglomeratic sandstones are present

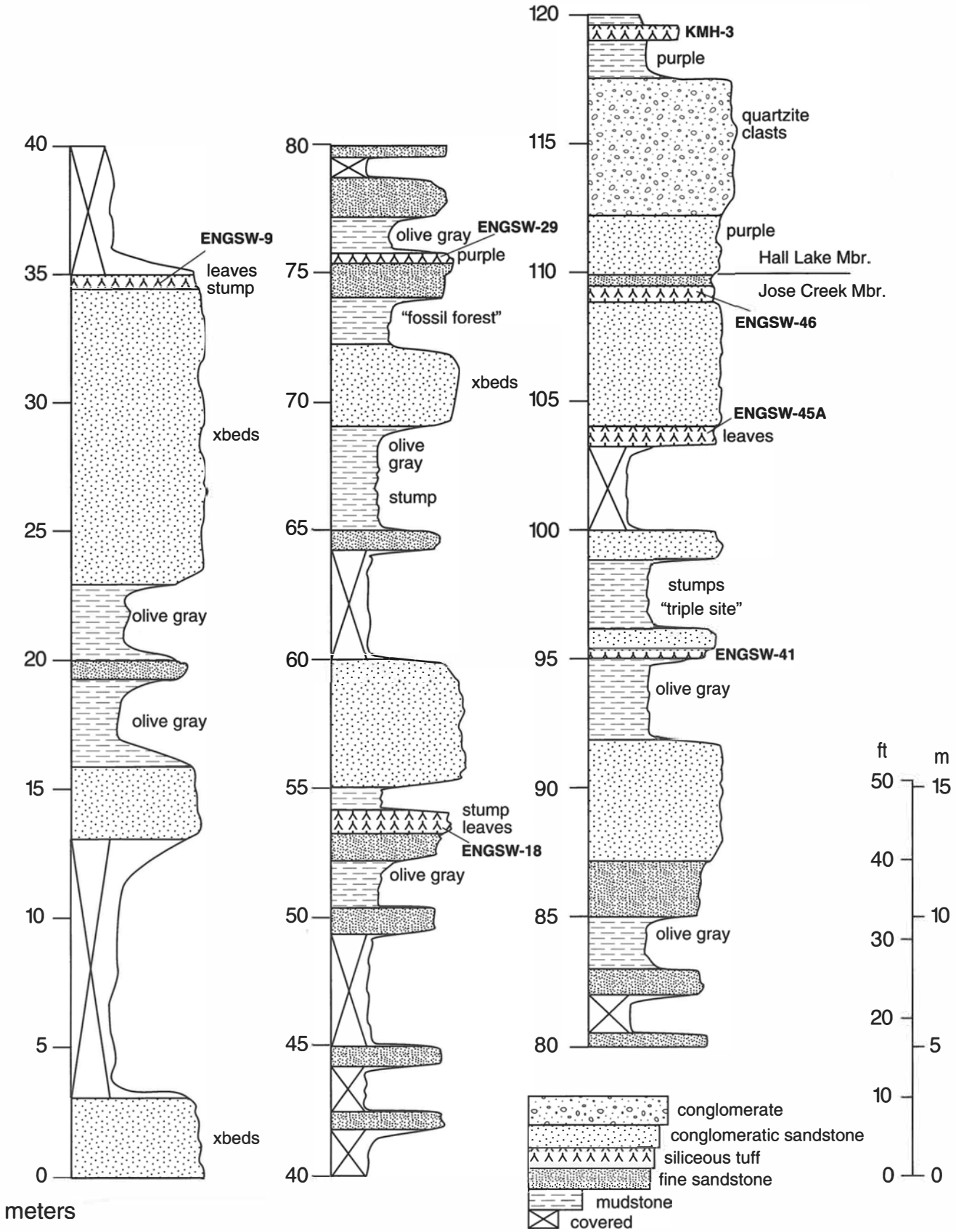

FIGURE 49—Measured section of the Jose Creek Member and lowermost Hall Lake Member of the McRae Formation (Upper Cretaceous; Maastrichtian) near McRae Canyon, southwestern Engle quadrangle. xbeds = crossbeds. **ENGSW-9, 18, 29, 41, 45A,** and **46** and **KMH-3** refer to siliceous tuffs in Table 2.

FIGURE 50—Thin ledge of highly fractured, tan fallout tuff in the Jose Creek Member of the McRae Formation (Upper Cretaceous; Maastrichtian) near McRae Canyon. This tuff is located between 34 and 35 m (111 and 115 ft) on the measured section of Fig. 49. Hammer is 25 cm (9.8 inches) long.

FIGURE 52—Cobble conglomerate near the base of the Hall Lake Member of the McRae Formation (Upper Cretaceous; Maastrichtian) near McRae Canyon. Most of the clasts are quartzite of unknown provenance. Hammer is 25 cm (9.8 inches) long.

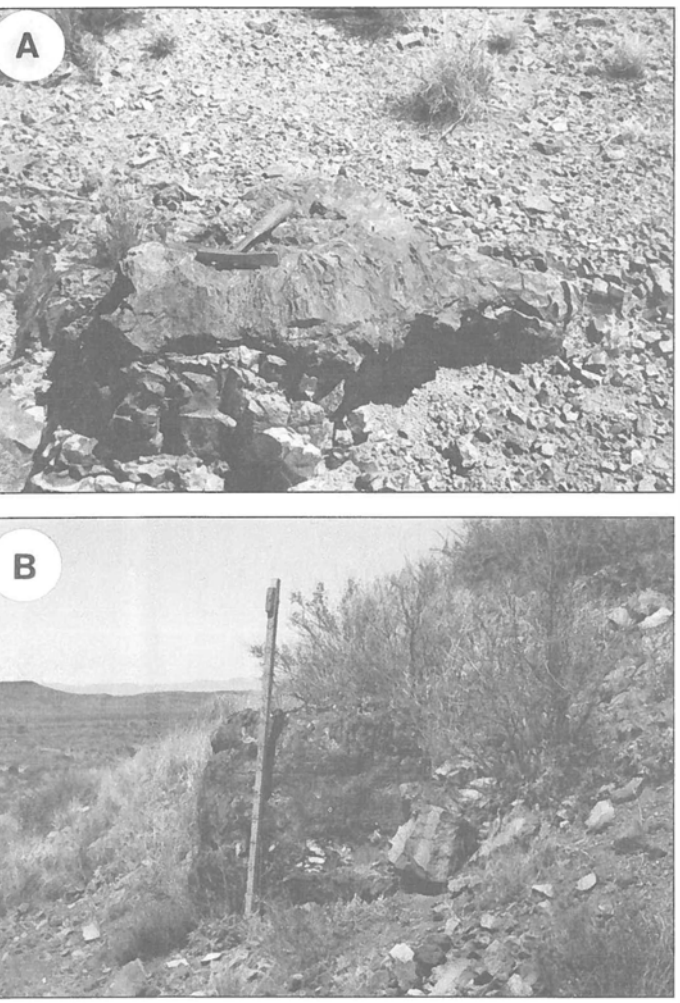

FIGURE 51—In situ petrified stumps in the Jose Creek Member of the McRae Formation (Upper Cretaceous; Maastrichtian) near McRae Canyon. **A**—Angiosperm stump located at the "fossil forest" site of the measured section of Fig. 49. Hammer is 25 cm (9.8 inches) long. **B**—Conifer stump approximately 1 m (3.3 ft) in diameter. Jacob's staff is 1.5 m (4.9 ft) long.

throughout the outcrop area and range in thickness from 1.5 to 10 m (49 to 33 ft). The sandstones are medium to coarse grained and contain lags, lenses, or isolated clasts of pebbles, cobbles, and small boulders. Many conglomeratic sandstone beds are traceable laterally for up to a kilometer, although locally they may pinch out within a few hundred meters. Trough crossbeds are common, and horizontal laminae, ripple cross-laminae, and imbrication are locally present. Most commonly ridge formers, some conglomeratic sandstones weather as rounded slopes. In contrast to the conglomeratic sandstones, cobble and boulder conglomerates are present only in the southernmost exposures of the Jose Creek Member. Up to 10 m (33 ft) thick, the conglomerates are either grain supported with imbrication and thin sandstone lenses or are matrix supported and lack any internal layering. Intermediate-composition volcanic rocks, most commonly andesite porphyry, constitute the gravel-sized clasts, although gray and white chert pebbles are locally present near the base of the member and a pebble layer containing pink and red quartzite clasts was observed in the Engle quadrangle. Four $^{40}Ar/^{39}Ar$ ages from altered andesite clasts at the base of the Jose Creek Member range in age from 43.3± 0.7 to 67 ± 2.9 Ma (Esser, 2003b). These dates are not considered to be reliable.

Most slope-forming intervals of the Jose Creek Member are underlain by interbeds of mudstone and thin, <1 m (<3 ft), fine-grained sandstone. Mudstones are olive gray or dark green in color, although bluish-green and light-purple colors are also present locally, especially near the top of the member. Mudstones generally have a blocky structure and commonly contain root traces, some of which are replaced by a red mineral identified by Buck (1992) as the zeolite heulandite. Interbedded with mudstones are ledge-forming, brown to tan, very fine to fine-grained sandstones. Ripple cross-laminae and horizontal laminae are locally present within the sandstones, but many beds lack current structures as a result of modification by root traces and burrows.

The least common rock type of the Jose Creek Member is siliceous tuff, which is most common in the upper half of the member. Although relatively thin, 0.3–1 m (0.98–3.3 ft), siliceous tuffs form laterally continuous ledges that display a closely spaced system of vertical joints (Fig. 50). Most siliceous tuffs weather to a light-tan or gold color, but are light green or gray on a fresh surface. In addition, there are also varieties of siliceous tuffs that weather to white or light-purple colors. The light-pur-

ple variety resembles chert in outcrop and is most common in the upper part of the member. Bushnell (1953, 1955) referred to all of the siliceous tuffs as chert. Most of the siliceous tuffs lack any evidence of internal stratification, but a few display graded bedding, horizontal laminae, or ripple cross-laminae. Root traces may also be present in some beds. Petrographically, the siliceous tuffs consist primarily of a microcrystalline mosaic of quartz and clay and variable amounts of sand-sized crystals of feldspar, quartz, and biotite, which exist as either randomly scattered grains or as discrete laminae. A few samples display relict platy and cuspate glass shards recrystallized to microcrystalline quartz, as well as quartz crystals with euhedral bipyramids and embayed margins. Bulk chemical composition and trace element types and abundances are similar to those of silicic tuffs described by Winchester and Floyd (1977; Table 2). Five of the siliceous tuffs plot in the rhyolite field and four in the rhyodacite-dacite field on the SiO_2 versus Zr/TiO_2 variation diagram of Winchester and Floyd (1977).

Also common in the Jose Creek Member are leaf fossils and petrified wood. The plant fossils exist as impressions on bedding planes in sandstones, as well as in siliceous tuffs. Several of the tuffs in the Engle quadrangle have produced a large collection of leaves described by Upchurch and Mack (1998). At least 50 species of leaves have been collected, including ferns, conifers, cycads, and broadleaf Angiosperms. In addition, petrified conifer, Angiosperm, and palm wood are common as float in the Jose Creek Member and also exist locally as in situ stumps (Fig. 51), the largest of which is a conifer measuring 1.7 m (5.6 ft) in diameter. At two locations at the measured section (Fig. 49), referred to as the "fossil forest" and "triple site," more than one in situ stump is present, allowing determination of the spacing between the trees when they were alive.

Hall Lake Member

The Hall Lake Member is characterized by purple color of both mudstones and sandstones. Four rock types are present in the member, including mudstone, sandstone, quartzite-clast conglomerate, and pink, siliceous tuff. The most abundant rock type is slope-forming, purple, maroon, or light-green mudstone. The mudstone commonly has a blocky texture, and some beds display slickensides and meter-scale, concave-up fractures interpreted to be wedge-shaped peds. Also common in the mudstones are calcic nodules and tubules interpreted to be stage II morphology calcic paleosols (Buck, 1992; Buck and Mack, 1995). In a few cases, the nodules and tubules have coalesced into massive beds of carbonate that represent a stage III morphology calcic paleosol.

Sandstones of the Hall Lake Member are purple or pink, medium-grained, and range in thickness from 1 to 15 m (33 to 49 ft). The thickest sandstones are multistory in character, with individual stories bounded by erosional surfaces floored by conglomerate and/or rip-up clasts of mudstone and/or pedogenic carbonate. At Kettle Top Butte, a thick, 3 m (9.8 ft), lateral accretion set is preserved. Sedimentary structures include trough crossbeds, planar crossbeds, horizontal laminae, and straight to sinuous, horizontal burrows located near the top of some beds. Gravel-sized clasts are primarily volcanic, mostly andesite porphyry, although quartzite and granite clasts are locally present. The composition of the sand-sized fraction consists primarily of zoned plagioclase and volcanic rock fragments, and a minor amount of monocrystalline quartz (Table 1).

One of the most distinctive rock types in the Hall Lake Member is a thick, 2–10 m (6.6–33 ft), cobble and boulder conglomerate composed primarily of quartzite clasts (Fig. 52). This conglomerate is located 5–10 m (16–33 ft) above the base of the Hall Lake Member, although locally, because of deep scour, it directly overlies the Jose Creek Member. In many places the conglomerate is poorly cemented and is expressed as low hills or rounded knobs covered with loose gravel. The conglomerate becomes thinner and finer grained northward. Clasts are well rounded and grain supported, and imbrication is common. Quartzite clasts range in color from maroon, white, gray, and green. Also present are clasts of red granite and andesite porphyry. Two altered andesite clasts yielded $^{40}Ar/^{39}Ar$ ages of 70.82 ± 0.42 Ma and 89.7 ± 1.0 Ma from groundmass concentrate and biotite respectively (Esser, 2003b). The older date is spurious.

Another distinctive marker bed in the Hall Lake Member is a 1–2 m (3.3–6.6 ft) thick, ledge-forming, pink siliceous tuff, which is located stratigraphically above the quartzite-clast conglomerate and about 10–15 m (33–49 ft) above the base of the Hall Lake Member. The pink tuff lacks internal stratification and commonly is burrowed and/or rooted in its upper part. Petrographically,

TABLE 2—ICP chemical analyses of siliceous mudstones (ash-fall tuffs) of the McRae Formation. Stratigraphic positions of **ENGSW-9, 18, 29, 41, 45A, 46,** and **KMH-3** are shown in the Cretaceous stratigraphic column (Fig. 49); **ENGSW-FLOAT** and **ENGSW-PCH** are from the Jose Creek Member elsewhere in the quadrangle. **LOI** = loss on ignition.

	ENGSW-9 (wt%)	ENGSW-18 (wt%)	ENGSW-29 (wt%)	ENGSW-41 (wt%)	ENGSW-45A (wt%)	ENGSW-46 (wt%)	ENGSW-FLOAT (wt%)	ENGSW-PCH (wt%)	KMH-3 (wt%)
SiO_2 (wt%)	77.08	69.18	72.22	73.73	79.14	72.11	74.32	77.04	69.91
TiO_2 (wt%)	0.23	0.37	0.31	0.32	0.34	0.41	0.32	0.30	0.18
Al_2O_3 (wt%)	12.69	15.14	12.01	9.93	9.86	12.94	13.88	11.50	10.76
Fe_2O_3 (wt%)	0.91	3.55	4.62	5.92	1.80	3.30	0.69	2.30	1.73
MnO (wt%)	0.02	0.05	0.10	0.11	0.04	0.07	0.01	0.03	0.06
MgO (wt%)	0.20	0.66	0.68	0.81	0.33	0.58	0.05	0.20	1.16
CaO (wt%)	1.13	1.47	1.56	1.41	1.48	1.03	1.27	1.40	2.91
Na_2O (wt%)	7.28	7.08	4.87	3.07	2.91	3.25	7.82	4.74	0.27
K_2O (wt%)	0.00	0.16	0.39	0.66	1.99	3.72	0.04	1.10	0.49
P_2O_5 (wt%)	0.23	0.16	0.31	0.14	0.23	0.21	0.44	0.17	0.00
LOI (wt%)	1.14	2.14	3.16	3.93	2.54	2.67	1.08	1.50	10.80
Total (wt%)	100.91	99.96	100.23	100.03	100.66	100.29	99.92	100.28	98.27
	ppm	ppm	ppm	ppm	ppm	ppm	ppm	ppm	ppm
Sr (ppm)	74	399	350	227	292	296	135	386	>2500
Ba (ppm)	78	131	164	163	2115	2506	62	697	3118
Y (ppm)	21	27	31	21	31	30	26	23	18
Zr (ppm)	149	152	176	137	62	177	175	142	118
Sc (ppm)	2.8	4.7	6.8	8.7	7.2	6.7	4.7	4.4	14.7
V (ppm)	15	33	34	60	36	50	16	31	20

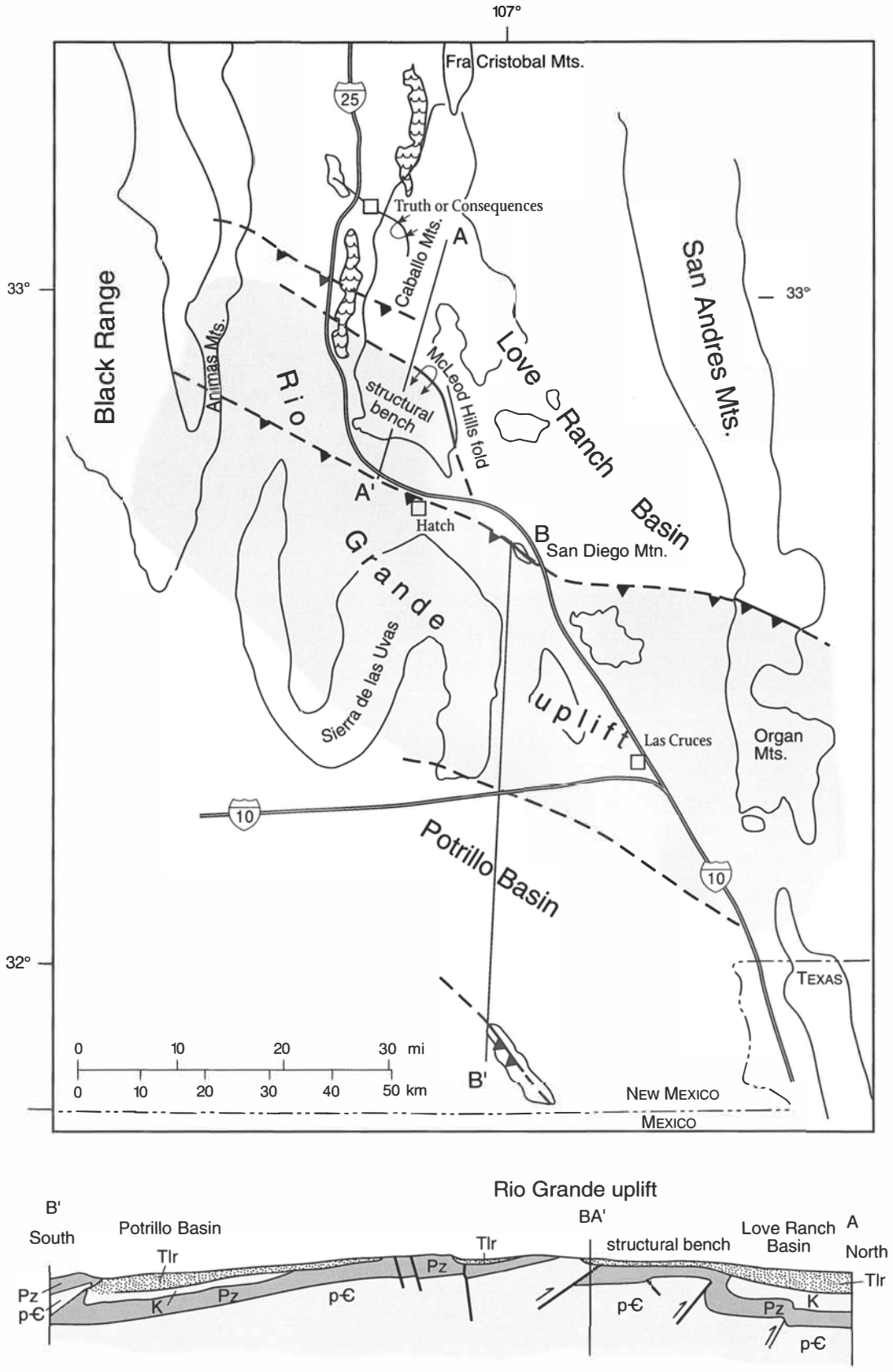

FIGURE 53—Tectonic map and diagrammatic cross section of Laramide Rio Grande uplift, Love Ranch Basin, and Potrillo Basin in south-central New Mexico. **p€** = Precambrian rocks; **Pz** = Paleozoic rocks; **K** = Cretaceous rocks; **Tlr** = Love Ranch Formation.

it is composed of relict platy and cuspate glass shards set in a microcrystalline matrix. Single sand-sized crystals of biotite, quartz, and feldspar are rare. The pink tuff is restricted to the Elephant Butte and Engle quadrangles.

Unlike the Jose Creek Member, plant fossils are rare in the Hall Lake Member. Stem and log impressions are rarely preserved along bedding planes of sandstones, and only one small, 30 cm (12 inches) diameter, in situ petrified stump was observed in the Engle quadrangle.

Depositional environments

The McRae Formation in the Elephant Butte and Engle quadrangles is interpreted to be fluvial in origin, although the type of fluvial system probably differed between the members. Thick sandstones and conglomeratic sandstones represent fluvial channels. In general, channel sandstone bodies are thicker and more multistory in character in the Hall Lake Member. Lateral accretion sets, indicative of point-bar deposition, have been observed in both members, but are not common, perhaps because outcrops are not favorably oriented to reveal them. Crossbed and imbrication paleocurrent data (Seager et al., 1997; Hunter, 1986) in the northern outcrop area indicate paleoflow primarily to the northeast and east-southeast.

Mudstone beds in the McRae Formation were deposited on floodplains by overbank flooding. Thin beds of fine sandstone interbedded with mudstone represent crevasse splays and are much more common in the Jose Creek Member. Floodplain sediment commonly displays evidence of pedogenesis in the form of root traces, blocky texture interpreted to be peds, and paleosol horizon development. In the case of the Jose Creek Member, the most mature paleosols are olive-gray in color and have well developed argillic B horizons characterized by the down-profile movement of clay (Buck, 1992; Buck and Mack, 1995). These paleosols resemble modern soils formed in subhumid regions (Buck and Mack, 1995; Levron, 1995). Leaf fossils in the Jose Creek Member, consisting of fern, conifer, cycad, and flowering plants, including palm, suggest a subtropical to paratropical forest (Upchurch and Mack, 1998). In contrast, Hall Lake paleosols were well oxidized and characterized by the accumulation of pedogenic carbonate and the development of wedge-shaped peds and slickensides. These features suggest a relatively dry climate with strongly seasonal precipitation (Buck and Mack, 1995).

Periodically during deposition of the upper half of the Jose Creek Member and the lowermost part of the Hall Lake Member the study area was inundated with fine volcanic ash. Many of the ashes were reworked by running water or wind prior to final deposition, and soils developed on some of the ash beds. The exact source of the volcanoes from which the ash erupted is unknown, but tuffs with a post-compaction thickness of 0.3–2 m (1–6.6 ft) suggest a fairly proximal source.

The coarsest McRae Formation is exposed in the Cutter and Upham quadrangles and consists primarily of conglomerate with minor amounts of sandstone and mudstone. Many of the conglomerates are very poorly sorted, matrix supported, and lack internal stratification, suggesting deposition as debris flows. Other conglomerates are better sorted and imbricated and have lenses and interbeds of crossbedded sandstones. These waterlaid conglomerates and sandstones indicate paleoflow to the northnortheast. The overall coarse grain size, presence of debris flows, and paucity of fine facies argue for an alluvial-fan origin for the McRae Formation in the southernmost outcrops.

Love Ranch Formation

Named by Kottlowski (1956) for exposures of conglomerate in the southern San Andres Mountains, the Love Ranch Formation crops out widely throughout south-central New Mexico. In the Caballo Mountains and vicinity outcrops are especially instructive because they document uplift and erosion of Laramide fault blocks (Rio Grande uplift) and deposition of syn- to post- tectonic detritus in the complementary Love Ranch Basin (Fig. 53; Seager and Mack, 1986; Seager et al., 1986, 1997). As a result, thickness, facies, and subcrop relationships of the Love Ranch Formation are variable, controlled by paleogeographic position. In the center of the Love Ranch Basin, corresponding to the northeastern part of the Caballo Mountains and adjacent Jornada del Muerto Basin, the Love Ranch Formation unconformably overlies Upper Cretaceous rocks and is as much as 900 m (2,952 ft) thick. To the south, on the Rio Grande uplift, in the central and southern part of the Caballo Mountains, the Love Ranch Formation is only 200–550 m (656–1,804 ft) thick and unconformably overlies deeply eroded Paleozoic and Precambrian rocks. Locally on the Rio Grande uplift, the Love Ranch Formation has filled a paleocanyon several hundred meters deep and approximately 6 km (3.7 mi) wide. Trending east or northeasterly, the paleocanyon was floored by Precambrian granite, above which stood stepped walls of Paleozoic limestone, all buried successively by Love Ranch canyon fill. The relationships are well exposed in the east-central part of the modern Red Hills (Fig. 2).

The Love Ranch Formation may be as old as Paleocene, but is probably mostly Eocene in age. In the Grimm and others exploration well in southern Doña Ana County, late Paleocene or early Eocene palynomorphs are present in the lower 250 m (820 ft) of a 2,100 m (6,889 ft) thick section of red beds that is correlated with the Love Ranch Formation (Thompson, 1982), but within a separate basin. The age of the top of the Love Ranch Formation is bracketed by its conformable contact with the Palm Park Formation, which has yielded K/Ar radioisotopic ages of 51.5 ± 2.6 and 42.4 ± 1.6 Ma, corresponding to late Eocene (Kottlowski et al., 1969; Clemons, 1979). Two clasts of altered andesite porphyry from a basal conglomerate yielded $^{40}Ar/^{39}Ar$ ages of 89.4 ± 2.2 and 86.47 ± 0.4 Ma (Esser, 2003a), both dates inconsistent with known ages of Laramide volcanic fields in the region (75 Ma), as well as with the paleogeography of Coniacian and Santonian strata in southwestern New Mexico.

Description

Although the Love Ranch Formation consists primarily of conglomerate, sandstone, and mudstone throughout the Caballo Mountains area, it is useful to describe sections in the Love Ranch Basin separately from those on the Rio Grande uplift, as significant differences distinguish deposits in each tectonic setting.

Outcrops in the Love Ranch Basin underlie much of the pedimented east-central flank of the Caballo Mountains, especially in the Cutter and Upham quadrangles, and they have been penetrated in the Exxon No. 1 Prisor well. In these areas, the base of the formation is marked by a boulder conglomerate 30–40 m (98-131 ft) thick. Widespread and tabular in shape, the conglomerate extends southwestward from the vicinity of Engle to the western reaches of Yoast Draw in the central foothills of the range, at which point it is overlapped toward the southwest by younger Love Ranch conglomerate. Grain size increases southwesterly, and at the overlap point subrounded boulders as much as 1.5 m (4.9 ft) in diameter compose much of the unit. Above the basal conglomerate, red conglomerate and interbedded conglomeratic sandstone, sandstone, mudstone, and gypsiferous mudstone compose the rest of the formation. Conglomerates increase in thickness and abundance southwestward toward the Rio Grande uplift as clast size increases from cobble to boulder in the same direction. Locally, however, trains of very large boulders weather from generally poorly consolidated conglomerate units throughout the outcrop area. Toward the north and east the ratio of sandstone and mudstone to conglomerate increases; in easternmost outcrops and in the Prisor well most of the 900-m (2,952-

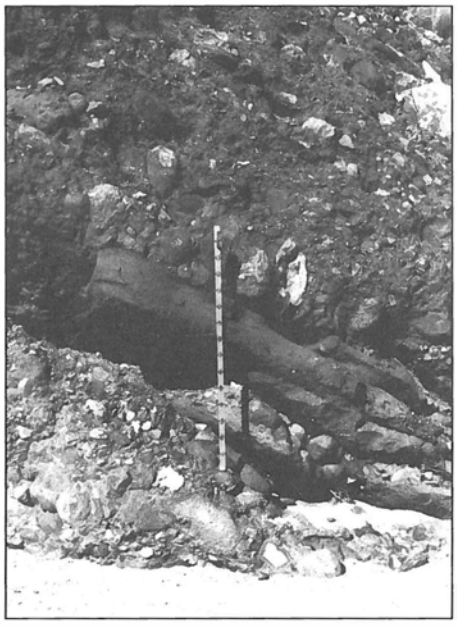

FIGURE 54—Conglomerate and interbedded sandstone of the Love Ranch Formation (Eocene) in Apache Canyon. Jacob's staff is 1.5 m (4.9 ft) long.

ft)-thick section is pink mudstone. Near Engle gypsiferous mudstone composes much of the Love Ranch Formation.

Significant vertical changes in stratigraphy also distinguish the Love Ranch Formation in the Love Ranch Basin. Within conglomerate units, clast composition changes upward. Intermediate-composition and felsic volcanic clasts compose the basal conglomerate, followed upward by the appearance of Abo siltstone and lower to middle Paleozoic clasts and finally by Precambrian clasts. Stratigraphically highest conglomerates may contain as much as 30% Precambrian detritus.

There are also upward changes in bedding and sedimentary structures. The lower two-thirds of the formation consists of upward-coarsening cycles of mudstone, sandstone, and conglomerate, each approximately 50 m thick. Conglomerate units are usually poorly sorted, clasts are subangular to subrounded and generally matrix supported. Conglomerates also often contain concentrations of very large, >1 m (>3.3 ft), boulders. Sandstone units display horizontal laminae. In contrast, conglomerate beds in the upper one-third of the formation contain well-rounded and well-sorted clasts, often imbricated and organized into sets of trough crossbeds or, locally, planar crossbeds. Many conglomerates have scoured bases and grade up into mudstone units with calcic nodules interpreted to be paleosols. In general, the formation becomes finer grained upward, as well as basinward.

Outcrops of the Love Ranch Formation on the Rio Grande uplift, specifically on the structural bench segment of the uplift (see section on Laramide structure), are exposed in fault blocks of the southern Caballo Mountains, south of Apache Canyon (Fig. 54). Although the formation consists largely of reddish conglomerate and conglomeratic sandstone on the bench as it does in the Love Ranch Basin, there are notable differences in the deposits on the bench. The basal volcanic conglomerate, so widespread in the basin, is absent on the structural bench. Instead, discontinuous beds of limestone, as much as 15 m (50 ft) thick locally form the base of the Love Ranch Formation, especially in the area near Hidden Tank. The limestones are medium bedded and contain oncolites (Fig. 55) interpreted to be of algal origin, as well as wavy and crinkly laminae and spar-filled tubes suggestive of tufa or travertine deposits.

FIGURE 55—Oncolitic(?) limestone in the Love Ranch Formation (Eocene) in Apache Valley. Lens cap is 5 cm (1.9 inches) in diameter.

Above the limestones and across the structural bench, conglomerates are notably coarser grained compared to those in the Love Ranch Basin, and they coarsen southwestward; boulders of lower Paleozoic limestone and Precambrian granite as large as 2 m (6.6 ft) in diameter are present on southernmost Caballo fault blocks. Clasts in the conglomerates are a mix of Precambrian, Paleozoic, and volcanic cobbles and boulders showing no notable systematic upsection change in composition. An exception to this generalization is the paleocanyon where basal beds consist of large angular boulders of lower Paleozoic clasts derived from adjacent canyon walls, followed upward by a mix of Precambrian, Paleozoic, and volcanic clasts. Conglomerates on the structural bench are generally poorly sorted, matrix supported, and contain local clusters of very large boulders. However, fining-upward, channel-shaped units containing trough crossbeds and grain-supported clasts are typical of clastic rocks in the paleovalley. Within the paleocanyon and elsewhere on the bench, mudstone, sandstone, and cobble conglomerate, as well as local bodies of sandy to granular micrite without allochems, mark the top of the Love Ranch Formation. These relatively finer grained strata demonstrate that the Love Ranch section on the bench becomes finer grained upward just as it does in the Love Ranch Basin.

Depositional environments

The Love Ranch Formation records a variety of non-marine environments, all closely tied to the evolution of the Rio Grande uplift. Coalescing alluvial fans compose the lower two-thirds of the formation in the Love Ranch Basin and most of the formation on the structural bench of the Rio Grande uplift. Sediment was delivered to the fans primarily by sheetfloods and debris flows as indicated by the disorganized, matrix-supported clasts of the conglomerates and by horizontal laminae in sandstones and conglomeratic sandstones. Clusters of boulders probably represent debris flow levees. Upward coarsening conglomerate units may represent prograding fan lobes. Mudstone units either represent deposition in interfan low areas or alluvial flats at the distal margin of fans. Calcic paleosols in both mudstones and sandstones suggest deposition in an arid or semi-arid climate. Gypsiferous mudstones near Engle are far out in the basin and probably are playa deposits.

The upper one-third of the Love Ranch Formation in the Love Ranch Basin is fluvial in origin and was deposited on a broad alluvial plain sloping eastward or northeastward away from the Rio Grande uplift. Well-rounded, grain-supported cobbles and trough- to planar-shaped crossbeds are consistent with a fluvial

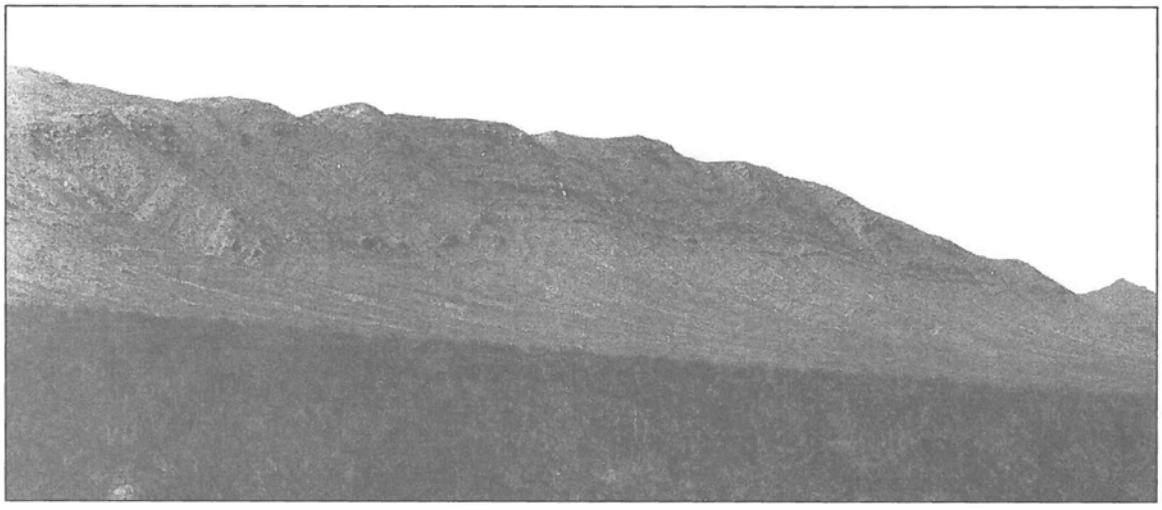

FIGURE 56—McLeod Hills fault-propagation fold exposed on Taylor Ridge. Note natural section of overturned anticline at left. View looks approximately west.

origin, and the coarse grains and predominantly sheet-like character of conglomerate beds suggests deposition by braided streams of low sinuosity. Occasional sets of planar crossbeds may represent shifting gravel and sand bars. Paleoflow to the northeast or north is indicated both by cobble imbrication and trough crossbeds. Mudstones with paleosols gradationally above conglomerate channels or sheets are floodplain deposits that were stable long enough to develop weak to moderately mature soil profiles. Fluvial deposition on the structural bench was largely but probably not entirely confined to the paleovalley as indicated by the better sorted, grain-supported and trough-crossbedded conglomerates in the paleocanyon section.

Eventually, sediment in the Love Ranch Basin aggraded high enough so that upper parts of the Love Ranch Formation overlapped and buried the structural bench segment of the Rio Grande uplift. In the process, the paleocanyon was backfilled with 550 m (1,804 ft) of sediment. Discontinuous limestone beds at the base and top of the Love Ranch Formation probably are the deposits of small fresh water lakes, perhaps fed by hot springs that occupied depressions on the bench both before it was buried by sediment, as well as during the final stages of burial.

Laramide structures

Tectonic setting

Using major contractile structures, unconformities, and the syntectonic to post-tectonic deposits of the McRae and Love Ranch Formations, Seager (1983), Seager and Mack (1986), and Seager et al. (1986, 1997) reconstructed the Laramide Rio Grande uplift and its adjoining basins (Fig. 53). Trending northwestward, the Rio Grande uplift is at least 140 km (87 mi) long and 50 km (31 mi) wide. It consists of one or two southwesterly tilted blocks, each bordered on the northeast by northeast-verging thrust faults or fault-propagation folds. As Figure 53 illustrates, the Rio Grande uplift locally consists of two main blocks, a structurally high, southwest-tilted block, named main uplift, which was widely and deeply eroded into Precambrian basement during the Laramide orogeny, and an adjoining, structurally lower block, named structural bench, consisting mostly of broadly arched Paleozoic strata. Broad basins filled with synorogenic to post-orogenic clastic rocks flank the uplift on both the northeastern and southwestern sides. The southwestern basin, named Potrillo Basin (Seager and Mack, 1986), contains as much as 2,100 m (6,889 ft) of lower Tertiary clastic strata (Thompson, 1982), but the character of its basin fill as well as the extent and geometry of the basin is not well known. In contrast, the Love Ranch Basin on the northeastern flank of the uplift is better understood because of widespread outcrops of the Love Ranch and McRae Formations, which filled the basin and overlapped the uplifts, and because of data provided by the Exxon no. 1 Prisor oil test. Collectively, these data permit interpretations of the kinematic evolution and depositional history, not only of the Love Ranch Basin but also for the Rio Grande uplift (Seager et al., 1997).

Parts of the structural bench and Love Ranch Basin, as well as the major fault-propagation fold that separates them, are well exposed in the Caballo Mountains and on its eastern piedmont slopes (Fig. 53). In the following section, we first discuss these structures and then summarize the tectonic evolution of the Caballo area during the Laramide orogeny, using the structural features as well as sedimentologic data from the Love Ranch and McRae Formations.

McLeod Hills fault-propagation fold

Because it forms the boundary between the Love Ranch Basin and structural bench section of the Rio Grande uplift, the McLeod Hills fault-propagation fold is of special importance. The longest and most prominent of the Laramide structures in the area, the fault-propagation fold extends from east of the Rincon Hills north-northwestward a distance of 19 km (11.8 mi) before it bends to a more westerly course and then is cut off by the late Cenozoic Caballo normal fault. Northwest of the Caballo fault, the fold probably continues, hidden beneath the Tertiary rocks in Apache graben; its trend projects into the Palomas Basin at a point just north of the Red Hills. The belt also probably continues southward, past the Rincon Hills, but there it is truncated by the late Cenozoic east Rincon Hills normal fault and buried by alluvium and Camp Rice sedimentary rocks.

The structure of the McLeod Hills fault-propagation fold is relatively simple and best expressed in the southern part of the McLeod Hills, a limestone ridge located east of Red House Mountain (Fig. 56). Kelley and Silver (1952) named this ridge Taylor Ridge and referred to the prominent fold that forms the ridge crest as Taylor Ridge anticline. The structure is at least 2 km (1.2 mi) wide and actually consists of an overturned syncline on the east and an overturned anticline on the west (Fig. 57). Both structures face or verge toward the northeast, and dips in the overturned limb are commonly from 40° to 60° southwest, locally less than 30°. Axial surfaces dip southwest also at moderate

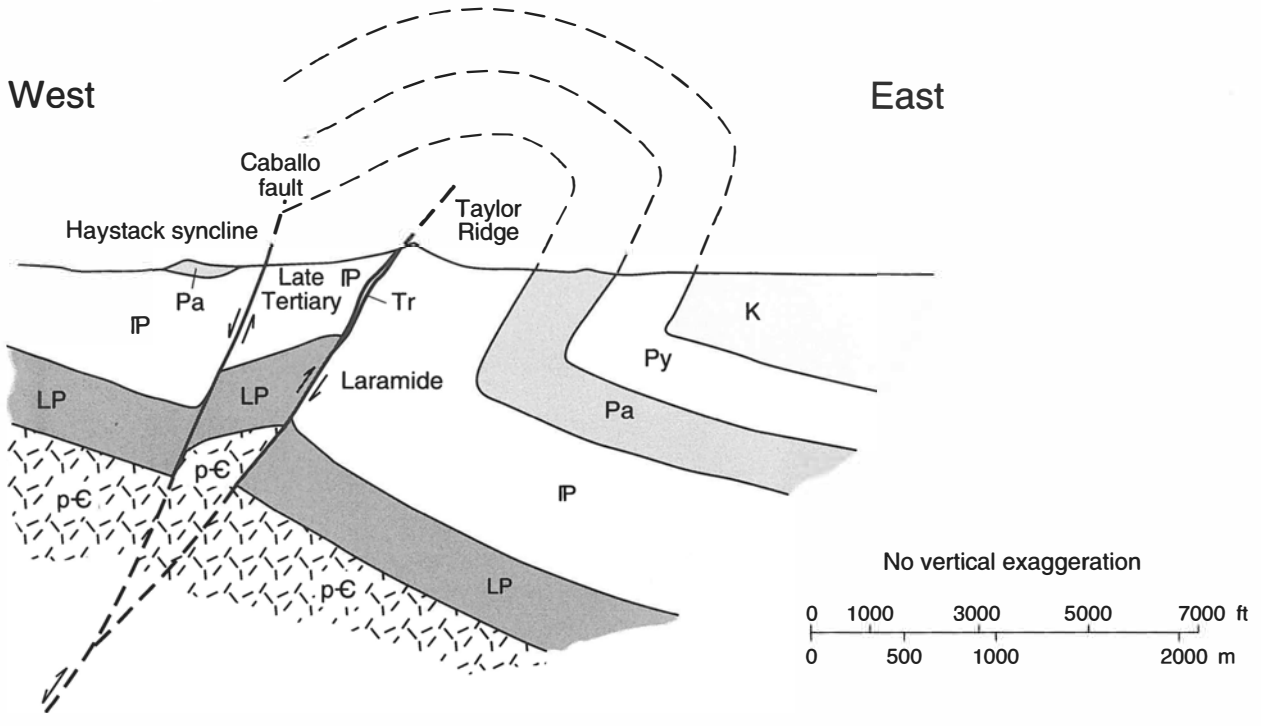

FIGURE 57—Cross section of McLeod Hills fault-propagation fold across Taylor Ridge. **p€** = Precambrian; **LP** = Lower Paleozoic rocks; **IP** = Pennsylvanian rocks; **Pa** = Abo Formation; **Py** = Yeso Formation; **K** = Cretaceous rocks, undifferentiated; **Tr** = rhyolite dike.

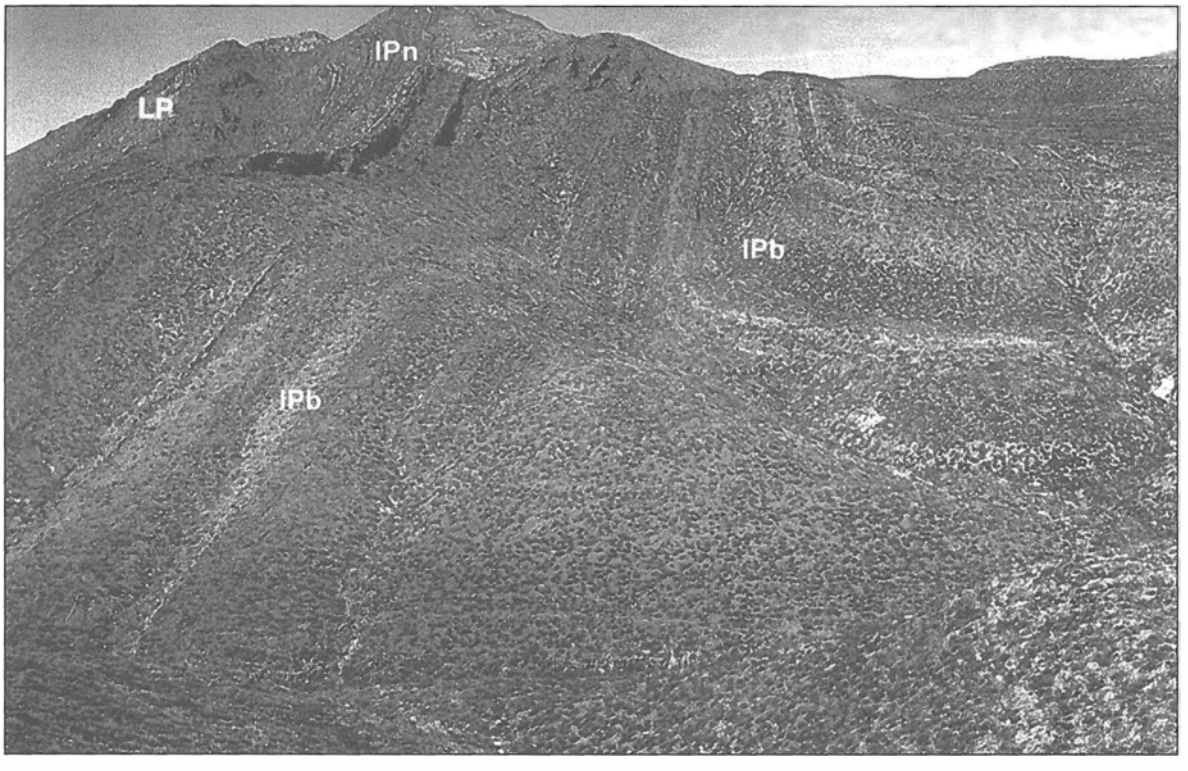

FIGURE 58—McLeod Hills fault-propagation fold exposed in footwall of Caballo fault south of Apache Canyon. View looks northwest. Trace of synclinal hinge extends diagonally from upper right to lower left, and strata in the left part of the picture are overturned, dipping 50°–80°SW. **LP** = Lower Paleozoic strata; **IPn** = Nakaye Formation; **IPb** = Bar B Formation.

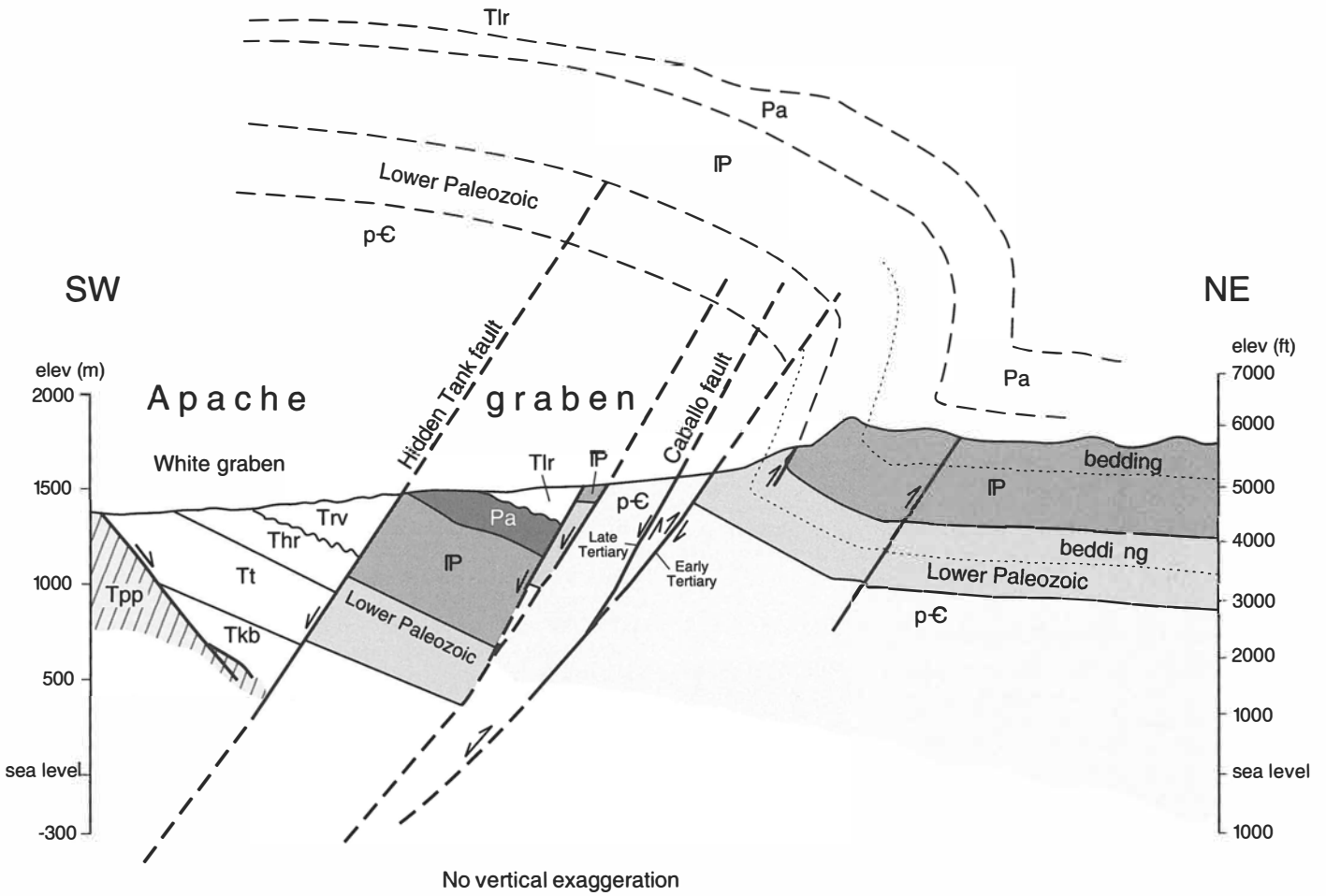

FIGURE 59—Cross section across Apache graben and Caballo fault block showing reconstruction of McLeod Hills fault-propagation fold. Note inversion of the fault-propagation fold by the Caballo fault. **p€** = Precambrian rocks; **IP** = Pennsylvanian rocks; **Pa** = Abo Formation; **Tlr** = Love Ranch Formation; **Tpp** = Palm Park Formation; **Tkb** = Kneeling Nun Tuff and Bell Top Formation; **Tt** = Thurman Formation; **Thr** = Hayner Ranch Formation; **Trv** = Rincon Valley Formation.

angles, although locally the folds appear to be nearly recumbent. Amplitude of the folds exceed 1.5 km (0.9 mi) on Taylor Ridge, but elsewhere along the belt it probably approaches 1.8 km (1.1 mi). Thrust faults displace Pennsylvanian strata in the core of the anticline along the length of Taylor Ridge. The faults approximately follow the axial surface; stratigraphic separation is less than 100 m (328 ft) in Pennsylvanian strata, but probably increases downward, as Figure 57 illustrates.

At the northern end of Taylor Ridge, the anticline-syncline pair bifurcates into two pairs, both verging northeastward. The eastern anticline-syncline pair continues north-northwestward for 4 km (2.5 mi) before dying out into a regional east dip. The western pair of folds bends abruptly westward at the northern tip of Taylor Ridge toward the late Tertiary Caballo fault, which truncates the anticline. The overturned syncline curves back northwestward parallel to the Caballo fault and is exposed in its footwall (Fig. 58) for a distance of 9.5 km (5.9 mi) before it, too, is cut off by the Caballo fault and downdropped below Tertiary sedimentary rocks in Apache Valley. Cross-section reconstructions of the syncline in the Caballo fault footwall and anticline buried beneath Apache Valley indicate overall geometric similarity with the folds on Taylor Ridge (Fig. 59). However, the overturned limb of the anticline-syncline pair is much more deeply eroded in the Caballo fault footwall, and this permits reconstruction of the fault-propagation fold down to the level of Precambrian rocks. Most importantly, reverse faults following the axial surface of the anticline, which only slightly offset Pennsylvanian strata in the anticline at Taylor Ridge, can be seen to penetrate basement in the footwall of the Caballo fault, resulting in Precambrian rocks being thrust over strongly overturned lower Paleozoic rocks (Fig. 60) for a distance of 3 km (1.9 mi). Other structures exposed in the deeper levels of the folds are (1) thrust faults within the overturned limb of the folds, most notably localized by the Percha Shale; (2) short, north to northeast-trending steep faults that obliquely transect the overturned fold limb and terminate within the Percha Shale—some of these display significant, 300 m (984 ft), strike separation and probably have an important component of strike slip; (3) many small folds, warps, and wrinkles in the overturned limb; and (4) discontinuous thrusts along the synclinal axial surface, which have carried overturned beds eastward onto the right-side-up limb of the syncline.

In summary, the McLeod Hills fault-propagation fold consists of an overturned anticline-syncline pair, bifurcating into two pairs locally, that is vergent toward the northeast and exhibits structural relief of more than 1.5 km (0.9 mi). The synclinal axial surface is locally broken by thrust faults, but the axial surface of the anticline is more generally followed by a thrust that increases in throw downward into basement and dies out upward, probably in Upper Pennsylvanian strata. The geometry of the structure closely fits that of a fault-propagation fold.

FIGURE 60—Basement thrust fault in core of McLeod Hills fault-propagation anticline, exposed in footwall of Caballo fault south of Apache Canyon. View is to the southeast. Thrust fault extends diagonally from lower right toward upper center part of picture and passes beneath dark backpack on arroyo floor. The fault dips southwestward (right) approximately 36°, and Precambrian granite on right is thrust over overturned El Paso strata on left.

Structural bench of Rio Grande uplift

The southwestern, uplifted side of the McLeod Hills fault-propagation fold is the structural bench, a major block at the northern margin of the Rio Grande uplift (Fig. 53). All of the Cenozoic fault blocks of the southern Caballo Mountains, from the Red Hills to Red House Mountain, as well as a large part of Apache graben, are coextensive with the structural bench. Beyond these, the bench projects southward into the Hatch–Rincon Basin and west-northwestward into the Palomas Basin.

The general structure of the bench and the depth of erosion can be gaged by examining the unconformity at the base of the Love Ranch Formation (Fig. 61). The overall pattern of pre-Love Ranch erosion suggests arching of Paleozoic strata along a northwest-trending hinge zone, located 5–6 km (3.1–3.7 mi) southwest of the McLeod Hills fault-propagation fold (Fig. 62B). Structural culminations along the hinge are suggested by areas of deeper erosion into Pennsylvanian, lower Paleozoic, or Precambrian rocks, while the saddles along the hinge, as well as the flanks of the arch, are less deeply eroded. Apparently the culmination along the northwestern part of the hinge localized the deep northeast-draining paleocanyon seen now in the Red Hills (Fig. 62A). Precambrian rocks constituted the floor of the canyon, whereas lower and upper Paleozoic rocks formed the canyon walls. In general, erosion of the arch stripped 1,000–1,450 m (3,280–4,757 ft) of Cretaceous and upper Paleozoic rocks from the structural bench, although as much as 1,850 m (6,070 ft) of sedimentary rock and Precambrian granite was removed from the paleocanyon. All of the structures and topography on the bench were eventually buried by Love Ranch clastics

Another notable feature of the structural bench is exposed in the Derry Hills. Two southwest-vergent, overturned anticline-syncline pairs trend northwesterly (Fig. 61) in outcrops on the eastern flank of the hills (Seager and Mack, 1991). The belt is only 1 km (0.6 mi) wide and is exposed along strike for a distance of 1.6 km (1.0 mi). Axial surfaces of both anticlines and synclines dip approximately 40°NE and are followed by thrust faults, which are notably more continuous in the anticlines. The eastern fold pair is structurally higher than the western pair; collectively they exhibit approximately 450 m (1,476 ft) of structural relief. Younger normal faults that follow axial plane thrusts have inverted the western structure. Seager and Mack (1991) have interpreted these fault-propagation folds as back thrusts on the southwestern flank of the structural bench.

Structures in the Love Ranch Basin

Three groups of contractional structures were mapped in the Love Ranch Basin: the Cutter foldbelt, northern Caballo folds, and Putnam anticline and related synclines.

Cutter foldbelt

The Cutter foldbelt consists of nine anticlines and synclines that trend northwesterly across much of the Cutter quadrangle. Most distal of all of the exposed intrabasinal folds, the Cutter foldbelt is developed almost entirely within the Crevasse Canyon Formation. The folds are gentle to open, symmetrical structures as much as 12 km (7.4 mi) in length, with parallel hinges that plunge gently southeastward or are nearly horizontal. Locally small domes and basins are present, the result of low culminations and depressions along hinges. Fold wavelengths are approximately 2.3 km (1.4 mi), and amplitudes do not exceed 200 m (656 ft). In sections normal to strike, the foldbelt is a broad, low anticlinorium. Both northeast and northwest-trending faults of small displacement cut the foldbelt, at least some of which may be strike-slip or thrust faults, respectively.

The Cutter foldbelt formed before deposition of the McRae Formation. Evidence of this may be seen in the Aleman Draw area, where folded and faulted Crevasse Canyon Formation is overlain by less deformed Jose Creek Member of the McRae. The angular discordance becomes more pronounced toward the southwest and is especially striking in the Yoast Draw area. The unconformity indicates a latest Cretaceous age for the foldbelt, the earliest date for Laramide shortening in the Caballo area.

Northern Caballo folds

The northern Caballo folds comprise three groups of folds that extend in an en echelon pattern from the eastern slopes of Timber Mountain to the northern tip of the range. Best expressed in Paleozoic strata, the folds all trend northerly to northwesterly, and most cross the crest of the range diagonally (Mason, 1976). All verge northeastward to eastward, and most have the overall form of the McLeod Hills fault-propagation fold, although the northern Caballo folds are smaller, shorter, lack notable thrusts, and often consist of more than one pair of folds. Kelley and Silver (1952) and Mason (1976) described three belts in some detail: the North Ridge belt at the northern tip of the range; the Palomas Gap belt, extending southeastward from Palomas Gap; and the Granite Wash belt, located 2–4 km (1.2–2.5 mi) north of the divide at the head of Longbottom Canyon. We shall refer to a fourth group, located on the eastern slope of Timber Mountain as the Timber Mountain folds.

The North Ridge, Palomas Gap, and Granite Wash belts are each 3–6 km (1.9–3.7 mi) in width. The major structure in each belt is an overturned syncline located along the northeastern flank of the belt, and this is generally followed by two asymmetric or overturned anticlines and a syncline lying above and to the west of the syncline. Overturned limbs dip as little as 40°, and the axial surfaces commonly dip westward at 25°, locally as low as 10°–15° (Kelley and Silver, 1952). Amplitudes of the fold belts range from 760 m (2,493 ft) for the North Ridge belt to as little as 400 m (1,312 ft) for the other two. All of the folds step Paleozoic strata down northeastward into the Love Ranch Basin in a stair-step fashion. Folds in the North Ridge belt are interpreted to have been continuous, with similar structures in the southeastern Mud Springs Mountains, separated now by the Hot Springs fault (Fig. 61).

The Timber Mountain folds display most of the characteristics of the other fold belts with two exceptions. First, the Timber Mountain folds are not arranged en echelon with its neighbor, the Granite Wash belt. Rather, the two may be interpreted to be continuous, in spite of the facts that individual fold hinges cannot be traced across the Longbottom fault and that the Granite Wash belt trends north-northwesterly, whereas the Timber Mountain belt trends northerly. Second, although they verge eastward, none of

the Timber Mountain folds are overturned. They are monoclinal-like flexures that gradually die out southward.

The northern Caballo folds are younger than the Crevasse Canyon Formation, which is deformed in the North Ridge folds. Whether they are pre-McRae (latest Cretaceous) in age or post McRae (early Tertiary) is not known with certainty. However, all of the structures are probably fault-propagation folds, similar in geometry and trend with the McLeod Hills structures, and their main function was to accommodate subsidence of the southwestern flank of the Love Ranch Basin. Consequently, they may most easily be interpreted to be Love Ranch in age, early Tertiary.

Putnam anticline and adjacent growth syncline

The Putnam anticline, named and described by Kelley and Silver (1952), trends and plunges east-southeasterly from the northern flank of Timber Mountain into the Love Ranch Basin. The fold is prominently displayed by nearly elliptical outcrops of Pennsylvanian and Permian strata near the base of the mountain, but becomes partly hidden by alluvium farther east where Cretaceous and lower to middle Love Ranch beds are folded. The fold is approximately 15.5 km (9.6 mi) long and 1.6 km (1.0 mi) wide, narrowing eastward. Although the structure is closed at the level of Pennsylvanian rocks in the core, it plunges easterly at modest angles at the level of Permian rocks. Vergent toward the north, the axial plane dips approximately 70° south; only locally is the northern limb overturned, but it is otherwise steep. Amplitude of the western part of the fold is approximately 750 m (2,460 ft), but this decreases eastward as the fold narrows, becoming particularly low and somewhat obscure as it passes through Love Ranch strata.

The northern limb of the Putnam anticline is broken by a reverse fault of small displacement, 50 m (164 ft) or less. Traced westward, the fault passes out of the Putnam anticline and cuts downsection, eventually transecting lower Paleozoic rocks and Precambrian granite in Longbottom Canyon in the western slopes of the range. Named Longbottom fault for the excellent exposures in Longbottom Canyon, the fault maintains its steep southerly dip, but stratigraphic separation increases westward with depth to approximately 400 m (1,312 ft) at the Precambrian–Bliss contact. Throughout the length of the fault, the southern hanging wall is upthrown, in spite of 100–200 m (328–656 ft) of late Tertiary inversion of the structure, discussed in a later section.

The Longbottom reverse fault and Putnam anticline are clearly linked both spatially and kinematically, as Kelley and Silver (1952) suggest. The fault and fold represent different levels of erosion of a major fault-propagation fold, whose growth during deposition of the Love Ranch Formation is confirmed by adjacent syndepositional (growth) synclines.

The synclines on both flanks of the Putnam anticline exhibit the characteristic geometry of growth folds (Riba, 1976; Anadon et al., 1986; Lawton and Trexler, 1991; DeCelles et al., 1995). They can be traced part way across the Love Ranch Basin, broadening and becoming more gentle, open folds as they plunge southeastward. Both McRae and lower to middle Love Ranch Basin deposits are folded within the synclines, but there is a progressive upward decrease in dip within the core of the folds (Seager et al., 1997). Oldest McRae or Love Ranch beds dip moderately, whereas successively younger Love Ranch strata are progressively less deformed. The upper one-third of the Love Ranch is not folded, containing only a low regional eastward dip, and is probably separated from the folded Love Ranch strata below by an inconspicuous unconformity. These relationships can best be seen in the southern syncline 1–5 km (0.6–3.1 mi) south of Yoast Draw in the Upham quadrangle and in the northern syncline less than 1 km (0.6 mi) north of Yoast Draw. Between the two synclines, a low, narrow, rather obscure anticline is along the projected hinge of the Putnam anticline.

The upward decrease in dip in the cores of the two synclines is opposite to that expected in concentrically folded synclines. Riba (1976), Anadon et al. (1986), Lawton and Trexler (1991), DeCelles et al. (1995), and Lawton et al. (1999) attribute such fold geometry to synchronous deposition and folding of strata and refer to such structures as growth synclines or progressive unconformities. The upward decrease in dip results partly from somewhat thicker deposits of sediment accumulating in the downfolding hinge areas, and also documents progressively decreasing accumulated strain in the younger beds through time. The upward flattening of dip and broadening of growth synclines also affect adjacent anticlinal hinges by causing them to become progressively lower, narrower, and more poorly expressed, like the eastern part of the Putnam anticline. They may also be sites of syntectonic erosion. The growth synclines in the Love Ranch Basin indicate they, as well as the Putnam anticline, were folded during deposition of the lower to middle part of the Love Ranch Formation. The synclines probably controlled local patterns of deposition of Love Ranch fan deposits, and the Putnam anticline may have been a minor source of clastics, including reworked Love Ranch sediment (Seager et al. 1997).

Laramide tectonic evolution

In the 10 Ma interval between Campanian and late Maastrichtian time, an interval for which there is no rock record in the Caballo Mountains, earliest events in the Laramide orogeny took place. Lava flows and debris-flow breccia of intermediate and silicic composition were emplaced across the Caballo area, perhaps spreading there from the Hillsboro region of the Black Range, where the remnants of a 75 Ma stratovolcano and 68 Ma intrusive are known (Hedlund 1977; Kelley and Chapin, 1997). Contractional stress also began to affect the region, producing the northwest-trending, gentle folds of the Cutter foldbelt, as well as broader uplift of the volcanic sequence in the Caballo Mountains area.

The sedimentary record of this earliest Laramide deformation is contained in the McRae Formation of latest Maastrichtian and possibly early Tertiary age. Paleocurrent data, grain size and facies distribution, and clast composition indicate the source of the McRae was the uplifted Upper Cretaceous volcanic sequence located southwest of the McRae outcrops (Seager et al., 1997). Presumably this was an incipient Rio Grande uplift. Most of the McRae volcanic detritus bypassed the northeastern flank of the uplift to be deposited in a distal piedmont slope or basin floor position. Axial drainage carried much of the McRae volcanic detritus, as well as Precambrian clasts from unknown sources, southeastward (Seager et al., 1997). Upper parts of the Jose Creek and Hall Lake Members of the McRae gradually onlapped the piedmont slope but never extended more than approximately one-third of the way between the basin floor and summit of the uplift. The lack of significant McRae sediment on upper to middle parts of this slope suggests that the northeastern flank of the uplift dipped gently northeastward and functioned primarily as a sediment transport surface. Apparently, at this time the Rio Grande uplift was a broad, low domal uplift or anticlinorium, rather than the asymmetrical fault- and fold-bounded structure that it evolved into.

The amount of time represented by the unconformity between the McRae and Love Ranch Formations is not known. A gap of as much as 10 m.y. or as little as 1 m.y. may separate them. If the longer interval proves accurate, then the McRae and Love Ranch Formations may represent separate Laramide contractional events, rather than semi-continuous deformation lasting from Maastrichtian well into Eocene time. At any rate, the Love Ranch Formation records the most significant phase of Laramide shortening in south-central New Mexico, most of which took place in Paleocene and/or Eocene time.

The basal boulder conglomerate of the Love Ranch Formation probably records renewed or accelerating uplift of the Rio Grande uplift as well as continued erosion of Upper Cretaceous

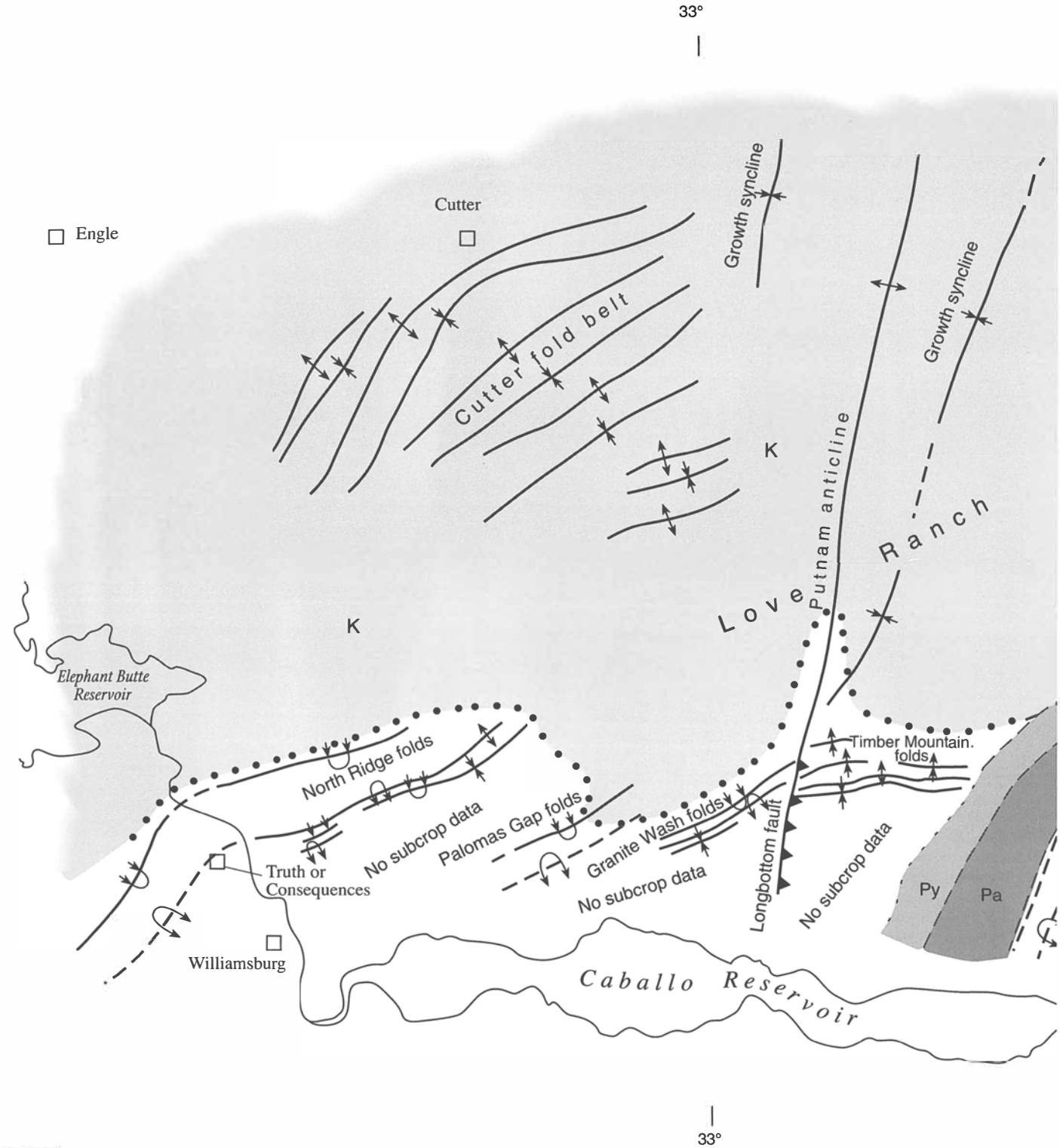

FIGURE 61—Tectonic map of Laramide structural features in the Caballo Mountains area. Love Ranch subcrops are also shown, which reveal depth of erosion and structures in the Love Ranch Basin, on the structural bench, and on the main uplift. Cross sections **A–A′** and **B–B′** are shown in Fig. 62.

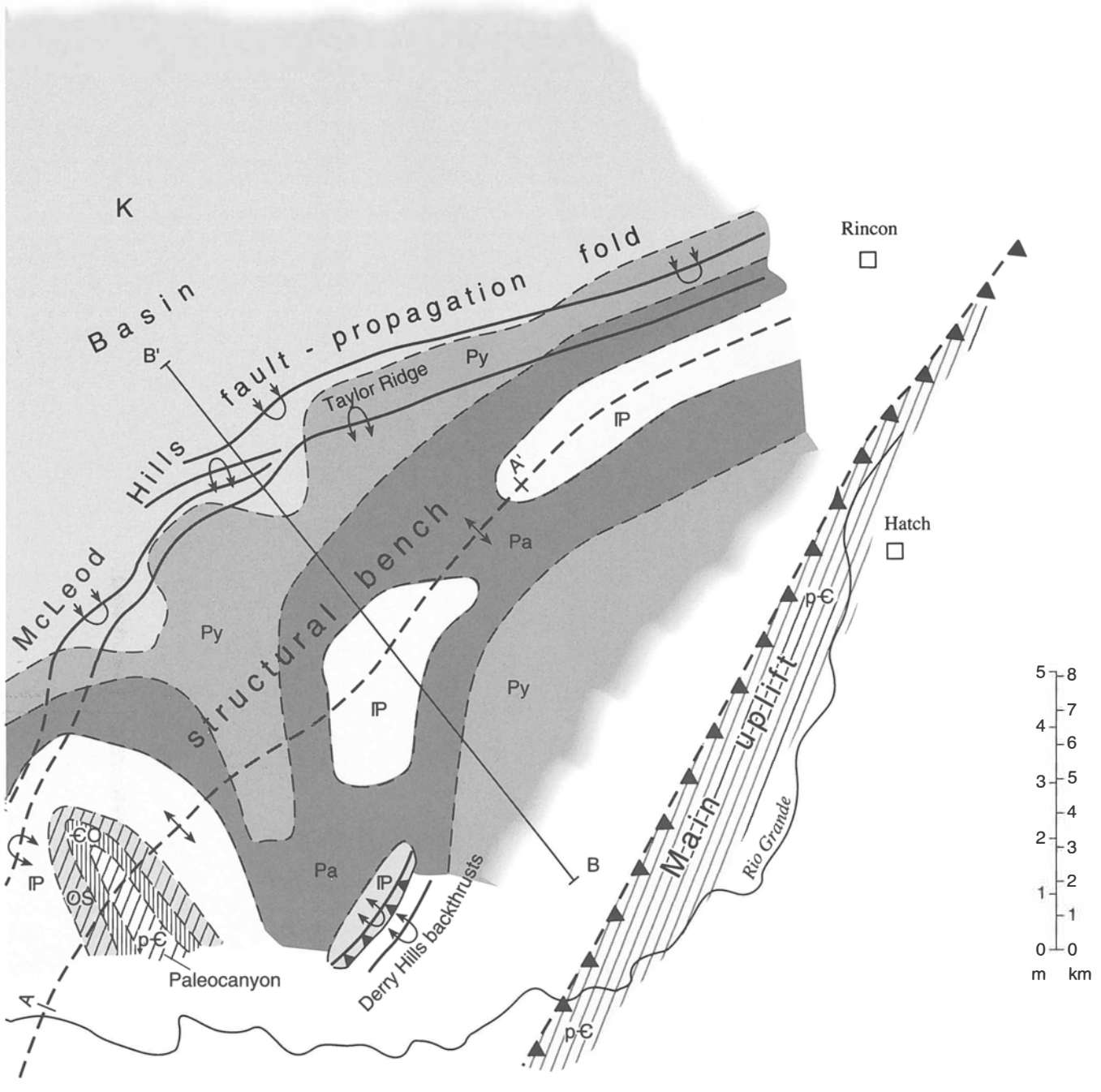

Geologic contact, moderate to good control on location

Boundary of area with no subcrop data

Monocline

Anticline

Syncline

Overturned anticline

Overturned syncline

Thrust fault

dashed where projected and approximately located

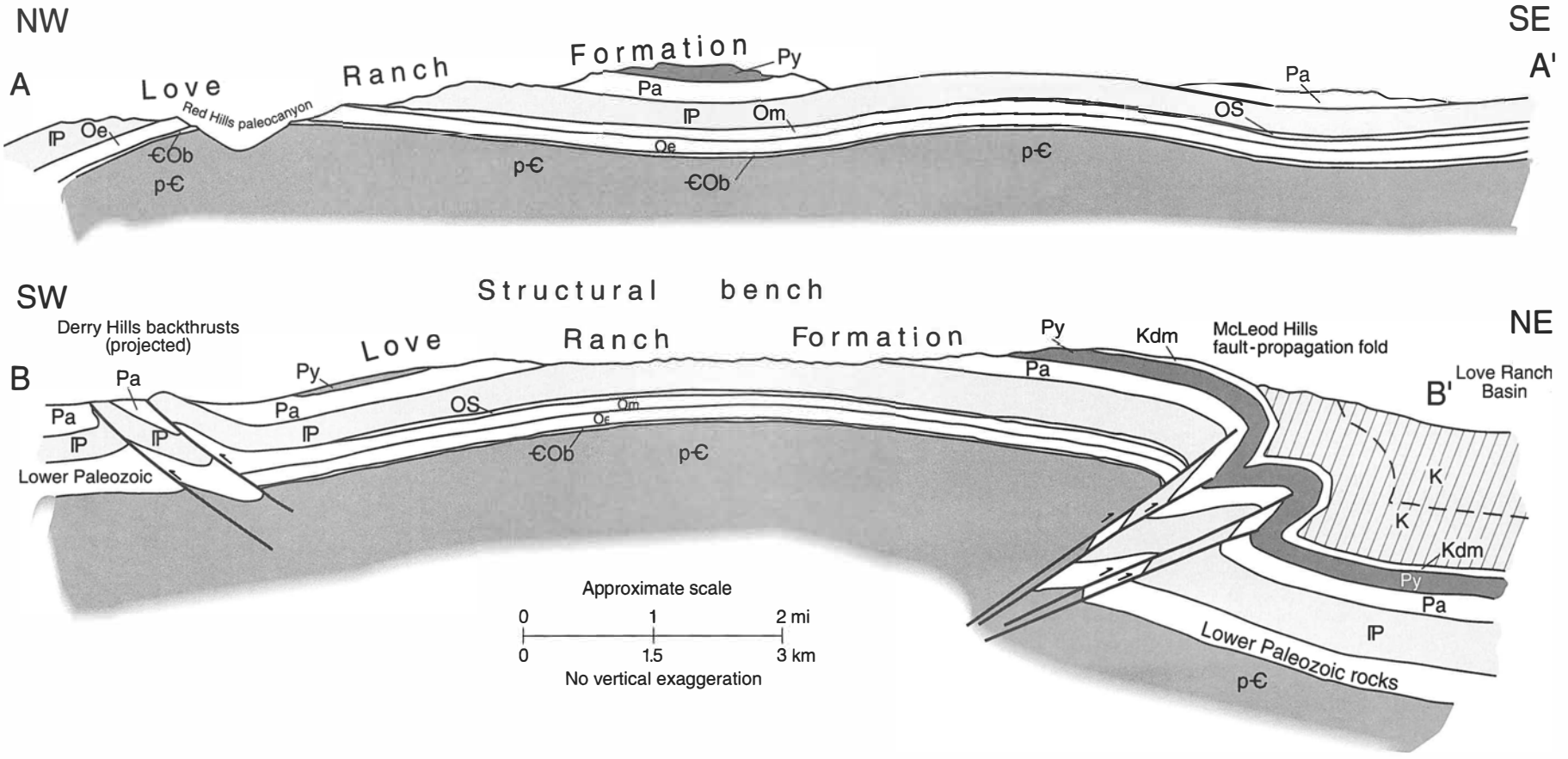

FIGURE 62—Reconstruction of Laramide structure and topography along sections **A–A′** and **B–B′** (Fig. 61) on structural bench. The reconstruction is based on patterns of Love Ranch subcrops. **p€**= Precambrian rocks; **€Ob** = Bliss Sandstone; **Oe** = El Paso Formation; **Om** = Montoya Formation; **OS** = Fusselman Dolomite and Percha Shale; **IP** = Pennsylvanian rocks; **Pa** = Abo Formation; **Py** = Yeso Formation; **Kdm** = Dakota Sandstone and Mancos Shale; and **K** = Cretaceous rocks, undifferentiated.

volcanic rocks from its summit. Because the conglomerate thins toward the source uplift and forms a widespread sheet far down on its northeast-sloping piedmont slopes, it seems unlikely that the uplift at this stage was asymmetrical or fault bounded. Rather, the broad, symmetrical uplift and wide, flanking transport surfaces that characterized the uplift during McRae time persisted into early Love Ranch time.

Following deposition of the basal conglomerate of the Love Ranch Formation, the Love Ranch Basin quickly deepened and broadened, expanding southwestward to a steep margin formed by the growing McLeod Hills fault-propagation fold. The structural bench above the fold, as well as the main uplift of the Rio Grande uplift, eroded rapidly and deeply, providing detritus that filled the Love Ranch Basin. Initially, most of the gravel and sand derived from the main uplift bypassed the structural bench via canyons incised into the bench, such as the one exposed in Red Hills.

The lower two-thirds of the Love Ranch Formation in the Love Ranch Basin was deposited as alluvial fans that sloped northeastward toward alluvial flats or playas near the basin center. The locus of proximal alluvial fan deposition shifted progressively southwestward toward the basin margin, a response to the increasing asymmetry of the basin and growth of McLeod Hills fault-propagation fold. Depositional patterns within the basin were also locally controlled by the actively forming Putnam anticline and its associated growth synclines. Toward the end of Love Ranch time, large fluvial systems drained the uplift, spilling northeastward across the basin toward ephemeral lakes south of Engle. By this time, the growth synclines were inactive, the Rio Grande uplift had been deeply eroded, and uplift-to-basin relief greatly reduced. Upper parts of the Love Ranch Formation onlapped and backfilled canyons on the structural bench (Fig. 63) and buried the remainder of the bench and all but the highest peaks of the main uplift. By late Eocene time, as much as 900 m (2,952 ft) of clastic sediment had filled the Love Ranch Basin, whereas less than one-quarter of that thickness buried the structural bench.

Conglomerate clasts within the Love Ranch Formation record progressive erosional unroofing of the Rio Grande uplift from the volcanic carapace down to its Precambrian core. Moreover, interpretations of the erosional history and topographic relief in the uplift may be estimated from the exposure gate, or range of formations represented by clasts in the conglomerate at any one horizon (Graham et al., 1986). The association of Precambrian, Paleozoic, and volcanic clasts near the lower middle part of the Love Ranch Formation suggests a section of rocks nearly 2.5 km (1.6 mi) thick was exposed in the uplift (Seager et al., 1997). In view of the low dips inferred on both the structural bench and main uplift, the uplift was probably a gently tilted, arched fault block with cuestas and strike valleys as expectable topographic forms. In view of this, topographic relief on the uplift of 1–2 km (0.6–1.2 mi) may be reasonable; the depth of the Red Hills paleocanyon confirms at least 1 km (0.6 mi) of local topographic relief on the structural bench. (Fig. 62A).

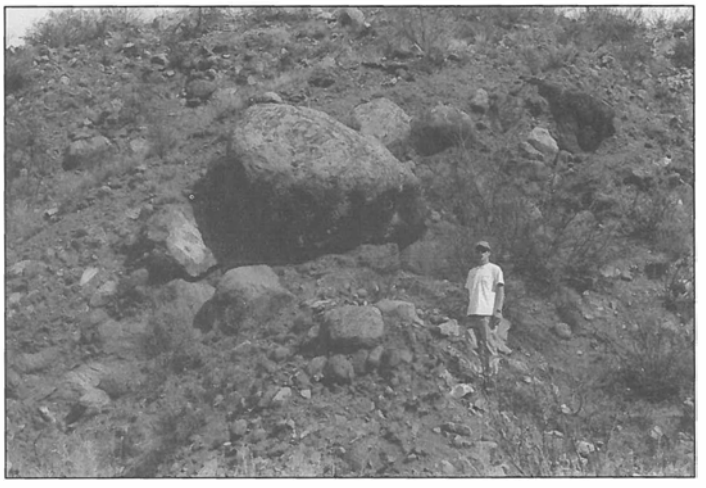

FIGURE 63—Boulder conglomerate of the Love Ranch Formation (Eocene) that infilled the northwestern part of the paleocanyon described in the text. Largest boulder belongs to the Ordovician Montoya Formation.

The upward-fining character of the Love Ranch Formation is notable, not only in the basin but also on the structural bench, where lacustrine beds are locally present at the top of the formation. The upward-fining character is partly a product of the progressive southwestward shift in alluvial fan depocenters with time, causing more proximal facies to be replaced by more basinward sediments. Control on this upward-fining process was structural, caused by the growing structural margins and asymmetry of the basin. Erosional and depositional processes were operating simultaneously and in a complementary way. Gradual reduction in basin-to-uplift topography, aggradation of the basin, onlap, and eventual burial of the uplift combined to broaden the basin with time. Proximal facies were progressively replaced by more distal ones, resulting in an upward decrease in grain size. Thus, structural, geomorphic, and depositional processes operating together within both basin and uplift can result in upward-fining sequences in foreland basins such as the Love Ranch Basin. Furthermore, such sequences can record both the structural kinematic evolution of both uplift and basin, as well as its geomorphic and depositional history.

Eocene volcanic arc rocks

The absence of volcanism during the Laramide orogeny throughout south-central New Mexico and across much of the western U.S. has been attributed to shallowing of the Farallon plate as it subducted beneath North America (Coney and Reynolds, 1977; Dickinson and Snyder, 1978). The same low-angle subduction may be responsible for the Laramide orogeny itself by providing strong compressive or shearing coupling between the Farallon plate and the North American craton as far inland as central New Mexico, Colorado, and Wyoming (Dickinson and Snyder, 1978). As the subducting plate began to steepen in Eocene time, the effects of the Laramide contraction waned, uplifts were leveled by erosion, basins filled by sediments, and arc volcanism was reestablished across southern New Mexico (McMillan, 1998). In the Caballo Mountains, the record of this volcanism is a thick apron of volcaniclastic and associated strata named Palm Park Formation that accumulated on the flanks of andesitic volcanoes.

Palm Park Formation

The Palm Park Formation was named by Kelley and Silver (1952) for exposures in Palm Park, located adjacent to Red House Mountain in the southern part of the Caballo Mountains. Mapped extensively throughout south-central New Mexico, the formation has also been correlated with the Rubio Peak Formation in the Silver City region (Elston, 1957), the Spears Formation in the Socorro–Datil region (Tonking, 1957; Osburn

and Chapin, 1983), and with the Orejon Andesite and Cleofas Andesite of the Las Cruces area (Dunham, 1935; Seager et al, 1976; Seager, 1981). In the Caballo Mountains, the formation crops out widely in Apache Valley and in the McLeod syncline, as well as in Palm Park. However, only the upper part of the formation is exposed at the type area, and outcrops are rather poor. Excellent, accessible outcrops of all parts of the formation are present throughout Apache Valley, the best and most extensive ones being in the walls of, or adjacent to, the many shallow arroyo systems that drain the valley. Consisting primarily of soft volcaniclastic rocks of andesitic composition, the formation weathers to varicolored, but prevailingly purplish-gray badlands with low relief, often covered by a veneer of Quaternary alluvial fan gravel.

Based on radiometric ages of lava flows or intrusive rocks, present elsewhere in the formation, the Palm Park is mostly, if not entirely, late Eocene in age, from 51.5 ± 2.6 to 42.4 ± 1.6 Ma (Kottlowski et al, 1969; Clemons, 1979). These dates are in general agreement with those of the Rubio Peak Formation and associated rocks, which include ages ranging from 44.7 to 36.7 Ma (Loring and Loring, 1980; Clemons, 1982). The Palm Park Formation exhibits a gradational contact with the underlying Love Ranch Formation and is probably disconformable with overlying volcanic units of the Bell Top Formation.

Regionally, the Palm Park–Rubio Peak–Spears Formations range from 600 m (1,968 ft) to 1,000 m (3,280 ft) thick, but locally they wedge out across the remnants of Laramide mountains (Seager and Mayer, 1988) or thicken to as much as 1,525 m (5,003 ft) in volcanic centers (e.g. Elston, 1957). Although a complete section is nowhere exposed in the Caballo Mountains, the formation is approximately 630 m (2,066 ft) thick, based on measurements from cross sections. Although the formation has not been formally subdivided into members, upper, middle and lower parts are distinctive enough to warrant separate descriptions.

Description

The basal 100 m (328 ft) or so of the formation is well exposed in the lower reaches of Apache Canyon, adjacent to the Red Hills fault, as well as in fault blocks on the southwestern flank of Apache Valley. This part of the formation consists largely of boulder conglomerate derived from Paleozoic and Precambrian rocks as well as from hypabyssal or volcanic porphyries of intermediate composition. Similar to clasts in the upper Love Ranch Formation in terms of provenance, rounding, sorting, and composition, Palm Park clasts are embedded in a matrix of gray to purplish-gray tuffaceous mudstone, very different from the brownish-red, non-volcanic matrix of the Love Ranch Formation. Conglomerate units appear to be discontinuous along strike, grading locally to finer-grained sections containing discontinuous beds of fresh-water limestone as much as 2 m (6.6 ft) thick.

Above the basal conglomerate, the thick, middle part of the Palm Park Formation consists of predominantly gray, bluish-gray, purplish-gray, green, white, or red mudstones and breccia with lesser amounts of sandstone. All are tuffaceous and andesitic in composition. Breccia and sandstone units are 3–15-m- (9.8–49-ft-) thick lenticular bodies, channel form in cross section, and are enclosed by mudstone units. Clasts in breccia are supported by mud, fine sand, or silt matrix and generally range in size from pebble to cobble. Boulder breccias are rare in the Palm Park of the Caballo Mountains, although they comprise significant parts of the formation elsewhere. Sandstones are poorly sorted, often contain laminae parallel to bedding or, more rarely, small-scale trough crossbeds. Although breccia and sandstone beds form low hills and ridges, mudstone units generally weather to badland topography.

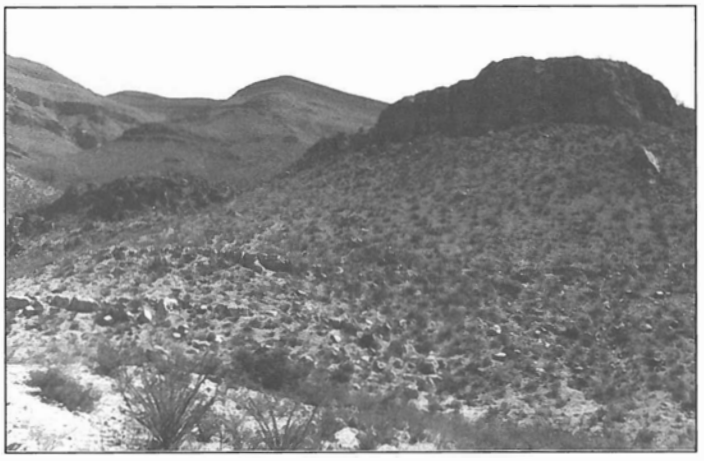

FIGURE 64—Travertine mound (upper right) in Palm Park Formation, with thinner-bedded fresh-water limestone outcrops in foreground. Apache Canyon enters picture from lower left, and view looks northeastward to Paleozoic strata in the Caballo fault block.

Discontinuous lenses of fresh-water limestone distinguish the upper part of the Palm Park Formation, especially in the northern part of Apache Valley. Collectively as much as 60 m (197 ft) thick, individual limestone beds range from 1 to 4 m (3.3 to 13 ft) thick and are interbedded with red, cream, or gray mudstone. The limestone beds thicken and thin along strike, often pinching out within short distance, <0.25 km (<0.2 mi), or building into prominent mounds as much as 15 m (49 ft) thick (Fig. 64). Medium to thick bedded, the limestones are gray, tan, or cream in color, generally fine grained, and contain significant amounts of randomly oriented, dark-colored flakes, chips, and filaments, which may be of algal origin. In contrast, limestone mounds usually reveal well-developed, coarse travertine textures.

Depositional environments

Rocks in the lower, middle, and upper parts of the Palm Park Formation represent changing environments during the late Eocene in the Caballo Mountains area. The poorly sorted, mud-supported conglomerate in the lower part of the formation may be interpreted to be debris flow deposits that accumulated on alluvial fans adjacent to the erosional remnants of the Laramide Rio Grande uplift. Finer-grained clastic rocks that grade laterally into conglomerates probably represent interfan low areas or distal fan environments, which were locally the sites of fresh water ponds or cienegas as suggested by interbedded algal limestone. The bulk of the Palm Park Formation clearly records extensive deposition of mudflows and volcanic lahars on the distal portions of volcanic aprons, presumably surrounding andesitic stratovolcanoes or other volcanic edifices in the region. Breccia units probably represent channelized mudflows, whereas mudstones may record overbank flooding, and at least some sandstone bodies may be interpreted as fluvial in origin. The tuffaceous character of the rocks indicates abundant ash was either falling directly on active lahars or was being carried in huge quantities from sources upstream. Upper limestone beds have been studied by Chafetz et al. (1991) who interpreted them to be hydrothermal tufa deposits. The thick limestone mounds containing travertine textures clearly are deposits that accumulated at the sites of hot springs, whereas the thinner bedded, discontinuous lenses of algal limestone probably represent cienegas, small ponds, or lakes fed by the hot springs.

Latest Eocene–Neogene extension and the Rio Grande rift

Beginning in latest Eocene time, basalt-rhyolite volcanism commenced across south-central New Mexico accompanied by the development of broad sedimentary basins, an indication that extensional deformation had begun. Increasing extensional strain is suggested by the outpouring of huge volumes of plateau basaltic andesites later in the Oligocene, fed in part at least, by a system of west-northwest-trending fissures. Dramatic rifting of the crust and formation of the Rio Grande rift followed during the Neogene. The record of this impressive series of events is recorded in some detail by the Bell Top, Uvas, Thurman, Hayner Ranch, Rincon Valley, and Palomas/Camp Rice Formations, collectively more than 2,500 m (8,200 ft) thick in the Caballo Mountains and adjacent areas (Fig. 65).

Bell Top Formation

The Bell Top Formation was named by Kottlowski (1953) for exposures of volcanic and volcaniclastic rocks at Bell Top Mountain in the Sierra de las Uvas. Subsequently, the formation was recognized in neighboring ranges, including the Caballo Mountains. Establishing Bell Top terminology in the Caballos was an outgrowth of mapping of the original Thurman Formation in the Rincon Hills area, first named and described by Kelley and Silver (1952). As they defined it, the Thurman included a tripartite division of lower rhyolite and sedimentary rocks, medial basalt flows, and upper, white, tuffaceous sandstone. In 1973, Seager and Hawley recognized that the lower and middle units corresponded respectively to the Bell Top Formation and Uvas Basaltic Andesite of the Sierra de las Uvas. Subsequent studies in the Caballo Mountains have retained Bell Top and Uvas terminology and restricted Thurman Formation to the white tuffaceous sandstone above the Uvas Basaltic Andesite (e.g. Seager et al, 1982). Excellent exposures of the Bell Top Formation are present at Point of Rocks, Rincon Hills, Black Hills, and in the northern part of Apache Valley. All localities are readily accessible by graded dirt road except the Rincon Hills. Consisting of resistant ash-flow tuff and softer sedimentary rocks, the formation typically forms a series of cuestas and strike valleys.

A latest Eocene–early Oligocene age for the Bell Top Formation is established by radiometric dates from ash-flow tuffs interbedded throughout the formation. Single sanidine $^{40}Ar/^{39}Ar$ ages range from 35.7 Ma for a tuff near the base (tuff 3) to 28.6 Ma for a tuff at the top (tuff 7) of the formation (McIntosh et al., 1991). A minor disconformity may separate basal Bell Top tuffs from underlying Palm Park strata, but the upper part of the formation intertongues with overlying Uvas Basaltic Andesite, at least in exposures south and east of the Derry fault. North of the fault, Uvas basaltic flows pinch out, and in Apache Valley Bell Top rocks are unconformably overlain by Thurman Formation or locally by Rincon Valley Formation.

As much as 450 m (1,476 ft) thick in the Sierra de las Uvas, the Bell Top Formation thins in all directions. At Point of Rocks, 170 m (558 ft) of Bell Top was measured, including a tongue of Uvas Basaltic Andesite. The formation is 170 m (558 ft) thick in the Rincon Hills–Black Hills area (Seager and Hawley, 1973), but thins northward to Apache Valley where it is approximately 80 m (262 ft) thick. A wide array of rock types make up the formation regionally, including basaltic flows and flow-banded rhyolite in addition to ash-flow tuffs and volcaniclastic sedimentary rocks. In the Sierra de las Uvas, where the most complete section is exposed, the following members (with radiometric ages) are present in ascending order: tuff 2; basalt; tuff 3, 35.7 ± 0.2 Ma; tuff 4, 35.0 ± 0.4 Ma; tuff 5, 34.8 Ma; lower sedimentary unit; tuff 6, 33.6 Ma; upper sedimentary unit; and tuff 7, 28.6 ± 0.8 Ma (McIntosh et al., 1991). Tuff 5 and younger members are generally present in the Caballo Mountains.

Based on similar radiometric dates, stratigraphic position, and lithologic characteristics, McIntosh et al. (1991) suggest that several of the Bell Top tuffs are outflow sheets that may be correlated with caldera sources in distant parts of southwestern New Mexico. In particular, they believe that ash-flow tuff 5 is the distal part of the Kneeling Nun ash-flow tuff sheet whose source was the Emory cauldron, located in the Black Range, 50 km (31 mi) west of the Caballo Mountains. Ash-flow tuff 6 correlates with the Box Canyon Tuff, derived from the Schoolhouse Mountain cauldron situated 200 km (124 mi) west of the Caballos, and ash-flow tuff 7 is the Vick's Peak Tuff, derived from the Nogal Canyon cauldron in the San Mateo Mountains, 100 km (62 mi) north of the Caballo Range.

Kneeling Nun Tuff/ash-flow tuff 5

Named for the Kneeling Nun, a rock monolith that overlooks the open pit copper mine at Santa Rita, the Kneeling Nun Tuff is one of the most widespread ash-flow tuff sheets in southern New Mexico (Kuellmer, 1954; Jicha 1954; Elston, 1957). Its source cauldron, the Emory cauldron in the Black Range, was described by Elston et al. (1975) and Abitz (1986). An $^{40}Ar/^{39}Ar$ age of 34.9 Ma obtained from the Kneeling Nun Tuff corresponds almost exactly with the 34.8 Ma age of tuff 5 of the Bell Top Formation (McIntosh et al., 1990, 1991, 1992).

The prominent orange-weathering, cliff-forming tuff in the northern part of Apache Valley is probably Kneeling Nun Tuff (Fig. 66). Overlying the Palm Park Formation, the tuff marks the base of the Bell Top Formation. It is succeeded by the lower sedimentary member of the Bell Top, or locally by the upper sedimentary member. Approximately 30 m (98 ft) thick, the tuff probably represents a distal facies of the Kneeling Nun outflow sheet. Lithologically, it is similar to the Kneeling Nun at the type area as well as in the Emory cauldron. Crystals of quartz, sanidine, biotite, plagioclase, and sphene comprise approximately 30% of the volume of the tuff, and these are imbedded in a matrix of glass shards and distinctive pink or lavender, uncollapsed, crystal-rich pumice fragments. A simple cooling unit, the tuff is poorly welded or entirely unwelded, weathering to pale pink, salmon, or cream colored, bold cliffs that display the smooth planar surfaces typical of columnar joints (Fig. 67).

South and east of the Derry fault, outcrops of the basal Bell Top tuff are assigned to tuff 5. The tuff is well exposed at Point of Rocks and in the Rincon Hills–Black Hills–Palm Park area, forming prominent cuestas at each locality (Fig. 68). Like the Kneeling Nun Tuff, tuff 5 unconformably(?) overlies the Palm Park Formation and is overlain by the lower sedimentary member of the Bell Top Formation. As much as 21 m (69 ft) thick in Point of Rocks, tuff 5 is 5–17 m (16–56 ft) thick or less in the Rincon Hills–Black Hills area. Local irregularity in thickness is due to channels incised into the top of the unit prior to deposition of overlying Bell Top conglomerate. Like the Kneeling Nun Tuff, ash-flow tuff 5 is crystal and pumice rich. However, Clemons (1976) points out differences in the ratios of quartz, feldspar, and biotite in the two tuffs, and the fact that tuff 5 is sphene-free, whereas the Kneeling Nun always contains that mineral. Furthermore, tuff 5 contains abundant bipyramidal quartz, is prevailingly gray in color rather than orange or pink, and pumice lumps are chalky white rather than pale red or lavender. Clemons (1979) also indicates that Kneeling Nun Tuff underlies tuff 5 in the Goodsight Mountains. In view of these differences, the Kneeling Nun Tuff and ash-flow tuff 5 were differentiated on geologic maps of Apache Valley and the southern parts of the range, although both units probably represent the same outflow sheet.

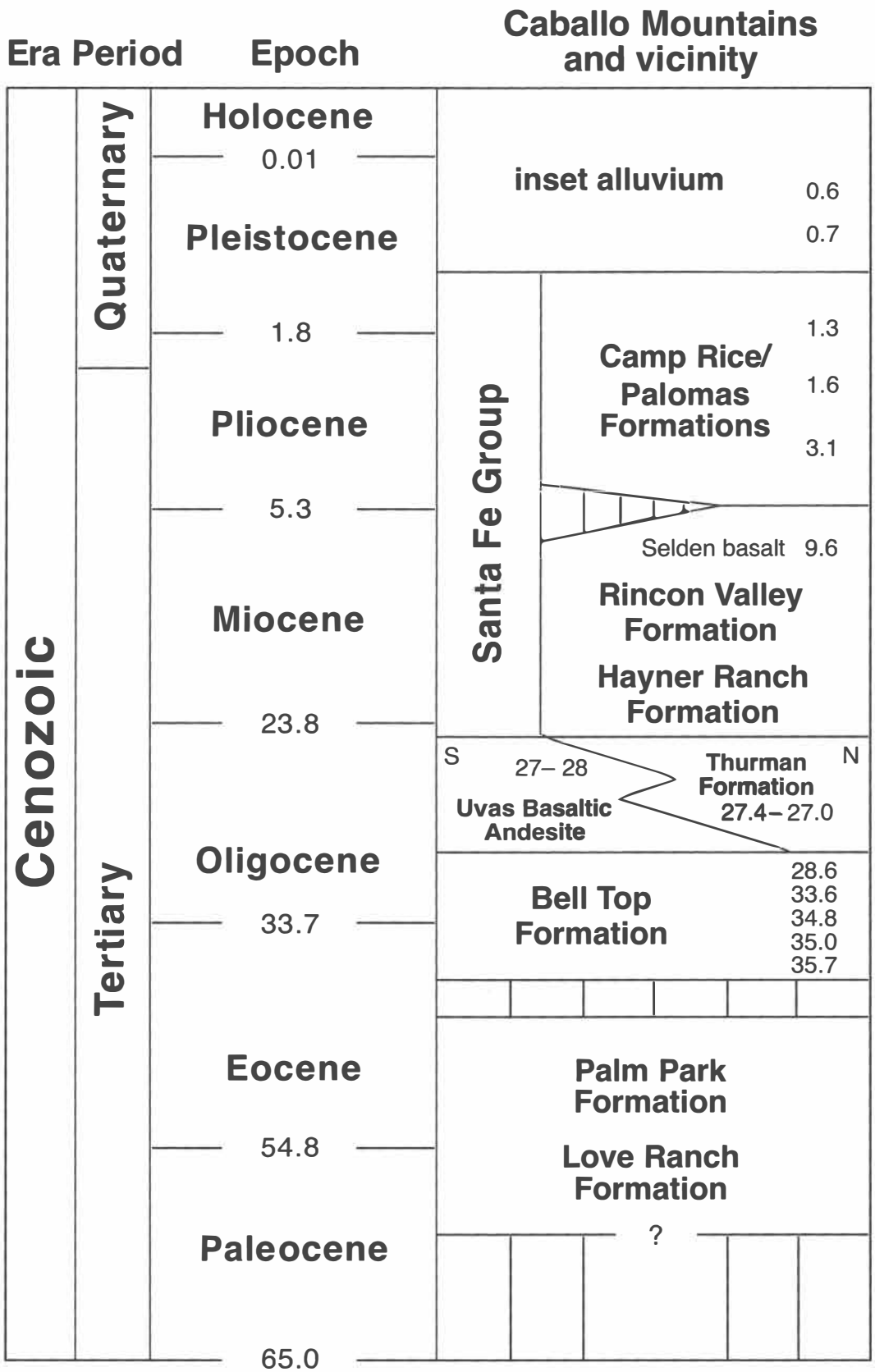

FIGURE 65—Cenozoic correlation chart for southern New Mexico. Numbers are radioisotopic dates of volcanic rocks in millions of years, adapted from Kortemeier (1982), Seager et al. (1984), McIntosh et al. (1991), Mack et al. (1993), Boryta (1994), and Mack et al. (1996). Boundaries for the epochs in millions of years are taken from the DNAG time scale (Palmer and Geissman, 1999).

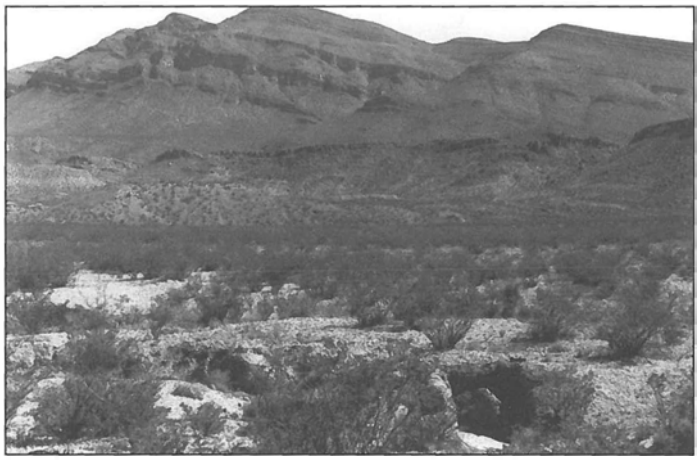

FIGURE 66— Caballo fault block in the background with Tertiary strata exposed in Apache (White) graben in the foreground. The prominent dark cuesta near the middle of the photo is Kneeling Nun Tuff, below which are Palm Park beds. The low peak in shadow in the left center part of photo is the Palm Park travertine deposit pictured in Fig. 64.

FIGURE 67—Kneeling Nun Tuff (left) and ash-flow tuff 6 (center right), separated by thin, slope-forming lower sedimentary member of the Bell Top Formation. Units are exposed on north slope of Apache Canyon. View looks north.

Ash-flow tuff 6

Ash-flow tuff 6 is well exposed at Point of Rocks, throughout the Rincon Hills–Black Hills area, and in most of the northern part of Apache Valley (Fig. 67). A ledge-forming, simple cooling unit, ash-flow tuff 6 conformably overlies the lower sedimentary member of the Bell Top Formation in each area and is succeeded upward by the upper sedimentary member.

Although tuff 6 is approximately 11–15 m (36–49 ft) thick throughout the southern Caballo Mountains, it is locally absent in Apache Valley, owing to erosion by streams that deposited conglomerate at the base of the upper sedimentary member. Crystal rich, tuff 6 contains broken crystals of quartz, sanidine, biotite, and plagioclase in a matrix of devitrified ash. Like tuff 5, tuff 6 is medium gray in color. However, fewer and smaller crystals, the lack of bipyramidal quartz, and the absence of conspicuous large pumice fragments distinguish tuff 6 from tuff 5 in faulted outcrops.

Sedimentary members of the Bell Top Formation

Sedimentary rocks occupy a stratigraphic position above ash-flow tuff 5/Kneeling Nun Tuff and the top of the Bell Top Formation. Where ash-flow tuff 6 is present, it serves to divide the sedimentary rocks into lower and upper sedimentary members. In the Caballo Mountains and vicinity, the sedimentary member(s) increase in thickness toward the east-southeast from 47 m (154 ft) near Pass Tank (NE¼ sec. 34 T16S R4W) to just less than 200 m (656 ft) at Point of Rocks (SE¼ sec. 22 and NW¼ sec. 26 T17S R2W) and in the Rincon Hills (SE¼ sec. 23 and NE¼ sec. 26 T18S R3W). In addition to sedimentary rocks, the upper sedimentary member at Point of Rocks also contains a basalt lava flow and associated cinder conglomerate (Fig. 69).

Description

The sedimentary member(s) of the Bell Top Formation consist of three rock types, tuffaceous sandstone, conglomerate, and shale. Tuffaceous sandstones are distinctly whitish to light gray in

FIGURE 68—View southeastward across lowlands of Palm Park to cuesta of ash-flow tuff 5, which nearly rims the valley. Beyond, are the Rincon Hills (with tower), flat-topped San Diego Mountain, the Doña Ana Mountains, and on the skyline, the Organ Mountains.

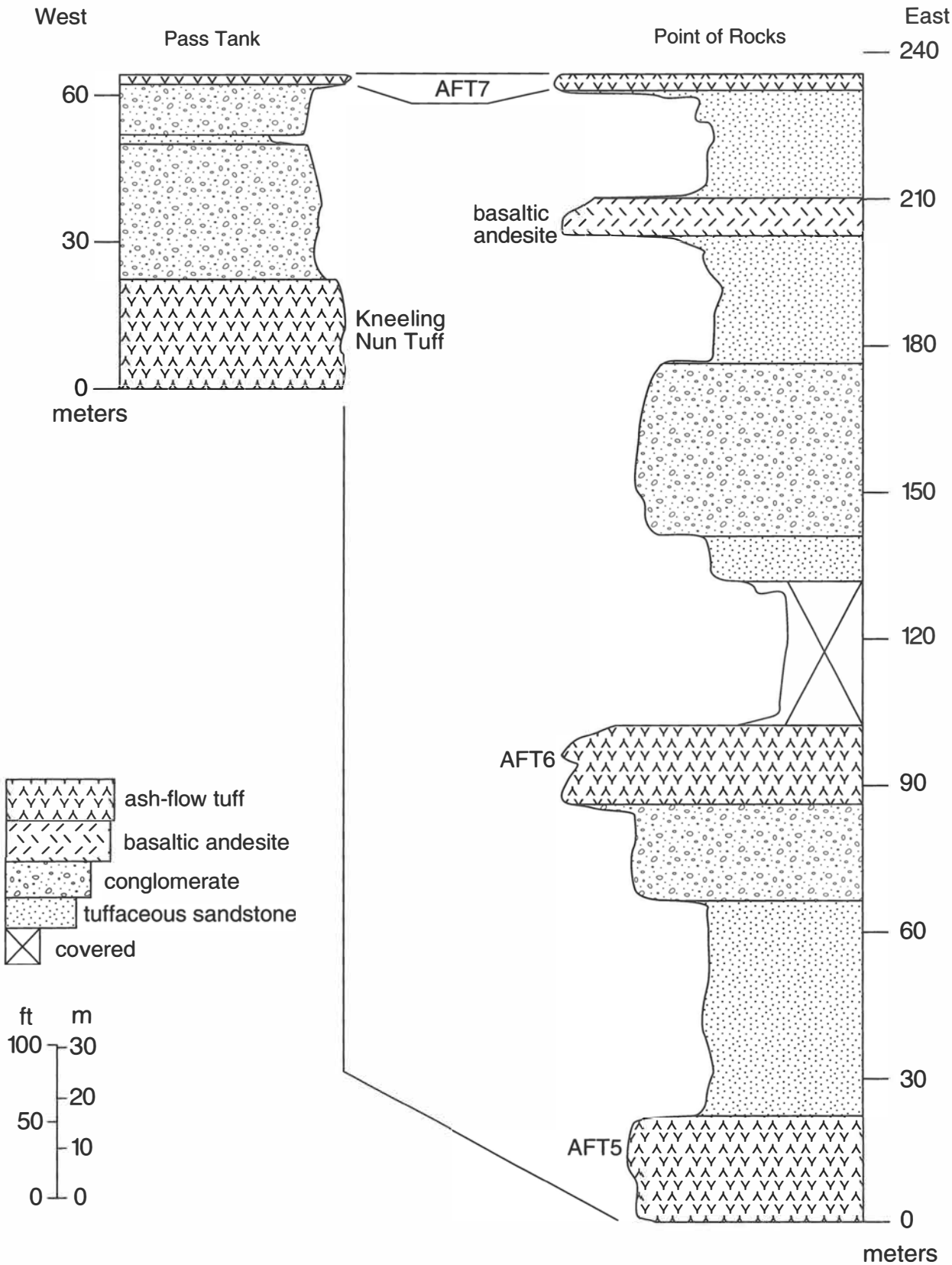

FIGURE 69—Measured section of the Bell Top Formation (lower Oligocene) at Pass Tank in Apache Canyon (NE¼ sec. 34 T16S R4W) and at Point of Rocks (SE¼ sec. 22 and NW¼ sec. 26 T17S R2W).

color, medium to thin bedded, and fine to medium grained. Most beds have layers or scattered granules and small pebbles of white pumice. The majority of beds are relatively thin, <1 m (<3.3 ft), and laterally continuous for tens of meters, although broad, shallow channels are also present. Graded beds and horizontal laminae are common, and small-scale trough crossbeds are rare. A few beds are massive and consist of gravel-sized clasts of pumice or epiclasts floating in a matrix of sand or finer sediment. In thin section, the tuffaceous sandstones are composed of a subequal mixture of glass shards and/or pumice, and crystals of quartz, sanidine, and biotite.

Conglomerates dominate the section at Pass Tank, and are also present in both the lower and upper sedimentary members at Point of Rocks (Fig. 70). The conglomerates are medium to thin bedded and display both poorly sorted, matrix-supported and moderately well sorted, grain-supported varieties. The latter commonly contains lenses and thin beds of coarse sandstone, which may be massive or have horizontal laminae or trough crossbeds. Imbrication is also common in the grain-supported conglomerates and indicates paleoflow primarily to the east-southeast (Mack et al., 1994a). Grain size of the conglomerates ranges from boulders up to 1 m (3.3 ft) in length to pebbles and granules, and generally decreases to the east-southeast.

The conglomerates are composed of clasts of andesite porphyry, ash-flow tuff 5 and Kneeling Nun Tuff, and well-rounded clasts of Precambrian metamorphic and granitic rocks, Paleozoic limestone and dolostone, and Abo siltstone. Because of excellent rounding, the Precambrian and Paleozoic clasts are interpreted to be recycled from the Love Ranch Formation. Most of the andesite clasts are derived from the Palm Park Formation, although a few may represent Upper Cretaceous volcanic gravel reworked out of the Love Ranch Formation. One of the uppermost conglomerates at Point of Rocks also contains a few clasts of flow-banded rhyolite, which were probably derived from the Cedar Hills vent zone, located south of the Caballo Mountains (Mack et al., 1994a).

The least common rock type in the sedimentary member(s) is red sandy shale. Generally less than 1 m (3.3 ft) thick, the red shale is not present everywhere the sedimentary member(s) is exposed. The shale has a blocky fabric and locally contains small root traces.

Depositional environments

The abundance of glass shards and pumice in the tuffaceous sandstones indicates they represent fallout tephra that was reworked by sedimentary processes. Plinian eruptions presumably mantled the countryside with largely sand-sized tephra, which was quickly redistributed toward topographically low areas by sheetfloods, shallow streamflows, or debris flows. Following the terminology of Smith (1991), Mack et al. (1994a) referred to these rocks as "syneruption facies."

Once the fallout tephra was removed from upland areas, bedrock was exposed and supplied gravel and sand to the Bell Top Basin. Mack et al. (1994a) referred to these rocks as "post-eruption facies." The coarse grain size and paucity of interbedded fines within the post-eruption facies suggest they were deposited on alluvial fans. Most of the post-eruption conglomerates were deposited by sheetflood or streamflood processes, although the matrix-supported variety probably represents debris flows. Paleoflow on the fans was to the east-southeast (Mack et al., 1994a). Red mudstone probably accumulated between fans or beyond the toes of the fans in an alluvial-flat setting.

Ash-flow tuff 7 (Vick's Peak Tuff)

Good outcrops of ash-flow tuff 7 are present at Point of Rocks, Black Hills, and in the northern part of Apache Valley. Only 3 m (9.8 ft) thick or less, tuff 7 is discontinuous along strike and is missing altogether in the Rincon Hills area. Ledges and cuestas

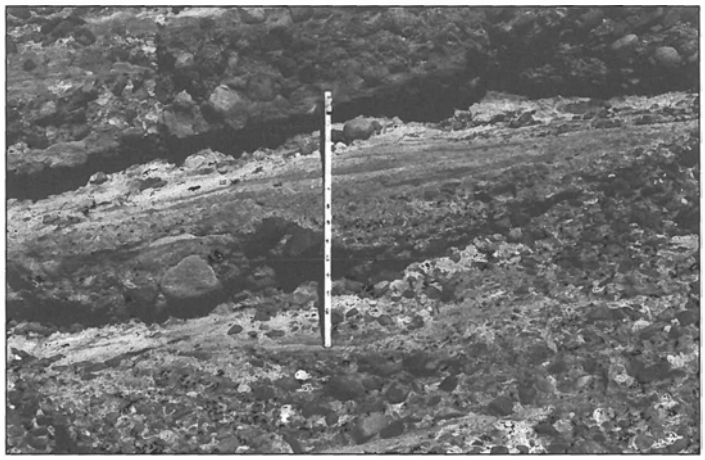

FIGURE 70—Conglomerates and sandstones of the Bell Top Formation (lower Oligocene) in Apache Canyon. Jacob's staff is 1.5 m (4.9 ft) long.

are the favored landforms, and often these conspicuously mark the top of the Bell Top Formation. Tuff 7 is conformable with both the underlying upper sedimentary member of the Bell Top and overlying Uvas Basaltic Andesite, with two exceptions. In Apache Valley, tuff 7 generally is succeeded by the Thurman Formation as a result of the pinchout of intervening Uvas flows. Also in Apache Valley, at the south end of White graben, tuff 7 is locally overlapped by the Miocene Rincon Valley Formation, the contact an angular unconformity. A simple cooling unit, tuff 7 is a dark, grayish-brown, fine-grained, moderately welded tuff that consists mostly of glass shards and pumice fragments.

Rhyolite dikes

Rhyolite dikes crop out in only two places in the Caballo Mountains. The first occurrence is approximately 1 km (0.6 mi) south of Bob's Tank on the southeastern flank of Timber Mountain. There, a discontinuous flow-banded rhyolite dike, dipping steeply (~60°) trends west northwest and for a distance of 2 km (1.2 mi) cuts successive beds of Abo, Bar B, and Nakaye strata. The southerly portion of the dike lies adjacent to a dike of basaltic andesite, the two having apparently intruded along the same fissure. A second rhyolite dike closely follows the anticlinal crest of the McLeod Hills fault-propagation fold on Taylor Ridge. Approximately 5 km (3.1 mi) long, the dike dips west, following a thrust fault in the core of the anticline, but locally diverging into one limb of the fold or the other. Nowhere more than 15 m (49 ft) thick, the dike consists of unfoliated, nearly aphyric rhyolite that weathers to cream or gray. The rhyolite is younger than the Laramide folds and thrusts, which structurally control its position and attitude, and older than the normal faults at the southern end of Haystack syncline, which dismember it. The dikes are considered to be Oligocene in age, probably related to silicic volcanic activity associated with the Bell Top Formation.

Uvas Basaltic Andesite

Named by Kottlowski (1953) for exposures in the Sierra de las Uvas, the Uvas Basaltic Andesite is part of a vast sheet of flood basaltic andesite that once covered most of southwestern New Mexico and northern Chihuahua (Cameron et al., 1989). In the Socorro area, the basalts are known as La Jara Peak Andesite (Tonking 1957), in the Black Range–Silver City area as the Bear Springs Basalt (Elston, 1957). Outcrops of Uvas Basaltic Andesite in the Caballo Mountains are confined to the Rincon Hills and Point of Rocks in the southern part of the range and Jornada del Muerto, respectively. The latter outcrops are easily accessible from I–25 and are representative of outcrops within the range. Dark-gray, vesicular, basaltic-appearing flows comprise most of the formation, forming low cuestas or moderately high, rounded hills.

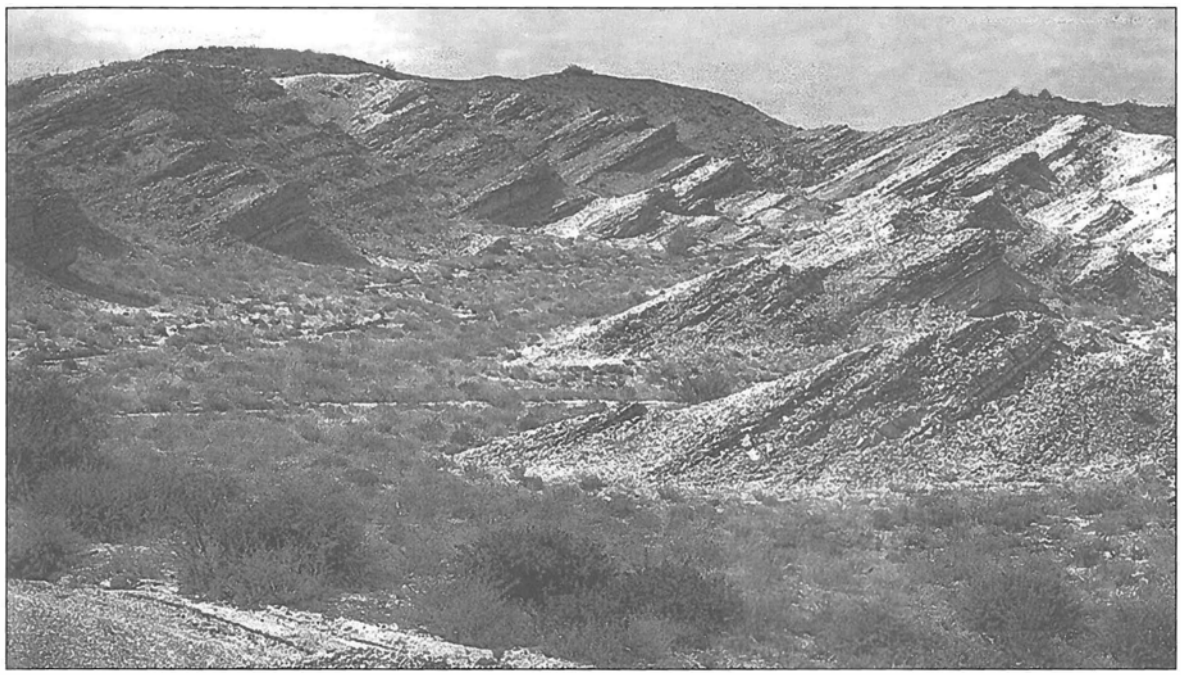

FIGURE 71—Tilted, white Thurman sandstone and mudstone exposed in Johnson Spring Arroyo area. View looks northwest.

Radiometric dates from the Uvas Basaltic Andesite establish its age between 27 and 28 Ma (late Oligocene; Clemons, 1979), consistent with a date of 28.1 Ma from a flow within the Bear Springs Basalt near Hillsboro (Seager et al, 1984). The Uvas Basaltic Andesite intertongues both downward with underlying Bell Top rocks and upward with overlying Thurman Formation.

As much as 250 m (820 ft) thick in the Sierra de las Uvas, the Uvas Basaltic Andesite thins northward to 103 m (338 ft) thick in the Rincon Hills to a pinchout somewhere between the Derry fault and southern Apache Valley. In the central and northern Apache Valley, the formation is absent between the Bell Top and Thurman Formations. In Point of Rocks, the Uvas Basaltic Andesite is probably more than 150 m (492 ft) thick.

Description

Grayish-brown to dark-gray vesicular, amygdaloidal flows distinguish the Uvas Basaltic Andesite, although some flows are massive, non-vesicular, and exhibit platy jointing. Silica content ranges between 49% and 60%, consistent with a classification as basaltic andesite rather than true basalt. Two to three tongues of white, tuffaceous Thurman sandstone or pink sandstone define the intertonguing relationship of the two formations in the Rincon Hills.

More than forty mafic dikes, probably correlative with Uvas Basaltic Andesite flows, trend west-northwest across the Caballo Mountains, and especially, across the pedimented strata of the northeastern piedmont slope. At Point of Rocks, one of these dikes transects Bell Top Formation and merges upward into flows of Uvas Basaltic Andesite, a relationship indicating the dike fed one of the flows and is late Oligocene in age. Esser (2003a) obtained an $^{40}Ar/^{39}Ar$ age of 26.8± 0.68 Ma for this dike. The dikes are generally basaltic in composition and range from aphyric to coarsely prophyritic. One dike observed near Apache Gap Tank contains > 50% plagioclase phenocrysts, each 0.5–1.0 cm (0.2–0.4 in) in length. From 2 to 6 m (6.6 to 20 ft) in width, the dikes range in length from less than 1 km (0.6 mi) to more than 6 km (3.7 mi). The longest dikes are part of a swarm that crosses Cretaceous outcrops on the pedimented northeastern flank of the range. Where dikes transect these Cretaceous or other sandstone beds, they hold up low ridges; where they cut more resistant limestone beds, they weather to narrow trenches, often with steep sides. Locally, the dikes occupy faults of relatively minor displacement, but most of the dikes were emplaced along fissures lacking offset.

Mode of emplacement

The thick pile of Uvas Basaltic Andesite lava flows in the Sierra de las Uvas region, together with exposed vents, including plugs, cinder cones, and diatremes, suggests the Uvas Basaltic Andesite in that area formed a small, compound shield volcano composed of several types of central vents (Clemons and Seager, 1973). Flows spread out radially from the center, but in the Caballo Mountain region, they pinched out within Bell Top and Thurman sedimentary units. The presence of basaltic andesite dikes merging upward into flows at Point of Rocks indicates that some flows were emplaced as fissure eruptions, a regionally significant mode of emplacement, judging from the widespread, plateau-forming aspect of these basaltic andesites (Cameron et al., 1989). Further, the west-northwest-trending dikes in the Caballo area are evidence that a north-northeast–south-southwest directed extensional stress field prevailed in south-central New Mexico during the late Oligocene.

Thurman Formation

The Thurman Formation was named by Kelley and Silver (1952) for a thick sequence of sedimentary and volcanic rocks exposed in Thurman Arroyo, which drains Palm Park and the Black Hills. Seager and Hawley (1973) subdivided the Thurman Formation in the Rincon Hills into upper and lower Thurman formations separated by the Uvas Basaltic Andesite. They recognized that the lower Thurman Formation in the Rincon Hills was equivalent to the upper part of the Bell Top Formation of the Sierra de las Uvas. Subsequently, the designation upper and lower Thurman has been abandoned in the Caballo Mountains in favor of the names Bell Top Formation, Uvas Basaltic Andesite, and Thurman Formation, in ascending order (e.g. Seager et al., 1982). Besides the excellent exposures in the Rincon Hills, the Thurman Formation crops out widely in Apache Valley. The white sandstone that forms much of the formation and by which it is readily recognized, forms spectacular, barren, white badlands in both

areas, but especially in the Johnson Spring Arroyo area (Fig. 71) of the Rincon Hills (Seager and Hawley, 1973). However, it is most easily accessible in Apache Valley.

The age of the Thurman Formation is based on reversal magnetostratigraphy and $^{40}Ar/^{39}Ar$ ages of single sanidine crystals extracted from sandstone beds within the formation. Although ages of 34.9, 33.5, and 27.7 Ma have been obtained, most dates cluster around 27.4 Ma (Boryta, 1994; Boryta and McIntosh, 1994). The intertonguing relationships of basal Thurman beds and Uvas Basaltic Andesite is also consistent with an age of 27–28 Ma for the Thurman Formation. At the top of the formation in Apache Valley, the Thurman intertongues with overlying conglomerate of the Hayner Ranch Formation, or locally is angularly unconformable beneath Rincon Valley or Camp Rice/Palomas strata.

Complete sections of the Thurman are exposed in the Rincon Hills, where it is 388 m (1,273 ft) thick, and in Apache Valley, where it is 508 m (1,666 ft) thick. Kelley and Silver (1952) also reported that 285 m (935 ft) of Thurman Formation was penetrated in the Barney Iorio No. 1 Fee well in the Palomas Basin (sec. 25 T14S R5W). Kieling (1993) measured sections in both the Rincon Hills and Apache Valley, describing six lithofacies.

Description

Kieling's (1993) study of the Thurman Formation provided important information about the age, thickness, stratigraphy, and depositional environments of the six lithofacies she described. The thin-bedded sandstone lithofacies and massive sandstone lithofacies compose the bulk of the formation. The thin-bedded sandstone lithofacies consists of planar-bedded, white to light-gray, medium-grained sandstone. Highly tuffaceous, the sandstone contains abundant glass shards and pumice, as well as single crystals of sanidine, quartz, plagioclase, and biotite. The massive sandstone lithofacies is compositionally similar, but is unsorted, unlayered, and often contains cobbles of basaltic or other volcanic rocks "floating" in a matrix of sand. Single beds of massive sandstone may exceed 10 m (33 ft) thick. Less common is the crossbedded sandstone lithofacies. Compositionally identical to the massive and thin-bedded sandstone, the crossbedded sandstone lithofacies is distinguished by trough crossbeds in sets that seldom exceed 1 m (3.3 ft) thick. Even less abundant is the conglomerate lithofacies, which consists of grain-supported volcanic cobbles and pebbles confined to shallow channels less than 1 m (3.3 ft) thick. The fifth and sixth lithofacies include massive pink mudstone in beds as much as 2 m (6.6 ft) thick, and at least four white fallout-tuff units, each approximately 0.2 m (0.7 ft) thick. Whereas massive sandstone lithofacies distinguish the Thurman Formation in the northern part of Apache Valley, fine-grained, thin-bedded sandstone, crossbedded sandstone, and mudstone lithofacies are relatively more common farther south in the Rincon Hills.

A notable series of clastic dikes cuts the Thurman Formation in the northern part of Apache graben. As much as 30 cm (12 in) thick, the dikes range in texture from coarse-grained sandstone to fine, sandy mudstone. Their source appears to be a fine sandstone/mudstone unit 10 m (33 ft) thick at the base of the formation, and from there the dikes extend upward approximately 100 m (328 ft). No dikes cut middle and upper parts of the formation. Most of the dikes trend N10°E–N30°E, dip steeply, and are roughly orthogonal to bedding. A few trend N25°W, parallel to a weakly developed set of joints. The trend of dikes and joints suggests the dikes invaded a conjugate fracture system, but little or no offset of bedding is present along either dikes or joints. Orientation of the conjugate fracture system suggests approximate east-west extension, a contrast with the north-northeast–south-southwest extension indicated by upper Oligocene basaltic dikes.

Depositional environments

Except perhaps for the rare conglomerate beds, the Thurman Formation represents syneruption sediments and fallout ash deposited on the distal part of an alluvial apron (Walton, 1979; 1986; Smith, 1991; Kieling, 1993; Mack et al., 1994a). Massive, poorly bedded sandstones were probably deposited by debris flows, whereas thin-bedded sandstone represents deposition by sheetfloods, an interpretation consistent with thin, laterally continuous bedding, horizontal laminae, and the lack of crossbedding. Grain-supported cobble conglomerate and crossbedded sandstone probably indicate deposition in shallow channels associated with sheetflood runoff, whereas mudstones are either very distal mudflow deposits or alluvial-flat sediments. At least four times, fallout tephra accumulated on the alluvial apron and was buried before it was eroded.

The predominant date of 27.4 Ma suggests that most of the tephra in the Thurman Formation was derived from the 27.4 Ma Mount Withington caldera (McIntosh et al, 1986, 1991), located 80 km (50 mi) north of the Caballo Mountains. Consistent with this interpretation are two lines of sedimentological evidence described by Kieling (1993). First, southward dispersal of Thurman sand is suggested by trough-crossbed paleocurrent data. Second, more distal lithofacies, including fine-grained sheetflood and shallow-channel sandstone and alluvial-flat mudstone, compose a larger percentage of the more southerly Rincon Hills section, whereas the predominantly debris flow facies in Apache Valley is more proximal. Thus, the Thurman Formation appears to be a distal part of the volcaniclastic apron that spread southward from the Mount Withington caldera.

Although the Thurman Formation is thick in the southern Caballo Mountains, the formation is too limited geographically to determine if its distribution was controlled by early rift grabens. Clearly, the fine-grained character of the formation, even adjacent to major faults of the southern Caballo range, indicates that if these faults were active they had not created significant topographic relief during Thurman deposition. On the other hand, syndepositional faulting and associated earthquakes could have triggered emplacement of clastic dikes into the lower part of the formation. Alternatively, the dikes may simply have been the product of rapid loading of water-saturated sand and mud by the overlying thick sequence of Thurman sands.

Hayner Ranch Formation (Santa Fe Group)

The Hayner Ranch Formation was named by Seager et al. (1971) for about 800 m (2,624 ft) of conglomerate, sandstone, and shale exposed near San Diego Mountain. In addition, 500 m (1,640 ft) of fine-grained sediment at San Diego Mountain originally assigned to an "unnamed transitional unit" are now considered to belong to the Hayner Ranch Formation, bringing the total at the type section to 1,300 m (4,265 ft; Mack et al., 1998a). A comparable thickness of the Hayner Ranch Formation is exposed in the Caballo Mountains and vicinity. The most complete sections are (1) in Caballo and Pulido Canyons, southeastern part of the Caballo quadrangle; (2) in Apache Valley, northern part of the McLeod Tank quadrangle; (3) along the southwest flank of Red House Mountain, southern McLeod Tank and northern Hatch quadrangles; (4) in the Rincon Hills and adjacent Black Hills, central and western parts of the Rincon quadrangle, respectively; and (5) in the northern Sierra de las Uvas, south-central part of the Hatch quadrangle.

In the Caballo Mountains, the base of the Hayner Ranch Formation is transitional with the underlying Thurman Formation. Over a stratigraphic interval of approximately 50 m (164 ft), white tuffaceous sandstones of the Thurman Formation are interbedded on the scale of from 5 to 20 m (49 to 66 ft) with gray pebble and cobble conglomerates and sandstones of the Hayner Ranch Formation. The upper contact of the Hayner Ranch Formation may be locally conformable with the Rincon

FIGURE 72—Cobble conglomerates of the Hayner Ranch Formation (upper Oligocene–lower Miocene) in Apache Valley.

Valley Formation, marked by the change to more reddish colors, as well as by the appearance of angular clasts of Paleozoic rocks. In general, however, the Hayner Ranch–Rincon Valley contact is an angular unconformity.

The Hayner Ranch Formation cannot be directly dated, because it lacks index fossils and datable volcanic rocks. However, it can be bracketed between latest Oligocene and late Miocene, based on stratigraphic position (Fig. 65). The age of the base of the Hayner Ranch Formation is constrained by the transitional contact with the Thurman Formation, which has been interpreted by Boryta (1994) and Boryta and McIntosh (1994) to be between 27.4 and 27.0 Ma, based on radioisotopic dating of detrital sanidines and reversal magnetostratigraphy. Similarly, the Hayner Ranch underlies the Rincon Valley Formation, which contains the 9.6 Ma Selden basalt (Seager et al., 1984). Consequently, the age of the top of the Hayner Ranch Formation is no younger than late Miocene.

Description

The Hayner Ranch Formation in the Caballo Mountains and vicinity is primarily composed of gray, moderately cemented conglomerate, with lesser amounts of sandstone, shale, and limestone. In the southernmost Rincon Hills, however, the formation is tightly cemented and prevailingly red or dark brown, the result of local silicification, alteration, and mineralization along late Tertiary faults. The coarsest, most poorly sorted, and thickest-bedded conglomerates are located directly adjacent to the Red House Mountain and Caballo fault blocks, where boulders up to 1 m (3.3 ft) in length are common. To the west and southwest, the conglomerates are thinner bedded, finer grained, and better sorted (Fig. 72). Imbrication is common in the thin-bedded conglomerates, and some of the conglomerates have thin interbeds or lenses of coarse sandstone. Imbrication measurements indicate westward and southwestward paleoflow (Mack et al., 1994b). Clasts in the conglomerates are subangular to subrounded and consist of a variety of volcanic rock types, with chert, carbonates, red siltstones, and red granite appearing only near the top of the formation. The latter three clast types are commonly much better rounded than associated volcanic clasts.

Interbedded with conglomerates are distinct beds ranging from 1 to 5 m (3.3 to 16 ft) thick of medium- to coarse-grained sandstone. Granules and pebbles are locally present in the sandstones as scattered clasts or as discrete lenses. The dominant sedimentary structures are graded beds, horizontal laminae, and cut-and-fill structures. Crossbeds are rare.

Much less common than conglomerate and sandstone are thin, <1 m (<3.3 ft), beds of red to brown, sandy mudstone and tan to red argillaceous very fine sandstone. These fine-grained rocks have a blocky fabric and lack sedimentary structures. A few beds have scattered calcic nodules and tubules 2–3 cm (0.8–1.2 in) in diameter that resemble stage II morphology calcic soils (Gile et al., 1981).

The least common rock type in the Hayner Ranch Formation are four thin limestones, which are best exposed in the Rincon Hills. Generally less than 2 m (6.6 ft) thick, the limestones are interbedded with fine conglomerates and sandstones. The limestones are primarily composed of microcrystalline calcite and are devoid of allochems, although a few beds contain ostracods and one has stromatolites (Kieling, 1994; Mack et al., 1994b).

In the northern Sierra de las Uvas, about 30 m (98 ft) of cobble and boulder conglomerates of the Hayner Ranch Formation occupy a paleocanyon cut into the Uvas Basaltic Andesite. The paleocanyon is approximately 200 m (656 ft) wide and 1 km (0.6 mi) long. Imbrication paleocurrents and northward fining of the conglomerates indicate northerly paleoflow of the canyon fill sediment.

Depositional environments

The abundance of conglomerate and granular, pebbly sandstone indicate that most of the Hayner Ranch Formation was deposited on alluvial fans (Mack et al., 1994b). The coarsest, most poorly sorted conglomerates probably were deposited as debris flows, while the thin-bedded, imbricated conglomerates were deposited by sheetfloods and streamfloods. Thin mudstones were most likely deposited between fans or on alluvial flats beyond the toes of the fans, and thin limestones probably represent small, carbonate-precipitating lakes (Mack et al., 1994b). Overall coarsening toward the east-northeast together with west-southwest-directed paleocurrents suggests that the southern Caballo and Red House Mountain fault blocks were the source of sediment of the Hayner Ranch Formation. Moreover, composition of the clasts in the Hayner Ranch Formation suggests that the Uvas, Thurman, Bell Top, Palm Park, and Love Ranch Formations were exposed in the fault blocks. The latter Formation supplied the anomalously well-rounded clasts of Precambrian granite and Paleozoic carbonate and siltstone found in the upper part of the Hayner Ranch Formation.

The paleocanyon infilled with Hayner Ranch conglomerate in the northern Sierra de las Uvas is an exception to the model of derivation of the Hayner Ranch Formation from the Caballo and Red House Mountain fault blocks. The conglomerates in the paleocanyon were derived from the Uvas Basaltic Andesite and were dispersed northward. Similarly, Hayner Ranch strata at the type section at San Diego Mountain and in the Selden Hills were derived from the south (Mack et al., 1994b).

Rincon Valley Formation (Santa Fe Group)

The Rincon Valley Formation was named by Hawley et al. (1969) and Seager et al. (1971) for exposures at San Diego Mountain and in the Cedar Hills. In the Caballo Mountains, the Rincon Valley Formation is best exposed in those locations described above for the Hayner Ranch Formation. Up to 600 m (1,968 ft) thick at the type section, the Rincon Valley Formation has a comparable thickness in the Caballo Mountains. The Rincon Valley Formation conformably overlies the Hayner Ranch Formation at its type locality, although in the Caballo Mountains area the contact is generally an angular unconformity. The Rincon Valley Formation may be distinguished from the Hayner Ranch Formation in the Caballo Mountains by overall redder colors and by an abundance of angular Paleozoic clasts, but these criteria do not always apply elsewhere in the region. Throughout southern New Mexico, including the Caballo Mountains and the type section, the Rincon Valley Formation is unconformably overlain by the Camp Rice or Palomas Formations. Although its

age is poorly constrained, the formation is considered to be late Miocene in age. In Selden Canyon, the Rincon Valley Formation has within it the Selden basalt, which has been radioisotopically dated at 9.6 Ma (Seager et al., 1984). The upper age limit is constrained by the age of the oldest dates for the Camp Rice and Palomas Formations, which are between 4.5 and 5 Ma (Mack et al., 1998b).

Description

The Rincon Valley Formation is composed of conglomerate, sandstone, and red, locally gypsiferous mudstone. The relative abundance of the rock types varies laterally. The formation is coarsest near the Caballo and Red House Mountain fault blocks and fines to the west, southwest, and south. Most conglomerates are medium- to thin-bedded and consist of moderately well sorted, imbricated pebbles, cobbles, and small boulders. Many of the thin beds are laterally continuous for tens of meters with little or no thickness change, while others consist of broad, 10 m (33 ft), shallow, 1 m (3.3 ft), channels. Decimeter-scale couplets of gravel and coarse sand are common in the thin-bedded conglomerates. Imbrication paleocurrent data indicate westward and southwestward paleoflow (Mack et al., 1994b). A few conglomerates are medium bedded, poorly sorted, and matrix supported. Red medium- to coarse-grained sandstones are also present, generally as lenses or thin beds intercalated with conglomerate. Gravel-sized clasts in the conglomerates and sandstones consist of volcanic rocks and angular clasts of Pennsylvanian limestone and red Abo siltstone.

In and directly adjacent to Rincon Hills, and extending northwestward to the mouth of Berrenda Creek, the Rincon Valley Formation is characterized by thick, red mudstones, thin, <1 m (<3.3 ft), sandstones, and gypsum (Fig. 73). The mudstones have a blocky fabric, and many contain displacive crystals of selenite gypsum. The sandstone beds are medium grained, locally contain pebbles, and display horizontal laminae. In the Rincon quadrangle (sec. 8 T19S R2W) the red mudstone is interbedded with thin, <30 cm (<12 in), laterally continuous beds of selenite gypsum.

In the northern Sierra de las Uvas, paleocanyon-fill conglomerates of the Hayner Ranch Formation are overlain by fine sandstones, pebble conglomerates, and mudstones of the Rincon Valley Formation. Unlike farther north, the Rincon Valley Formation at this location has north to northwest-directed paleocurrents and consists primarily of volcanic clasts, including flow-banded rhyolite (Mack et al., 1994b).

Depositional environments

The northern and eastern exposures of the Rincon Valley Formation in the Caballo Mountains and vicinity were deposited on alluvial fans, an interpretation supported by the abundance of coarse-grained conglomerates. Thin-bedded, imbricated conglomerates and sandstones probably represent sheetfloods, whereas the less common, poorly sorted conglomerates may be debris flows. Coarsening toward the east-northeast together with west to southwest-directed paleocurrents suggests derivation from the Caballo and Red House Mountain fault blocks (Mack et al., 1994b). A decrease in the ratio of volcanic to sedimentary clasts in the Rincon Valley Formation compared to the Hayner Ranch Formation suggests "unroofing" of Paleozoic sedimentary rocks in the Caballo and Red House Mountain fault blocks. The angularity of limestone and siltstone clasts points to a first-cycle origin, rather than reworking from the Love Ranch Formation.

Thick, red mudstones and interbedded gypsum were deposited in alluvial flat and playa lake environments. The bedded gypsum may represent precipitation of gypsum on the floor of the saline lake, whereas interbedded sandstones probably represent

FIGURE 73—Playa lake facies of the Rincon Valley Formation (upper Miocene) consisting of red gypsiferous mudstone (recesses) and bedded selenite gypsum (ledges) near the town of Rincon.

deposition by sheetfloods that spread from the toes of the fans onto the alluvial flat and into the playa lake during times of desiccation (Mack et al., 1994b). Exposed as far north as the mouth of Berrenda Creek in the Garfield quadrangle, the gypsiferous mudstone facies is probably also present in the subsurface of the modern Palomas Basin.

The Rincon Valley Formation exposed in the northern Sierra de las Uvas was deposited on distal fans and alluvial flats and was part of a broad, northwest-flowing fan system derived from source areas to the south in the Doña Ana Mountains and Cedar Hills vent zone (Mack et al., 1994b).

Palomas and Camp Rice Formations (Santa Fe Group)

The sedimentary record of the most recent phase of crustal extension in the southern Rio Grande rift is the Palomas Formation in the Palomas Basin and the Camp Rice Formation in the Hatch–Rincon Basin and basins farther south (Fig. 65). The Camp Rice Formation was named by Strain (1966) in the Hueco Basin of west Texas, and the name was subsequently applied in southern New Mexico (Hawley et al., 1969; Hawley and Kottlowski, 1969; Seager et al., 1971, 1982, 1987). Lozinsky and Hawley (1986a, b) defined the Palomas Formation in the Palomas Basin for sediment and sedimentary rocks coeval to the Camp Rice Formation. The Palomas Formation is well exposed along canyon walls and in badlands at the mouths of incised drainages that emanate from the Caballo Mountains and the Black Range (Fig. 2). The best exposures of the Palomas Formation east of Caballo Reservoir and the modern Rio Grande are in Red, Longbottom, Wild Horse, Granite, Bat Cave, Pulido, Caballo, Apache, and Green Canyons. Among those drainages heading in the Black Range, the best exposures of the Palomas Formation are in the canyons and badlands of Palomas, Seco, Las Animas, Percha, Tierra Blanca, and Berrenda Creeks. In addition, the Palomas Formation west of Caballo Reservoir and the modern Rio Grande is also well exposed in drainages that head in the Animas Mountains or within the Palomas Basin, such as Kelly, Montoya, and Sibley Canyons. In the Rincon quadrangle, the Camp Rice Formation is best exposed along the canyon walls of Rincon Arroyo and its tributaries, while in the Hatch quadrangle, it crops out along drainages north of the Rio Grande and in badlands and cliffs adjacent to the mesa in the southwestern and southern parts of the quadrangle.

The Camp Rice and Palomas Formations are Pliocene to early Pleistocene in age, based on a combination of (1) a Blancan and lower Irvingtonian vertebrate fauna (Hawley et al., 1969; Tedford, 1981; Lucas and Oakes, 1986; Repenning and May, 1986;

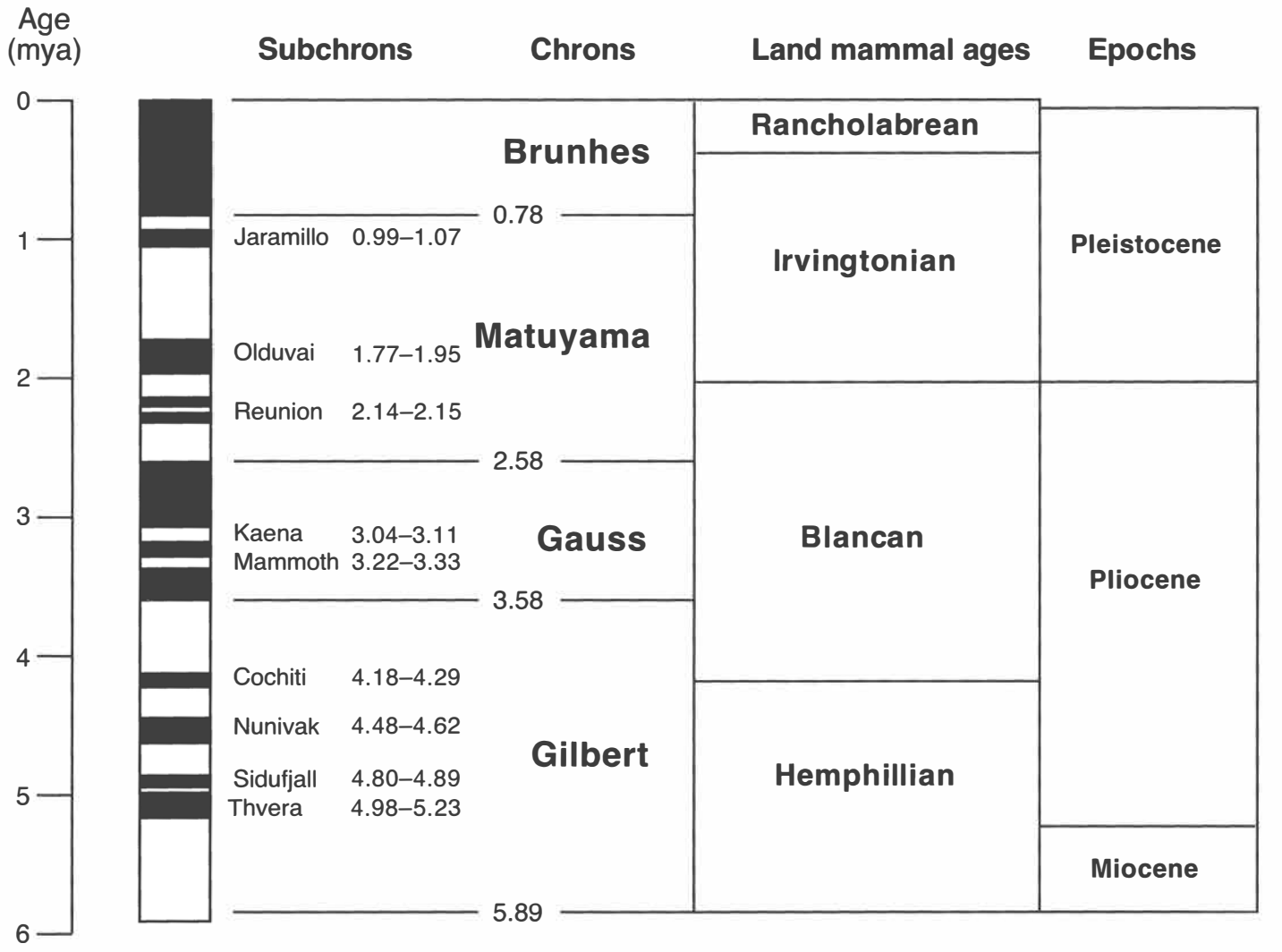

FIGURE 74—Polarity reversal time scale and land mammal ages, adapted from Berggren et al. (1995). In this and subsequent figures, black refers to normal (north) magnetic polarity and white refers to reversed (south) polarity.

Vanderhill, 1986; Morgan et al., 1998); (2) radioisotopic and tephrochronologic ages of interbedded and overlying ash fall deposits, basalt flows, and pumice-clast conglomerates (Reynolds and Larsen, 1972; Seager et al., 1975; Bachman and Mehnert, 1978; Kortemeier, 1982; Seager et al., 1984; Mack et al., 1996, 1998b); and (3) reversal magnetostratigraphy (Vanderhill, 1986; Repenning and May, 1986; Mack et al., 1993, 1996, 1998c; Leeder et al., 1996a).

The most accurate dates for the Palomas and Camp Rice Formations come from reversal magnetostratigraphy, calibrated to the polarity reversal time scale (Fig. 74) by radioisotopic dates of interbedded pumice-clast conglomerates. These data bracket the age of the formations between about 5 and 0.78 Ma (Mack et al., 1993, 1998c; Leeder et al., 1996a). At Rincon Arroyo and at Hatch Siphon, radioisotopically dated pumice-clast conglomerates provide tie points to the polarity reversal time scale (Fig. 75). At Hatch Siphon, a 3.12 Ma pumice conglomerate is present within a section that is primarily Gauss age with both subchrons (Mammoth and Kaena) represented. At Rincon Arroyo, about 50 m (164 ft) of Gauss-age strata are overlain by an equal thickness of Matuyama-age strata, in which all four subchrons are represented (two Reunion, Olduvai, and Jaramillo). A radioisotopically dated pumice conglomerate, 1.59 Ma, occupies the position between the Olduvai and Jaramillo subchrons. At Hatch Siphon, Rincon Arroyo, and elsewhere in the Palomas Basin (Figs. 75, 76), the constructional top of the Camp Rice and Palomas Formations is younger than the Jaramillo subchron, but does not appear to cross the Matuyama–Brunhes boundary, indicating an age no younger than 0.78 Ma. At Garfield East and West, a thick, composite section appears to include Gilbert-age strata (Fig. 76). The younger three subchrons of the Gilbert chron are present at Garfield West with reversed polarity beneath, suggesting a lower limit of 4.98 Ma for the Camp Rice Formation at this location. Gilbert-age strata were also recognized by Repenning and May (1986) in axial-fluvial sediment near Truth or Consequences. Because the Gilbert-age strata at Garfield West are axial-fluvial facies, it indicates the ancestral Rio Grande entered southern New Mexico nearly 5 Ma ago.

The Camp Rice and Palomas Formations unconformably overlie the Rincon Valley or older formations along uplift margins and in the Hatch–Rincon Basin. In most locations in the Palomas Basin the basal contact is buried. The constructional top of the formations is widely exposed as a gently sloping geomorphic surface capped by a stage IV or V petrocalcic paleosol. In the Palomas Basin, the surface at the top of the Palomas Formation is referred to as the Cuchillo surface (Lozinsky, 1986), but it is called the Jornada I surface and the La Mesa surface above piedmont facies and axial-fluvial facies, respectively, of the Camp Rice Formation (Gile et al., 1981). The maximum exposed thickness of the Camp Rice and Palomas Formations in the Caballo

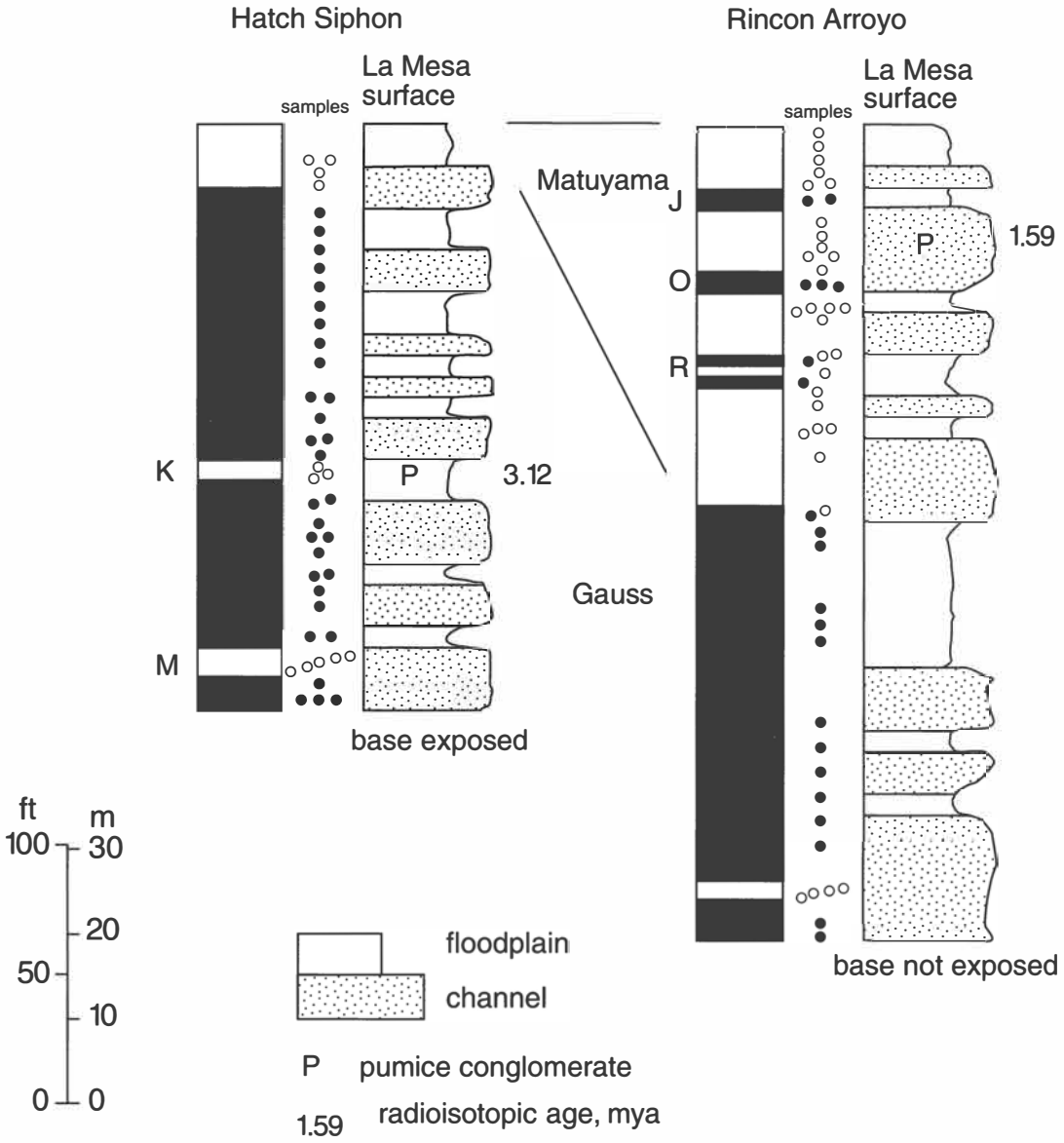

FIGURE 75—Magnetostratigraphy of the Camp Rice Formation (Pliocene–Pleistocene) at Hatch Siphon and Rincon Arroyo. Compare to the polarity reversal time scale of Fig. 74. **J** = Jaramillo subchron; **O** = Olduvai subchron; **R** = Reunion subchron; **K** = Kaena subchron; **M** = Mammoth subchron.

Mountains and vicinity is approximately 100 m (330 ft), although the Palomas Formation may be thicker in the center of the Palomas Basin where the base is not exposed. Along the eastern flank of the Caballo Mountains, the Palomas Formation represents thin, <20 m (<66 ft), pediment and alluvial-fan gravels that cap the highest mesas.

Description

Throughout the Caballo Mountains and vicinity, the Camp Rice and Palomas Formations are generally divided into piedmont and axial-fluvial map units. Both units contain significant accumulations of pedogenic as well as other types of authigenic carbonate, and both units embrace a variety of volcanic rocks. In the following sections each is described separately.

Piedmont facies

The piedmont facies, which refers to sediment deposited on alluvial fans and alluvial flats, consists of interbedded gravel/conglomerate, sand/sandstone, and mudstone. The piedmont facies in particular is well exposed along the walls of incised drainages, and it is possible to trace the sediment from proximal to distal settings on both the eastern and western sides of the basin (Figs. 77, 78). The conglomerates and sandstones are generally well lithified directly adjacent to the Caballo Mountains, but are more likely to be unconsolidated elsewhere.

Grain-supported gravels/conglomerates are common throughout the Palomas and Hatch–Rincon Basins. Ranging in thickness from less than 1 m to 7 m (3.3 to 23 ft), the conglomerates commonly display a channel morphology in suitably oriented outcrops. Most conglomerates are moderately well sorted and may display graded beds, trough and planar crossbeds, imbrication, and thin lenses of sand/sandstone (Fig. 79). Much less common and restricted to proximal settings are poorly sorted, matrix-supported to grain-supported conglomerates that lack any internal layering (Fig. 80). Those conglomerates in the Palomas Basin exposed west of Caballo Reservoir and the Rio Grande are composed almost exclusively of volcanic clasts derived from the Animas Mountains and Black Range, while

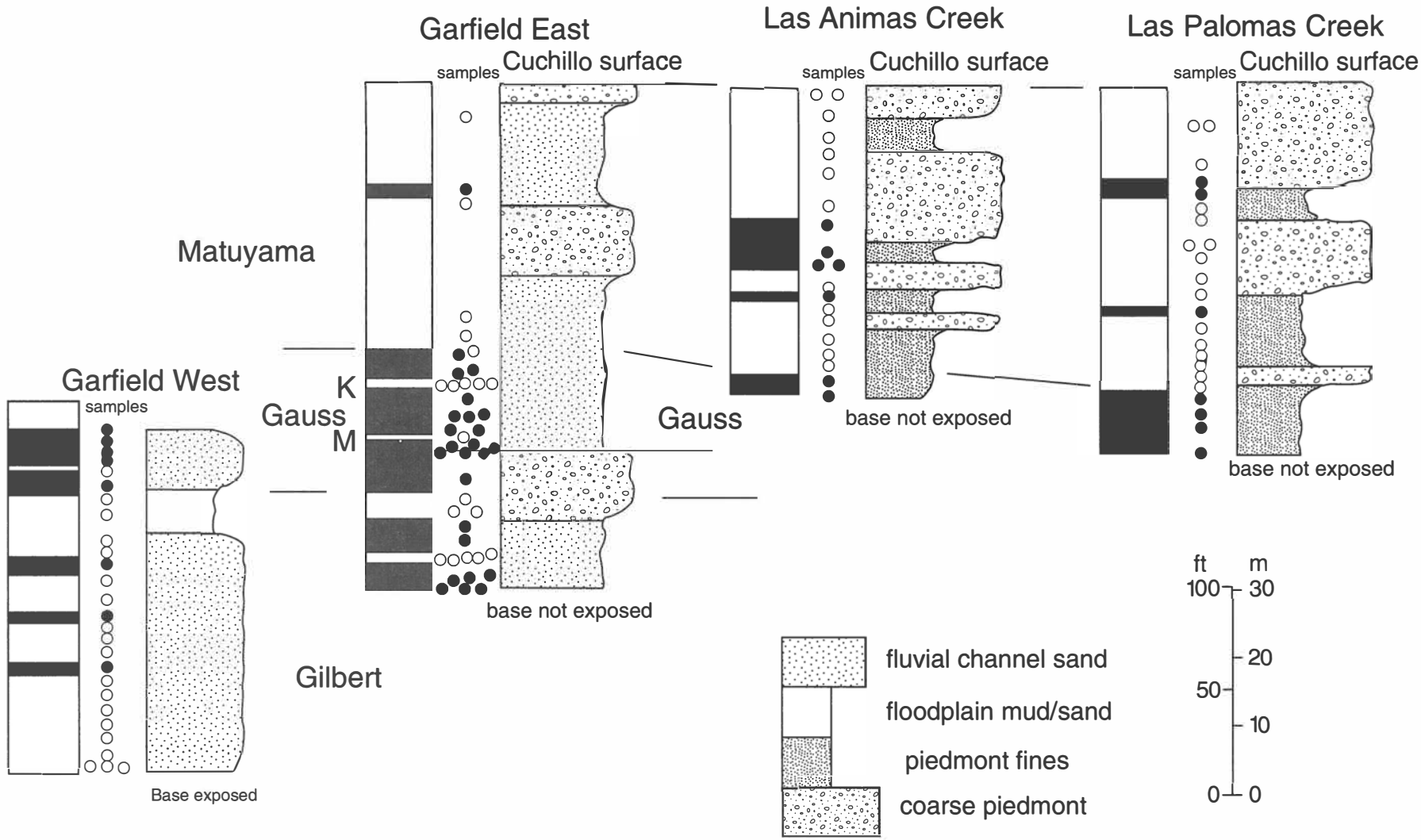

FIGURE 76—Magnetostratigraphy of the Palomas Formation (Pliocene–Pleistocene). Compare to the polarity reversal time scale of Fig. 74. K = Kaena subchron; M = Mammoth subchron.

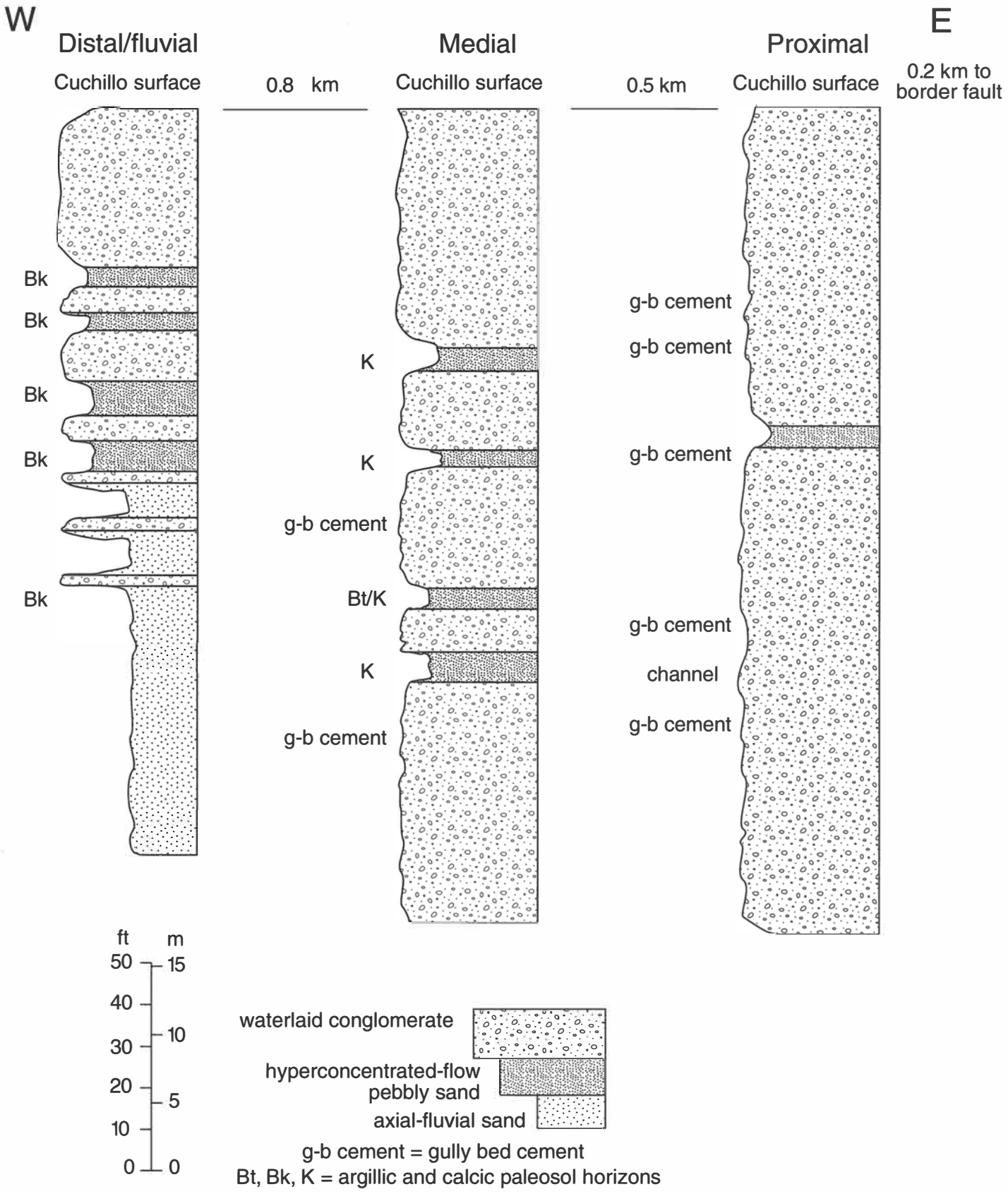

FIGURE 77—Measured sections of footwall-derived alluvial-fan and axial-fluvial sediment of the Palomas Formation (Pliocene–Pleistocene) in Granite Canyon.

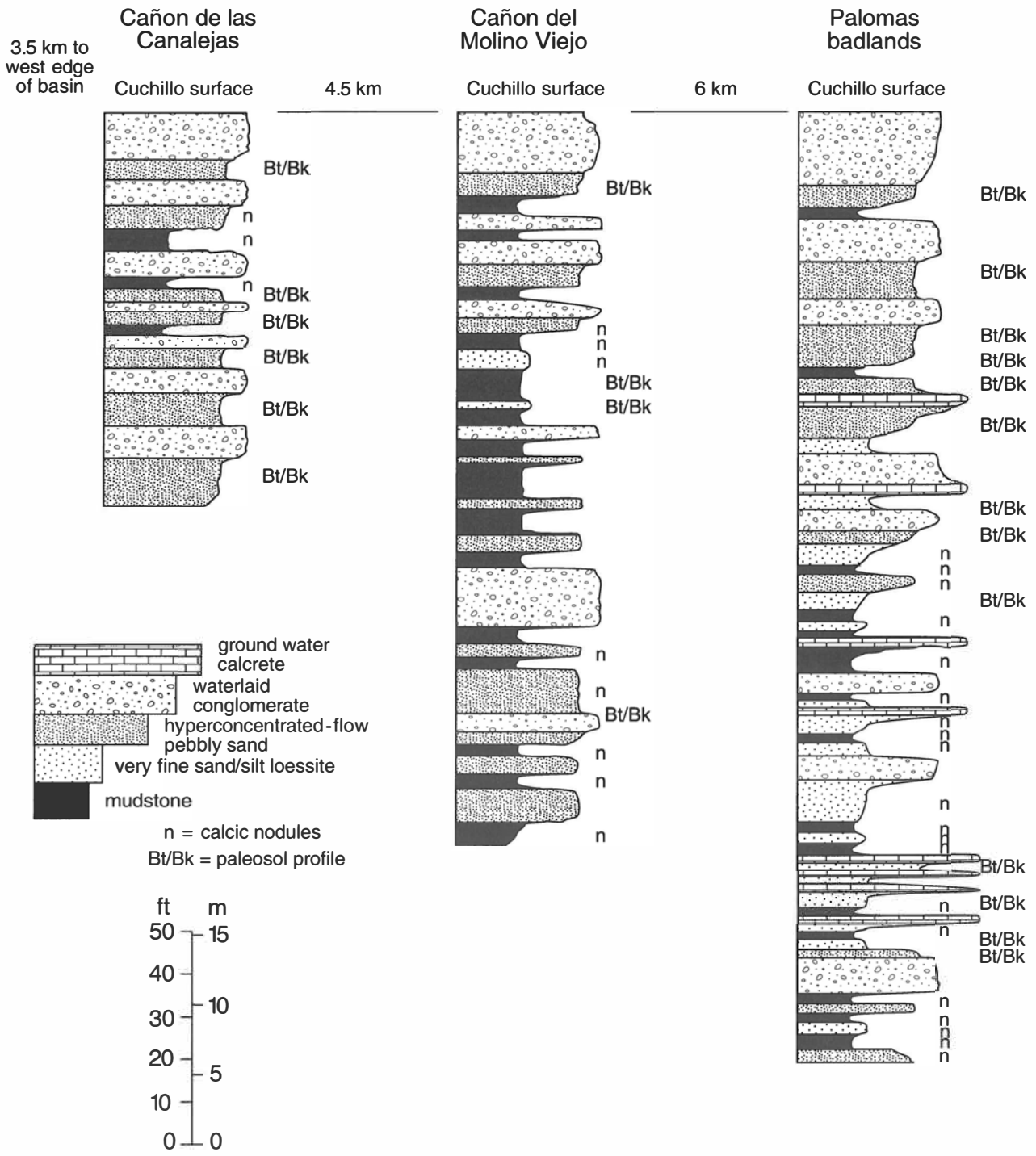

FIGURE 78—Measured sections of hanging-wall-derived, alluvial-fan sediment of the Palomas Formation (Pliocene–Pleistocene). Cañon de las Canalejas (SW¼ sec. 12 T14N R6W): Cañon del Molino Viejo (SE¼ sec. 17 T14S R5W); Palomas badlands (SW¼ sec. 25 and NE¼ sec. 26 T14S R5W).

conglomerates directly adjacent to the Caballo, Red Hills, and Rincon Hills blocks consist of clasts of Precambrian metamorphic and granitic rocks, Paleozoic sedimentary rocks, and lesser amounts of Tertiary volcanics.

Equally as common as grain-supported conglomerate, particularly in medial and distal settings of the piedmont facies, is poorly sorted pebbly and cobbly sand in beds 0.5–6 m (1.6–20 ft) thick. Many of these beds consist of granules, pebbles, and small cobbles floating in a matrix of argillaceous very fine, fine, or medium sand, and lack any evidence of internal layering. Another variety of pebbly sands consists of discontinuous beds and lenses of weakly grain supported granules and pebbles in a sand matrix (Fig. 81). The basal and upper contacts of the gravel lenses are not well defined, and they have very weakly developed normal grading. The pebbly sands were interpreted by Mack and Leeder (1999) and Mack et al. (2002) to have been deposited by hyperconcentrated flows characterized by high sediment-to-water ratios.

Rarely, sand/sandstone in the piedmont facies west of Caballo Reservoir exists in beds less than 2 m (6.6 ft) thick. The

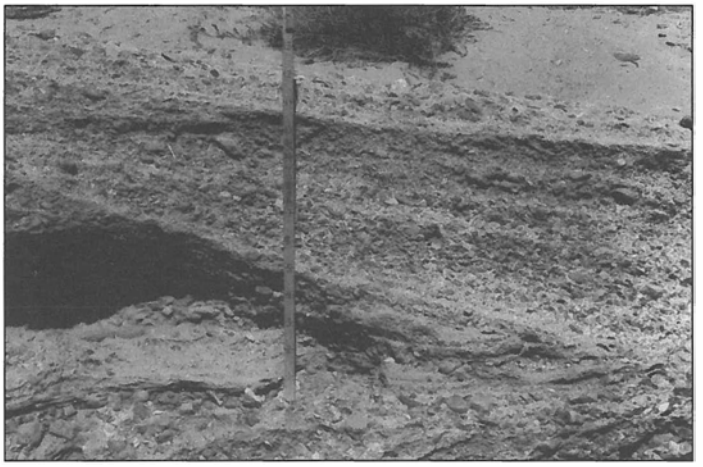

FIGURE 79—Crossbedded alluvial-fan conglomerate derived from the Caballo Mountains footwall, Pliocene–Pleistocene Palomas Formation, Caballo Canyon. Jacob's staff is 1.5 m (4.9 ft) long.

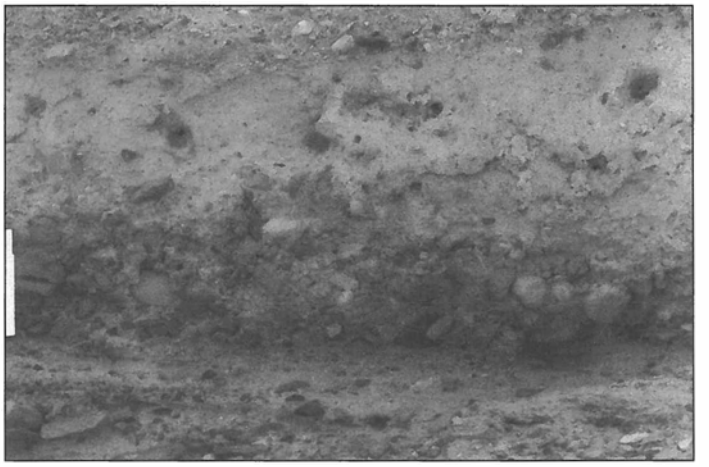

FIGURE 81—Pebble conglomerate and pebbly sand deposited by a hyperconcentrated flow, Pliocene–Pleistocene Palomas Formation, Caballo Canyon. Bar scale is 15 cm (5.9 in) long.

FIGURE 80—Very poorly sorted alluvial-fan conglomerate of probable debris-flow origin derived from the Caballo Mountains footwall, Pliocene–Pleistocene Palomas Formation, Granite Canyon. Jacob's staff is 1.5 m (4.9 ft) long.

FIGURE 82—Axial-fluvial sand overlain by siltstone and blocky red mudstone, which in turn is overlain by alluvial-fan conglomerates, Pliocene–Pleistocene Palomas Formation, Caballo Canyon. Bar scale is 2 m (6.6 ft) long.

sand/sandstones are either medium to coarse grained with horizontal laminae or trough crossbeds or are massive and very fine grained. In addition a few thin, <1.5 m (<4.9 ft), very well sorted fine sands are interbedded with conglomerates in Apache and Bat Cave Canyons. Like the sand/sandstone, red mudstones are relatively thin, <1 m (<3.3 ft), and rare in the piedmont facies. Primarily exposed along the western margin of Caballo Reservoir and in a few locations where the piedmont facies interfingers with the axial-fluvial facies east of Caballo Reservoir, the mudstones have a blocky fabric and some have meter-scale, concave-upward fractures interpreted to be wedge-shaped peds (Fig. 82).

Axial-fluvial facies

The axial-fluvial facies in the Palomas Basin consists primarily of pebbly to cobbly fine, medium, or coarse sand, rarely cemented, to sandstone. Trough crossbeds and horizontal laminae are common, and ripple-cross laminae are locally present at the tops of sand beds. The axial-fluvial sands exist as multistory sheets with story boundaries marked by low-angle erosion surfaces mantled by lags of gravel and/or rip-up clasts of mudstone and carbonate.

Mack and Leeder (1999) recognized three facies of axial-fluvial strata along the eastern margin of the Palomas Basin, based on the abundance and nature of the gravel fraction. The least common facies is only locally exposed at the base of the formation and consists of about 5 m (16 ft) of well-rounded pebble and small cobble conglomerate and interbedded sand with horizontal laminae and trough and planar crossbeds. The most common facies, pebbly sand, is characterized by well-rounded pebbles dominated by volcanic rocks, most of which were derived from upstream sources (Fig. 83). Almost as abundant as the pebbly sand is bimodal-clast gravelly sand, which has two distinct populations of gravel (Fig. 84). The finer mode is identical in size, rounding, and composition to the pebbles in the pebbly sand facies, but the coarser mode consists of cobbles and boulders of angular granitic, metamorphic, and sedimentary clasts that can be correlated with rocks exposed in the Caballo and Red Hills footwall uplifts. Presumably, these locally derived clasts were too large to be efficiently transported by the river.

Locally, red mudstone and tan siltstone intercalated on the scale of centimeters occupy the top of a channel-fill sequence. In Rincon Arroyo, the channel sands/sandstones are interbedded with massive, fine sand and red mudstone in beds 0.3–2 m (1.0–6.6 ft) thick.

Paleosols and other authigenic carbonate

A prominent component of both the piedmont and axial-fluvial

FIGURE 83—Trough crossbedded, pebbly sand of the axial-fluvial facies of the Pliocene–Pleistocene Palomas Formation, Caballo Canyon. Jacob's staff is 1.5 m (4.9 ft) long.

FIGURE 85—Paleosol in floodplain sand of the Camp Rice Formation, Rincon Arroyo. Dark horizon is a Bt horizon, which overlies a Bk horizon with stage II morphology calcic nodules. Hammer is 25 cm (9.8 in) long.

FIGURE 84—Axial-fluvial facies of the Pliocene–Pleistocene Palomas Formation with bimodal-clast channel lags, consisting of pebbles from upstream sources, and cobbles and small boulders derived from the Caballo Mountains footwall. Jacob's staff is 1.5 m (4.9 ft) long.

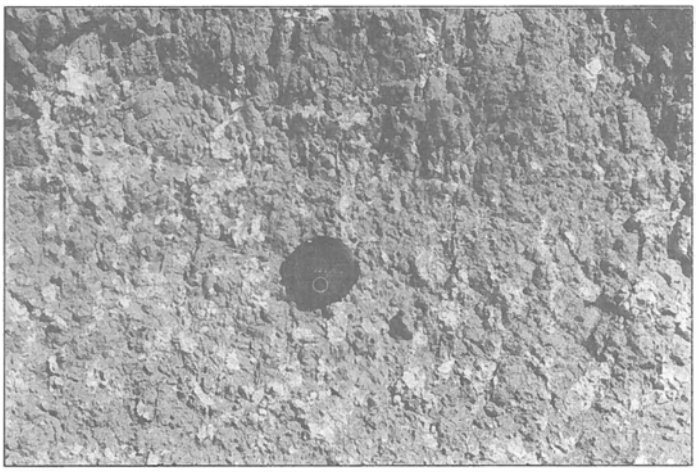

FIGURE 86—Paleosol developed in distal alluvial-fan mudstone, Palomas Formation, south of Palomas Creek. Upper dark horizon has prismatic peds and is a Bw horizon; lower horizon is a stage II-morphology, Bk horizon. Lens cap is 5 cm (2 in) in diameter.

facies of the Camp Rice and Palomas Formations is authigenic carbonate (Mack et al., 2000). Many of the mudstones and fine sandstones contain calcic paleosols (Figs. 85, 86; Mack and James, 1992; Mack et al., 2000). Complete profiles of the paleosols consist of a thin, <10 cm (<3.9 in), gray to tan A horizon, overlying a dark-brown argillic B (Bt) or structural B (Bw) horizon up to 50 cm (20 in) thick, which in turn overlies a calcic B or K horizon 30–100 cm (12–39 in) thick. Root traces are common in all three horizons. The argillic and structural B horizons have blocky, prismatic, and locally wedge-shaped peds, and the argillic B horizon is distinguished from the structural B horizon by clay coats (argillans) around sand grains and/or peds (Figs. 87, 88). The calcic B horizon is most commonly composed of scattered nodules and vertically oriented tubules of microcrystalline calcite, representing stage II morphology of Gile et al. (1966). In some cases, the calcic B horizon is a massive bed of carbonate, corresponding to a K horizon of stage III morphology. Many of the paleosols were truncated before burial, such that the A and all or part of the Bw/Bt horizons were removed.

Also common in the Camp Rice and Palomas Formation are beds of authigenic carbonate interpreted to have precipitated from shallow ground water. Some of the ground-water carbonate beds are about 0.5 m (1.6 ft) thick and are characterized by sharp basal contacts and gradational upper contacts consisting of an upper fringe of nodules and vertically oriented tubules related to precipitation in the capillary fringe above the water table (Fig. 89; Mack et al., 2000). Other ground-water carbonates are interpreted to be related to shallow ground-water flow and deposition at springs, and in the Palomas Basin are restricted to the distal piedmont sediment exposed west of Caballo Reservoir. Some of these ground-water carbonates are thin, <30 cm (<12 in), and consist of a dense mat of horizontal calcified roots (Fig. 90). Others are up to 2 m (6.6 ft) thick and are laterally persistent for kilometers (Fig. 91). The thicker variety has a sharp base and top and consists of over 90% micrite. A distinctive fenestral fabric in the upper part of these thick carbonates suggests that degassing may have played a role in carbonate precipitation (Mack et al., 2000).

A relatively uncommon type of authigenic carbonate is restricted to proximal and midfan conglomerates and is especially well exposed in Granite Canyon (Fig. 92). This type of authigenic carbonate consists of thick, 1 m (3.3 ft), laterally persistent beds of conglomerate plugged with white micrite that fills interstices between the gravel-sized clasts and coats the clasts,

FIGURE 87—Photomicrograph of pedogenic clay coats around skeletal sand grains (free grain argillans) in a Bt horizon, Pliocene–Pleistocene Palomas Formation. Bar scale is 0.25 mm (0.1 in) long.

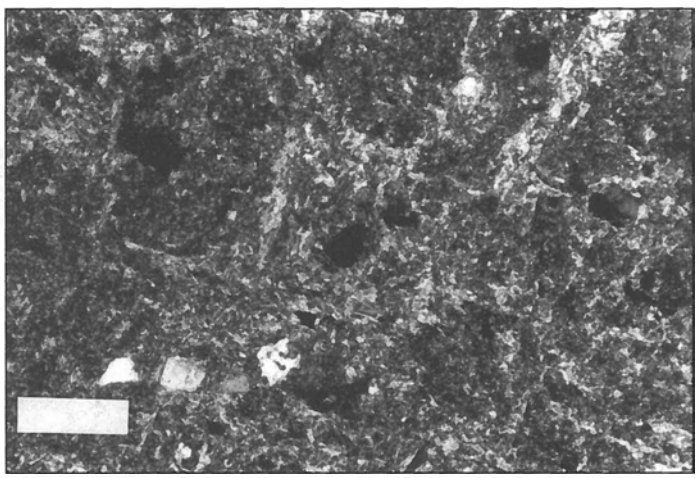

FIGURE 88—Photomicrograph of pedogenic clay coats around clay-rich peds (ped argillans) in a Bt horizon, Pliocene–Pleistocene Palomas Formation. Bar scale is 0.25 mm (0.1 in) long.

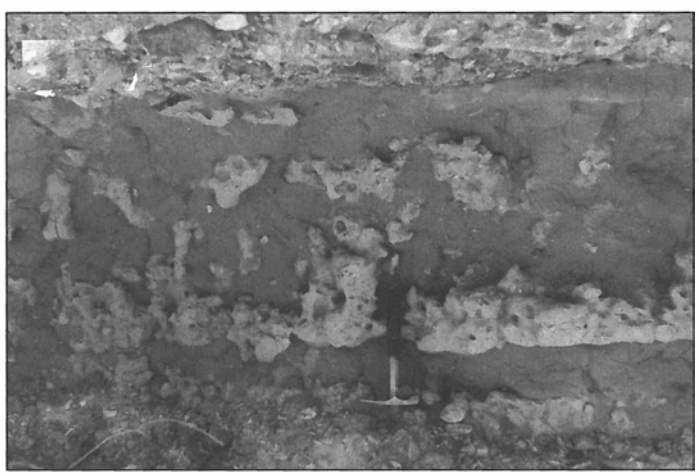

FIGURE 89—Authigenic calcite precipitated near the water table and in the capillary fringe above the water table, Pliocene–Pleistocene Palomas Formation, Granite Canyon. Hammer is 25 cm (9.8 in) long.

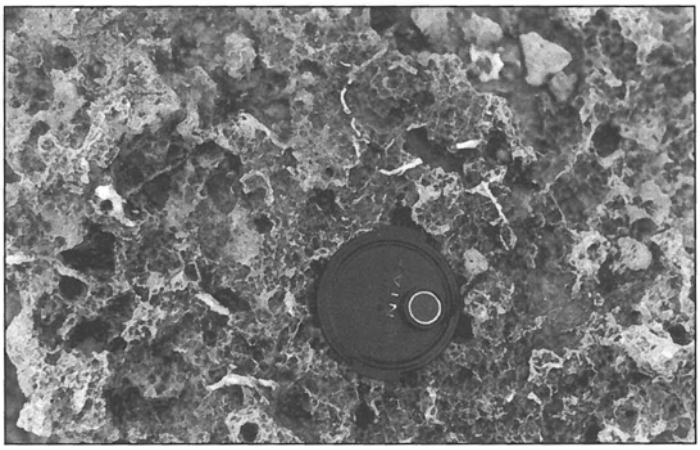

FIGURE 90—Bedding plane of calcified root mat, distal hanging wall-derived sediment of the Pliocene–Pleistocene Palomas Formation, Palomas Canyon. Lens cap is 5 cm (2 in) in diameter.

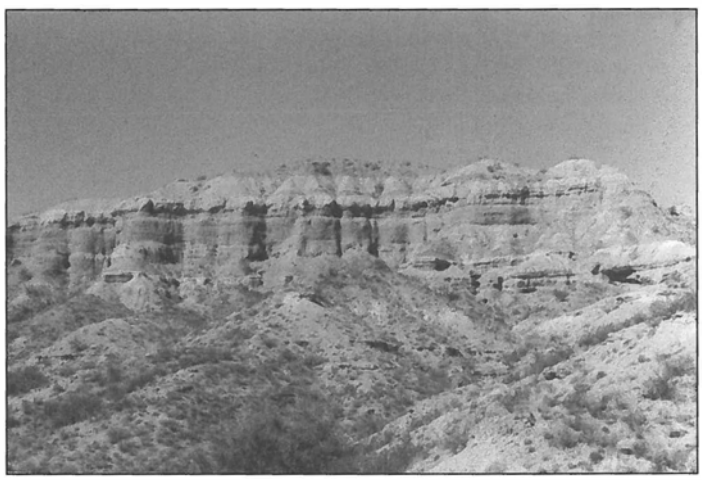

FIGURE 91—Near top of cliff is a 2-m- (6.6-ft-) thick bed of light-colored authigenic carbonate precipitated by laterally flowing, shallow ground water, Pliocene–Pleistocene Palomas Formation, Palomas Canyon.

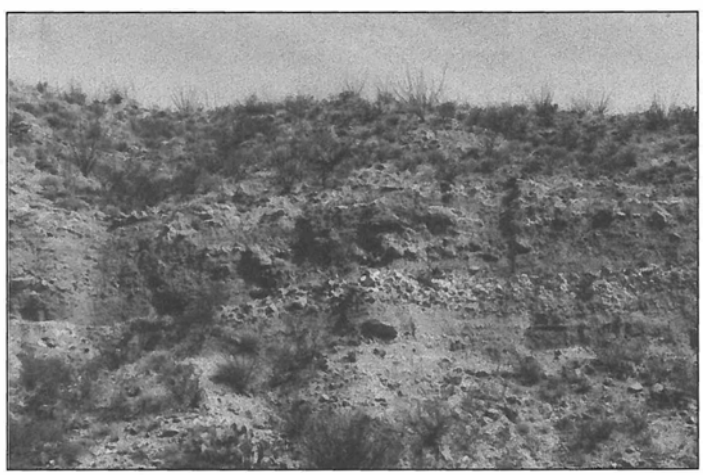

FIGURE 92—Proximal alluvial-fan conglomerate with two prominent light-colored horizons of gully bed cement, Pliocene–Pleistocene Palomas Formation, Granite Canyon.

FIGURE 93—Close up of lower horizon of gully bed of Fig. 92. Note thick coats of authigenic carbonate preferentially on undersides of clasts. Hammer is 25 cm (9.8 in) long.

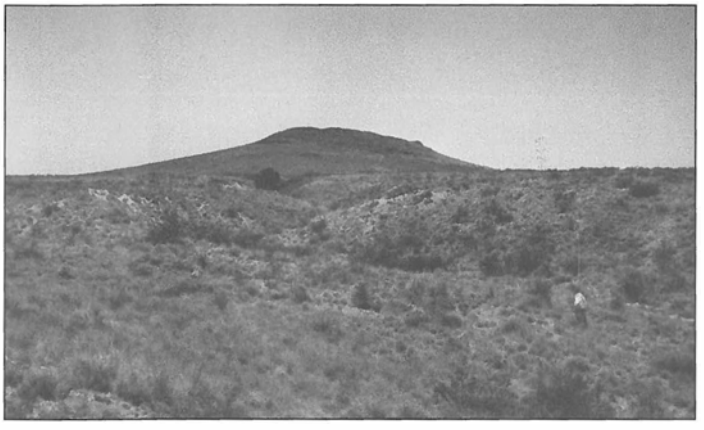

FIGURE 94—Pliocene cinder cone, southern part of Engle quadrangle.

preferentially on the undersides (Fig. 93). Many of the beds also display thin, <10 cm (<4 in), laminar to brecciated caps of carbonate. Conspicuous by their absence, however, are root traces, peds, or any evidence of soil horizons above or below the authigenic carbonate. This variety of authigenic carbonate is interpreted as gully bed cement (cf. Lattman, 1973), which forms when storm and/or spring runoff infiltrates the floor of gravel channels, evaporates, and precipitates authigenic carbonate between and around the gravel clasts. That evaporation was the dominant process of precipitation is indicated by thicker coats of carbonate on the undersides of the clasts. Once the bed was plugged with carbonate, water could not infiltrate it, instead ponding on the surface and precipitating the laminar cap. The absence of soil features or horizons indicates that gully bed cement is not a true paleosol.

Volcanic rocks in the Camp Rice and Palomas Formations

In addition to sediment and sedimentary rocks, the Camp Rice and Palomas Formations also locally contain interbedded volcanic rocks. The volcanic rocks include basalt flows, pumice-clast conglomerates, and fallout ash beds.

The oldest basalt flow, dated by the K–Ar method at 4.5 ± 0.1 Ma, underlies the Palomas Formation in exposures along NM–152 approximately 12 km (7.4 mi) east of Hillsboro (Seager et al., 1984). Two other basalt flows within the Palomas Formation are of similar age. One is located within piedmont conglomerates on the upthrown side of the Caballo fault in the

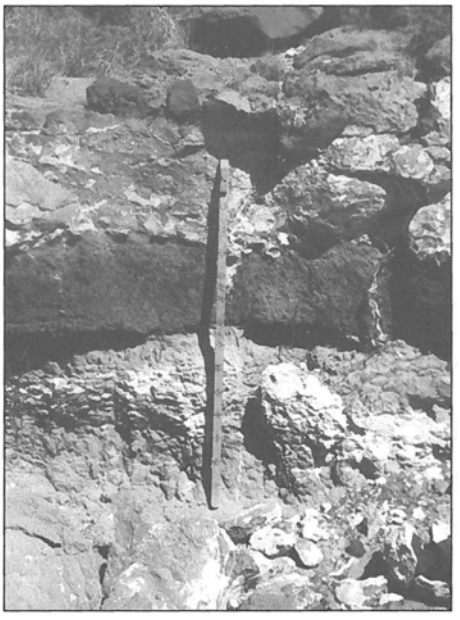

FIGURE 95—Dark layer of cinders overlying a calcic paleosol and underlying a basalt lava flow, Engle quadrangle. Cinders and lava flow were derived from the cinder cone pictured in Fig. 94. Jacob's staff is 1.5 m (4.9 ft) long.

northwest part of the Apache Gap and southwest part of the Palomas Gap quadrangles and has been dated at 3.1 ± 0.1 Ma (Seager et al., 1984), while the other occupies the narrows of Elephant Butte Reservoir, is interbedded with axial-fluvial sand, and has been dated at 2.9 ± 0.3 Ma (Bachman and Mehnert, 1978).

Basalt lava flows issued from five cinder cones and a single shield volcano in the Engle and northernmost Palomas Gap quadrangles, all of which are still prominent, relatively uneroded features of the landscape (Fig. 94). Although some of the flows spread short distances eastward from their vents, the major volume of flows moved westward or northward toward the Palomas Basin, flooding the stable piedmont slopes that represent the top of the lower Palomas Formation. Generally, single flows overlie the lower Palomas, but near the pair of cinder cones in the northwestern part of the Engle quadrangle two or more flows are present. Locally, up to a meter of unconsolidated cinders deposited by pyroclastic fallout directly overlie the lower part of the Palomas Formation (Fig. 95). Bachman and Mehnert (1978) dated a cinder cone in the southwestern corner of the Engle quadrangle using the K–Ar method at 2.1 ± 0.4 Ma, an age that probably applies equally well to the rest of the cinder cones and basalt flows nearby. Warren (1978) studied the basalts that issued from the cinder cones in the Engle quadrangle and found them to be alkalic basalts with 46% SiO_2. Textures are typically pilotaxitic with a groundmass of feldspar, titanomagnetite, brownish clinopyroxene, olivine, and brown glass. Phenocrysts of olivine constitute up to 10% of the basalt.

Warren (1978) also described three groups of inclusions from basalt flows exposed north of the Engle quadrangle: (1) green lherzolite, (2) single megacrysts of clinopyroxene, spinel, anorthoclase, and olivine, and (3) pyroxenites and granulites. Bright emerald-green chromium diopside is a conspicuous component of many lherzolite xenoliths, which are otherwise dominated by granular olivine. Pyroxenites include both websterites and harzburgites, whereas granulites consist of quartz and feldspar. Warren (1978) concluded that the lherzolite xenoliths and most megacrysts originated in the upper mantle at depths of 30–40 km (19–25 mi), whereas the granulites and anorthoclase

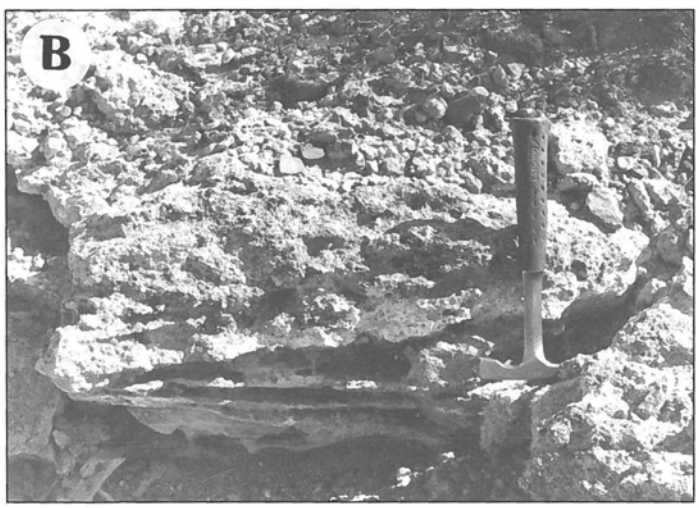

FIGURE 96—Pumice-clast conglomerates derived from the Jemez volcanic field, Pliocene–Pleistocene Camp Rice Formation, Rincon Arroyo. **A**—lower part of pumice conglomerate consisting of pebbles, cobbles and boulders of pumice. **B**—upper crossbedded pumice granules. Radioisotopic analysis of sanidine from the lower pumice gives an age of 1.59 Ma, suggesting the pumice was derived from the lower Bandelier eruption (Mack et al., 1996). Hammer is 25 cm (9.8 in) long.

megacrysts were derived from the lower crust at depths of 28–30 km (17–19 mi).

Particularly well preserved is the basalt cinder cone at Black Hills, located in the east-central part of the Cutter quadrangle (NE¼ sec. 34 T14S R2W). Approximately 0.5 km (0.3 mi) in diameter, the cone straddles the Jornada Draw fault, with the western half of the cone constructed on eroded Crevasse Canyon Formation and the eastern half overlying the Palomas Formation. The excellent state of preservation of the cone suggests a Pliocene–Quaternary age, and this is confirmed by an $^{40}Ar/^{39}Ar$ age of 2.04 ± 0.36 Ma obtained from lava on the flank of the cone (Esser, 2003a).

Pumice-clast conglomerates are interbedded with fluvial sediment of the Camp Rice Formation in southern New Mexico, including sites in the Hatch and Rincon quadrangles (Mack et al., 1996). The oldest is exposed at Hatch Siphon (NE¼ sec. 9 T19S R4 W) and consists of 0.5 m (1.6 ft) of pebbles and small cobbles of pumice. $^{40}Ar/^{39}Ar$ analysis provides an age of 3.12 ± 0.03 Ma, which corresponds to its position within the Kaena subchron of the Gauss chron (Fig. 75; Mack et al., 1996). At Rincon Arroyo (SW¼ sec. 35 T18S R2W), a pumice-clast conglomerate is present in the upper part of the Camp Rice Formation and has been dated at 1.59 ± 0.02 Ma, an age that is consistent with its position

FIGURE 97—The "Las Palomas ash" of the Pliocene–Pleistocene Palomas Formation, exposed just south of Red Canyon. Hammer is 25 cm (9.8 in) long.

between the Olduvai and Jaramillo subchrons of the Matuyama chron (Fig. 75; Mack et al., 1996). The pumice-clast conglomerate at Rincon Arroyo consists of two parts (Fig. 96). A laterally discontinuous lower layer up to 0.5 m (1.6 ft) thick is composed of cobbles and boulders of pumice and a minor amount of other clasts. The more laterally persistent upper part is up to 2 m (6.6 ft) thick and is composed of crossbedded granules and small pebbles of pumice mixed with fluvial sand. The pumice-conglomerates at Hatch Siphon and Rincon Arroyo are derived from the Jemez volcanic field; the older one is related to eruptions recorded in the Puye Formation, and the younger one corresponds to the lower Bandelier Tuff eruption. Presumably, these eruptions dammed the ancestral Rio Grande with pumice that subsequently broke free and spread quickly downriver as pumice floods (Mack et al., 1996).

Four fallout ash beds are interbedded with the Palomas Formation in the Palomas Basin. Three of the ash beds are located east of Caballo Reservoir, in Red Canyon (NE¼ SW¼ sec. 33 T14S R4W), Wild Horse Canyon (SW¼ SW¼ sec. 29 T15S R4W), and an unnamed canyon north of Ash Canyon (SW¼ NE¼ sec. 20 T15S R4W). The other ash is located west of the reservoir in North Kelly Canyon (NW¼ NE¼ sec. 11 T15S R5W). The ash in Red Canyon was previously designated the "Las Palomas ash" by Lozinsky and Hawley (1986b). The ash beds are 1.3–4.6 m (4.3–15 ft) thick and are laterally discontinuous. The ashes at Red Canyon, north of Ash Canyon, and Kelly Canyon extend laterally less than 30 m (98 ft), before being truncated by overlying alluvial-fan channels. The ash at Wild Horse Canyon is exposed over an area of about 0.1 km² (0.06 mi²). All four ashes are white to light gray and consist primarily of glass shards and secondarily of silt to fine sand-sized quartz, sanidine, plagioclase, and biotite. The lower part of each of the ashes is structureless and probably represents largely unmodified fallout tephra (Fig. 97). A well-bedded upper part, exhibiting horizontal laminae, ripple cross-laminae, and/or burrows, was probably reworked by water or wind and living organisms. None of the ashes have been radioisotopically dated, but the age of the Red Canyon (Las Palomas) ash and the Wild Horse Canyon ash can be estimated using reversal magnetostratigraphy (Fig. 98). The Red Canyon (Las Palomas) ash projects stratigraphically into a section interpreted to be entirely Matuyama in age. This fact, plus the substantial thickness and a position only about 10 m (33 ft) below the Cuchillo surface, suggests the Red Canyon ash is related to one of the Bandelier eruptions in the Jemez volcanic field. A similar position beneath the Cuchillo surface of the North Kelly and north-of-Ash Canyon ashes suggests they too may be related to

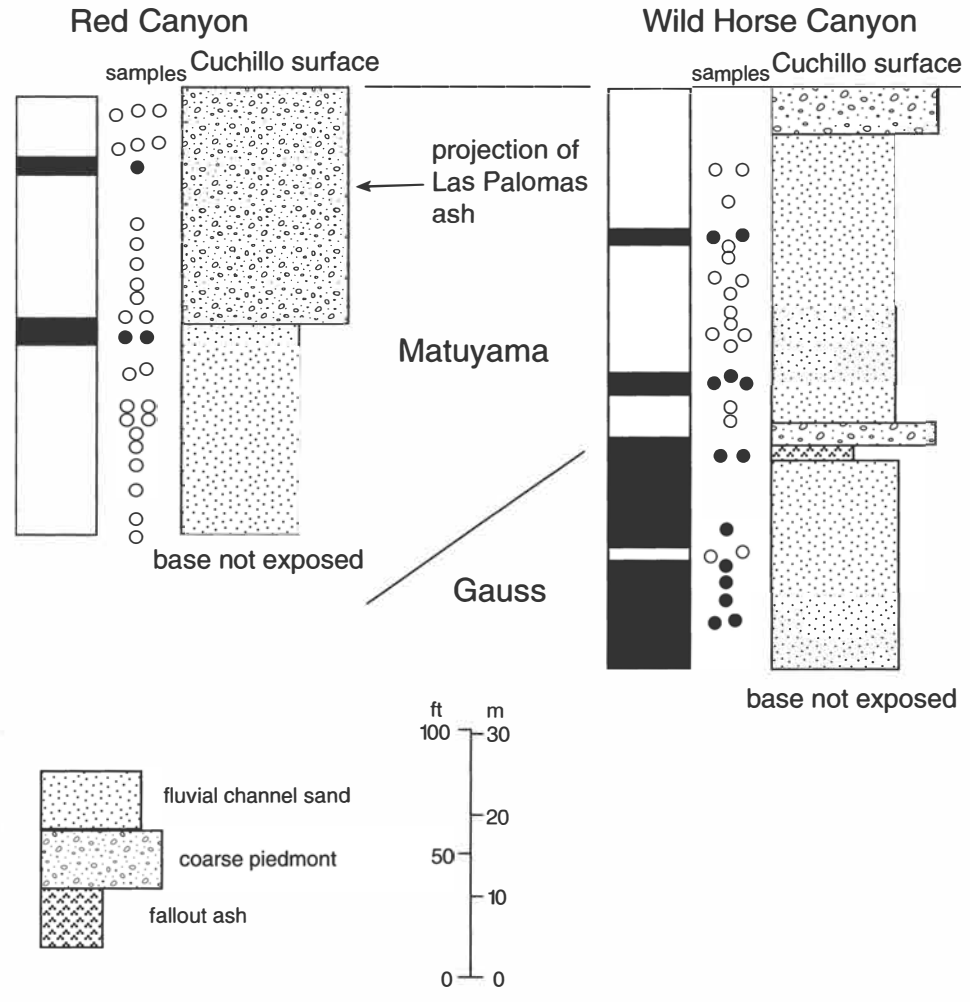

FIGURE 98—Magnetostratigraphy of two fallout ash-bearing sections of the Pliocene–Pleistocene Palomas Formation on the eastern side of the Palomas Basin. Compare to the polarity reversal time scale of Fig. 74.

one of the Bandelier eruptions. However, the Wild Horse Canyon ash is below the Matuyama–Gauss boundary, and must therefore be older than 2.6 Ma. The origin of the Wild Horse Canyon ash is not known, although its substantial thickness also suggests derivation from the Jemez volcanic field.

Finally, a thin, 0.5 m (1.6 ft), fallout ash is located in a railroad cut near the Grama siding in the Rincon quadrangle (NW¼ sec. 15 T18S R2W; Seager and Hawley, 1973). A fission track date of 0.754 ± 0.2 (Kortemeier, 1982) and normal polarity (Mack et al., 1993) suggest a correlation with the Bishop Tuff. The Grama ash occupies an inset surface, suggesting local downcutting by Rincon Arroyo had begun before 0.75 Ma, which is consistent with the interpretation that regional downcutting by the Rio Grande and its tributaries began at or near the Matuyama-Brunhes boundary, at 0.78 Ma (Mack et al., 1993, 1998b).

Depositional environments

The geographic distribution of the piedmont and axial-fluvial facies of the Camp Rice and Palomas Formations is controlled primarily by basin symmetry (Mack and Seager, 1990). In the Palomas half graben, footwall-derived alluvial fans, which deposited the piedmont facies, have a short radial length, extending only a few kilometers into the basin. In contrast, the hanging wall-derived fans occupy a broad belt up to 20 km (12 mi) wide that covers over half of the basin. The slopes of the paleofans, as preserved by the Cuchillo geomorphic surface, also differ between the two fans systems. Footwall-derived paleofans were steeper (1.1°–4.4°), compared to slopes of the hanging wall-derived fans (<1°; Mack and Leeder, 1999; Mack et al., in press a). The floodplain of the axial-fluvial system was narrow, <5 km (<3.1 mi) wide, and located directly adjacent to the footwall blocks of the Palomas Basin. In contrast, in the Hatch–Rincon full graben, the axial-fluvial system extended to within a kilometer (0.6 mi) or less on both sides of the basin. Moreover, axial-fluvial sediment in the Hatch–Rincon Basin contains a greater proportion of overbank fines and stage II calcic paleosols than that in the Palomas Basin, which contains mostly multistory channel sands with little or no floodplain sediment preserved (Mack and James, 1993).

The distribution of piedmont and axial-fluvial facies in the Palomas Basin conforms to theoretical models of asymmetrical subsidence of half grabens (Leeder and Gawthorpe, 1987). Footwall-derived alluvial fans are small, because they have small catchment areas on the footwall scarp. Much larger catchments in the hanging-wall mountains resulted in extensive fans deposited on the hanging-wall dip slope of the basin. The ancestral Rio Grande was positioned near the footwall block, because this was the site of maximum subsidence and because it was restricted on the west by the large hanging wall-derived fans. Frequent avulsions of the ancestral Rio Grande across the narrow floodplain inhibited preservation of overbank fines, resulting in fluvial sediment dominated by channel sands. In the symmetrically subsiding Hatch–Rincon Basin, however, the ancestral Rio Grande was able to move across almost the entire width of

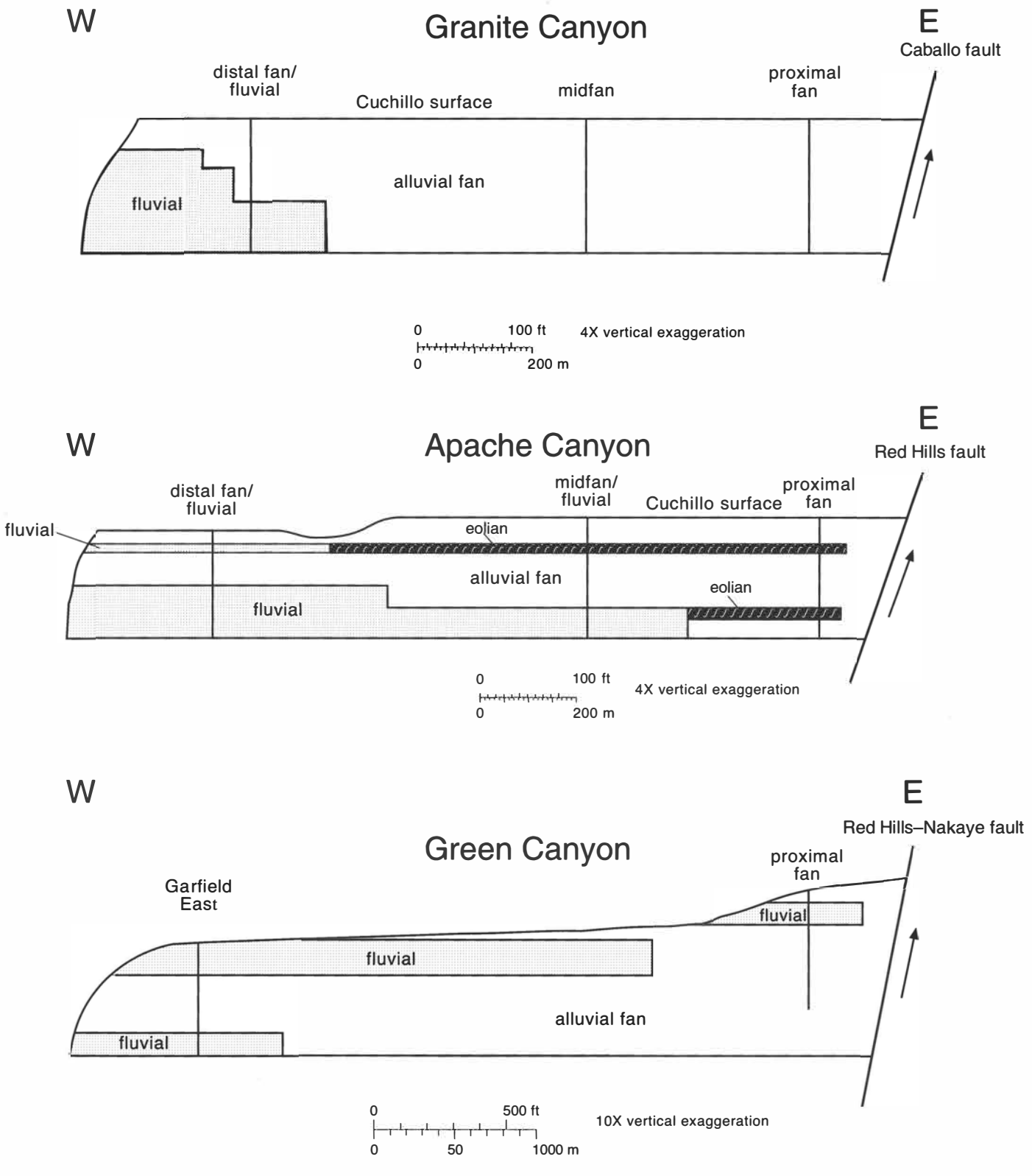

FIGURE 99—Interbedded axial-fluvial and footwall-derived, eolian, and alluvial-fan sediment of the Pliocene–Pleistocene Palomas Formation along the eastern side of the Palomas Basin, adapted from Mack and Leeder (1999).

the basin. Consequently, overbank mudstones and fine sands, many of which have stage II calcic paleosols, had a much higher preservation potential, because at any one location on the floodplain there was a long time period between reoccupations of the river channel.

The axial-fluvial and footwall-derived piedmont facies are complexly interbedded along the eastern margin of the Palomas Basin (Mack and Leeder, 1999; Mack et al., 2002). North of Caballo Canyon, there is in the lower part of the Palomas Formation, a mappable interval 80 m (262 ft) thick composed of axial-fluvial sediment. This axial-fluvial lithosome extends to within about 1 km (0.6 mi) of the Caballo border fault in Granite

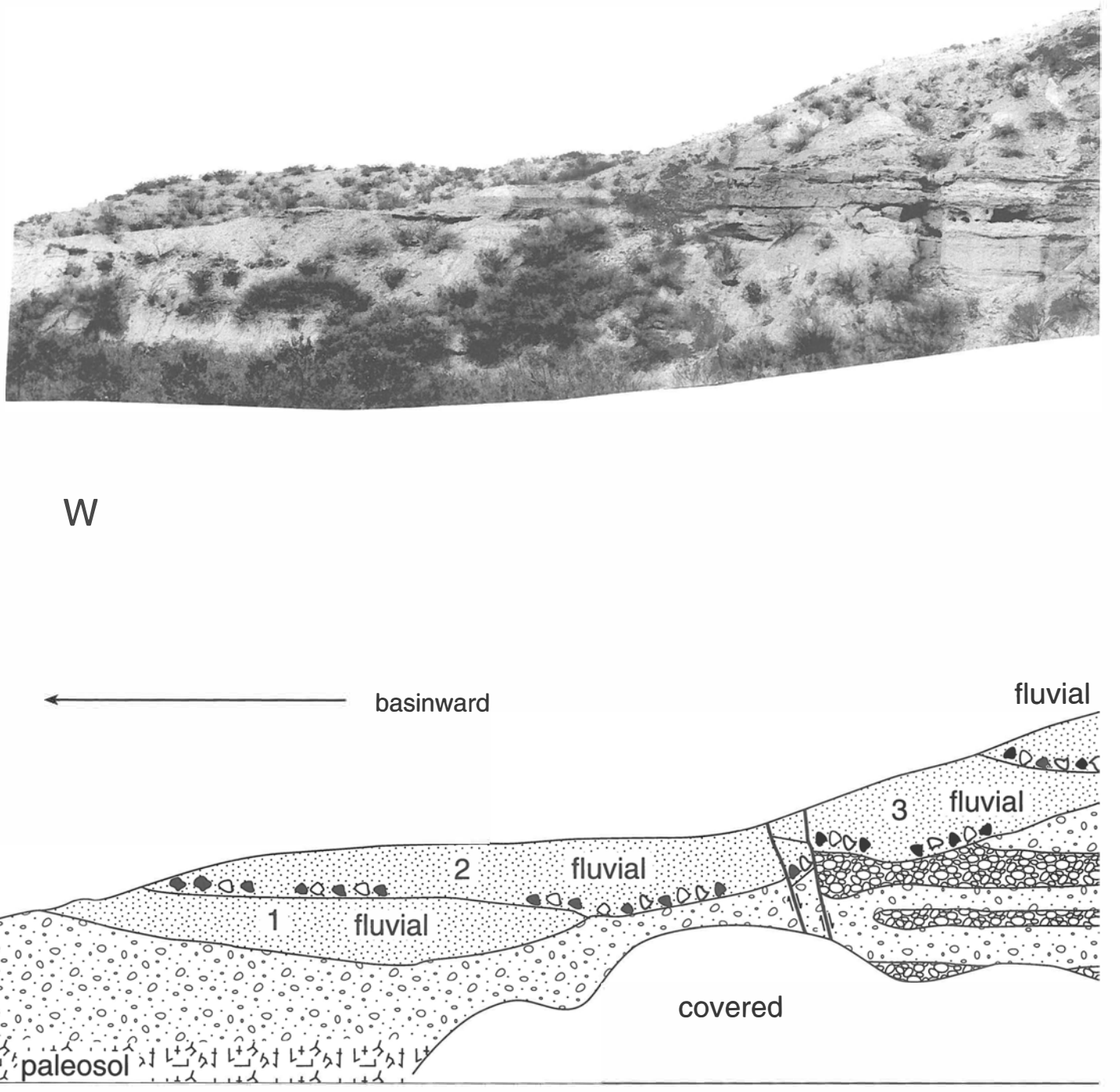

FIGURE 100—View to the north of cliff face of the Pliocene–Pleistocene Palomas Formation, illustrating toe cutting of the footwall-derived alluvial fans by the ancestral Rio Grande. River flowed toward viewer and the footwall uplift is to the viewer's right. Axial-fluvial facies defines an onlap relationship in which each successively younger fluvial channel is positioned closer to the footwall uplift (adapted from Mack and Leeder, 1999). Located at SE¼, SW¼ sec. 30 T16S R4W.

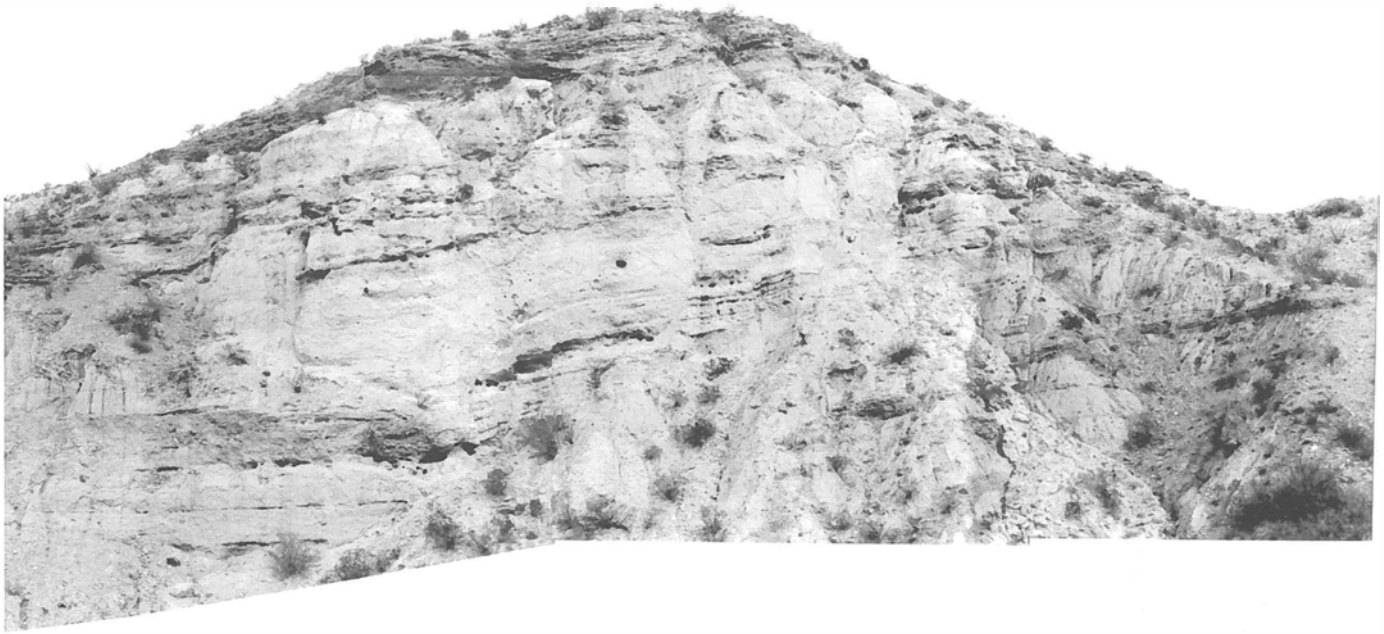

E

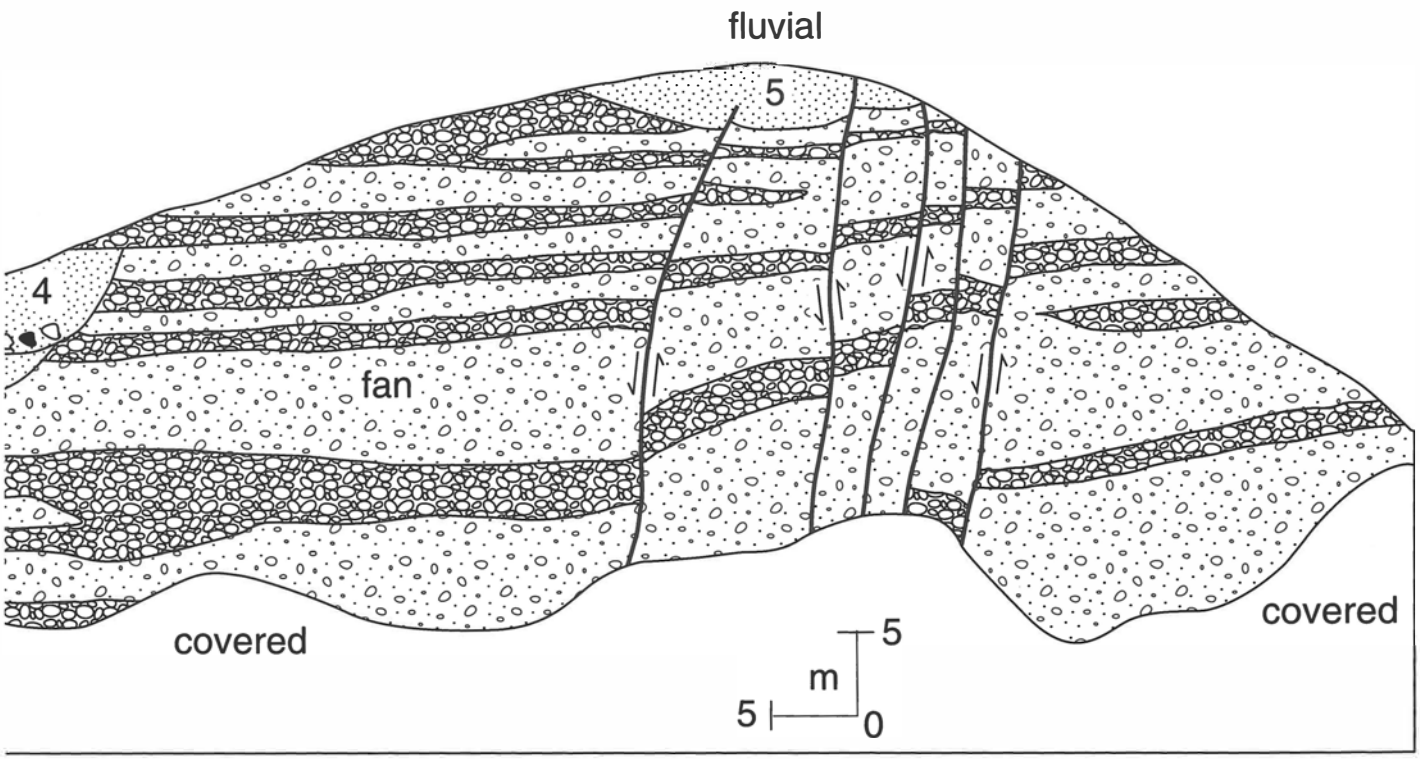

Canyon and is overlain by about 30 m (98 ft) of piedmont conglomerate that prograded over a kilometer (0.6 mi) into the basin (Fig. 99; Mack and Leeder, 1999; Mack et al., 2002). At Apache Canyon, there are two lithosomes of axial-fluvial sediment (Fig. 99). The lower one is about 35 m (115 ft) thick and extends to within 400 m (1,312 ft) of the border fault, whereas the upper one is much thinner (5 m; 16 ft) and only reaches to within 1.3 km (0.8 mi) of the border fault. As is the case farther north, the top of the Palomas Formation in Apache Canyon consists of about 8 m (26 ft) of piedmont conglomerate that prograded at least 1.5 km (0.9 mi) into the basin. The Apache Canyon sections are noteworthy because of the presence of several thin, 1.5 m (4.9 ft), beds of very well sorted eolian sand located upfan of the axial-fluvial lithosomes. Apparently, wind occasionally blew sand from the river onto the footwall-derived fans to a distance within 100 m (328 ft) of the border fault (Mack and Leeder, 1999). At Green Canyon, in the southern part of the Palomas Basin, there are three axial-fluvial lithosomes, each overlain by piedmont conglomerate (Fig. 99). Each successively younger fluvial lithosome extends closer to the Red Hills border fault, the youngest one reaching to within about 100 m (328 ft) of the fault. More than a dozen outcrops reveal that the axial river moved toward the footwall block by toe cutting the fans (Fig. 100), and Mack and Leeder (1999) and Mack et al. (2002) argued that basin tilting drove the river toward the footwall block. The difference in the number of fluvial lithosomes in the basin was a response to variations in the history of movement on the segments of the Caballo and Red Hills border faults.

Axial-fluvial and interbedded axial-fluvial and piedmont sediment is poorly exposed west of Caballo Reservoir and the Rio Grande. At the best exposures, in Kelly Canyon and in and south of Tierra Blanca Canyon, the axial-fluvial sediment contains a higher proportion of mottled overbank mudstone and fine sand representing crevasse-splays or small channels than is preserved along the eastern side of the basin (Mack et al., 2002). Unlike the eastern margin of the basin, there is no evidence at Kelly and Tierra Blanca Canyons of toe cutting of the hanging wall-derived alluvial fans by the axial river.

Mack and Leeder (1999) also recognized climatic cyclothems in the footwall-derived piedmont sediment of the Palomas Basin. The 3–10 m (9.8–33 ft) thick cycles are characterized by (1) calcic soil development and contemporaneous or subsequent channel incision to the fan toe, (2) deposition of horizontally bedded and crossbedded conglomerates by turbulent flow, and (3) deposition of pebbly sandstones by hyperconcentrated flows, which provide the parent sediment for the next generation of calcic paleosols (Fig. 101). Each cyclothem developed within a time scale of approximately 150 kyrs and was a response to climatically driven changes in sediment yield from the footwall scarps. Hanging-wall-derived strata in the Palomas Basin have similar cyclothems, although near the toes of the fans well-sorted, massive eolian sands and red mudstones are also present.

Finally, the presence of basalt cinder cones in the Engle and northernmost Palomas Gap quadrangles may have a structural origin. Mack and Seager (1995) defined the Cutter Sag area as a transfer zone, in which strain was transferred from the Caballo–Hot Springs fault to the Walnut Canyon fault that borders the western side of the Fra Cristobal Range. The Cutter Sag transfer zone is a north-dipping ramp cut by a series of northeast-trending normal faults. Pliocene cinder cones appear to be concentrated within the transfer zone.

Late Quaternary and Holocene deposits

The Cuchillo and Jornada I/La Mesa surfaces represent the constructional tops of the Palomas and Camp Rice Formations, respectively, as well as the culmination of basin filling on both sides of the Caballo Mountains about 0.78 Ma (Lozinsky and Hawley, 1986a,b; Seager and Hawley, 1973; Mack et al., 1993, 1998c). Sediments either inset below these formations or deposited on them are thin, <30 m (98 ft), but widespread alluvial deposits of late Pleistocene to Holocene age, deposited in a variety of modern or near-modern settings. Broadly, the deposits fall into two groups. One group includes alluvium deposited by the Rio Grande and its tributaries as they entrenched themselves and partially backfilled valleys during the last 0.78 Ma. These deposits, which are associated with a notable stepped sequence of terraces adjacent to the Rio Grande and along its tributary sideslopes, are prominent along the western and southern piedmont slopes of the Caballo Range. The second group of sediments, located on the eastern piedmont slopes of the range, consists of alluvium that is or has been in transit toward the closed basin floor of the Jornada del Muerto. These sediments accumulated outside the Rio Grande drainage network, at least originally. Headwaters of Rio Grande tributaries are beginning to erode the deposits locally.

Rio Grande valley-fill alluvium

Two groups of valley-fill alluvium are generally distinguished on geologic maps of the Caballo Mountains, based on age: older valley-fill alluvium (Qvo) and younger valley-fill alluvium (Qvy).

Older valley-fill alluvium

Description

Older valley-fill alluvium comprises deposits associated with a stepped sequence of three major and several lesser terraces that are conspicuous along the length of the Rio Grande, as well as in the walls of its major tributary arroyos (Gile et al, 1981). The terraces represent the constructional tops of underlying alluvial or fluvial deposits, the deposits and their surfaces collectively known as morphostratigraphic units (Gile et al, 1981). Inset against any older rock unit above range-boundary faults, but mostly against units of the Palomas or Camp Rice Formation below the faults, each of the three major morphostratigraphic units reveals the former position of the Rio Grande and its floodplain as well as alluvial fans and arroyo floors that were graded to or close to the floodplain. The highest and oldest of the major terraces grades to 45–60 m (148–197 ft) above the modern river floodplain, intermediate terraces to 45 m (148 ft) above the floodplain, and lower terraces to 20–30 m (66–98 ft) above the floodplain. The higher terraces, above 30 m (98 ft), are correlative with the Tortugas surface of the Las Cruces area, which together with underlying associated alluvium constitutes the Tortugas morphostratigraphic unit. The lower major surface, at 20 m (66 ft) above the floodplain, is the Picacho surface, the top of the Picacho morphostratigraphic unit (Ruhe, 1964, 1967; Hawley, 1965; Hawley and Kottlowski, 1969; Gile et al., 1981). Based on scattered mammalian fossils and radiometric dates from both overlying and underlying alluvium, the Picacho and Tortugas deposits are middle to late Pleistocene in age (Gile et al, 1981).

As much as 20 m (66 ft) thick where they crop out in bluffs adjacent to the Rio Grande floodplain, both the Tortugas and Picacho morphostratigraphic units thin upslope toward the mountains, becoming thin pediment veneers above the range-boundary faults. Both units consist mainly of unconsolidated, poorly sorted, boulder-cobble gravel, gravelly sand, and sand, with lesser amounts of clay. Deposits adjacent to the floodplain locally include well-sorted, well-rounded, gravel containing clasts from both local and upstream sources. Sets of planar crossbeds as much as 1 m (3.3 ft) thick are common in these deposits. Upslope from the river bluffs, Tortugas and Picacho alluviums are derived entirely from local sources. The clasts are poorly sorted, either grain or mud supported, and both horizontal and trough crossbedding is common. Trains of boulders are usually conspicuous along paleodrainage-ways. Although the Picacho and Tortugas alluvium are nearly identical lithologically, the oldest, highest Tortugas deposits differ by their thick, 1 m (3.3 ft), stage IV petrocalcic soils in uppermost beds, which tightly

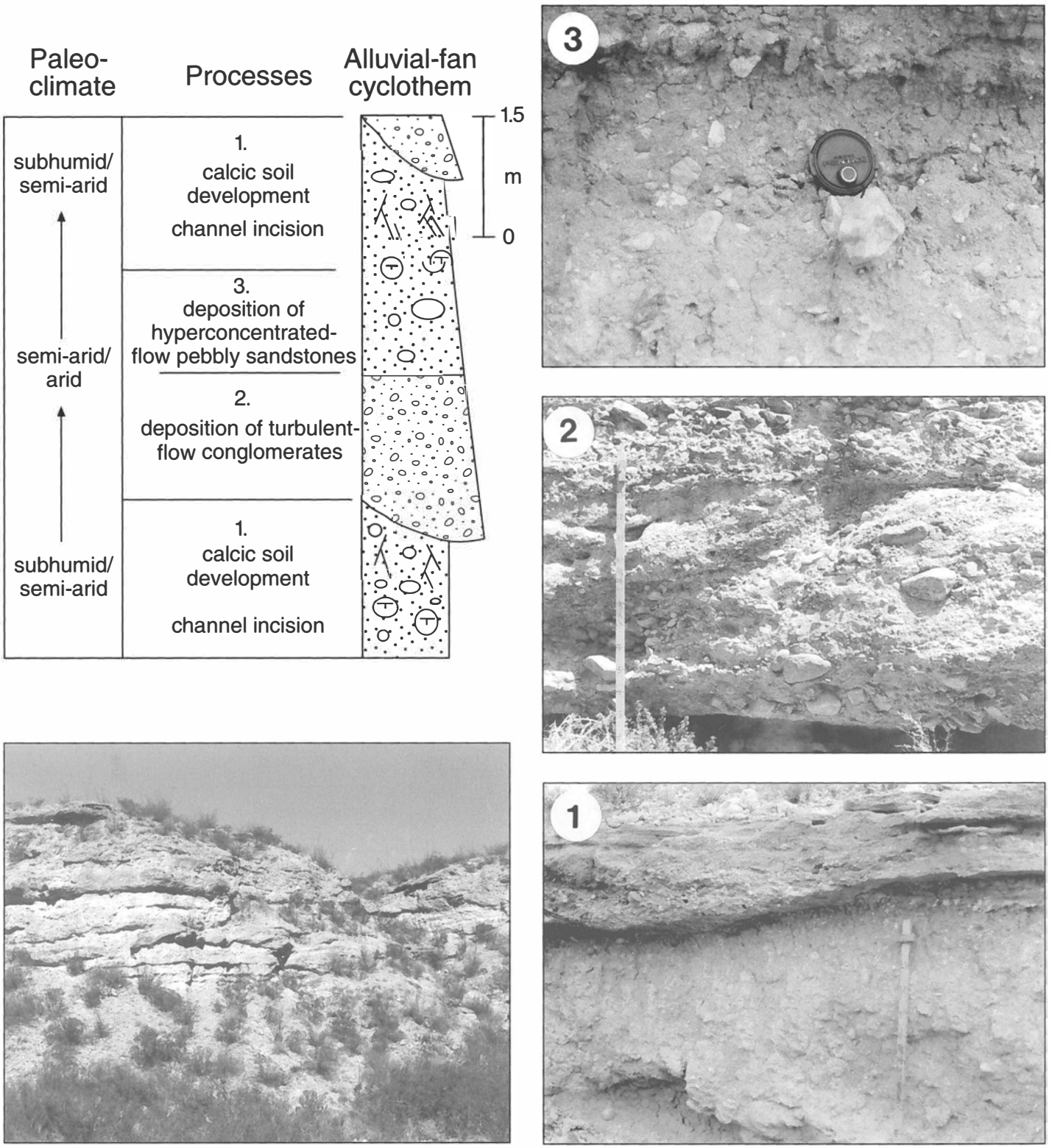

FIGURE 101—Climatic cyclothems in footwall-derived sediment of the Pliocene–Pleistocene Palomas Formation, adapted from Mack and Leeder (1999).

cement sediment. In contrast, younger Tortugas and Picacho alluviums generally exhibit soil profiles characterized by stage III or II soil carbonate as much as 0.5 m (1.6 ft) thick, which provide modest or weak cementation.

Younger valley-fill alluvium

Description

Younger valley-fill alluvium comprises the deposits of the modern Rio Grande channels and floodplain, as well as all arroyo, alluvial fan, and colluvium that is graded to within a few meters of the floodplain. The deposits correlate with the Leasburg, Fillmore, and historical morphostratigraphic units of Hawley and Kottlowski (1969) and Gile et al. (1981) in the Las Cruces area. Oldest parts of the deposits, associated with the Leasburg surface, may be as much as 15,000 years old, Wisconsonian in

age. Radiocarbon dates as as old as 9,400 yrs have been reported from charcoal in alluvial fans that have prograded onto the floodplains (Hawley and Kottlowski, 1969; Seager and Hawley, 1973).

Younger valley-fill alluvium is lithologically similar to older valley-fill alluvium. Well-sorted sand and gravel containing interbedded clay and silt lenses are as much as 21 m (69 ft) thick beneath the Rio Grande floodplain, as determined from water-wells (Conover, 1954; King et al., 1971). On piedmont slopes above the valley floor, younger valley-fill alluvium consists of more poorly sorted, locally derived sand and gravel. Generally less than 10 m (33 ft) thick, younger valley-fill alluvium is non-indurated, except for the uppermost few centimeters that may contain incipient (stage I) soil development, including clay accumulation and thin coatings of filamentary carbonate on clasts or fine-grained material.

Depositional environments

Older valley-fill deposits include both fluvial and piedmont-slope alluvium. Fluvial deposits of the Rio Grande are distinguished by the well-sorted sand and gravel beds exposed in bluffs along the river's floodplain as well as by the distant source of well-rounded clasts. Planar crossbeds in gravel indicate deposition on large transverse river bars. Both older and younger piedmont-slope deposits still preserve much or all of their original depositional form, making interpretations of depositional environments easy. Both groups of alluvium include poorly sorted deposits of arroyo floors, alluvial fans, pediment veneers, and slope colluvium, any of which may be left as terraces adjacent to active arroyo channels or canyon walls. Trains of boulders on fans or within arroyos are probably debris flow levees, whereas more widespread sheets of alluvium are the products of sheetfloods. Fan and arroyo deposits grade to and interfinger downslope with river alluvium, indicating a process of fan progradation onto the floodplain, trimming of fan toes by the river, and repeat of the cycle many times. Examples of these processes are abundant on the modern floodplain throughout the length of the river.

The stepped sequence of terraces associated with the Tortugas, Picacho, Leasburg, and Fillmore morphostratigraphic sequences resulted from at least five episodes of downcutting by the Rio Grande and its tributaries in the last 780,000 yrs, each episode followed by an interval of partial backfilling and valley-floor stability (Hawley and Kottlowski, 1969; Gile et al, 1981). According to Gile et al. (1981), the cycles of downcutting and deposition were probably climatically controlled, driven by waxing and waning flow of the Rio Grande in northern New Mexico and Colorado. In particular, glacial periods were probably times of huge river discharge and downcutting, whereas deposition and backfilling of valleys may have been the dominant process during inter-glacial periods (Gile et al., 1981).

Closed-basin alluvium

Closed-basin deposits on the eastern piedmont slopes of the Caballo range are different in several respects from Rio Grande valley deposits. The closed-basin alluvium includes no fluvial sediment, rather consisting of a relatively thin veneer of sand and gravel on widespread pediment surfaces. Less eroded than Rio Grande valley deposits, inset terraces are generally low in relief or absent altogether, and the terraces as well as all depositional landforms are graded to playa lakes near the center of the Jornada del Muerto. Like the Rio Grande valley-fill alluvium, closed-basin deposits can be subdivided into two groups: older closed-basin alluvium and younger closed-basin alluvium.

Older closed-basin alluvium

Description

Older closed-basin alluvium comprises at least two and probably three generations of deposits, mostly on piedmont slopes, that onlap or are inset below the Palomas/Camp Rice Formations. Inset relationships are typical of fan-head trenches in the upper parts of Palomas/Camp Rice fans, whereas the lower reaches of those fans are buried by younger alluvium. The "crossover line" between inset and onlap relationships is often near the middle of the fan. Ten meters or less in thickness, the deposits and their constructional upper surfaces correlate with the Picacho and Tortugas morphostratigraphic units in the Rio Grande valley (Hawley, 1965; Ruhe, 1964; 1967; Hawley and Kottlowski, 1969; Gile et al., 1981). Gravel, sand, and loamy sediment comprise most of the deposits, grain size varying with proximity to the mountain front or with the size of clasts in underlying conglomerate beds, such as Camp Rice, Love Ranch, or McRae Formations, which may be local sources of gravel. Silt and clay, locally gypsiferous, distinguish distal parts of alluvial fans as well as adjacent playas. Although the sediments are nearly unconsolidated, ground-water cementation by calcite has locally indurated them, as in Aleman Draw. Uppermost beds are also tightly or moderately cemented by pedogenic carbonate or clay. Stage IV soil carbonate is typical of the highest, oldest deposits, whereas stage III or stage II carbonates distinguish lower, younger basin fill.

Younger closed-basin alluvium

Description

Younger closed-basin alluvium includes actively moving sediment on present arroyo floors as well as deposits graded to within a meter or two of arroyo floors or to the surface of playa lakes near the center of the Jornada del Muerto. Less than 15,000 years old, the deposits correlate with the Leasburg, Fillmore, and historic alluvium of the Rio Grande valley (Gile et al., 1981). Like older closed-basin alluvium, younger deposits are also inset against older alluvium in fan-head trenches, but overlap more distal parts of the fans, particularly downslope from the Jornada Draw fault. Consisting almost entirely of gravel, sand, silt, and clay, the latter locally gypsiferous on playa lake beds, the deposits are unconsolidated, although the uppermost few centimeters may be weakly coherent owing to accumulations of clay or organic material in weakly developed soil. Soil carbonate is either absent or present only as fine filaments or thin coatings.

Depositional environment

Because of their youth and position on piedmont slopes leading to closed-basin floors, neither older nor younger closed-basin alluvial units have been substantially modified by erosion. Consequently, depositional environments are reflected in landform morphology as well as by lithologic character of deposits. The alluvium accumulated on the floors of arroyos (where shallow incision has left many remnants as low terraces) as thin, widespread pediment veneers, hillside colluvium, playa lake beds, and adjacent alluvial flats, and both small and very large alluvial fans. The stepped terraces developed in this closed-basin setting are clearly not a product of valley cutting by the Rio Grande. Rather, they may be formed by progressive entrenchment of arroyos within mountain uplands caused either by steady-state downcutting or by episodic, accelerated erosion caused by uplift of the range by movement on range-boundary faults.

Neogene extensional structure

The Neogene structure of the Caballo Mountains is dominated by various grabens, horsts, and tilted blocks formed by movement on moderate to high-angle normal faults (Fig. 102). The Neogene age of these faults is clear from the fact that they transect and offset Laramide structures, as well as all of the Tertiary formations, and a few substantially displace Quaternary alluvium. Movement on the large faults or fault systems can also be related to contemporaneous deposition of Neogene alluvial fans (Hayner Ranch/Rincon Valley/Palomas–Camp Rice Forma-

tions) on hanging-wall blocks, followed by deformation of fan sediment as fault movement progressed. Locally, the position and trend of major normal faults are controlled by Laramide thrust faults, resulting in structural inversion of the older structures by the younger. Although normal faults are the prevailing mode of Neogene deformation, folds are also important. These range in scale from small drag folds along faults to domal, semidomal, or synclinal structures that are coextensive with large fault blocks.

The array of Neogene structures in the Caballo Mountains offers insight into several aspects of extensional tectonics that may be applicable to other rifts. First, the internal geometry of some fault blocks permits interpretations of their kinematic evolution. Second, the close association of faults with dated basin-fill deposits provides a basis for understanding the timing of individual fault movements as well as changing patterns of fault activity across basin/uplift margins. Finally, the overprinting of Laramide structures by Neogene faults emphasizes the important effect of structural inversion on the geometries of extensional structures in parts of the southern Rio Grande rift, as well as the extent to which Laramide deformation controls Neogene fault trends and locations.

In the following section, major Neogene faults and fault blocks will be described, paying particular attention to the geometry of the structures and, where evidence is available, to Laramide controls of faulting, structural inversion, timing of fault movements, and kinematic structural evolution. This discussion, combined with the preceding description of synorogenic sedimentary and volcanic rocks, provides a basis for interpreting the Neogene tectonic evolution of fault blocks within the Caballo Mountains area and then for summarizing the evolution of the Rio Grande rift in south-central New Mexico.

Caballo–Hot Springs fault

The Caballo–Hot Springs fault (Fig. 102) is one of the major range-boundary normal faults in the southern Rio Grande rift. More than 42 km (26 mi) in length, the fault is broadly convex toward the west, trending north-northeasterly in its northern half to southeasterly in its southern reaches, the change in trend taking place midway along its length near Flordillo Canyon. The eastern footwall of the fault is the triangle-shaped Caballo uplift, tilted eastward from 10° to 20° in the manner of an enormous trap-door structure (Fig. 103). The more complex, down-dropped, hanging-wall block is broken into several fragments by faults that branch from or intersect the Caballo–Hot Springs fault, including, among many others, the major Red Hills and Williamsburg–Mud Springs faults. Consequently, hanging-wall structures range from the deep Palomas and Engle Basins to a variety of shallow grabens, half grabens, and tilted blocks at intermediate structural levels, such as the Mud Springs and Red Hills uplifts, Apache graben, Hidden Tank fault block, and Nakaye horst (Fig. 102).

Kelley and Silver (1952) applied the terms Hot Springs and Caballo faults to northern and southern segments of the fault that overlap modestly 6 km (3.7 mi) south of Truth or Consequences, the area of overlap enclosing a lozenge-shaped block at an intermediate structural level they informally named northern red hills (Fig. 102). North of the overlap, the Hot Springs fault forms the western margin of the Caballo uplift as well as the eastern limit of both the Mud Springs uplift and Engle Basin.

The southern extent of the Hot Springs fault is less precisely known. It is apparently truncated by the Williamsburg–Mud Springs fault at the southern edge of the northern red hills. Harrison and Chapin (1991) and Cather and Harrison (2002) believe the Hot Springs fault continues beyond this junction southwestward across the Palomas Basin, buried beneath gravels of the Palomas Formation, but revealed by the gravity and aeromagnetic data of Kucks et al.. (2001). Based on our study of Kucks et al. (2001) maps and the gravity maps of Ramberg and Smithson (1975) we believe that the buried fault in the Palomas Basin is a northeastern extension of the Goodsight fault, which terminates against the Red Hills fault in the vicinity of Caballo dam (Fig. 102).

South of the overlap of the Hot Springs and Caballo faults, the Caballo fault extends to the southern tip of the Caballo uplift, transecting a variety of structures in its hanging wall, most notably the Red Hills fault, Apache graben, and Hidden Tank fault. Based on one exposure near Longbottom Canyon, the Caballo fault dips 50° west. Bushnell (1953), Lozinsky (1986), and Mason (1976) indicate the Hot Springs fault dips from 65° to 78° west. The courses of parts of both the Hot Springs and Caballo faults were partly controlled by west-dipping Laramide reverse faults. This is especially clear for the southern part of the Caballo fault, where it follows a basement thrust in the core of the McLeod Hills fault-propagation fold for a distance of 12 km (7.4 mi). A similar relationship apparently exists between the Hot Springs fault and the core of an overturned Laramide fold south of Truth or Consequences (Mason, 1976). Because Laramide and late Tertiary movements were opposed, inversion of the Laramide structures has occurred. The resulting unusual relationships between hanging-wall and footwall rocks will be reviewed in the section on structural inversion, p. 100.

Maximum stratigraphic separation on the Caballo–Hot Springs fault is probably achieved near the midpoint of the fault in the vicinity of Timber Mountain, the structurally highest part of the footwall uplift. Using gravity data of Keller and Cordell (1983), Gilmer et al. (1986) calculated as much as 1.6 km (1.0 mi) of basin fill on the hanging wall of the Caballo fault. Maximum stratigraphic separation of 6.5–6.6 km (4–4.1 mi) may be estimated by combining this thickness with the exposed thickness of Precambrian rocks below Timber Mountain as well as with 4.6 km (2.9 mi) of Phanerozoic strata that crop out above the Precambrian and that presumably are present beneath basin fill in the hanging wall. From Timber Mountain, throw gradually decreases both toward the north and the south as successively younger footwall strata intersect the Hot Springs/Caballo faults. Abrupt decreases in separation also occur at intersections with major footwall and hanging-wall structures and where inversions of Laramide structures have occurred. According to Warren (1978), the Hot Springs fault dies out northward within the Palomas Formation near the Fra Cristobal uplift. South of Timber Mountain, the Caballo fault eventually dies out southward within the Haystack syncline. Thus, stratigraphic separation on the Caballo–Hot Springs fault varies from zero at the tips to a maximum near the midpoint of the arc-shaped fault at Timber Mountain.

Although the Caballo uplift is a relatively simple eastward-tilted block, there are a variety of structures that locally modify the shallow easterly dip. Most of these are Laramide folds, including the McLeod Hills fault-propagation fold, the Putnam anticline, and various other fold belts described under Laramide structures. The Longbottom fault (Fig. 102), an easterly trending Laramide reverse fault that passes into the Putnam anticline, is a conspicuous transverse fault that passes across the range just north of Timber Mountain and Longbottom Canyon. Both the topographic crest of the range as well as Paleozoic strata are lowered several hundred meters on the north side of the fault, the result of Laramide reverse movement on the fault. Renewed late Tertiary displacement was down to the south as described in the section on inversion structures.

Controversy persists regarding the origin of the Hot Springs fault. Harrison and Chapin (1990), Cather and Harrison (2002), and Harrison and Cather (in press,) believe the fault was initiated during the Laramide orogeny as a major strike-slip fault. Kelley and Silver (1952) and Mason (1976), among others, including ourselves, regard the fault as essentially a late Tertiary

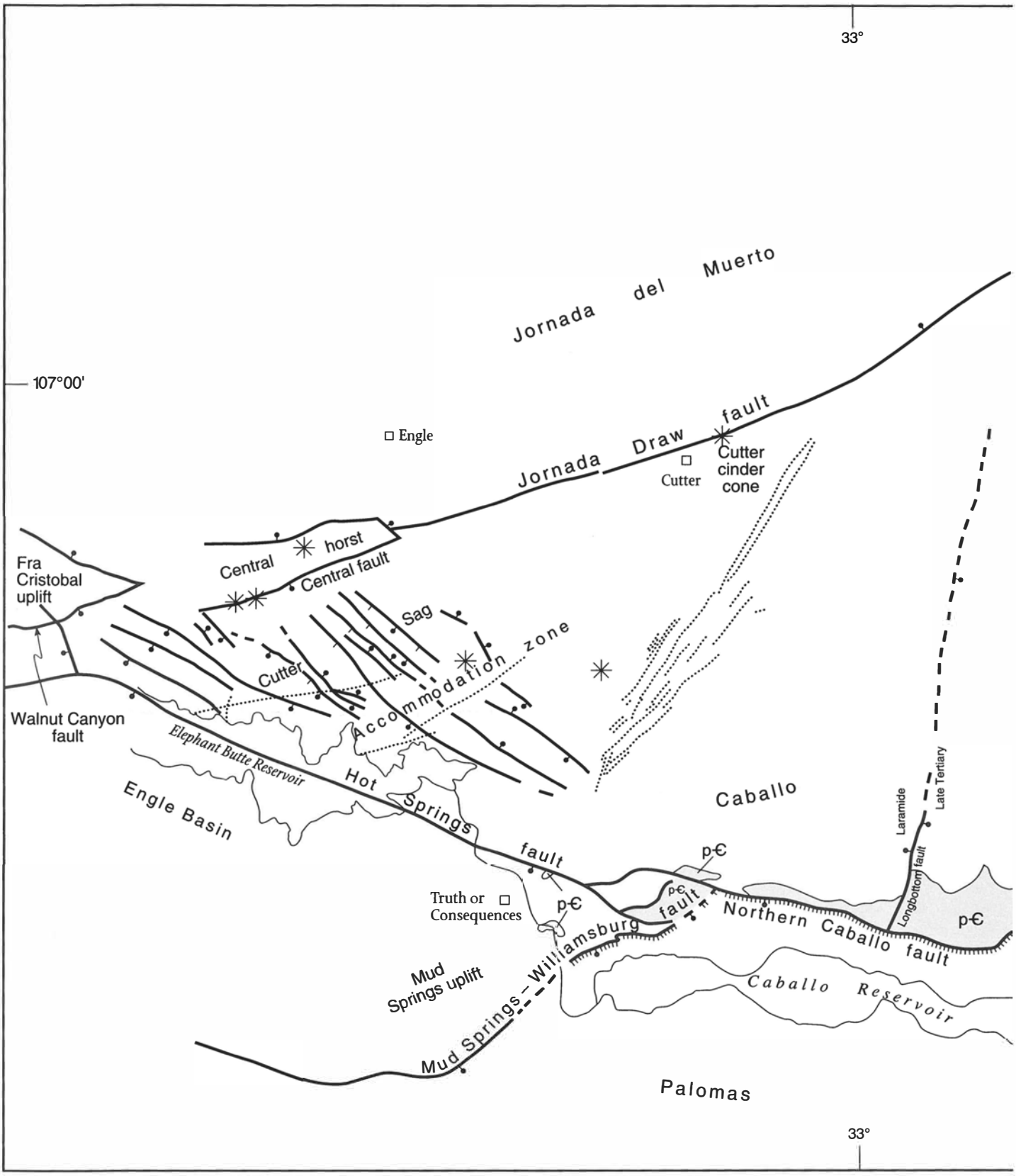

FIGURE 102—Tectonic map of latest Oligocene and Neogene extensional structures and dikes in Caballo Mountains and vicinity. Data is from quadrangle maps shown on Fig. 1 and, for the southern Fra Cristobal Mountains, from Kelley (1955) and Warren (1978). Goodsight fault based on data from Ramberg and Smithson (1975) and Kucks et al. (2001).

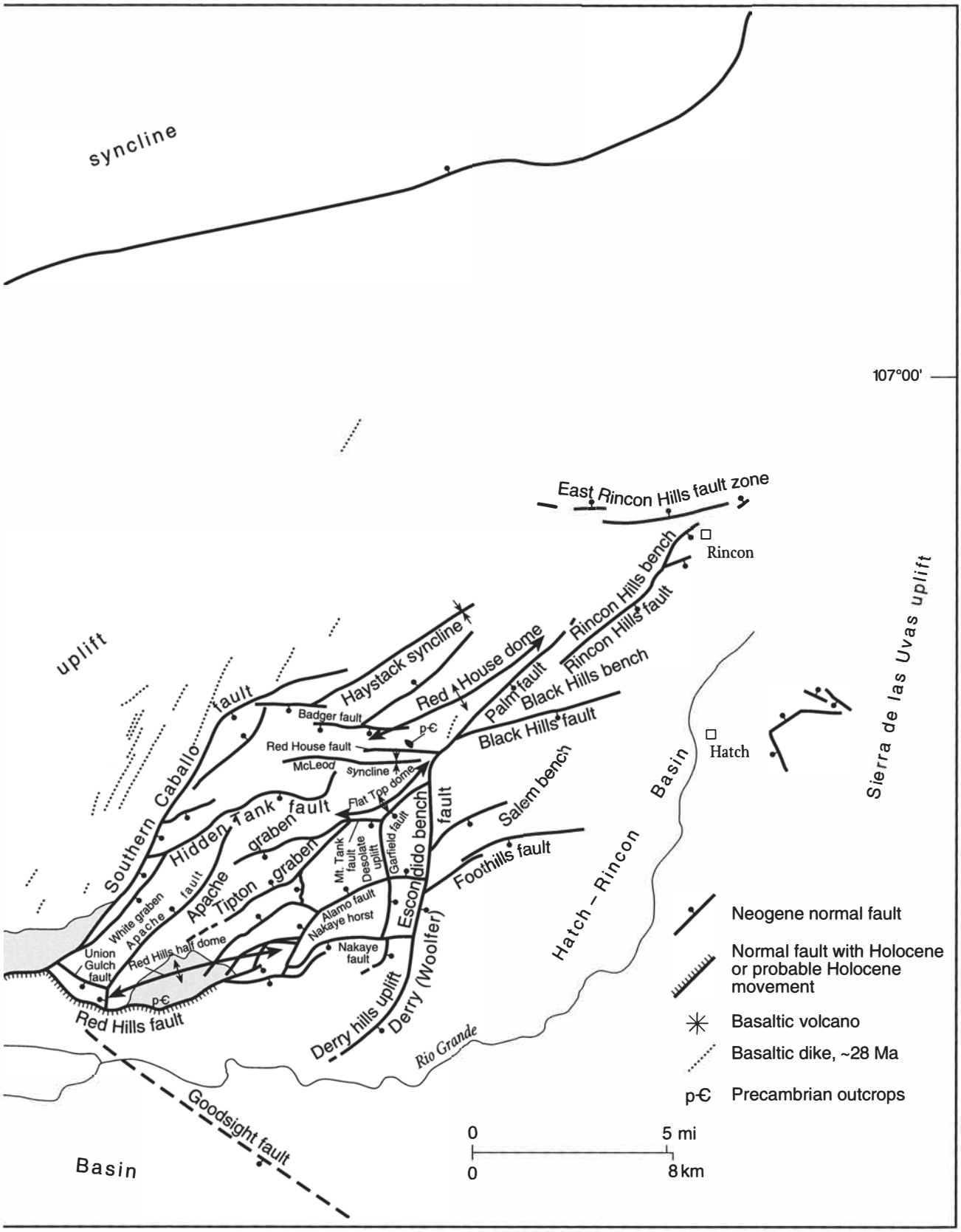
syncline
107°00'
East Rincon Hills fault zone
Rincon
Rincon Hills bench
Rincon Hills fault
Palm fault
Black Hills bench
Black Hills fault
Haystack syncline
Red House dome
Badger fault
p-€
Red House fault
McLeod syncline
Flat Top dome
Garfield fault
Mt. Tank fault
Desolate uplift
Escondido bench fault
Salem bench
Foothills fault
Hidden Tank fault graben
Tipton graben
Apache fault
White graben
Apache fault
Union Gulch fault
Red Hills half dome
Alamo fault
Nakaye horst
Nakaye fault
Red Hills fault
Derry hills uplift
Derry (Woolfer)
Hatch – Rincon Basin
Hatch
Sierra de las Uvas uplift
Rio Grande
Goodsight fault
Basin
uplift
Southern Caballo fault
Neogene normal fault
Normal fault with Holocene or probable Holocene movement
Basaltic volcano
Basaltic dike, ~28 Ma
p-€ Precambrian outcrops
0 5 mi
0 8 km

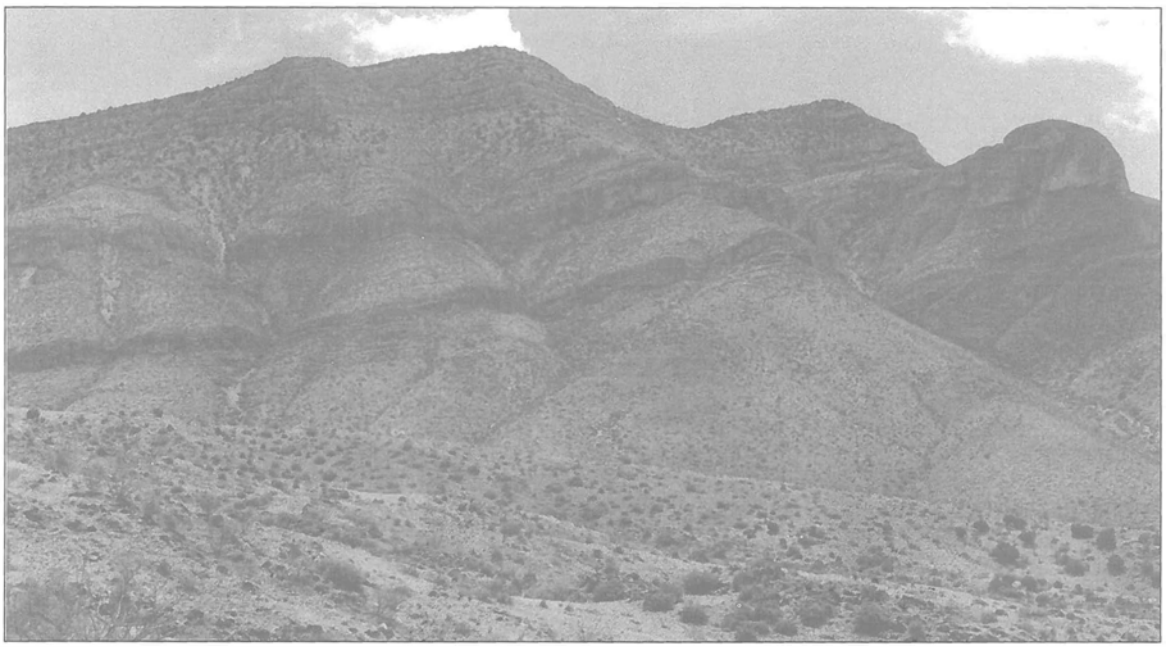

FIGURE 103—Eastward tilted footwall of Caballo fault as seen on southern slopes of Burbank Canyon. Precambrian granite and metamorphic rocks crop out in foreground, lower Paleozoic strata form lower cliffy outcrops on canyon wall, and Pennsylvanian beds cap mountaintop. View looks southeast.

structure. However, Mason (1976) and we recognize that segments of the fault probably followed Laramide reverse faults in the northern Caballo foldbelt just south of Truth or Consequences (see section on structural inversions). At any rate, relatively little is known about the Neogene history of movement on the Hot Springs fault because no Neogene basin-fill deposits older than Pliocene–Pleistocene Palomas Formation have been identified in either the hanging wall or footwall. Offset of the upper part of the Palomas Formation in the Elephant Butte area, together with as much as 90 m (295 ft) of displacement of 2.1 Ma basalts, indicates movement at least as late as early to middle Pleistocene time for the northern segment of the fault (Machette, 1987). There is no evidence for late Pleistocene or Holocene movement.

In contrast to the Hot Springs fault, the history of the Caballo fault is better appreciated. At least the southern part of the fault (southern Caballo fault; Fig. 102) was initiated in latest Oligocene or early Miocene time and was intermittently active until middle Pleistocene time. Earliest movements are documented by fanglomerate of the Hayner Ranch Formation exposed adjacent to the fault in Apache graben. Composed of locally derived boulders and cobbles of middle Tertiary volcanic rocks, the fanglomerate was derived from the east, presumably from the newly formed footwall of the southern Caballo fault. Repeated movements through the Neogene are indicated by the angular unconformity with overlying Rincon Valley Formation; by the proximal fanglomerate of the Rincon Valley Formation itself, whose clasts record erosion of lower Tertiary and upper Paleozoic strata from the footwall; by the angular unconformity between Rincon Valley Formation and overlying Palomas Formation; and by the proximal fanglomerate of the Palomas Formation, whose clasts are derived from formations now exposed in the footwall escarpment. In contrast to the southern Caballo fault, inactive for at least the last 0.7 Ma, the northern Caballo fault, located between the Red Hills and Williamsburg–Mud Springs fault (Fig. 102), has been repeatedly active throughout the Quaternary and into Holocene time (Foley et al., 1988; Machette, 1987).

North of its junction with the Red Hills fault, the northern Caballo fault is marked by a conspicuous piedmont scarp 2–45 m (6.6–148 ft) in height. The lower scarps transect Picacho-age alluvial fans (Qvo), whereas progressively higher scarps truncate progressively older Tortugas and Palomas deposits. This is a clear indication that higher scarps are composite, the result of multiple faulting events in Quaternary time.

Machette (1987) and Foley et al. (1988) have studied the northern Caballo fault scarps in order to judge (1) most recent movement on the fault, (2) recurrent intervals between major earthquakes, and (3) magnitude of potential earthquakes that may affect Caballo or Elephant Butte dams. To solve these problems, they produced detailed maps of the northern Caballo fault and the offset Quaternary units along the fault, excavated trenches across the fault to study offset alluvial units and soils, and made scarp-height vs scarp-slope angle studies. Based on these efforts, Machette (1987) and Foley et al. (1988) concluded that the northern part of the Caballo fault underwent multiple episodes of movement from middle Pleistocene to Holocene, the most recent of which was probably less than 5,000 yrs ago. Machette (1987) speculates that the recurrence interval along the Caballo fault is probably approximately 100,000 yrs, and Foley et al. (1988) estimate maximum credible earthquake potential for the Caballo fault at magnitude 7.25.

The piedmont scarps associated with the Caballo fault continue northwestward along the Williamsburg–Mud Springs fault and southeastward along the Red Hills fault. Southeast of its junction with the Red Hills fault, the southern Caballo fault does not disturb upper Palomas strata or the Cuchillo surface, indicating this southern segment of the fault has been inactive for at least the last 0.7 Ma.

Red House and Palm faults

At the southern tip of the (southern) Caballo fault, throw is transferred westward across a narrow accommodation zone to the Red House and Palm faults, movements on which have raised the prominent Red House fault block (Fig. 102). The Red House fault trends northerly and extends for a distance of 3 km (1.9 mi) along the western base of Red House Mountain. Throw increases from north to south along the fault, and near its northern tip, where throw is approaching zero, slip is transferred eastward to the en echelon Badger and an unnamed fault. While these en echelon faults are also structural boundaries of the Red

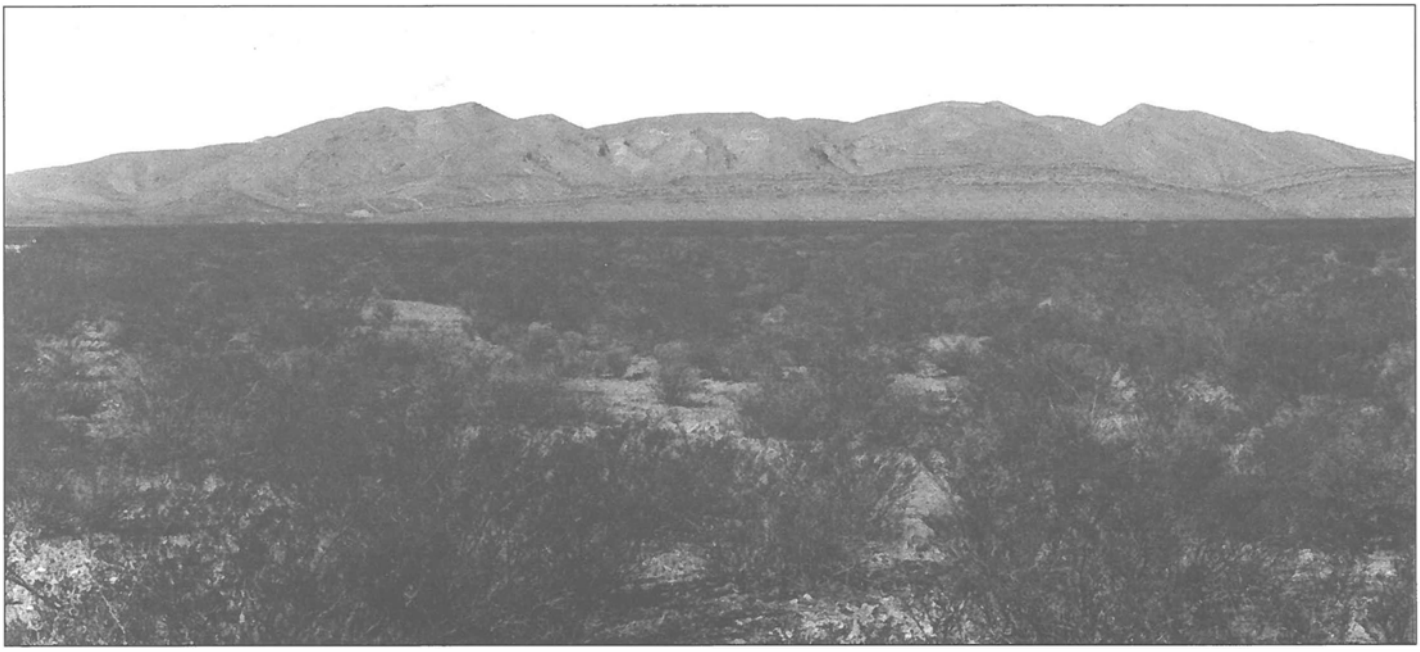

FIGURE 104—Red House Mountain viewed from the east. Summit of the range is along hinge of Red House dome. Note plunge of dome toward both southeast and northwest.

House uplift, they serve at the same time as the connecting structural links in the accommodation zone between the Caballo and Red House faults. Like its neighboring en echelon transfer faults, the Red House fault dips 50°–65° west and is downthrown to the west. At its southern end, the Red House fault appears to obliquely intersect and be truncated by the Palm fault, but may also be interpreted to abruptly bend into the southeasterly trend of the Palm fault. Maximum stratigraphic separation along the Red House fault is close to 900 m (2,952 ft) near its intersection with the Palm fault.

The northwestward-trending Palm fault forms the southwestern boundary of the Red House block. Although the southeastern limits of the fault are unknown because of burial by the Camp Rice Formation, the Palm fault can be traced for 9 km (5.6 mi) to its intersection with the Red House fault. Northwest of the intersection, the fault bends abruptly westward, becoming the Derry fault as it does so. The Palm fault dips 50°–60° southwest and is downthrown toward the southwest. Stratigraphic separation probably exceeds 1,800 m (5,906 ft) near its intersection with the Red House fault but decreases to 1,000 m (3,280 ft) or less at the southeastern edge of Red House Mountain.

Because of the oblique intersection of the Red House and Palm faults, the uplifted Red House block is triangular in shape. Steep, west- and southwest-facing footwall escarpments rise 365 m (1,197 ft) above the surrounding lowlands, whereas more gentle dip slopes reflect the overall tilt of the block 25° toward the northeast. The dip slope also constitutes the western limb of the Haystack syncline, which borders the uplift on the east.

The central structure of the Red House block is a northwest-trending, doubly-plunging anticline, whose hinge approximately follows the topographic crest of the range (Fig. 104). The culmination of the dome is located just east of the intersection of the Palm and Red House faults, where stratigraphic separation is greatest. The northwestward and southeastward plunges from this culmination correspond to decreasing throws on the boundary fault zones. Although the northeastern limb of the dome forms the northeastern dip slope of the fault block, the southwestern limb is exposed in the steep footwall escarpment. Dipping moderately southwest, this limb is broken by many branching and anastomosing antithetic normal faults, downthrown toward the summit of the dome, all of which are truncated by the Red House and Palm faults.

Clearly, doming of strata in the Red House block is related to movement on the Red House–Badger and Palm faults rather than to any compressional event. Because a similar style of doming distinguishes other fault blocks in the southern Caballo Mountains, they all may share a common kinematic evolution. This idea is developed in the section on extensional folds.

Because the Caballo, Red House, and Palm faults compose a nearly continuous through-going fault system, it is not surprising that these faults share a common history of movement. Like the southern Caballo fault, earliest movement on the Red House–Palm faults in latest Oligocene or early Miocene time is documented by thick proximal fanglomerate of the Hayner Ranch Formation deposited on the hanging wall of the Palm fault. Clasts in the fanglomerate prove that the Bell Top and Uvas volcanic rocks were exposed in the incipient Red House uplift. Subsequent fault movements are recorded by alluvial fan deposits of the Rincon Valley Formation, whose imbricated clasts also confirm the Red House block as the source and document progressive erosion into lower Tertiary and upper Paleozoic strata. Local angular unconformities between folded and faulted Hayner Ranch strata and less deformed Rincon Valley beds, such as the excellent example in the Rincon Hills (Seager and Hawley, 1973), also confirm movement on the Palm or related faults during the Miocene. Like the southern Caballo fault, the Palm and Red House faults have apparently been inactive since at least middle Pleistocene time, a conclusion supported by the fact that undeformed uppermost Palomas or Camp Rice deposits lie across the fault traces at several localities.

Rincon Hills, Black Hills, and Salem benches

South and southwest of the Palm and Derry faults, three structural benches step Tertiary and older rocks down into the Hatch–Rincon Basin. Arranged en echelon in a left-stepping pattern, each bench trends northerly or northwesterly, the group spanning a distance of 18 km (11 mi) along the northern margin of the Hatch–Rincon Basin. Each of the benches is relatively narrow, only 1.6–5 km (1.0–3.1 mi) in width, and each is bordered on the west by a normal fault, downthrown to the west or southwest. From southeast to northwest, the benches and boundary faults are: Rincon Hills bench and Rincon Hills fault (Central

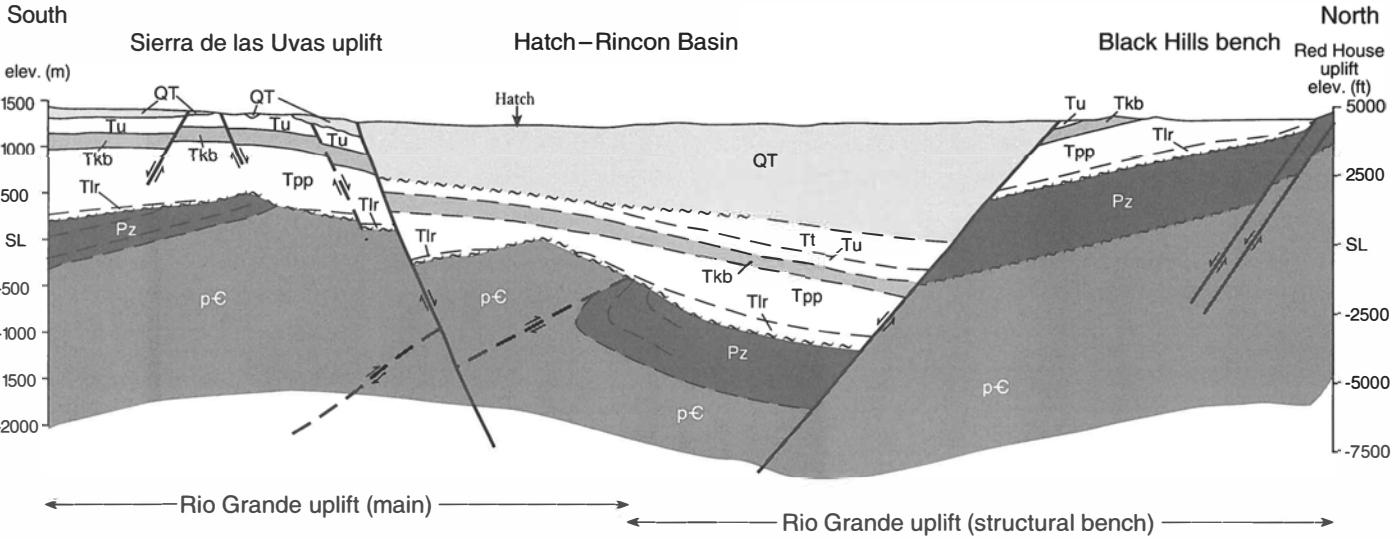

FIGURE 105—North-south cross section across Hatch–Rincon Basin. Note Laramide Rio Grande uplift buried beneath Tertiary formations. **p€** = Precambrian rocks; **Pz** = Paleozoic rocks; **Tlr** = Love Ranch Formation; **Tpp** = Palm Park Formation; **Tkb** = Bell Top Formation; **Tu** = Uvas Basaltic Andesite; **Tt** = Thurman Formation; **QT** = Hayner Ranch, Rincon Valley, and Camp Rice Formations, undifferentiated.

fault of Seager and Hawley, 1973); Black Hills bench and Black Hills fault; and Salem bench and Foothills fault. As illustrated in Figure 102, the Foothills fault is a splay off the Derry fault, the Black Hills fault is a splay off the Palm fault, and the Rincon Hills fault represents an eastward transfer of extensional strain from the southern tip of the Black Hills fault. Although none of these faults appears to be more than 8 km (5 mi) in length, construction of cross sections suggests stratigraphic separations may approach 1,200 m (3,937 ft), at least along the Black Hills fault. This relatively large displacement seems necessary because of the thick section of basin fill exposed in the hanging wall.

Middle Tertiary volcanic and sedimentary rocks are widely exposed in both the Rincon Hills and Black Hills benches. Generally dipping southward at shallow to moderate angles, these strata may comprise the down-faulted southern limb of the Red House dome. More significant, however, are the widespread outcrops on the benches of tilted, faulted and broadly folded Hayner Ranch and Rincon Valley fanglomerate.

Several lines of evidence indicate the Hayner Ranch and Rincon Valley alluvial fan deposits were derived entirely from the Red House uplift rather than from any part of the structural benches on which they now crop out. First, Hayner Ranch and Rincon Valley fanglomerate exposed in Salem bench increase in grain size toward the Red House block, becoming very coarse grained proximal fanglomerate at the Red House–Palm fault junction. Second, outcrops of the two formations on the Rincon Hills and Black Hills benches contain abundant clasts of Love Ranch and upper Paleozoic formations, strata that are still buried beneath the Tertiary volcanic rocks on both benches but capped Red House Mountain during the Miocene. Third, exposures of the Rincon Valley Formation, downthrown against the Black Hills fault, are midfan rather than proximal facies. And finally, the Rincon Hills fault disrupts playa and lacustrine facies of both the Hayner Ranch and Rincon Valley Formations. From these relationships, it seems clear that during most of the Miocene, alluvial fans of the Hayner Ranch and Rincon Valley Formations spread south and southwestward into the Hatch–Rincon Basin from their sources in the Red House uplift; the structural benches had not yet formed.

Sometime during the latest Miocene or early Pliocene, following deposition of Rincon Valley fans and playa sediment, faulting stepped basinward, forming the Salem, Black Hills, and Rincon Hills benches. Judging from piedmont scarps and displacement of Camp Rice strata, each of the bordering faults has continued to be active into the middle or late Quaternary.

Hatch–Rincon Basin

The Hatch–Rincon Basin is a northwest-trending graben that separates the Sierra de las Uvas from uplifts in the southern Caballo Mountains. Approximately 35 km (21.7 mi) long, the southeastern part of the basin is only 12 km (7.4 mi) wide near the town of Rincon, but it broadens to the northwest where it merges with the southern part of the Palomas Basin. Judging from the symmetrical distribution of fluvial and piedmont slope facies of the Camp Rice Formation, the basin has subsided symmetrically for the last 4–5 Ma (Mack and Seager, 1990). Even today, the graben controls the course of the Rio Grande, which flows near the basin center.

Although the basin has been a graben since the late Miocene or early Pliocene, it was a half graben throughout most of the Miocene, when a thickness of as much as 1.5 km (0.9 mi) of Hayner Ranch and Rincon Valley Formations was deposited in it (Fig. 105). The distribution and composition of lithofacies in these formations, together with their northeast dip, are consistent with deposition in a half graben, deepening northeastward, whose footwall uplift was Red House Mountain and whose hanging-wall dip slope was an ancestral Sierra de las Uvas (Mack et al., 1994b). During latest Miocene or early Pliocene time, faulting stepped basinward from both flanks, creating the structural benches on the northern flank, disrupting the hanging wall dip slope on the southern flank, and converting the half graben to a full graben.

Derry fault

The Derry fault (Woolfer fault of Kelley and Silver, 1952), together with the Palm fault, forms the northern margin of the modern Hatch–Rincon Basin (Fig. 102). Although the Palm and Derry faults appear to be a continuous fracture, the term Derry fault is applied to the segment extending westward from the Red House fault–Palm fault intersection. From this junction, the Derry fault extends westward for a distance of 8 km (5 mi) before bending to a more northwesterly strike, forming the southwestern margin of the Derry Hills as it does so. Northwest of the Derry Hills, the fault is buried beneath upper Quaternary alluvium at the mouth of Green Canyon. The fault is downthrown toward the south or southwest, and at two localities its dip of 65° south or southwest can be measured.

The Derry fault truncates several structures in both hanging-wall and footwall blocks, causing stratigraphic separation to vary

dramatically along strike. For example, maximum stratigraphic separation of approximately 1,860 m (6,102 ft) was measured where Montoya strata at the base of the Nakaye horst are juxtaposed against Hayner Ranch strata on the Salem bench. East and west of the border faults of the Nakaye horst, stratigraphic separation abruptly decreases to 1,200 m (3,937 ft) or less. Smaller but no less abrupt changes in separation occur as the Derry fault transects the Foothills fault and Salem bench, both structures comprising parts of the hanging wall of the Derry fault.

The Derry fault apparently was not initiated until latest Miocene or early Pliocene time, following deposition of Hayner Ranch and Rincon Valley basin fill. Although these formations crop out in the hanging wall adjacent to the Derry fault, only midfan lithofacies are generally present, evidence that the Derry fault was either not present, or its footwall uplift was too subdued to be an important source of clastics. On the other hand, Pleistocene movement on the Derry fault is indicated by offset of all except the youngest deposits of the Camp Rice Formation and the Cuchillo (Jornada I) surface. Movement on the Foothills fault, a basinward splay of the Derry fault, has continued into middle to late Pleistocene time, judging by the fault truncation of the youngest Camp Rice strata. However, post-Camp Rice inset terraces and fans adjacent to this fault are not broken.

Garfield fault

A major fault splay from the Derry fault into its footwall uplift is named Garfield fault (Kelley and Silver, 1952). Approximately parallel to the Derry fault and located 1–2 km (0.6–1.2 mi) north of it, the Garfield fault extends approximately 10 km (6.2 mi) westward from its junction with the Derry fault. The western end of the fault is buried beneath alluvium between the Derry Hills and Nakaye horst. Like the Derry fault, the Garfield fault is downthrown to the south, but its dip is unknown. Stratigraphic separations along the length of the Garfield fault are variable because of its intersections with faults of modest to large displacement in both hanging wall and footwall. Maximum stratigraphic separation of 810 m (2,657 ft) was measured where the fault transects the Nakaye horst, but separations of only 100–200 m (328–656 ft) are also obvious where the fault truncates structurally lower footwall blocks.

The structural block nearly enclosed by the Garfield and Derry faults is the Escondido bench (Fig. 102). It may be viewed as an intermediate structural step between the footwall uplifts of the Garfield fault and the Hatch–Rincon Basin. The western part of the bench consists of the downfaulted, southern part of the Nakaye horst, a horst that is more prominent in the footwall uplift on the northern side of the Garfield fault. The structurally low, eastern part of Escondido bench consists mostly of southwest-dipping, upper Paleozoic rocks, the southwestern flank of the Flat Top uplift/anticline. Because both the Nakaye horst and Flat Top anticline are truncated and offset by the Garfield fault, the fault is apparently somewhat younger than these structures.

The footwall uplift of the Garfield fault is a major fault block that exposes a variety of extensional structures. With the exception of the Nakaye horst and Flat Top anticline, all of these structures terminate at the Garfield fault. From west to east, the footwall blocks are (1) Nakaye uplift, a northerly trending, synclinal-shaped horst that is bordered on the west by Nakaye fault and on the east by the Alamo fault zone; (2) the Desolate uplift, a broad, fractured, half-dome shaped structure that plunges north beneath Apache graben; (3) the Flat Top uplift, a north-northwest-trending domal structure that is raised and tilted eastward by a combination of movement on the north-trending Mountain Tank fault and Garfield fault; and (4) the McLeod syncline, a shallow synclinal-shaped half graben whose hanging-wall dip slope is the eastern flank of the Flat Top uplift/anticline and whose footwall uplift is the Red House uplift. Collectively, these structures form not only the footwall of the Garfield fault but also the southern and southwestern rim of Apache graben, located to the north.

The Flat Top fault block is of special interest because of its structural similarity with the Red House uplift. Each uplift is triangular in plan view, formed by intersecting north and northwest-trending normal faults. Each uplift features a prominent, doubly plunging symmetrical anticline that trends northwesterly, a course that parallels the resultant vector of the two boundary faults. The plunges of both folds correspond to decreasing throws on the bounding faults, and the summit of each dome is adjacent to the region of maximum stratigraphic separation. In each uplift, the western limb of the anticline is truncated and offset by the boundary fault zones. There are two main differences between the two structures: (1) the scale, the Red House uplift being three times larger than the Flat Top uplift, and (2) the lack of extensive antithetic faulting in the western limb of the Flat Top fold. Small thrust faults break the core of the Flat Top fold, whereas none have been identified in the Red House structure. The similarities in geometry suggest that both uplifts share a common kinematic evolution, discussed further in the section on extensional folds.

Because few Neogene rocks are present on either hanging wall or footwall, the age of the Garfield fault cannot be more closely determined than post-Palm Park, pre-uppermost Camp Rice. Presumably the fault was initiated with and has had a history of movement similar to the Derry fault.

Red Hills fault

The Red Hills fault is an important normal fault in the southern Caballo Mountains. It, together with the northern Caballo and Williamsburg-Mud Springs faults, forms a continuous, recently active fault zone along the eastern margin of the Palomas Basin (Fig. 102). The Red Hills fault branches southwestward from the Caballo fault near Flordillo Canyon, then in a course that is broadly convex to the west, extends southward a distance of nearly 8 km (5 mi) before branching into several splay faults, including the Nakaye fault, that extend the fault zone another 6 km (3.7 mi) farther south. The fault zone finally terminates against the Derry fault at the southern end of the Nakaye horst. The Red Hills fault dips 63°–68° west, and slickensides suggest a small component of right slip. Stratigraphic separation must vary considerably along the fault because the fault truncates major structures in the footwall, such as Apache graben and the Red Hills half dome. Using 1.6–2.3 km (1.0–1.4 mi) of basin fill calculated by Gilmer et al. (1986) and Harder et al. (1986) for the eastern Palomas Basin, we speculate that maximum stratigraphic separation may approach 3 km (1.9 mi) along the central part of the Red Hills half dome, where Precambrian rocks are structurally highest. From there, throw decreases northward and more dramatically southward, particularly on the Nakaye fault and other southern splays, where only a few hundred meters or less of stratigraphic separation are present.

The footwall uplift of the Red Hills fault exposes two important structures, Apache graben and the Red hills half dome. Apache graben crosses the northern end of the footwall uplift obliquely before being truncated by the Red Hills fault. It is described in the next section. South of the graben and separated from it by the Apache fault, is the broad Red Hills half dome. Approximately 6 km (3.7 mi) in length, the northerly trending hinge of the half dome parallels the Red Hills fault. Red Precambrian and lower Paleozoic (?) granite form the core of the half dome, whereas Paleozoic and lower Tertiary rocks plunge both to the north and south along the hinge and dip eastward along the eastern flank. The plunging southeastern flank of the half dome is further modified by several normal faults, each of which step the Phanerozoic section down eastward into the southern part of Apache graben. On its western side, the half dome is truncated by the Red Hills fault.

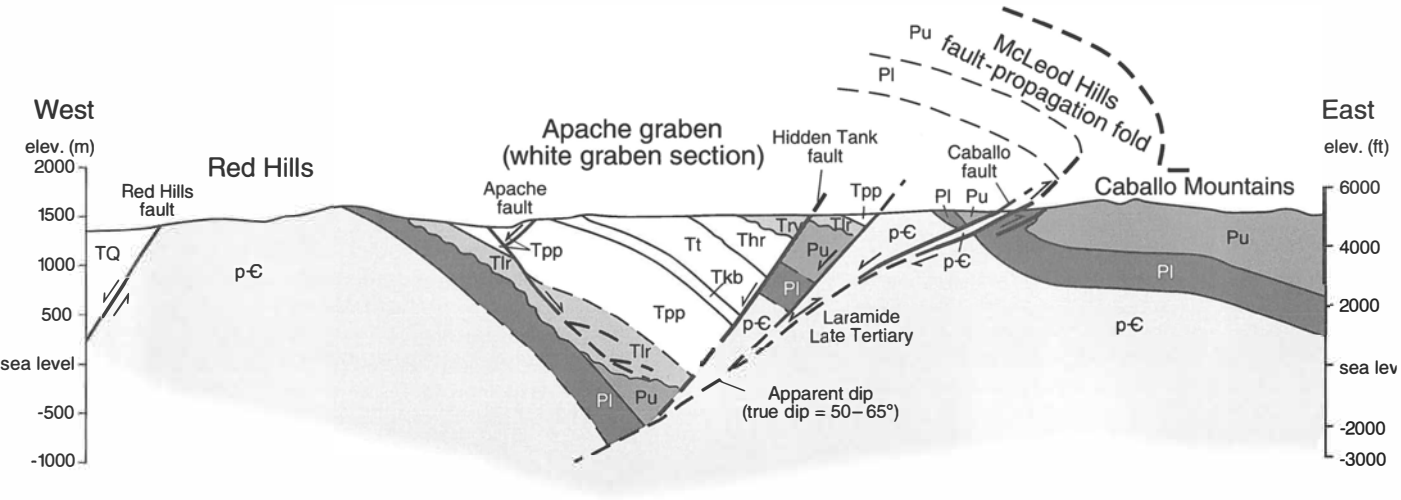

FIGURE 106—Cross section showing structure of Apache graben (White graben section). Note structural inversion of McLeod Hills fault-propagation fold by Neogene Caballo fault. **p-€**= Precambrian rocks; **Pl** = lower Paleozoic rocks; **Pu** = upper Paleozoic rocks; **Tlr** = Love Ranch Formation; **Tpp** = Palm Park Formation; **Tkb** = Kneeling Nun Tuff and Bell Top Formation; **Tt** = Thurman Formation; **Thr** = Hayner Ranch Formation; **Trv** = Rincon Valley Formation; **TQ** = Palomas Formation and older basin-fill deposits.

The Red Hills half dome is similar in several respects to the Red House and Flat Top domes, but dissimilar in others. Similarities include a fold hinge whose course is determined by the trend of the bounding fault zone(s), plunges of hinge lines that seem to correlate with decreasing throws on boundary fault zones, approximate cross sectional and longitudinal symmetry, and the presence of antithetic faults in the limb adjacent to the boundary fault. The widely exposed core of Precambrian/lower Paleozoic (?) basement and absence of much of the western limb of the Red Hills half dome are conspicuous differences between it and the other two domes. The general similarity of the Red Hills half dome and the Flat Top and Red House domal uplifts, however, suggests a common kinematic evolution of these fault blocks, discussed in the section on extensional folds.

Like the Derry and Garfield faults, the Red Hills fault is a much younger structure than the Caballo–Red House–Palm fault system. Movement on the Red Hills fault truncated, uplifted, and tilted alluvial fan deposits of the Hayner Ranch and Rincon Valley Formations back toward their source uplifts, the Caballo and Red House blocks. Thus, the Red Hills fault was initiated in latest Miocene or Pliocene time after deposition of the Rincon Valley Formation, and it has contributed in a major way to the breakup of the eastern flank of the ancestral Palomas Basin.

The Red Hills fault has been active during the late Pleistocene and probably Holocene. A prominent piedmont scarp marks its course from Flordillo to Apache Canyon and can be traced locally along the base of the Red Hills. Scarp heights range from a few meters to several tens of meters, and the youngest morphostratigraphic units offset by the fault are Picacho fans and terraces, approximately 50–150 ka years old. Although Machette (1987) and Foley et al. (1988) discussed the Red Hills fault scarp, they did not map, trench, or make morphometric studies of it. In view of its continuity with the northern Caballo and Williamsburg faults, which have demonstrable Holocene movement, it is likely that the Red Hills fault has also been active during the Holocene.

Apache graben

One of the largest and most important structures in the southern Caballo Mountains is Apache graben (Fig. 102). Rimmed by the Caballo uplift on the east, by the Flat Top and Desolate uplifts on the south, and by the Nakaye–Red Hills uplift on the west, the graben is nearly surrounded by elevated Paleozoic and Precambrian rocks. In contrast, the graben exposes thick sequences of Tertiary strata, including the "early rift" and Laramide syn- or post-orogenic rocks that are crucial in reconstructing the tectonic evolution of the Caballo Mountains. Approximately 9 km (5.6 mi) long in a north-northwest direction, the graben narrows from more than 6 km (3.7 mi) wide at its southern end to 2 km (1.2 mi) wide at its northern end, where it is truncated nearly at right angles by the Red Hills fault. The overall geometry of the graben also changes from south to north along its length.

The northern half of the Apache graben is basically a northeasterly tilted half graben whose footwall uplift is the Caballo and Hidden Tank uplifts, the latter a major structural bench of the Caballo block (Fig. 106). The hanging-wall dip slope of the half graben is formed by the east-dipping flank of the Red Hills uplift. Modifying the dip slope is Apache fault, downthrown northeastward a few hundred meters toward the deep part of the half graben. The Apache fault converts the downdip portion of the half graben into an asymmetrical graben in which "early rift" fanglomerate is preserved and where upper Paleozoic rocks are near sea level (Fig. 106). Named White graben (Seager and Mack, 1998) because of the conspicuous outcrops of white Thurman strata in the southern part of the graben, the structure narrows southward and terminates against the Hidden Tank fault. Throughout its length, White graben, the deepest structure within Apache graben, can be viewed as a simple antithetic graben on the downthrown side of the Caballo–Hidden Tank fault system.

South of the termination of White graben, the rest of Apache graben widens, changing to a "graben in graben" structural style. Blocks of Tertiary and Paleozoic strata are stepped down eastward from the Red Hills–Nakaye uplift axis as well as westward from the Caballo uplift. Between the two oppositely facing series of fault blocks, Tipton graben, the structurally lowest, keystone-shaped block, trends north-northwest for a distance of 5 km (3.1 mi) near the middle of Apache graben. Opposing dips in the fault blocks on either side of the central keystone graben create an overall domal geometry in the "graben in graben" structure. We view the domal structure as the result of rotation of fault blocks on oppositely dipping normal faults rather than from collapse of an arch. Southward, along the trend of Apache graben, Paleozoic strata rise and emerge at the surface as the Desolate uplift in the footwall of the Garfield fault. The broad tilting and extensive fracturing of these Paleozoic rocks may be interpreted as representative of the down-plunge, subsurface structure of Apache graben.

Within White graben, the deepest part of Apache graben, faulted and tilted Hayner Ranch and Rincon Valley Formations are unconformably overlain by undeformed alluvial fans of the upper Palomas Formation. The relationship indicates that Apache graben formed during the latest Miocene or early Pliocene, and has been tectonically inactive during much of the Pleistocene. The fact that the graben is largely a product of the eastward tilting of the Red Hills uplift and northward tilting of the footwall of the Garfield fault indicates that all of these structures formed concurrently in latest Miocene to early Pleistocene time.

Palomas Basin

The Palomas Basin is one of the major basins in the southern Rio Grande rift. It extends southward from the Williamsburg–Mud Springs fault, which limits its northern extent, some 65 km (40 mi) to the vicinity of the Derry Hills, where it merges with the Hatch–Rincon Basin. Twenty-five km (16 mi) in width, the basin is essentially a half graben, as indicated by both surface and gravity data (Keller and Cordell, 1983; Gilmer et al., 1986). Eastward-dipping volcanic and sedimentary rocks in the Animas Mountains and Black Range form the hanging-wall dip slope, whereas the Mud Springs, central Caballo Mountains, and Red Hills represent footwall uplifts along the deep eastern side of the basin. Based on seismic and gravity data, Gilmer et al. (1986) and Harder et al. (1986) suggest Neogene basin fill in the eastern part of the basin may be as much as 1.6–2.3 km (1.0–1.4 mi) thick. Maximum structural relief of the basin's eastern margin may approach 6.5 km (4 mi) adjacent to the northern Caballo fault.

An ancestral Palomas Basin was apparently initiated in early Miocene time with inception of the Caballo–Red House–Palm fault systems along its eastern border, followed by deposition of the Hayner Ranch and Rincon Valley Formations primarily as footwall fan deposits. By latest Miocene or early Pliocene time, faulting stepped basinward from both sides of the basin, narrowing it by 25 km (16 mi) or more and fragmenting its margins into various fault blocks.

The disruption of the basin was especially extensive along its eastern flank, where outlying fault blocks of the southern Caballo Mountains were shaped. By latest Miocene or Pliocene time a new through-going fault boundary was established along the eastern side of the modern Palomas Basin, formed by the Red Hills fault, the northern segment of the Caballo fault, and the Williamsburg–Mud Springs fault. Piedmont scarps along almost the entire length of this system indicate continued subsidence of the Palomas Basin or uplift of its footwall into the Holocene (Foley et al., 1988; Machette, 1987; Machette et al., 1998).

Williamsburg–Mud Springs fault

Foley et al. (1988) and Machette (1987) referred to the Williamsburg fault (Fig. 102) as the northern Caballo fault and labeled the piedmont scarp that marks its position the Williamsburg scarp. In their 1998 report, Machette et al. called the fault the Williamsburg section of the Caballo fault. We shall refer to the fault as the Williamsburg fault because we view it as a splay off the Caballo–Hot Springs fault zone, analogous to the Red Hills fault in that respect. The junction of the Williamsburg fault with the Caballo fault is located near the southern edge of the northern red hills. Striking northwestward from this junction, the Williamsburg fault seemingly truncates the Hot Springs fault and continues to the Rio Grande floodplain, marked discontinuously throughout its length by piedmont scarps.

Northwest of the floodplain, the fault reappears along the southwestern base of the Mud Springs uplift, where Kelley and Silver (1952) applied the name Mud Springs fault. The fault's course turns northerly at the northern end of the Mud Springs uplift, truncating footwall strata as it does so. North of the Mud Springs uplift, the fault can still be identified by piedmont scarps cutting the Palomas surface (Machette et al., 1998).

The Williamsburg and Mud Springs faults are clearly parts of the same fault zone, both normal faults, downthrown to the southwest, and together they form the northern boundary of the Palomas Basin across a distance of nearly 33 km (20 mi). From their studies of the Williamsburg scarp, Foley et al. (1998) and Machette (1987) determined that the Williamsburg fault had been active during the Holocene. They conclude that, because of the nearly continuous late Pleistocene or Holocene scarps, the Williamsburg–Mud Springs, northern Caballo, and Red Hills faults currently function as a single, through-going active fracture system that marks the northern and eastern edge of the Palomas Basin.

Cutter Sag accommodation zone

Bushnell (1953) named the Cutter Sag, and Kelley (1955) characterized it as a physiographic and structurally low embayment of the Jornada Basin located between the northern Caballo and southern Fra Cristobal Mountains. Mack and Seager (1995) interpreted the Cutter Sag to be an accommodation zone across which extensional strain was transferred from the Hot Springs fault of the northern Caballo uplift to the Walnut Canyon and Main Central faults of the Fra Cristobal uplift (Fig. 102). The two north-trending fault zones and uplifts overlap in a right en echelon pattern, the ramp-like accommodation zone occupying the space between them. Both the Hot Springs and Walnut Canyon–Main Central faults dip westward at moderate angles, and all transect sediments or lava flows in the Palomas Formation, indicating Quaternary movement.

The Cutter Sag accommodation zone is a northwesterly dipping ramp, surfaced by Cretaceous sedimentary rocks of the Crevasse Canyon and McRae Formations. The slope of the ramp is approximately 5°, but it is interrupted by a system of northeast-trending normal faults, most of which are downthrown to the northwest. Spaced 0.8–1.6 km (0.5–1.0 mi) apart, the faults dip at moderate angles, and most exhibit slickenside rakes of 80° or more. Among the few faults that have significant strike-slip components, both right-lateral and left-lateral motion are represented. All of the ramp faults have displacement of 150 m (492 ft) or less, and none extend beyond the boundaries of the ramp.

According to the classification of Faulds and Varga (1998), the Cutter Sag accommodation zone is a typical example of an overlapping, synthetic accommodation zone. However, the northeast-trending normal faults appear to be unusual compared to other similar accommodation zones. Mack and Seager (1995) suggested the faults may be the product of simple shear between the westward-moving hanging wall of the Walnut Canyon fault and the relative eastward movements of the footwall of the Hot Springs fault. Alternatively, the faults may be related to stretching of strata on the plunging northeastern flank of the Caballo uplift (Mack and Seager, 1995).

Another notable feature of the Cutter Sag accommodation zone is the seven basaltic cinder cones constructed on the ramp or on bordering faults. A series of basaltic lava flows, dated by the K–Ar method at 2.1 Ma (Bachman and Mehnert, 1978) have issued from the cones and moved down the ramp toward the adjoining Engle Basin. Basaltic volcanism appears to be controlled by fractured ramps in other accommodation zones in East Africa (Ebinger, 1989a, b) and southern New Mexico (Mack and Seager, 1995), and may be similarly controlled on the Cutter Sag accommodation zone.

Jornada Draw fault

The Jornada Draw fault is a major, through-going normal fault that crosses the southern part of the Jornada del Muerto and may be regarded as the eastern boundary of the Caballo uplift (Fig. 102). Named by Seager and Mack (1995) for Jornada Draw, an

ephemeral stream whose course across the Jornada del Muerto is controlled by the fault, it extends 64 km (40 mi) south-southeastward from the vicinity of Engle to south of Point of Rocks. Locally, the fault's position is also revealed by strings of small playa lakes, low scarps, or by small groups of bedrock hills, such as Prisor Hill and Upham Hills. Downthrown to the east, a single exposure of the fault at Aleman Draw indicates a dip of 60° east. Maximum stratigraphic separation of approximately 564 m (1,850 ft) was measured along the central part of the fault at Prisor Hill, where uppermost Love Ranch Formation and upper members of the Bell Top Formation are juxtaposed. From this area, stratigraphic separations apparently decrease both to the north and south. Like most of the outlying faults beyond the boundaries of the main Caballo uplift, the Jornada Draw fault formed relatively late in the evolution of the range.

Although the age of initiation of the Jornada Draw fault is not known precisely, it certainly pre-dates the cinder cone constructed on the fault near Cutter. A 2.1 Ma age for this cone is suggested by its similarity to other cones and flows in Cutter Sag, dated by Bachman and Mehnert (1978). Seager and Mack (1995) argued that the fault was probably initiated in latest Miocene or Pliocene time because the only synorogenic deposits that crop out or have been drilled on the hanging wall are the Pliocene–Pleistocene Palomas/Camp Rice Formations. The most recent movement displaced the La Mesa surface south of Point of Rocks approximately 400 ka ago, judging from the age of the offset surface (900–780 ka; Mack et al., 1993, 1998c) and the development of unfaulted stage III–IV calcic soils on the scarp (Seager and Mack, 1995). Near Engle, Quaternary movement along the northern part of the fault has offset the Cuchillo surface as well as the cinder cone near Cutter between 5 and 30 m (16 and 98 ft), but this activity has been dated no more closely than less than 780–900 ka, the age of the Cuchillo surface.

The Jornada Draw fault breaks the hinge region of the Jornada del Muerto syncline, a major downwarp created by the eastward tilting of the Caballo fault block and the westward-tilting of the San Andres fault block. Uplift and eastward tilting of the Caballo block commenced as early as late Oligocene or early Miocene time, continuing to the present. By Pliocene time, the structural relief between the Caballo uplift and Jornada del Muerto syncline had grown to approximately its present value, 3.3 km (2 mi). Seager and Mack (1995) suggested that initiation of the Jornada Draw fault near the hinge of the Jornada del Muerto syncline in Pliocene time may have been required to accommodate further differential movement between uplift and basin. They argued that the position, trend, length, and sense of movement of the Jornada Draw fault are consistent with this hypothesis.

Structural inversion

Parts of the Caballo, Hot Springs, Longbottom, and other late Tertiary faults follow and apparently are localized by pre-existing Laramide reverse faults. The normal slip on the late Tertiary faults is opposite to the thrust or reverse slip on the earlier faults, resulting in inversion of the older structures and unusual stratigraphic relationships along the faults.

From the Haystack syncline northward to Apache Canyon, the Caballo fault closely follows the axial-surface reverse fault in the McLeod Hills fault-propagation anticline. Both faults dip approximately 60° west, and it is likely that at depth the two faults are represented by a single fracture, although at the surface they are approximately 200 m (656 ft) apart. Movement on the reverse fault was west side up, whereas the Caballo fault is downthrown to the west, and that has led to structural inversion. The structurally highest part of the McLeod Hills fault-propagation anticline now forms the hanging wall of the Caballo fault. The inversion creates structural complexities along the fault, such as local zones of apparent zero or low stratigraphic separations, or even reversals in apparent sense of up or down movements.

A good example of apparent zero displacement is located 3 km (1.9 mi) southeast of Apache Canyon. Here, both hanging wall and footwall of the Caballo fault expose Precambrian rocks juxtaposed against the fault in spite of throw that probably exceeds 1.5 km (0.9 mi; Figs. 59; 106). The unusual relationship can be understood when it is realized that the Precambrian rocks in the hanging wall were originally in the structurally high core of the Laramide fault-propagation anticline, then dropped to their present position by movement on the Caballo fault. The inversion has nearly returned the Precambrian rocks to their pre-Laramide position; thus the juxtaposition of the Precambrian rocks across the fault approximates a "null" point in the inversion (Williams et al., 1989).

A second example of a Laramide reverse fault that became partly inverted by late Tertiary normal movement is the Longbottom fault. The fault trends east-west and dips steeply south. The inversion did not return the Paleozoic section in the hanging wall or footwall to the null position, so the fault remains strikingly reverse in its sense of displacement today. Evidence for inversion comes from slices of rock within the fault zone that are out of stratigraphic order. For example, near the western tip of the fault both hanging wall and footwall of the fault expose Precambrian granite, but a horse of El Paso limestone occupies the fault zone between them. The two faults bounding the horse dip southward, the southern one being reverse in geometry, the northern one, which dips 50°, being normal. An identical relationship is present along the fault where it crosses the range north of Timber Mountain. Abo beds within a fault slice are juxtaposed against Montoya strata to the south and Pennsylvanian strata to the north, a relationship that is impossible for a fault that has undergone wholly reverse or normal movements. Structural inversion of an original reverse fault by later normal movement can easily result in the observed relationships as illustrated in Figure 107.

A third, particularly instructive example of structural inversion is located in the footwall of the Caballo fault 1.6–2 km (1–1.2 mi) southeast of Apache Canyon. At this locality, the overturned syncline at the eastern margin of the McLeod Hills fold belt trends east-west and is truncated by the Caballo fault (Fig. 108). At highest exposed levels of the syncline, in Bar B and upper Nakaye strata, the south-dipping axial surface is unbroken, but a reverse fault develops lower in the Nakaye along the axial surface, extending downward into the Percha Shale. Below the Percha, however, the fault becomes normal, separating overturned Fusselman and Pennsylvanian strata in the hanging wall from right-side-up Fusselman and older formations in the footwall. At one point, a horse of out-of-stratigraphic-order Nakaye limestone is enclosed by south-dipping faults; the limestone is juxtaposed against Percha Shale in the southern hanging wall and against Fusselman Dolomite in the northern footwall (Fig. 108). The southern fault is reverse, the northern is normal. Like the Longbottom fault, two periods of movement are required to produce such an extraordinary, but diagnostic relationship. Laramide reverse faulting along the axial surface of the overturned syncline was followed by normal movement along the same fault, resulting in negative structural inversion. A null point between reverse movement in upper parts of the axial surface and normal movement in lower parts is present within the Percha Shale where stratigraphic separation apparently becomes zero. Inversion on this fault may have accompanied synthetic, late Tertiary movement along the Caballo fault.

A fourth example is controversial. Two kilometers (1.2 mi) southeast of Truth or Consequences, Precambrian rocks in the hanging wall of the Hot Springs fault are juxtaposed with steeply dipping Paleozoic stata in the footwall. At this point the Hot Springs fault is reverse, contradictory to numerous stratigraphic relationships elsewhere, which confirm normal movement (Kelley and Silver, 1952; Mason, 1976). Interpretations to

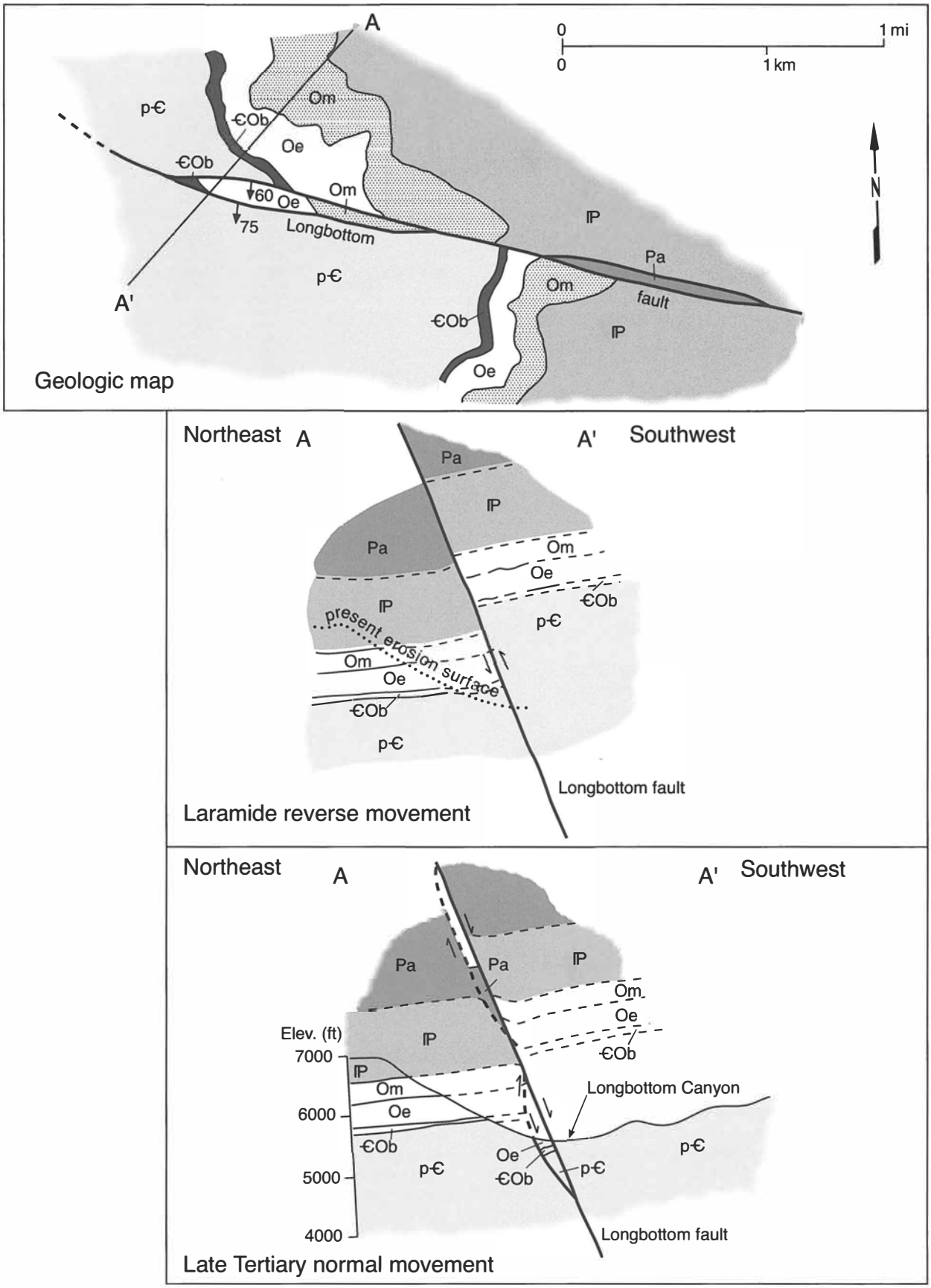

FIGURE 107—Geologic map of Longbottom fault with sections showing evolution of the fault. Laramide reverse movement is followed by late Tertiary normal movement, resulting in inversion of the structure. **p-€** = Precambrian rocks; **€Ob** = Bliss Formation; **Oe** = El Paso Formation; **Om** = Montoya Formation; **IP** = Pennsylvanian rocks; **Pa** = Abo Formation.

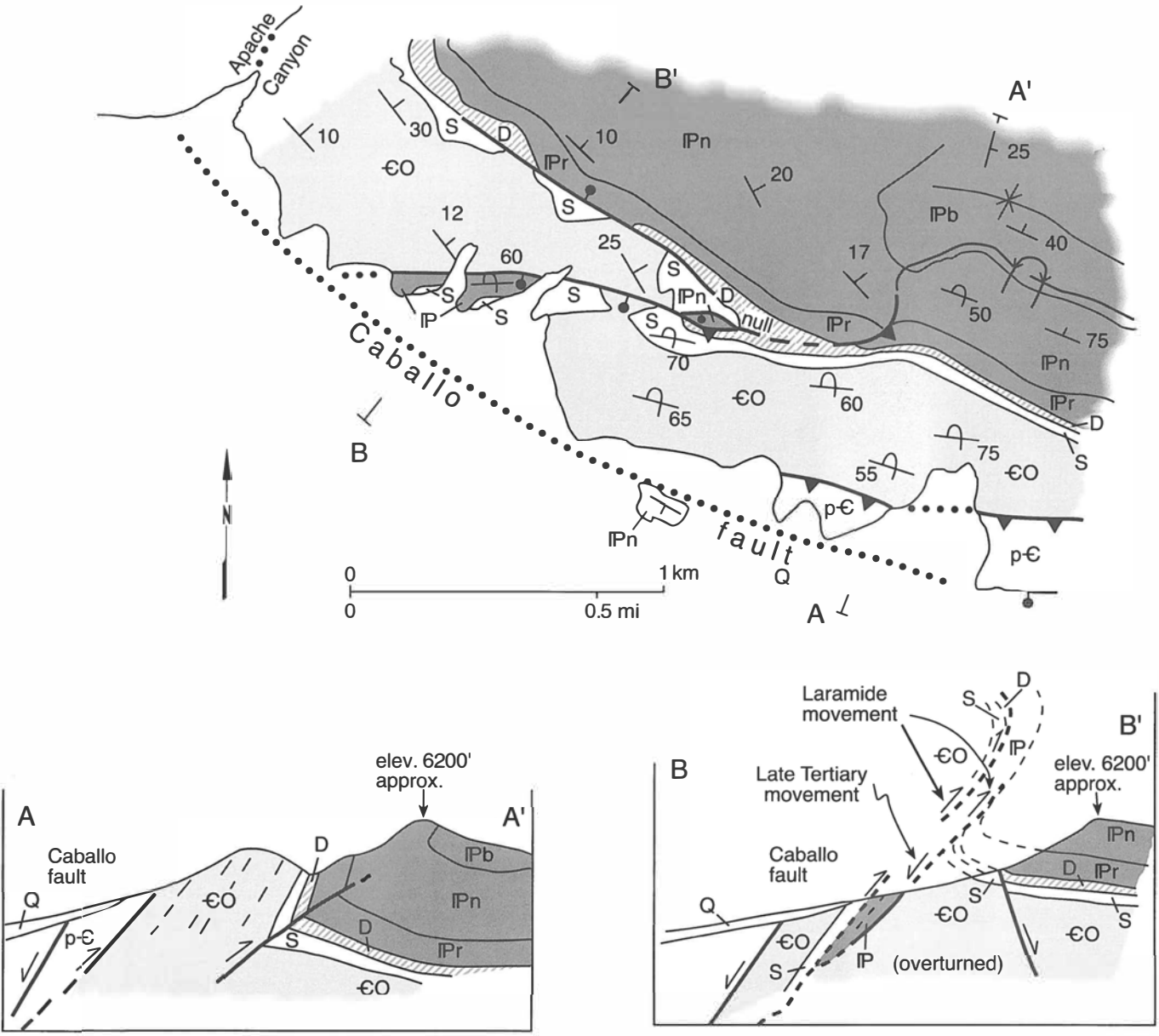

FIGURE 108—Simplified geologic map and cross sections of a negatively inverted reverse fault south of Apache Canyon. The reverse fault followed the axial surface of an overturned syncline during its Laramide origin, but underwent normal movement later, probably as a synthetic splay off the Caballo fault. Note local elimination of the Percha Shale in the overturned limb, probably a result of flexural-slip reverse faulting. **p-€**= Precambrian rocks; **-€O** = Bliss Sandstone and El Paso Formation; **D** = Percha Shale; **S** = Fusselman Dolomite; **PPr** = Red House Formation; **PPn** = Nakaye Formation; **PPb** = Bar B Formation; **PP** = Pennsylvanian rocks undifferentiated; **Q** = Quaternary rocks undifferentiated.

explain the anomalous relationships include strike-slip faulting and structural inversion.

Several authors have indicated that a component of strike slip may distinguish the Hot Springs fault. Kelley and Silver (1952) interpreted sinistral movement based on drag of bedding near Mescal Canyon. Thompson (1955) favored left-lateral slip for the fault in the Caballo Mountains but favored right-lateral slip near the Fra Cristobal Range. Bushnell (1953) also cited possible left slip, and Lozinsky (1986) indicated 460 m (1,509 ft) of right slip. None of these authors advocated large amounts of strike slip of either Laramide or Tertiary age, but all seemed to agree that late Tertiary movement involved oblique slip. In contrast, Harrison and Chapin (1990), Cather and Harrison (2002), and Harrison and Cather (in press) argue that the Hot Springs fault originated during the Laramide as a dextral strike-slip fault with 26 km (16.1 mi) offset. Evidence cited by these authors to support the hypothesis includes the following: slivers of pre-Cenozoic rock in the fault zone; offset of pinchouts of Percha Shale beneath the basal Pennsylvanian unconformity in the central Caballo Mountains and Mud Springs Mountains; offset and change in trend of folds between the northern Caballo and Mud Springs Mountains; offset of regional isopachs of lower Paleozoic rock units; pattern of folds on the east flank of the Caballo Mountains, interpreted to be second order en echelon folds associated with wrench faulting; and aeromagnetic and gravity data (Kucks et al., 2001) used to document offset Laramide structures and to extend the Hot Springs fault as a Laramide wrench fault southward to near the Mexican border. Collectively, the interpretation of this data would support Chapin and Cather's (1981) ideas of a dextral wrench fault zone along the eastern margin of the Colorado Plateau and that the Cutter Sag is a wrench basin.

Mason (1976) and we favor structural inversion rather than

strike slip along the Hot Springs fault to explain hanging-wall/footwall relationships near Truth or Consequences. We suggest that east-facing monoclinal flexures in the footwall of the Hot Springs fault were originally continuous with northeast-facing flexures in the Mud Springs Mountains, creating a northward convex, Precambrian-cored uplift not unlike the northern part of the Laramide structural bench bordered by the arcuate McLeod Hills fold belt farther south. Kelley and Silver's (1952) figure 23 shows the essential map geometry of this uplift. Precambrian rocks were structurally high in the uplift and may have been thrust up against the eastern limb along a west-dipping reverse fault. Subsequent movement on the Hot Springs fault utilized the west-dipping reverse fault along part of its course, dropping the Precambrian core downward to the west against the uplift's eastern limb, but not all the way to the null point. Thus, Precambrian rocks are downthrown against Paleozoic rocks along this part of the Hot Springs fault, a product of structural inversion rather than strike-slip faulting.

Evidence cited by Harrison and Chapin (1990), Cather and Harrison (2002), and Harrison and Cather (in press) to support 26 km (16.1 mi) of strike slip along the Hot Springs fault may be interpreted in other ways. As noted above, northwest and northerly trending structures in the northern Caballo and Mud Springs Mountains, rather than being juxtaposed by strike-slip faulting, may have been originally continuous, marking the boundary of an uplift whose Precambrian core lies beneath and south of Truth or Consequences. Because oblique folds are consistently northeast vergent, northeast-directed shortening rather than a north-south shear couple seems to us to be more consistent with their geometry. Also, these folds function as structural steps, dropping the Phanerozoic section down into the Love Ranch Basin. Slivers of pre-Cenozoic rocks in a fault zone are common in all types of fault zones, and we have already described how out-of-sequence rocks in fault slivers, such as those near Truth or Consequences, are an expectable consequence of structural inversion. Offset of outcrops of the Percha Shale may also be unrelated to strike-slip faulting.

Pennsylvanian subcrop patterns in the southern Caballo Mountains demonstrate that Late Mississippian or Early Pennsylvanian erosional truncation of older strata was irregular, governed, at least locally, by the pattern of tilted or gently folded beds (Fig. 17). Strata as old as Ordovician were exposed in the cores of uplifts, whereas Fusselman, Percha, and Lake Valley beds cropped out on the flanks only a few kilometers away. The presence of Percha Shale in the Mud Springs Mountains, 26 km (16.1 mi) north of a pinchout in the central Caballo Mountains, may be as easily ascribed to such irregular erosional truncation of broadly deformed Mississippian and older strata as to strike-slip faulting. Furthermore, palinspastic restoration of 26 km (16.1 mi) of dextral strike slip parallel to the Hot Springs fault would likely result in a stratigraphic mismatch across the fault. The sequence of Pennsylvanian/Percha/Montoya in the Mud Springs Mountains (Kelley and Silver, 1952; Maxwell and Oakman, 1990) would likely be juxtaposed with the Pennsylvanian/El Paso sequence that is exposed along the western flank of the Red Hills (Fig. 17), not with the Pennsylvanian/Percha/Fusselman sequence exposed at the Percha pinchout near Burbank Canyon. We note also that the Fusselman is missing beneath the Percha in the Mud Springs Mountains, another potential mismatch.

We also believe that, except for large middle Tertiary batholiths, patterns of gravity highs and lows in the southern Rio Grande rift almost exclusively reflect the distribution of late Tertiary basins and uplifts, not Laramide structure. Laramide structures, overprinted by the large, late Tertiary structures are very effectively obscured. While we disagree that the Hot Springs fault has a Laramide history of significant strike slip, we do acknowledge that, at least locally, the course of the Hot Springs fault is controlled by Laramide reverse faults, and that a small component of left or right slip may distinguish late Tertiary movement.

We conclude that the position of segments of the late Tertiary Caballo, Hot Springs, Longbottom, and other normal faults were controlled by pre-existing reverse faults in the cores of Laramide fault-propagation folds. Movement on the late Tertiary faults inverted Laramide structures by various amounts, creating a variety of structural complexities along the faults, including apparent zero stratigraphic separations, apparent reverse movement on normal faults, and fault slices of young rock that are enclosed by older rock on both hanging-wall and footwall sides. Such complexities encountered elsewhere, where Laramide structures are overprinted by late Tertiary extensional structures, may constitute evidence that structural inversion has occurred.

Extensional folds and their kinematic evolution

Two broad categories of folds associated with extensional fault blocks are recognized (Schlische, 1995). Longitudinal folds are parallel to the associated normal fault, commonly forming as a result of the propagation of a fault tip into a monoclinal flexure. Such folds have been referred to as forced folds by Withjack et al. (1990), fault-propagation folds by Mitra (1993), or drape folds by Stearns (1978) and Harding (1984). Transverse folds are also a result of displacement on normal faults, but they trend at right angles to the fault surface, although they may be elongated parallel to it. Transverse folds owe their shape to changes in the amount of slip on a fault along its length, from zero near the tips to a maximum near the central part, as well as to decreasing slip at right angles to the fault surface (Schlische, 1995). Thus transverse folds present a broad half-dome geometry in footwall uplifts and a half-basin shape in hanging-wall blocks. Of course, both transverse and longitudinal folds may be developed on a single fault block, creating a roughly domal structure that may be modified on one flank by normal faulting. In the Caballo Mountains, examples of all these extensional fold styles are present.

The Red Hills fault block is an excellent example of a transverse half dome that is elongated parallel to the Red Hills fault. Along-strike changes in fault displacement are responsible for the half-dome shape of the uplift. The structurally highest part of the uplift corresponds to the approximate midpoint of the Red Hills fault as well as to the region of maximum displacement. From this point, displacement decreases in both directions toward the fault tips, accompanied by younger footwall rocks intersecting the fault surface. In longitudinal profile, the arched structure of the fault block reflects the changing displacement on the Red Hills fault, and the eastward plunge of the structure corresponds to a decrease in slip perpendicular to the fault.

A longitudinal fold may once have existed adjacent to the Red Hills fault, the western limb of which has largely been removed by erosion. Westward-dipping strata are still present along the southern margin of the Red Hills half dome. Broken by antithetic faults and truncated by the Red Hills fault, these west-dipping strata, more than 1 km (0.6 mi) wide, may represent a drape fold that formed at the upper propagating tip of the Red Hills fault. If so, the Red Hills uplift would originally have been dome-shaped, a product of both transverse and longitudinal folding, and would have duplicated the geometry of both the Red House and Flat Top domes.

Both the Red House and Flat Top uplifts are elongated domal uplifts bordered on the west and southwest flanks by normal faults. They are seemingly excellent examples of extensional fault blocks in which transverse as well as longitudinal folding shaped the geometry of the uplift. Transverse folding on the Red House uplift was controlled by systematic changes in displacement on the Red House–Badger and Palm faults, from zero near the tip of the Badger fault to a maximum at the Red House–Palm fault junction to gradually diminishing values southeastward

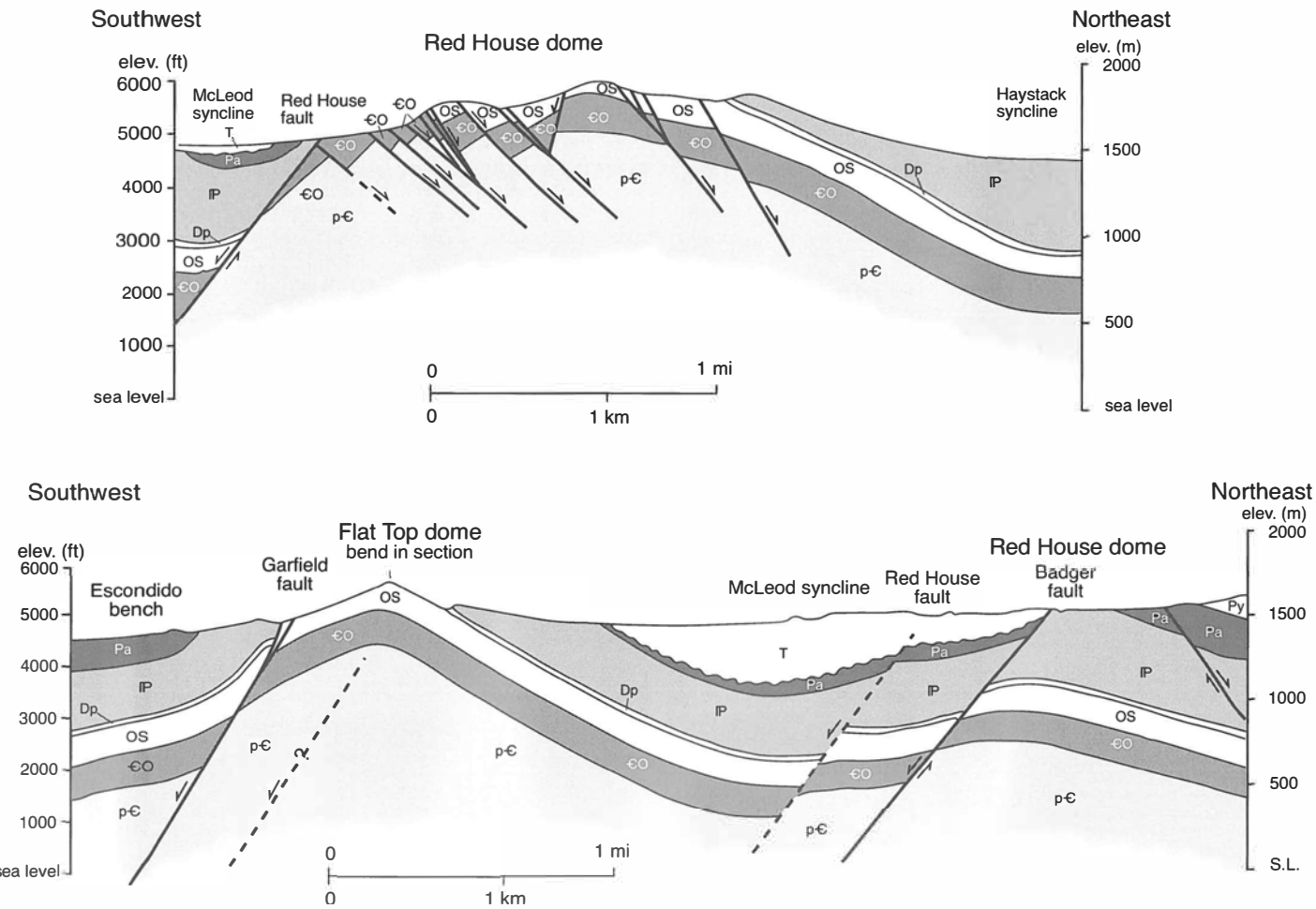

FIGURE 109—Cross sections through Red House and Flat Top domal uplifts and McLeod syncline. **p€**= Precambrian rocks; **€O** = Bliss Sandstone and El Paso Formation; **OS** = Montoya Formation and Fusselman Dolomite; **Dp** = Percha Shale; **IP** = Pennsylvanian rocks; **Pa** = Abo Formation; **Py** = Yeso Formation; **T** = Tertiary rocks.

along the Palm fault. The eastward plunge of the Red House dome reflects decreasing slip with distance from the fault. The longitudinal fold hinge approximately parallels the boundary faults, with the doubly plunging hinges again reflecting decreasing fault displacement toward the north and southeast. The western limb of the dome is broken by numerous east-dipping antithetic faults and is truncated by the Badger–Red House and Palm border faults (Fig. 109). The western limb of the longitudinal fold may record an early stage of forced drape folding of the sedimentary cover above an upward-propagating incipient range-boundary fault, as Figure 110 illustrates. Antithetic faults developed in the draped limb as it steepened. These seemingly represent fine natural examples of similar faults developed in model experiments (Schlische, et al., 2002). Eventually the Palm and Red House–Badger faults propagated through the sedimentary cover, truncating antithetic faults as well as bedding in the western limb of the dome. At this point the block may have isostatically rebounded somewhat, tilting it eastward, but the footwall longitudinal anticline and hanging-wall syncline (McLeod syncline) remain as testimony to the kinematic evolution of the fault block. Although the Flat Top anticline is smaller and antithetic faults are absent from the longitudinal fold, it is nearly identical in geometry to the Red House dome, and also probably in its kinematic evolution.

In summary, folds of extensional origin are an important aspect of the late Tertiary structure of the Caballo Mountains. They formed at the same time as, or just before, normal faulting. Some folds were broken into footwall anticlines and hanging-wall synclines by the propagating faults that formed them initially. The Caballo Mountain structures are particularly good examples of footwall anticlines, including transverse and longitudinal types as well as a combination of both. Well known in the subsurface because of their importance as oil traps in the North Sea, Libya, and the Gulf of Suez (Harding, 1984; Withjack et al., 1990; Robson, 1971), the Caballo blocks offer fine examples of outcropping analogues. Details of the structures, such as the array of closely spaced antithetic faults on the western limb of Red House Mountain, whose subsurface analogs may not be imaged by seismic techniques or understood by drilling, may be observed in these outcrops. Besides providing insight into the kinematic evolution of the Red House dome, such details can reveal the complexity that extensional folds in the subsurface may display.

Summary of Neogene tectonic evolution of the Caballo Mountains

Based on the trend of Uvas Basaltic Andesite dikes (Fig. 102), a north-northeast–south-southwest directed extensional stress field was established in the Caballo Mountains area by late Oligocene time, 27–28 Ma. The direction of late Oligocene extension was roughly parallel to the direction of contraction during the Laramide orogeny; thus, Laramide contractional structures and upper Oligocene dikes share the same northwesterly trend.

It is not clear whether the extension led to the formation of broad basins or fault-bounded structures during deposition of

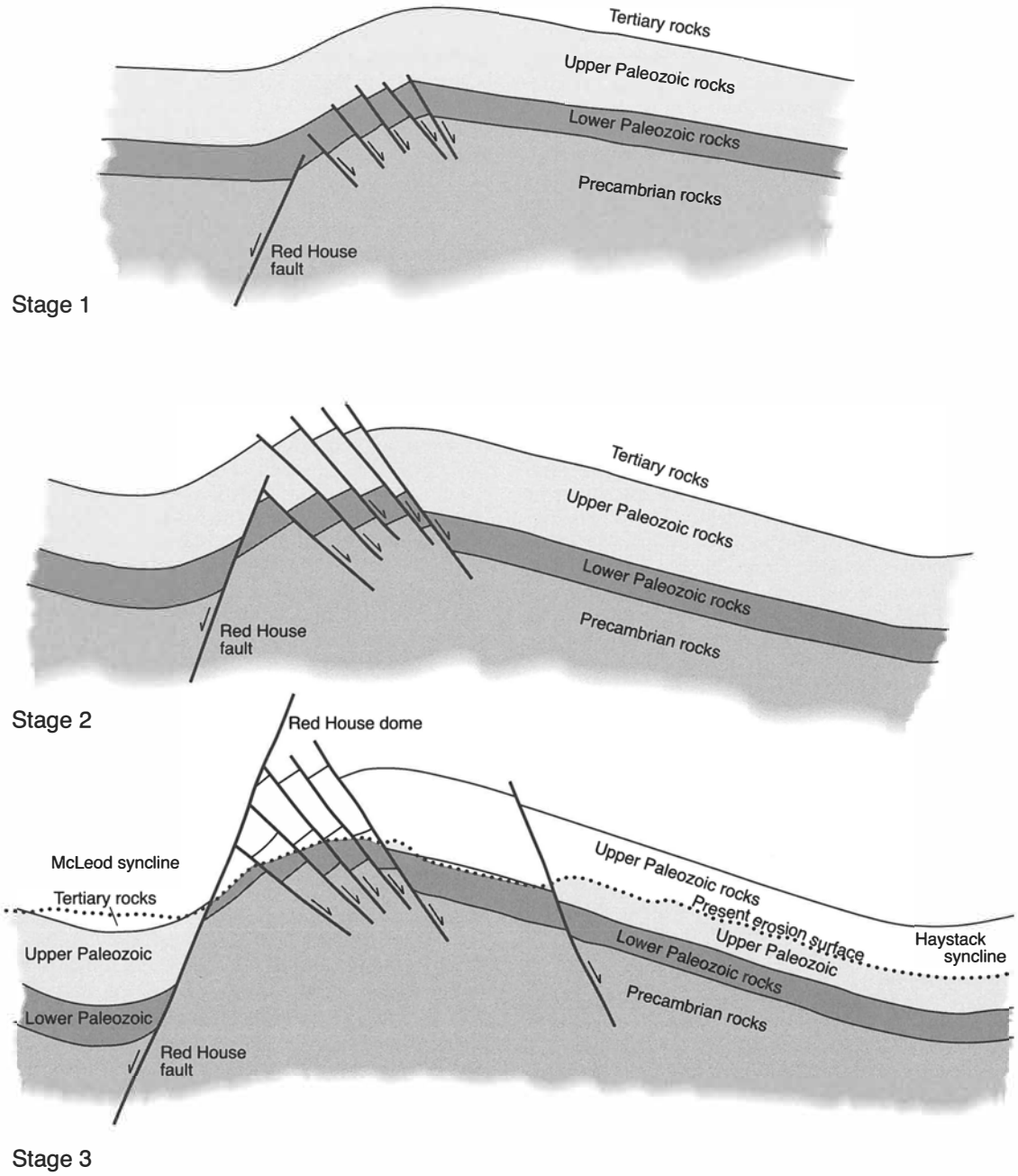

FIGURE 110—Diagrammatic cross sections illustrating evolution of dome-shaped, extensional fault-block uplifts in the southern Caballo Mountains. Stage 1—Draping of sedimentary cover over an upward-propagating basement fault. Stage 2—Boundary fault of uplift propagates into sedimentary cover; antithetic faults are well developed. Stage 3—Boundary fault propagates to surface, truncating antithetic faults and the drape fold and thereby creating a footwall anticline and hanging-wall syncline; isostatic uplift and tilting of the fault block may accompany this stage.

the Thurman Formation. Although the Thurman is locally more than 500 m (1,640 ft) thick, its fine-grained lithofacies provide little evidence that it accumulated in a fault-bounded basin, although the clastic dikes that cut the formation invite speculation that they were triggered by earthquakes. If an incipient Caballo uplift had formed, there was insufficient relief to supply coarse detritus to the basin.

Strong uplift of the southern Caballo–Red House fault blocks began in latest Oligocene or early Miocene time when the Caballo–Red House–Palm fault system was initiated, as documented by alluvial fan deposits of the Hayner Ranch Formation. These uplifts trend northwesterly, approximately normal to the direction of late Oligocene extension, and may be viewed as a product of the same north-northeast–south-southwest extension that began earlier in the Oligocene. However, the uplifts are also approximately parallel to Laramide reverse faults and fault-propagation folds, and the position of part of the southern Caballo fault was controlled by a pre-existing reverse fault. Apparently, the northwesterly trends of the southern Caballo and Red House faults were established through a combination of Laramide structural control and a regional north-northeast–south-southwest extensional stress field.

The Hayner Ranch Basin (Mack et al, 1994b) consisted of two sub-basins, an ancestral Hatch–Rincon Basin and an ancestral Palomas Basin, both half grabens, whose hanging-wall dip slopes were an ancestral Sierra de las Uvas uplift and the Black

Range, respectively. Subsidence of the two basins and uplift of the southern Caballo–Red House footwall blocks continued through the late Miocene, recorded by the Hayner Ranch Formation as well as by the Rincon Valley Formation. Changing clast composition in both the Hayner Ranch and Rincon Valley basin-fill deposits document erosion of the Caballo–Red House uplifts from Tertiary volcanic rocks down into Paleozoic carbonates. Judging from the presence of playa and lacustrine strata and lack of fluvial deposits in the Hayner Ranch and Rincon Valley Formations, the ancestral Palomas and Hatch–Rincon basins had only interior drainage.

According to Kelley and Chapin (1997), fission-track cooling ages indicate extensive uplift of Precambrian rocks 11–16 m.y. ago in the central part of the range and approximately 5 m.y. ago in the northern part. These data are consistent with substantial uplift of Precambrian rocks in the Caballo Mountains, although provenance data from the Rincon Valley and Camp Rice Formations indicate that the basement was not exposed until latest Miocene or early Pliocene time.

In latest Miocene or early Pliocene time, both the ancestral Hatch–Rincon and Palomas Basins were greatly modified as faulting stepped basinward from both the footwall and hanging-wall uplifts. The ancestral Hatch–Rincon Basin was dramatically narrowed as the Derry, Garfield, Foothills, Black Hills, and Rincon Hills faults broke the northern flank of the basin into a series of fault blocks and structural benches, while other faults along the northern margin of the Sierra de las Uvas broke the hanging-wall dip slope. The new faulting converted the Hatch–Rincon Basin from a half graben to a full graben. Faulting also stepped westward into the ancestral Palomas Basin to form the Red Hills, Nakaye, Derry, and perhaps the Mud Springs uplifts, as well as Apache graben. Older Hayner Ranch and Rincon Valley basin-fill deposits were uplifted and eroded away, except for the important sections preserved in White graben. The western flank of the Palomas Basin was modified by the rise of the Animas Mountains through Miocene hanging-wall fans derived from the Black Range. On the eastern side of the Caballo uplift, the through-going Jornada Draw fault was initiated, apparently to help accommodate the growing structural relief between the uplifted Caballo block and the downwarped Jornada del Muerto syncline.

The late Miocene to early Pliocene faulting narrowed the ancestral Palomas Basin by as much as 25 km (16 mi), shaped the modern outline of both uplifts and basins, and prepared the structural control for the Rio Grande which began to cross the basin early in the Pliocene. Furthermore, older faults such as the southern Caballo, Red House, and Palm faults apparently became inactive as faulting stepped basinward. Today, the active, through-going boundary fault of the Caballo uplift and Palomas Basin is composed of three different fault segments, the Red Hills, northern Caballo, and Williamsburg–Mud Springs faults. Holocene movement is documented for two of these, with all three likely to be active (Machette, 1987; Foley et al., 1988). The Palomas and Camp Rice Formations, as well as younger alluvium, are the sedimentary record of the uplift and erosion of the Caballo Mountains, evolution of the Rio Grande, and earthquake history of major Caballo faults for the last 4.5 Ma. In the following section, this summary is incorporated into a more regional account of the evolution of the southern Rio Grande rift.

Evolution of the Rio Grande rift in the Caballo Mountains and vicinity

The Rio Grande rift is a relatively narrow, < 100 km (< 62 mi), zone of middle and late Tertiary and Quaternary crustal extension traceable for approximately 1,100 km (682 mi) from central Colorado to south of El Paso, Texas (Olsen et al., 1987). Throughout its length the rift is characterized by thin continental crust, normal fault-block topography, high regional elevation, > 1,200 m (3,937 ft), high heat flow, and bimodal volcanism (Morgan et al., 1986). In southern New Mexico, the Rio Grande rift is bordered on the east by the Great Plains and merges westward with the Basin and Range, the latter boundary being placed near Deming, New Mexico, based on thinner continental crust beneath the Rio Grande rift and less evidence of Quaternary faulting in the Basin and Range (Woodward et al., 1978; Sinno et al., 1986).

The history of the Rio Grande rift is traditionally divided into two stages: an early stage that began in the latest Eocene and continued through most of the Miocene, and a later stage that began in latest Miocene or Pliocene and continues to the present day (Seager, 1975; Chapin and Seager, 1975). Chapin and Cather (1994) and Cather (1994) have modified that view somewhat by making the case in the middle and northern rift for rapid middle to late Miocene extension, preceeded and followed by slow extension. In the southern part of the rift, Mack et al. (1994a, b) have shown that a two-stage model for the southern Rio Grande rift is perhaps too simple, and that nearly continuous deformation from latest Eocene to Holocene was characterized by different fault blocks rising at different times. Indeed, in the southern Rio Grande rift, it is more instructive to consider three stages of development, based on a combination of normal faulting, basin development, and volcanism: (1) latest Eocene and Oligocene: bimodal rhyolite and basalt/basaltic andesite volcanism and minor block faulting and basin development; (2) latest Oligocene to latest Miocene: major block faulting and basin development and little volcanism; and (3) latest Miocene or Pliocene to recent: renewed or continued block faulting, basin development, and basalt volcanism. The results of these three stages are clearly evident in the Caballo Mountains and vicinity and are discussed below.

Latest Eocene and Oligocene bimodal volcanism and minor block faulting and basin subsidence

The latest Eocene and Oligocene epochs in southern New Mexico were dominated by bimodal volcanism. Explosive eruptions from calderas resulted in thick intra-cauldron fill and thinner outflow sheets of rhyolitic ash-flow tuffs. The main cauldrons in the vicinity of the Caballo Mountains were the Organ, Doña Ana, Emory, Nogal Canyon, and Mt. Withington cauldrons, which had major eruptions between 36.2 and 27.4 Ma (Fig. 111; Elston et al., 1975; Seager et al., 1976; Seager, 1981; McIntosh et al., 1991). At about the same time as eruption of the Organ and Doña Ana cauldrons, flow-banded rhyolite domes, dated at 35.4 Ma, were emplaced along the north-trending Cedar Hills vent zone (Seager and Clemons, 1975; Mack et al., 1998b). Also erupting at this time were thin basalt lava flows of the Bell Top Formation, as well as a major outpouring of basaltic andesite at around 27–28 Ma, corresponding to the Uvas Basaltic Andesite (Clemons, 1975). McMillan (1998) argued that the basalts and basaltic andesites of the Bell Top and Uvas Formations were derived by partial melting of the lithosphere induced by extension. The mafic melts locally caused partial melting of the crust, resulting in the voluminous rhyolitic eruptions. McMillan's model implies that regional extension in the southern Rio Grande rift began as early as 36.2 Ma, corresponding to the oldest dated ash-flow tuffs of the Organ Mountains cauldron. Cather (1990) arrived at a similar date for the onset of regional extension from his studies in the northern Datil–Mogollon volcanic field.

The earliest evidence of extensional uplift and complementary basin subsidence is shortly after 34.9 Ma, when the Goodsight–Cedar Hills depression developed. Mack et al. (1994a) interpreted the depression to be an east-tilted half graben, whose footwall consisted primarily of uplifted rhyolite domes of the Cedar Hills vent zone, and whose hanging wall was the ancestral Goodsight Mountains and its northward exten-

half graben, bordered on the north by the Caballo, Red House, and Palm faults, and on the south by a northeast-tilted hanging wall (Fig. 114). Footwall-derived and hanging-wall-derived alluvial fans and alluvial flats are easily distinguished by the distribution of facies, paleocurrents, and provenance (Mack et al., 1994b). The laterally restricted, footwall-derived, alluvial-fan conglomerates display southwest-directed paleocurrents and have a composition consistent with unroofing of the Uvas Basaltic Andesite and Bell Top, Palm Park, and Love Ranch Formations on the Caballo Mountains block. This relationship, plus a maximum thickness of 457 m (1,499 ft) of the Hayner Ranch Formation adjacent to the Caballo Mountains block, indicates approximately 1,615 m (5,298 ft) of stratigraphic separation along the Caballo–Red House Mountain–Palm fault system by the end of Hayner Ranch deposition. The footwall-derived alluvial fans graded basinward into an alluvial flat and small carbonate-precipitating lakes (Fig. 114; Mack et al., 1994b).

Hanging-wall-derived sediment of the Hayner Ranch Formation is exposed in the Sierra de las Uvas, Selden Hills, and at San Diego Mountain. The sediment is characterized by northeastward fining and northeast-directed paleocurrents, and consists of clasts of the Uvas Basaltic Andesite, Palm Park Formation, and flow-banded rhyolite (Mack et al., 1994b). The paleocanyon and its Hayner Ranch fill exposed in the northern Sierra de las Uvas appear to have been positioned along the northern edge of the hanging-wall source terrane.

The Caballo fault block continued to rise during middle and late Miocene time, corresponding to deposition of the Rincon Valley Formation (Fig. 115; Mack et al., 1994b). The addition of first-cycle Pennsylvanian and Permian clasts to the areally restricted, footwall-derived, alluvial-fan detritus of the Rincon Valley Formation, plus a maximum thickness of 610 m (2,001 ft), indicates an additional 854 m (2,801 ft) of stratigraphic separation on the border fault system of the Caballo Mountains block (Mack et al., 1994b). Moreover, Rincon Valley conglomerates near Hillsboro were derived from the Black Range hanging wall of an ancestral Palomas Basin, as indicated by eastward fining and eastward-directed paleocurrents. There is no evidence in the Rincon Valley Formation that the Animas fault block was active at this time.

A southern half graben also developed during deposition of the Rincon Valley Formation (Fig. 115; Mack et al., 1994b). This north-trending basin had as its footwall the Sierra de las Uvas and as its hanging wall the Doña Ana Mountains and Cedar Hills vent zone. The area between the two basins was occupied by a large alluvial flat and gypsum-precipitating playa lake. Although the northernmost outcrop of the playa lake facies is at the mouth of Berrenda Creek in the Garfield quadrangle, the lake probably extended northward into the present position of the Palomas Basin.

Finally, the 9.6 Ma Selden basalt erupted locally in the southern half graben during deposition of the Rincon Valley Formation (Seager et al., 1975, 1984). The Selden basalt heralded renewed volcanism in the southern rift, as well as the change from a lithospheric to an asthenospheric mantle source. According to McMillan (1998), enough crustal extension had taken place by the end of the Miocene to allow the asthenosphere to rise beneath the southern rift and experience decompression melting.

Latest Miocene to recent block faulting and volcanism

A major pulse of crustal extension began after deposition of the Rincon Valley Formation, in the latest Miocene or early Pliocene epochs. The major results of this extensional pulse were: normal faulting that dismembered previous basins, interconnected drainage in many of the new basins that resulted from the arrival of the ancestral Rio Grande, and renewal of basalt volcanism throughout the region.

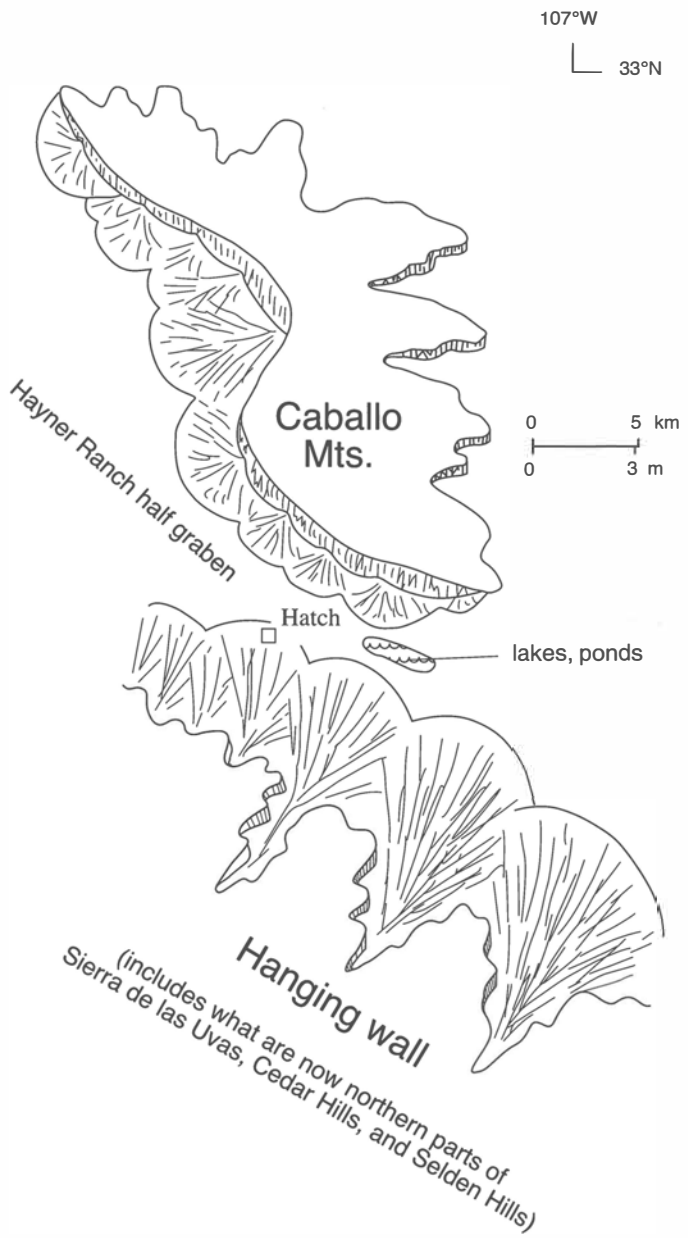

FIGURE 114—Paleogeography in the vicinity of the Caballo Mountains during latest Oligocene and early Miocene time, corresponding to deposition of the Hayner Ranch Formation. Adapted from Mack et al. (1994b).

During the most recent phase of crustal extension, activity continued on some previously initiated faults, such as the northern Caballo fault, the Ward Tank fault, and the Goodsight Mountains fault (Fig. 116). In addition, some faults appear to have grown laterally at this time, such as the Jornada fault, which ultimately linked the Doña Ana Mountains, San Diego Mountain, and the Rincon Hills (Mack et al., 1994c). However, most of the strain was transferred to new faults and fault blocks that occupied former Miocene basins, among them the Red Hills fault, the Jornada Draw fault, the East and West Robledo faults, the Cedar Hills fault, the Selden Hills fault, the Uvas fault, and faults associated with the Derry Hills and the adjacent region to the southeast (Fig. 116). The net effect was to create more but narrower basins compared to Oligocene and Miocene time and to produce the modern distribution of uplifts and basins.

During Pliocene and early Pleistocene time (5–0.78 Ma), the basins in the southern Rio Grande rift infilled with sediment of the Camp Rice and Palomas Formations. A notable arrival into

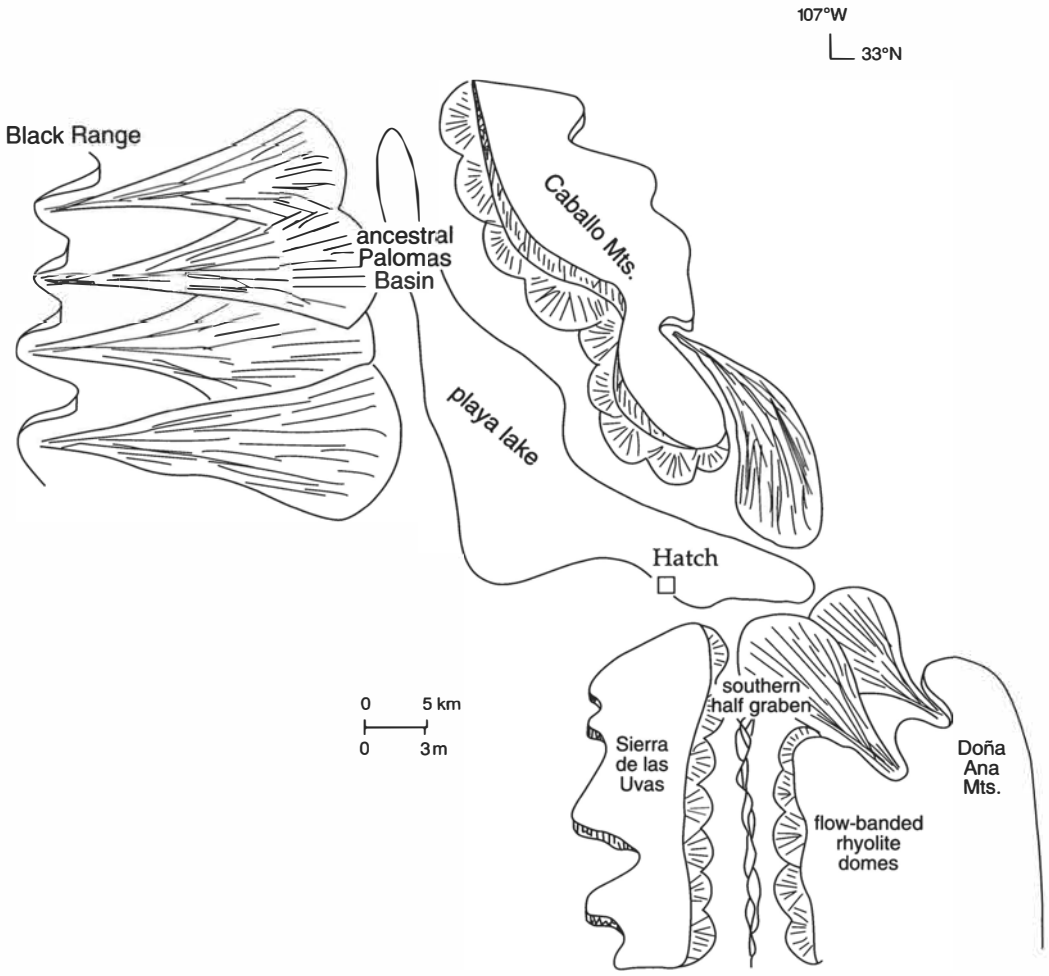

FIGURE 115—Paleogeography in the vicinity of the Caballo Mountains during late Miocene time, corresponding to deposition of the Rincon Valley Formation. Adapted from Mack et al. (1994b).

southern New Mexico at about 5 Ma was the ancestral Rio Grande, which periodically occupied six contiguous basins, the Palomas, Hatch–Rincon, Jornada del Muerto, Corralitos, Mesilla, and Tularosa/Hueco Basins (Fig. 117). The position of the river within a basin was controlled by basin symmetry (Mack and Seager, 1990), and the movement of the river to and from adjacent basins was controlled by faulting or deposition of basin-fill strata to the level of a topographic gap and consequent spillover into an adjacent basin (Mack et al., 1997). In the vicinity of the Caballo Mountains during this time, eruption of small amounts of basaltic lava from cinder cones was restricted to the margins of the Palomas Basin, to the Cutter Sag accommodation zone, and to the Jornada Draw fault (Seager et al., 1984; Mack and Seager, 1995). Several of the lava flows exposed east of Elephant Butte Reservoir probably flowed far enough to the west to temporarily dam or divert the ancestral Rio Grande.

Deposition of the Camp Rice and Palomas Formations ended approximately 0.78 Ma, when the ancestral Rio Grande and its tributaries began to alternately incise and backfill the basins. This process may have been initiated by and was probably subsequently driven by paleoclimatic changes related to northern hemisphere glaciations (cf. Gile et al., 1981). The paleoclimatically driven cycles of erosion and backfilling dominated the Palomas Basin during mid to late Pleistocene and Holocene, despite the fact that there was about 30 m (98 ft) of post-0.78 Ma movement on the Caballo fault, as indicated by offset of the Cuchillo surface. Apparently, paleoclimatic fluctuation has been a more important control on sedimentation than fault movement and basin subsidence during the last 0.78 Ma.

Plate-tectonic models for the Rio Grande rift

There is no consensus on the plate-tectonic origin or origins of the Rio Grande rift, although several different models have been proposed. The models generally fall into three categories: (1) those associated with subduction of the Farallon plate; (2) those related to crustal relaxation following Sevier and Laramide compression; and (3) those associated with the onset of transform motion between the North American and Pacific plates. Each of the models is described briefly below, but it is beyond the scope of this report to evaluate their relative merits. However, the excellent stratigraphic and structural record of the Rio Grande rift in the Caballo Mountains and vicinity should play an important role in any future attempt to test the plate-tectonic models.

A popular early model for the origin of latest Eocene, Oligocene, and Miocene extension and volcanism in the Rio Grande rift calls on back-arc extension related to the steepening of the Farallon plate following low-angle subduction during the Laramide orogeny (Coney and Reynolds, 1977; Lipman, 1980; Dickinson, 1981; Eaton, 1984). As the slab steepened, mantle flowed into the space formerly occupied by the subducting slab, triggering crustal extension and volcanism. However, Engebretson et al. (1984) and Elston (1984) argue that during mid-Tertiary time, the young, hot, buoyant Farallon plate should have continued to subduct at a very low angle or ceased sub-

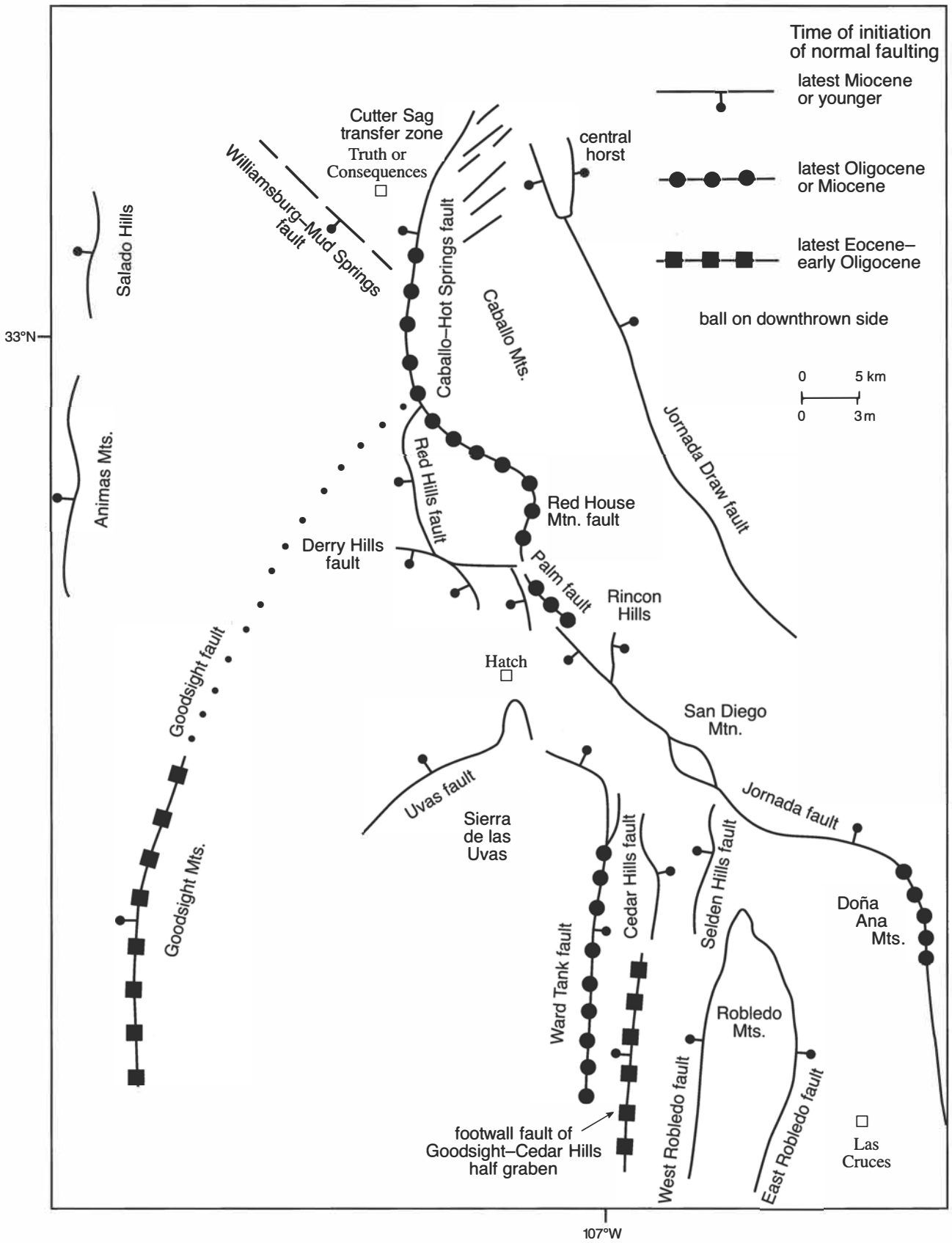

FIGURE 116—Distribution of faults initiated in latest Eocene–early Oligocene, latest Oligocene or Miocene, and latest Miocene or later time.

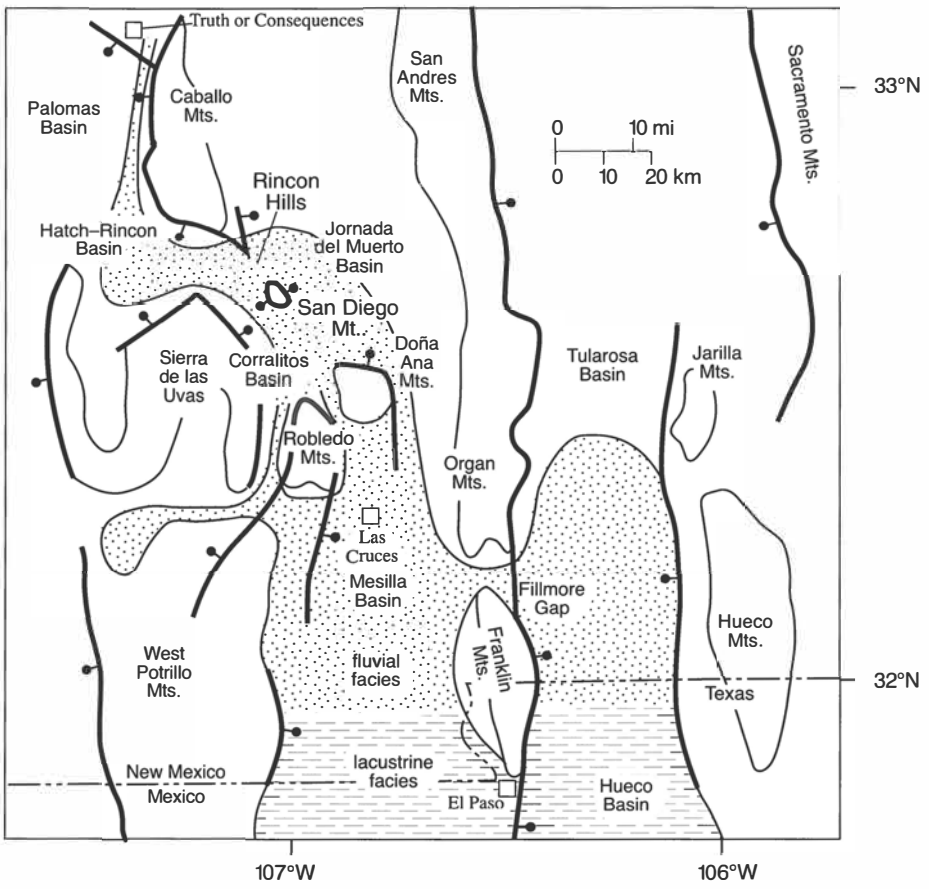

FIGURE 117—Distribution of faults (shown in bold line) active during latest Miocene, Pliocene, and early Pleistocene time, corresponding to deposition of the Camp Rice and Palomas Formations. Dot pattern shows distribution of axial-fluvial facies of the Camp Rice and Palomas Formations deposited by the ancestral Rio Grande.

duction altogether, rather than subduct at a steeper angle. In this variation, the hot Farallon plate underplated North America, causing partial melting and extension over a wide area.

A second model relates mid-Tertiary crustal extension in the Basin and Range and Rio Grande rift to a reduction of compressional stress and subsequent collapse of an overthickened crust created during Sevier and Laramide orogenesis (Coney and Harms, 1984; Wernicke et al., 1987; Dewey, 1988; Gans et al., 1989). The evidence for this model is the close correlation in space between the region of maximum compressional deformation during latest Cretaceous to Eocene time and subsequent crustal extension. The model provides a particularly compelling explanation for the large amount of extension associated with the mid-Tertiary core complexes in Arizona (Coney and Harms, 1984). Because there are apparently no core complexes in New Mexico, the explanation is less well suited as the origin of the Rio Grande rift. However, reactivation of Laramide structures clearly played a role in the evolution of the southern Rio Grande rift. The northwest-trending segments of the Caballo and Palm faults, as well as the northwest-trending Hayner Ranch Basin, are superimposed on northwest-trending structures in the Laramide Rio Grande uplift (cf. Seager and Mack, 1986; Seager et al., 1986, 1997).

Finally, a third group of models relates extension in the Basin and Range and Rio Grande rift to the onset of the San Andreas transform boundary, although there are several variations to this model. In one variation, distributed right-lateral shear created by the transform is responsible for crustal extension in the Southwest (Zoback and Thompson, 1978; Coney, 1987). A second variation considers extension and volcanism in the Southwest to be the result of the rise of the asthenosphere behind the detached and sinking Farallon plate (Dickinson and Snyder, 1978; Lipman, 1980; Seager et al., 1984; Humphreys, 1995). Yet a third variation on the San Andreas transform model calls upon transtension created by the relative motions of the North American and Pacific plates (Dokka and Ross, 1995). Because the San Andreas transform did not begin to form until about 30 Ma, it cannot be the cause of the earliest phase of extension in the southern Rio Grande rift, but may well have influenced the later stage of development.

Landslides

The combination of steep slopes and interbedded strong and weak sedimentary or volcanic rocks in the Caballo Mountains has yielded numerous landslides. They range in areal extent from more than 1 km^2 to 0.1 km^2 (0.24 to 0.04 mi^2) or less, and the largest is more than 4×10^6 m^3 (1.41×10^8 ft^3) in volume. Most are probably Quaternary in age, but at least one formed during the late Tertiary. Several types of landslides are present and may be best described using the classification of Cruden and Varnes (1996).

Cruden and Varnes (1996) followed Varnes (1978) in developing a classification scheme for landslides based on the kind of material involved in the slide and the type of movement. Rock, debris, and earth comprise the three types of material, whereas movements include falls, topples, slides, spreads, and flows. Falls involve falling, bouncing, or rolling of material downslope; toppling is the "foreward rotation out of the slope of a mass of soil or rock about an axis below the center of gravity of the displaced mass"; slides occur dominantly on surfaces of rupture or along thin zones of intense shear; spreads involve extension of a rock or soil mass combined with a general subsidence of the mass into a softer underlayer; and flows refer to the downslope movement of material in the manner of a viscous fluid, with or without the presence of water. Complex landslides can involve more than one type of movement. Examples of landslides using the Cruden and Varnes (1996) classification include rock fall, debris flow, rock slide, or earth flow. The classification is relatively easy to use if landslides are actually observed and the type of movement noted. More difficult is the classification of ancient landslides where the type of movement and presence or absence of water must usually be inferred. Although numerous, rock falls in the Caballo Mountains are of comparatively small volume. They are not shown on the geologic maps and are not described in this report. On the other hand, rock, debris, and complex slides, and perhaps flows, are notably large features of the Caballos and deserve some attention.

Rock slides are a common type of landslide in the Caballo Mountains. Two modes of sliding are represented, rotational slides and translational slides. For rotational slides, the hanging-wall blocks rotate back toward a listric rupture surface, producing a tilted, displaced block sometimes referred to as a toreva block. For translational slides the displaced mass slides downslope on a detachment surface, always a bedding plane in the Caballo Mountains, and often evolves into a debris slide as the strata fragment on a massive scale in the middle or downslope parts of the slide.

Rotational slides are common in the northern part of Apache Valley and in the McRae Canyon area. Nearly a dozen examples of rotational slides are present in Apache Valley, where cliffs of Kneeling Nun Tuff tower over lowlands underlain by soft Palm Park strata (Fig. 118a). The slides are as much as 0.5 km (0.3 mi) long, and all involve the downward slumping and backward rotation of blocks of Palm Park, Kneeling Nun, Bell Top, and locally Palomas Formations. The greatest amount of downward movement is 50–100 m (164–328 ft). Fractures that bound the slide blocks are typically spoon shaped, soleing out in fine-grained Palm Park strata. However, neither the toes of slide surfaces nor expectable compressional ridges have been identified, mostly because of the cover provided by post-slide sediments. The age of these slides is constrained between 780 ka and 50–100 ka, the ages of Palomas gravel involved in some of the slides and the age of inset, undeformed Picacho alluvium.

In the McRae Canyon area, rotational slides are present adjacent to the steep cliffs that border the incised drainage basin on the south, east, and north. The cliffs are capped by a basalt lava flow or flows that overlie a thin veneer of Palomas gravel. Beneath the Palomas Formation are gently dipping beds of the Cretaceous McRae Formation. The rotational slides consist of linear blocks a few tens of meters (50–150 ft) wide and usually less than 300 m (984 ft) long composed of basalt and Palomas Formation. The detachment surfaces are steep and appear to sole into either the lower part of the Palomas Formation or the Palomas–McRae contact. Most of the blocks dip from 5° to 30° toward the detachment surface, and the tops of the blocks have an elevation a few meters to tens of meters below that of the mesa from which they were derived. The majority of blocks moved only a short distance from the mesa, but a few extend a hundred meters or more into the valley and exist as klippe of basalt surrounded by the McRae Formation. An upper limit for the age of these rotational rock slides is younger than 2 Ma, the age of the basalt. Because the blocks are not in contact with younger sediment or geomorphic surfaces, a lower limit for their age cannot be determined.

A larger, ancient example of a rotational rock slide is preserved on Escondido bench south of Flat Top Mountain (Fig. 118b). In this area, Abo and Yeso strata dip 20°–30° southwesterly off the Flat Top dome, but they are overlain by a klippe of Palm Park beds, more than 1 km^2 (0.4 mi^2) in area, that dips 15°–30° northeast. The surface between the Permian and Palm Park rocks is a fault that dips southward less than 10°. In one gully, Abo beds, dipping southwest, are exposed below the Palm Park klippe. Both Permian and Palm Park strata, as well as the low-angle fault, are truncated by the high-angle Derry fault at the edge of the Escondido bench.

The geologic relationships suggest that the klippe of Palm Park strata is the erosional remnant of a once much larger rotational rock slide, derived perhaps from Flat Top Mountain to the north. As the block slid southwestward, it rotated back toward the northeast. The low-angle fault presumably represents the downslope, flatter part of a listric slide surface, whose up-dip, steeper part has been removed by erosion. The landslide clearly occurred before early to middle Pleistocene time, the date of the latest movement on the Derry fault. Most important, a source of Palm Park strata upslope of the slide no longer exists; it has been completely eroded away as has at least part of the landslide itself. These relationships suggest the slide may be at least as old as Pliocene if not older.

Translational rock and debris slides are also well represented in the Caballo Mountains. These are present on the eastern dip slope of the range, mostly within the interbedded limestone and shale of the Nakaye Formation, and to a lesser extent, the Bar B Formation (Fig. 118c). Bedding dips approximately 15° east, and the basal slide surfaces of the detached blocks or debris closely follow bedding, mostly within shales or at a shale-limestone contact (Fig. 119). The slides either moved directly down dip or somewhat obliquely across dip. One mass of rocky debris spilled into the upper reaches of ancestral Apache Canyon, backfilling it to a depth of 50 m (164 ft) or more. Most of the slides terminated downslope against cuestas or other types of rock ridges (Fig. 120). The slides range from wide, shallow, flat-bottomed spoon shapes to elongated lobes. The largest exceeds 1 km^2 (0.4 mi^2) in area and has a volume near 4.5×10^6 m^3 (1.6×10^8 ft^3) using calculations suggested by Cruden and Varnes (1996). The slides invariably consist of angular blocks or slabs of limestone as much as 100 m (328 ft) long that are randomly rotated, with dips as high as 90°. Top surfaces of the landslides are usually hummocky or otherwise irregular, featuring numerous undrained depressions. Breakaway scarps 20–30 m (66–98 ft) high are still preserved at the upper end of two of the largest slides (Fig. 121). An artificial cut in the toe of one large slide in the upper reaches of Apache Canyon reveals shattered but still intact limestone near the basal slide surface, whereas allochthonous blocks form the upper part of the slide.

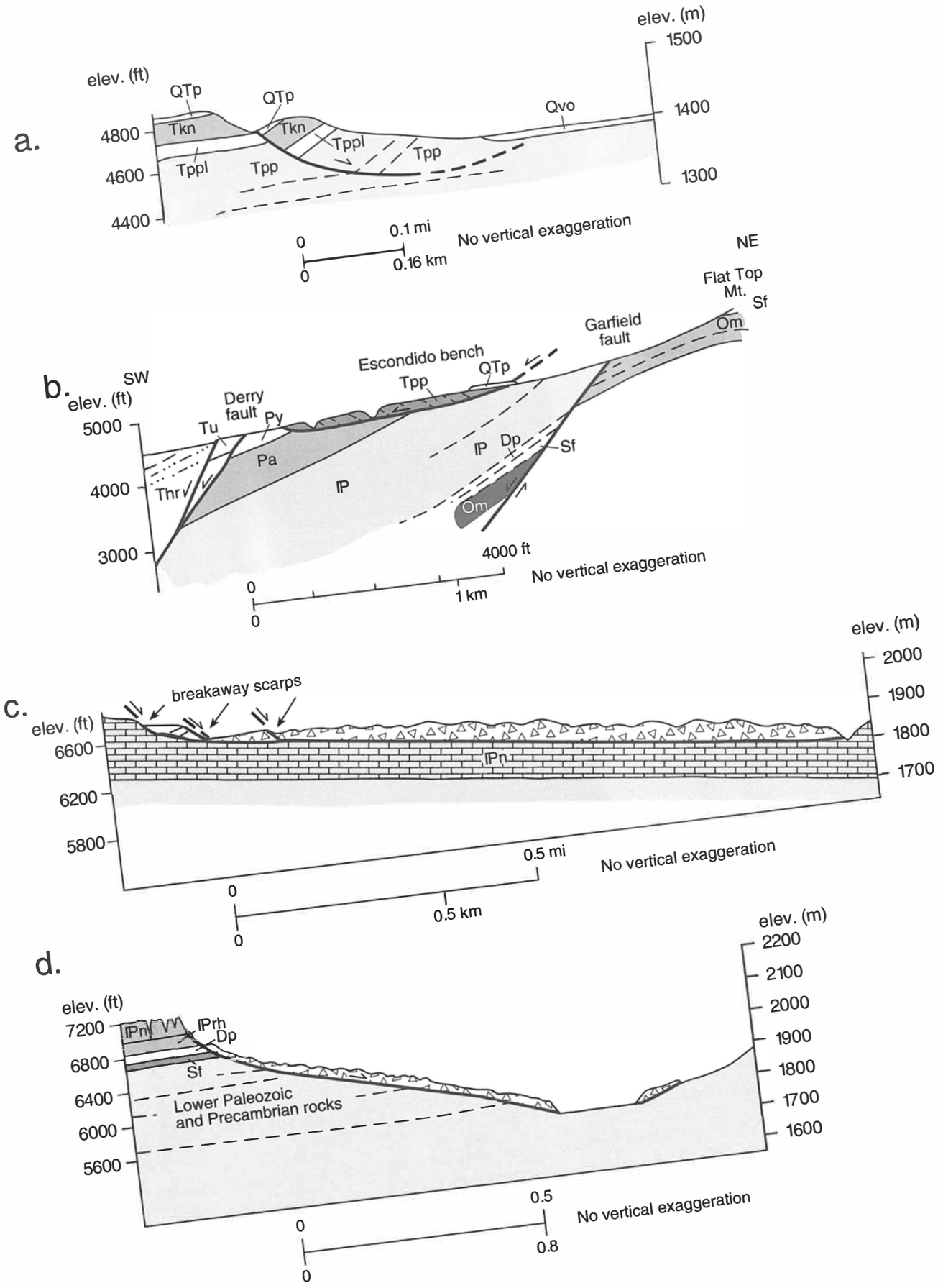
a.
elev. (ft)
elev. (m)
1500
1400
1300
4800
4600
4400
QTp
QTp
Tkn
Tkn
Tppl
Tpp
Tppl
Tpp
Qvo
0
0.1 mi
0
0.16 km
No vertical exaggeration
b.
SW
NE
elev. (ft)
5000
4000
3000
Derry fault
Tu
Py
Pa
Thr
lP
Escondido bench
Tpp
QTp
lP
Dp
Sf
Om
Garfield fault
Flat Top Mt.
Sf
Om
4000 ft
0
1 km
0
No vertical exaggeration
c.
elev. (m)
2000
1900
1800
1700
elev. (ft)
6600
6200
5800
breakaway scarps
lPn
0
0.5 mi
0
0.5 km
No vertical exaggeration
d.
elev. (m)
2200
2100
2000
1900
1800
1700
1600
elev. (ft)
7200
6800
6400
6000
5600
lPn
lPrh
Dp
Sf
Lower Paleozoic and Precambrian rocks
0
0.5
0
0.8
No vertical exaggeration

The classification of the slides seems fairly straightforward. They were probably initiated as rock slides, detached at the breakaway scarp that began moving downdip along shale beds or at a shale-limestone contact. As they increased in velocity and/or the toe compressed against bedrock ridges, they quickly fragmented into countless slabs and blocks, which continued to move down dip as debris slides, locally spilling into available canyons.

The rock/debris slides probably formed during the early to middle Pleistocene. They are young enough to still retain original scarp and surface morphology. However, the upper surfaces of the slides appear to grade to either near or above the Palomas fan surface, suggesting they are older than approximately 780 ka. Furthermore, most of the slides now mantle drainage divides, an inversion of topography having occurred since the slides were emplaced. Canyons as much as 50 m (164 ft) deep have been incised in bedrock along the margins of the largest slides, and the debris that once partially filled upper Apache Canyon has now been excavated to a depth of 20 m (66 ft) or more. Clearly, the slides are not recent features; an age of early to middle Pleistocene seems consistent with available data.

Landslides also are present along the steep western escarpment of the range. Most originated within cliffs of Red House and Nakaye limestone just below the summit of the range, but one was initiated on the dip slope of Nakaye limestone east of the summit and then poured into the upper reaches of Burbank Canyon. The largest landslides descended to the floors of Burbank and Apache Canyons (Fig. 118d), leaving narrow lobes of coarse boulders that mark the channels down which the debris moved. An estimated 1–1.5 x 10^6 m^3 (3.5–5.3 x 10^7 ft^3) of boulders comprise the largest landslides. Smaller dislodged masses came to rest on Percha Shale benches and slopes high on the escarpment, not having sufficient momentum to carry them to adjacent canyon floors.

It is difficult to classify these landslides, probably because they involved several kinds of movements. Initial movements may have involved rock topple, rock fall, or rock slide, or a combination of these processes. As the moving mass gained velocity and momentum they probably evolved into debris slides or small volume sturzstroms, a dry debris flow or rock avalanche that moves downslope very swiftly on a cushion of compressed air (Hsu, 1975).

Like the rock and debris slides on the eastern slopes of the range, the landslides on the western escarpment are probably Pleistocene in age. They partially filled the ancestral Apache and Burbank Canyons, but their toes have since been excavated by more recent drainage. The surfaces of the slides are graded approximately to the level of the Palomas fans, and upper Pleistocene alluvium is locally inset against the landslide masses.

From their studies of compound scarps in the Palomas Formation along the northern Caballo fault, Foley et al. (1988) and Machette (1987) concluded that recurrent movement along this fault took place throughout the early to middle Pleistocene. Our data suggest that major rock and debris slides were initiated during the same time interval throughout the Caballo Mountains, so it seems reasonable to assume that many of the

FIGURE 118—Diagrammatic sections of landslide types in the Caballo Mountains. **a**—Rotational block slide (toreva blocks). **b**—Ancient, deeply eroded rotational block slide on Escondido bench. **c**—Translational, fragmented block slides on the eastern dip slope of the Caballo Mountains. **d**—Debris flow (Sturzstrom) on steep canyon walls. **Om** = Montoya Formation; **Sf** = Fusselman Dolomite; **Dp** = Percha Shale; **IP** = Pennsylvanian rocks; **IPrh** = Red House Formation; **IPn** = Nakaye Formation; **Pa** = Abo Formation; **Py** = Yeso Formation; **Tpp** = Palm Park Formation; **Tppl** = Limestone beds in upper Palm Park Formation; **Tkn** = Kneeling Nun Tuff; **Tu** = Uvas Basaltic Andesite; **Thr** = Hayner Ranch Formation; **QTp** = Palomas Formation; **Qvo** = Older inset valley-fill alluvium.

FIGURE 119—Contact of debris-slide breccia of Fig. 120 with underlying unbroken Nakaye limestone bed. Slide surface (not visible) is a caliche-cemented zone of shear approximately 8 cm (3.1 in) thick lying just above the limestone bed. View looks approximately north, and slide surface dips 12° east (right).

FIGURE 120—Toe of large, spoon-shaped block/debris slide below Brushy Mountain on eastern dip slope of Caballo Mts. Landslide debris extends left (west) of the gully bottom and is approximately 50–60 m (164–197 ft) thick. Breakaway scarps are visible as two or three terraces at upper left of view. Nakaye beds crop out on right (east) side of foreground canyon and on skyline. View looks approximately northwest.

FIGURE 121—Breakaway scarp of large block/debris slide imaged in Figs. 119 and 120. Track follows base of scarp and landslide is to left. Note juniper trees on scarp for scale. The landslide is on eastern dip slope of the Caballo Mountains below Brushy Mountain. View looks south.

landslides were triggered by large earthquakes. To what extent water played a role in the downslope movements cannot be judged with confidence. However, most of the translational rock and debris slides are prevailingly free of mud, suggesting that they were essentially dry. Nevertheless, shale layers may have contained water, or water could have been concentrated at a shale-limestone boundary, which would have facilitated sliding, and the small-scale rotational rock slides in Apache Valley may have moved in response to excess moisture affecting the properties of Palm Park clay rather than earthquakes. Nevertheless, we conclude that, whereas water may have facilitated downslope movement or even initiated it in the case of the small toreva blocks, the large translational rock and debris slides, rock falls, and sturzstroms were probably triggered by Pleistocene earthquakes and were essentially dry when they moved. The close relationship of the large late Tertiary rotational rock slide on Escondido bench to the adjacent Derry fault invites speculation that it, too, may have been triggered by earthquake events along that fault.

Economic deposits

According to Endlich (1883), prospecting for mineral wealth in the Caballo Mountains began around 1883 or a little earlier. Possibly copper was produced shortly thereafter from mines near Palomas Gap, but mining began in earnest when gold was discovered about 1901 at the Shandon placers near the mouth of Apache Canyon (Harley, 1934). New discoveries of lead and copper were made near Palomas Gap in 1904 and 1905, followed by the discovery and production of small amounts of vanadium between 1909 and 1912 (Harley, 1934). As production of copper, lead, and vanadium waned after 1912, attention turned to fluorspar, iron, and manganese, mostly in response to the need for these commodities during World Wars I and II (Kelley and Silver, 1952). During the 1950s uranium prospecting revealed several occurrences in the Caballo Mountains (Melanco, 1952; Boyd and Wolfe, 1953; Boyd, 1955), but no economic deposits were developed. In the last few decades, most attention has focused on fluorspar (Williams, 1966; McAnulty, 1978), but with little or no production. Other commodities with proven or potential value include barite, gypsum, limestone, dolomite, caliche, sand, and gravel. Small amounts of coal have also been produced from Cretaceous rocks in the Mescal Canyon area, apparently used to treat vanadium ores from the Palomas Gap area around 1910 (Kelley and Silver, 1952).

According to Northrop (1959), the total value of copper, silver, gold, and lead won from the Caballo Mountains through 1952 amounted to no more than $200,000. Only a few hundred pounds of vanadium oxide were obtained from vanadinite at the leaching plant set up in Cutter (Harley, 1934), and approximately 34,100 tons of fluorite was shipped from the Caballo Mountains through 1954 (McAnulty, 1978). Similarly, the mountains have yielded only small tonnages of barite and manganese, and no iron ore has been produced for manufacture of steel, although some has been exploited as a color pigment (Kelley and Silver, 1952). Since 1955, no new discoveries of any of these commodities have been reported, and little or no ore shipped. It seems clear that hydrothermal mineralization in the Caballo Mountains is prevailingly feeble and scattered, a not surprising circumstance considering the lack of sizeable Cenozoic or Laramide intrusives in the area. In recent years occasional exploration efforts have focused on potential development of gypsum and limestone with little success, although sand, gravel, and caliche have been quarried successfully in several places.

Excellent summaries of the mineral deposits in the Caballo Mountains have been presented by Kelley and Silver (1952), Mason (1976), Williams (1966), and McAnulty (1978). These men integrated first-hand observations with earlier accounts of other geologists, many of whom worked in the area at the times the mines were active, including: Herrick (1898) on lead and copper; Leatherbee (1910), Larsh (1911), Allen (1911), and Hess (1913) on vanadium; Wells (1918) and Lasky and Wootton (1933) on manganese; Johnston (1928), Talmadge and Wootton (1937), and Clippenger (1949) on fluorite and barite; Kelley (1951) on iron; Lasky and Wootton (1933) on gold; and Keyes (1905) and Harley (1934) on the mineral deposits in general, with special emphasis by Harley (1934) on gold and vanadium. Williams et al. (1964) and Seager and Hawley (1973) described the occurrences of barite from the southern part of the mountains, and Staatz et al. (1965) and McLemore (1986) pointed out the presence of uranium and thorium-bearing minerals in the Red Hills. Kelley and Silver (1952), Tabet (1980), and Wallin (1983) recounted the geology of coal occurrences in the Mescal Canyon area.

Our examination of mineral deposits in the Caballo Mountains was at best cursory. The summary of the economic deposits that follows is based largely on the work of the authors named above, modified where appropriate by our observations. It is intended to serve the interested reader by providing location (Fig. 122) and production data of the mines and by abstracting the essential geologic relationships of the deposits.

Copper

There are two types of copper deposits in the Caballo Mountains: fissure vein deposits and sedimentary red bed deposits. Whereas the veins have yielded modest amounts of copper, the red beds are too feebly mineralized to be of commercial value.

The most important copper deposits in fissure veins are located approximately 2 km (1.2 mi) south of Palomas Gap on the western escarpment of the range. At this locality, a system of east-trending fissures cut Precambrian, Bliss, and El Paso rocks, the fissures being mineralized with hypogene bornite and chalcopyrite as well as supergene malachite, azurite, and chrysocolla. Small amounts of gold and silver are said to have been present, and the upper part of the veins contains fluorspar and galena. As much as 3 m (9.8 ft) wide and 240 m (787 ft) long, the veins contain copper mineralization primarily where they transect the Bliss Sandstone (Keyes, 1905; Harley, 1934). The principal workings are at the Marion (Victorio Chief) and Oohoo mines, the former located approximately 1 km (0.6 mi) south of the latter (Fig. 122). According to Harley (1934), approximately $100,000 worth of ore was taken from the Marion (Victorio Chief) mine, mostly copper, but some silver and gold.

Red bed copper deposits occur in the Abo Formation on the eastern flank of the range particularly east of Palomas Gap, where Harley (1934) described them in detail. We also found azurite and malachite in Abo outcrops much farther south in NW¼ sec. 17 T11S R3W. No structural controls are apparent at that locality, and several small prospects have explored the mineralized zone.

Lead

East and south of Palomas Gap, in the drainages of the south fork of Palomas Gap Creek and Lead Mine Canyon, small amounts of galena have been won from four distinct veins. The N70°–75°E trending veins are confined to the Bar B Formation, pinching out upward in the Abo as well as downward in basal Bar B and Nakaye strata. The veins carry galena as well as associated cerrusite, anglesite, vanadinite, pyromorphite, wulfenite, fluorite, and small amounts of barite and copper. Abandoned early in their development as sources of lead, the veins eventu-

along strike. The Independence (Bluejacket) mine is located west of the Caballo fault in the northern red hills. The fluorspar mineralization occurs in a brecciated fault zone, trending N15° –20°W, that juxtaposes Precambrian granite and lower Paleozoic sandstone. As much as 5 m (16 ft) wide, the ore-bearing zone can be traced for approximately 200 m (656 ft) before it is covered by alluvium. Veins at both the Illinois and Independence claims contained as much as 40–55% CaF_2 (Williams, 1966).

More noted for their content of vanadium and lead than for their fluorspar resources, the Palomas Gap group of mines includes the Governor group, Dewey, White Swan, Harding, Napoleon–Rosa Lee, and Cox mines (Fig. 122), described in some detail by Johnston (1928), Rothrock et al. (1946), and Williams (1966). Only about 2,000 tons of fluorspar were shipped from these mines or groups of claims, more than half of which came from the southernmost workings, the Cox mine (Williams, 1966; Fig. 122). With few exceptions, the fluorspar occupies northeast-trending fissure veins or brecciated fault zones, the longest traceable for approximately 400 m (1,312 ft). The veins are largely confined to the Bar B Formation.

McAnulty lists 12 fluorspar properties in the southern Caballo Mountains, only two of which produced modest tonnages of fluorspar, the Lyda K and Nakaye. Both deposits were described by Johnston (1928), Rothrock et al. (1946), and Williams (1966) as well as McAnulty (1978), although Rothrock et al. (1946) referred to the Nakaye property as the Alamo prospect.

The Lyda K mine, located on Precambrian rocks in the Red Hills, yielded approximately 2,650 tons of fluorspar ore from a northeast-trending fault zone named Lyda K fault. Although the fault cuts Paleozoic strata higher in the Red Hills, production of fluorspar was restricted to vein material within Precambrian granite. The fluorspar is associated with small amounts of galena as well as with massive jasperiod veins within the fault zone. As much as 30 m (98 ft) wide, the prominent fault zone and vein materials can be traced southwestward for several hundred meters (3,000 ft) across the Precambrian granite before they are truncated by the Red Hills fault and presumably dropped beneath the gravel of the Palomas Basin.

Located on the western flank of the Nakaye horst, the Nakaye (Alamo) workings yielded 5,471 tons of fluorspar ore through 1952, with no production recorded since then (McAnulty, 1978). Mineralization is both stratigraphically and structurally controlled. The east-trending Nakaye fault of McAnulty (1978) and Nelson (1974), which dips steeply southward, has localized small bodies of fluorspar where it transects Nakaye, Fusselman, and Montoya strata. The largest deposits, however, are stratabound replacement bodies within jasperized Fusselman Dolomite, which extends northward from its footwall cutoff with the Nakaye fault and dips gently eastward. Mineralization within the Fusselman is rather discontinuous over a distance of approximately 300 m (984 ft) and has been explored by several open cuts, shafts, and prospects. Some of the richer fluorspar lodes within the Fusselman are probably localized by minor, near-vertical fissures or faults.

Although other prospects in the southern Caballo Mountains have apparently produced little or no fluorspar, McAnulty (1978) indicates two prospects that may contain substantial reserves. The Alvarez prospect (Fig. 122) may have reserves of 30,000 tons of ore. Located on the southeastern flank of the Red Hills half dome, the prospects have explored mineralized fissures and stratabound jasperoid bodies in Pennsylvanian limestone adjacent to a northwest-trending fault. On the southwestern flank of Flat Top dome, the Gar Spar deposits contain probable reserves of 15,000–20,000 tons of 25+ % CaF_2 and ultimately could yield 100,000–150,000 tons of 20–25% CaF_2 (McAnulty, 1978). According to McAnulty (1978), the fluorspar is associated with jasperoid and a northwest-trending zone of faults of small displacement within Nakaye and Bar B strata.

Iron

Kelley (1949, 1951) described the iron deposits in the Caballo Mountains, which occur as oolitic hematite beds within the lower part of the Bliss Formation. Although the beds reach a thickness of nearly 4 m (13 ft) locally in Timber Mountain, average 25–35% iron and contain an estimated 63 million tons of minable iron ore, the deposits have never been exploited except as a source of hematite pigment (Kelley and Silver, 1952).

Manganese

Low-grade manganese deposits are widely scattered throughout the Caballo Mountains, according to Wells (1918) and Kelley and Silver (1952), both of whom gave informative summaries of their occurrence. The largest deposits, known as the Ellis claims, are located about 0.7 km (0.4 mi) northwest of Truth or Consequences. Interpreted to be hot springs deposits, the interested reader should refer to the detailed descriptions by Wells (1918) and Kelley and Silver (1952). Wells (1918) also describes a group of manganese prospects located "on both limbs of an anticline" approximately 9 km (5.6 mi) northeast of Derry. The description suggests the prospects are situated along the south-plunging hinge of the Red Hills half dome, but the precise location of the workings is in doubt. At any rate, Wells (1918) indicates only a few tons of psilomelane ore had been mined, some of high grade, from northerly, northwesterly, and easterly trending fissures, probably within Pennsylvanian and perhaps lower Paleozoic carbonates.

A third notable occurrence of manganese is in the Rincon Hills near Rincon, described by Wells (1918) and Seager and Hawley (1973). The Morgan claims, 2 km (1.2 mi) northwest of Rincon, produced 471 tons of psilomelane, wad, and associated limonite through July 1918 (Wells, 1918). The ore fills northwest-trending fissure veins and brecciated beds in the Hayner Ranch Formation and is associated with small amounts of barite. One and a half kilometers (0.9 mi) east-southeast of the Morgan claims, psilomelane was also worked in northwest-striking fissures in Hayner Ranch Formation at the Rincon mine, but the amount of ore shipped is not known. Seager and Hawley (1973) also describe small volumes of placer psilomelane near Rincon in the Rincon Valley and Camp Rice Formations, derived from the nearby veins.

Barite

Fine and Kennedy (1948), Clippinger (1949), and Williams et al. (1964) have described the barite deposits in the Caballo Mountains, the largest of which is the Palm Park deposit. Located adjacent to the Palm fault along the southwestern margin of Red House Mountain, the Palm Park deposit occurs within steeply dipping, silicified and faulted Fusselman Dolomite. Ore has been discontinuously mined for 600 m (1,968 ft) or more along the northwesterly strike of the dolomite. Overall, the deposits appear to be stratiform in shape, but locally faults and veins as much as 1.5 m (4.9 ft) wide transect the dolomite parallel to its strike, containing within them higher grade deposits of the bladed, white mineral. Four hundred tons of barite was shipped from the property before 1951, after which no further production is known (Williams et al., 1964). Much smaller barite deposits have been prospected near Palomas Gap and on the eastern flank of Red House Mountain near the southern end of Haystack syncline. Known as the Carolyn (Paxton) claims (Williams et al., 1964), the prospects at Palomas Gap have explored mineralization within northeast-trending fissures in Bar B limestone. A small horst of silicified Fusselman Dolomite is weakly mineralized along faults and in upper parts of the dolomite at Haystack syncline.

Gypsum and limestone

Beds of gypsum as much as 15 m (49 ft) thick compose much of the red siltstone-dolomite member of the Yeso Formation throughout its outcrop belt on the eastern flank of the range. The gypsum is massive but also interbedded with red siltstone and thin dolomite units. The beds vary in attitude from overturned to gently dipping. Enormous reserves are obviously present, but the outcrops are rather remote from markets and not easily accessible. Exploratory bulldozer excavations and drilling in the 1980s(?) took place in NW¼ sec. 11 T17S R3W.

Like gypsum, large quantities of both limestone and dolomite are present in the Caballo Mountains, but only a tiny fraction has been exploited. Pennsylvanian limestone in the Derry Hills was dug from small quarries, apparently for use as road metal. In the early 1980s, Portland Cement Company carried out a program of drilling and testing for cement-quality limestone in the McLeod Hills, sec. 23 T17S R3W. Their target was massive limestone beds in the Nakaye Formation. The drilling program was abandoned in the middle part of 1980. Because good quality limestone and dolomite is common near major New Mexico markets, it is doubtful that more distant deposits in the Caballo Mountains will soon be exploited.

Coal

Coal in the Caballo Mountains is restricted to the so-called "Engle coal field" (Lee, 1905), located along the Mescal Canyon drainage in the northeastern part of the range. Thin, discontinuous coal seams are confined to the lower 137 m (449 ft) of the Crevasse Canyon Formation (Wallin, 1983). Not more than 39 cm (15 in) thick in outcrop, the thickest and most continuous coal seam is associated with the top of the Gallup Sandstone (Wallin, 1983). In subsurface workings, this coal thickens to 46 cm (18 in), and several exploratory wells in the Engle field have intersected seams as much as 1.3 m (4.3 ft) thick (Tabet, 1980). According to Tabet (1980), the thicker beds of higher grade coal are probably subbituminous, but Wallin (1983) emphasizes the impurity of thin, localized seams and their habit of grading into carbonaceous shale.

Tabet and Frost (1978) identified three surface workings or prospects in the Engle field, all of which either produced from or explored the coal seam at the top of the Gallup Sandstone. The Southwestern mine (sec. 12 T14S R4W) apparently was the largest, reportedly furnishing the coal used to reduce vanadium ores from the Palomas Gap area (Kelley and Silver, 1952). At this mine (Fig. 122) the coal seam, 25–46 cm (9.8–18 in) thick, dips 80° eastward and was worked by a shaft and drift, 52 m (171 ft) and 44 m (144 ft) long, respectively. Little is left today to judge the extent of coal production from the other two mines or prospects, the Durham Ranch mine (Fig. 122) and Nogal seam (Wallin, 1983). The steep dips and thin and discontinuous nature of the coal beds make future production from the Engle field unlikely, in spite of a convenient railhead at Engle, only 16 km (9.9 mi) distant, and drill hole evidence that beds more than a meter (3.3 ft) thick are present in the subsurface.

Sand, gravel, and caliche

Sand and gravel suitable for construction has been quarried in several places along the Rio Grande between Rincon and Truth or Consequences. Well-sorted (poorly graded) sand and gravel comprise most of the fluvial facies of the Camp Rice and Palomas Formations, as well as fluvial facies of both younger and older inset valley fill. Most of these deposits are unlithified or nearly so, but locally the Camp Rice deposits are tightly indurated. Whereas sand and gravel deposits in the Camp Rice/Palomas Formations may attain a thickness of 50 m (164 ft) or more, inset fluvial deposits more than 15–20 m (49–66 ft) thick have not been observed. Deposits of interbedded fluvial and alluvial fan gravel are also common along the Rio Grande. The presence of angular, poorly sorted fan gravel in these mixtures naturally reduces the overall quality of the sand and gravel.

Caliche deposits suitable for road metal and fill material are widespread along the eastern rim of Rincon Arroyo where they form the caprock of the La Mesa surface. As much as 1 m thick, the deposits are easily accessible from I–25.

References

Abitz, R. J., 1986, Geology of mid-Tertiary volcanic rocks of the east-central Black Range, Sierra County, New Mexico—implications for a double-cauldron complex in the Emory cauldron; *in* Clemons, R. E., King, W. E., Mack, G. H., and Zidek, J. (eds.), Guidebook of the Truth or Consequences region: New Mexico Geological Society, Guidebook 37, pp. 161–166.

Ahlbrandt, T. S., Andrews, S., and Gwynne, D. T., 1978, Bioturbation in eolian deposits: Journal of Sedimentary Petrology, v. 48, pp. 839–848.

Algeo, T. J., and Seslavinsky, K. B., 1995, Reconstructing eustatic and epeirogenic trends from Paleozoic continental flooding records; *in* Haq, B. U. (ed.), Sequence stratigraphy and depositional response to eustatic, tectonic, and climatic forcing: Kluwer Academic Publishers, Dordrecht, Netherlands, pp. 209–246.

Allen, C. A., 1911, Vanadium deposits in the Caballo Mountains, New Mexico: Mining and Science Press, v. 103, pp. 376–378.

Allen, J. E., and Balk, R., 1954, Mineral resources of the Fort Defiance and Tohatchi quadrangle, Arizona and New Mexico: New Mexico Bureau of Mines and Mineral Resources, Bulletin 36, 196 pp.

Anadon, P., Cabrera, L., Columbo, F., Marzo, M., and Riba, O., 1986, Syntectonic intraformational unconformities in alluvial fan deposits, eastern Ebro Basin margins (NE Spain): International Association of Sedimentologists, Special Publication, no. 8, pp. 259–271.

Anderson, J. L., 1983, Proterozoic anorogenic granite plutonism of North America: Geological Society of America, Memoir 161, pp. 133–153.

Antisell, T., 1856, Geological report (Parke's surveys in California and near thirty-second parallel) U.S. Pacific Railroad Exploration: 33rd U.S. Congress and Session, Senate Executive Document 78 and House Executive Document 91, vol. 7, pt. 2, 204 pp.

Armstrong, A. K., Mamet, B. L., and Repetski, J. E., 1980, The Mississippian System of New Mexico and Arizona; *in* Fouch, T. D., and Magathan, E. R. (eds.), Paleozoic paleogeography of west-central United States, west-central U.S. Paleogeography symposium 1: Society of Economic Paleontologists and Mineralogists, Rocky Mountain Section, pp. 82–99.

Armstrong, A. K., Kottlowski, F. E., Stewart, W. J., Mamet, B. L., Baltz, E. H., Siemons, W. T., and Thompson, S., III, 1979, The Mississippian and Pennsylvanian (Carboniferous) systems in the United States—New Mexico: U. S. Geological Survey, Professional Paper 1110-W, 27 pp.

Bachman, G. O., and Mehnert, H. H., 1978, New K–Ar dates and the late Pliocene to Holocene geomorphic history of the central Rio Grande region, New Mexico: Geological Society of America, Bulletin, v. 89, pp. 283–292.

Batchel, S. L., and Dorobek, S. L., 1998, Mississippian carbonate ramp-to-basin transitions in south-central New Mexico—sequence stratigraphic response to progressively steepening outer-ramp profiles: Journal of Sedimentary Research, v. 68, pp. 1189–1200.

Ball, M. M., 1967, Carbonate sand bodies of Florida and the Bahamas: Journal of Sedimentary Petrology, v. 37, pp. 556–591.

Barron, E. J., Arthur, M. A., and Kauffman, E. G., 1985, Cretaceous rhythmic bedding sequences—a plausible link between orbital variations and climate: Earth and Planetary Science Letters, v. 72, pp. 327–340.

Bates, R. L., and Jackson, J. A., 1987, Glossary of geology, 3rd ed.: American Geological Institute, 788 pp.

Bauer, R. D., 1989, Depositional environments, sediment dispersal, and provenance of the Dakota Sandstone, Caballo Mountains, south-central New Mexico: Unpublished M.S. thesis, New Mexico State University, 64 pp.

Bauer, P. W., and Lozinsky, R. P., 1986, Proterozoic geology of supracrustal and granitic rocks in the Caballo Mountains, southern New Mexico; *in* Clemons, R. E., King, W. E., Mack, G. H., and Zidek, J. (eds.), Guidebook of the Truth or Consequences region: New Mexico Geological Society, Guidebook 37, pp. 143–149.

Berggren, W. A., Helgen, F. J., Langerlis, C. G., Kent., D. V., Obradovitch, J. D., Raffi, I., Raymo, M. E., and Shackleton, N. J., 1995, Late Neogene chronology—new perspectives in high-resolution stratigraphy: Geological Society of America, Bulletin, v. 107, pp. 1272–1287.

Berman, D. S., and Reisz, R. R., 1980, A new species of *Trimerorhachis* (Amphibia, Temnospondyli) from the Lower Permian Abo Formation of New Mexico, with discussion of Permian faunal distribution in that state: Annals of Carnegie Museum, v. 49, pp. 455–485.

Bilodeau, W. L., 1982, Tectonic models for Early Cretaceous rifting in southeastern Arizona: Geology, v. 10, pp. 466–470.

Blakey, R. C., 1990, Stratigraphy and geologic history of Pennsylvanian and Permian rocks, Mogollon Rim region, central Arizona and vicinity: Geological Society of America, Bulletin, v. 102, pp. 1189–1217.

Bond, G., 1978, Speculations on real sea-level changes and vertical motions of continents at selected times in the Cretaceous and Tertiary Periods: Geology, v. 6, pp. 247–250.

Bond, G., and Kominz, M. A., 1991, Disentangling Middle Paleozoic sea level and tectonic events in cratonic basins of North America: Journal of Geophysical Research, v. 96, pp. 6619–6639.

Boryta, J. D., 1994, Single-crystal $^{40}Ar/^{39}Ar$ provenance ages and polarity stratigraphy of rhyolitic tuffaceous sandstones of the Thurman Formation (late Oligocene), Rio Grande rift, New Mexico: Unpublished M.S. thesis, New Mexico Institute of Mining and Technology, 95 pp.

Boryta, J., and McIntosh, W. C., 1994, Single-crystal $^{40}Ar/^{39}Ar$ provenance ages and polarity stratigraphy of rhyolitic tuffaceous sandstones of the Thurman Formation (late Oligocene?), Rincon Hills and Caballo Mountains, New Mexico: New Mexico Geological Society, Spring Meeting Proceedings, p. 15.

Bowring, S. A., and Karlstrom, K. E., 1990, Growth, stabilization, and reactivation of Proterozoic lithosphere in the southwestern United States: Geology, v. 18, pp. 1203–1206.

Boyd, F. S., 1955, Some recent discoveries of uranium in Sierra County, New Mexico; *in* Fitzsimmons, J. P., Krusekopf, H. H., Jr., and Hayes, P. T. (eds.), South-central New Mexico: New Mexico Geological Society, Guidebook 6, p. 123.

Boyd, F. S., and Wolfe, H. D., 1953, Recent investigations of radioactive occurrences in Sierra, Doña Ana, and Hidalgo counties, New Mexico; *in* Kottlowski, F. E. (ed.), Guidebook of southwestern New Mexico: New Mexico Geological Society, Guidebook 4, pp. 141–142.

Bruno, L., and Chafetz, H. S., 1988, Depositional environment of the Cable Canyon Sandstone: a mid-Ordovician sandwave complex from southern New Mexico; *in* Mack, G. H., Lawton, T. F., and Lucas, S. G. (eds.), Guidebook of Cretaceous and Laramide tectonic evolution of southwestern New Mexico: New Mexico Geological Society, Guidebook 39, pp. 127–134.

Buck, B. J., 1992, Deterioration of paleoclimate in the Late Cretaceous indicated by paleosols in the McRae Formation, south-central New Mexico: Unpublished M.S. thesis, New Mexico State University, 69 pp.

Buck, B. J., and Mack, G. H., 1995, Latest Cretaceous (Maastrichtian) aridity indicated by paleosols in the McRae Formation, south-central New Mexico: Cretaceous Research, v. 16, pp. 559–572.

Budnick, R. T., 1986, Left-lateral intraplate deformation along the Ancestral Rocky Mountains—implications for late Paleozoic plate motions: Tectonophysics, v. 132, pp. 195–214.

Bushnell, H. P., 1953, Geology of the McRae Canyon area, Sierra County, New Mexico: Unpublished M.S. thesis, University of New Mexico, 106 pp.

Bushnell, H. P., 1955, Stratigraphy of the McRae Formation: Compass, v. 33, pp. 9–17.

Cameron, K. L., Nimz, G. J., Kuentz, D., Niemeyer, S., and Gunn, S., 1989, Southern Cordillera basaltic andesite suite, southern Chihuahua, Mexico—a link between Tertiary continental arc and flood basalt magmatism in North America: Journal of Geophysical Research, v. 94, pp. 7817–7840.

Caputo, M. V., and Crowell, J. C., 1985, Migration of glacial centers across Gondwana during Paleozoic Era: Geological Society of America, Bulletin, v. 96, pp. 1020–1036.

Cather, S. M., 1990, Stress and volcanism in the northern Mogollon–Datil volcanic field, New Mexico—effects of the post Laramide tectonic transition: Geological Society of America, Bulletin, v. 102, pp. 1447–1458.

Cather, S. M., and Harrison, R. W., 2002, Lower Paleozoic isopach maps of southern New Mexico and their implication for Laramide and Ancestral Rocky Mountain tectonism; *in* Lueth, V. W., Giles, K. A., Lucas, S. G., Kues, B. S., Myers, R., and Ulmer-Scholle, D. S. (eds.), Guidebook of White Sands: New Mexico Geological Society, Guidebook 53, pp. 85–102.

Cather, S. M., Chamberlin, R. M., Chapin, C. E., and McIntosh, W. C., 1994, Stratigraphic consequences of episodic extension in the Lemitar Mountains, central Rio Grande rift; *in* Keller, G. R., and Cather, S. M. (eds.), Basins of the Rio Grande rift—structure, stratigraphy, and tectonic setting: Geological Society of America, Special Paper 21, pp. 157–170.

Chafetz, H. S., Meredith, J. C., and Kocurek, G., 1986, The Cambro–Ordovician Bliss Formation, southwestern New Mexico, USA—progradational sequences on a mixed siliciclastic and carbonate shelf: Journal of Sedimentary Petrology, v. 49, pp. 201–221.

Chafetz, H. S., Utech, N. M., and Fitzmaurice, S. P., 1991, Differences in the $\delta^{18}O$ and $\delta^{13}C$ signatures of seasonal laminae comprising travertine stromatolites: Journal of Sedimentary Petrology, vol. 61, pp. 1015–1028.

Chapin, C. E., and Cather, S. M., 1981, Eocene tectonics and sedimentation in the Colorado Plateau–Rocky Mountain area: Arizona Geological Society Digest, vol. 14, pp 173–198.

Chapin, C. E., and Cather, S. M., 1994, Tectonic setting of the axial basins of the northern and central Rio Grande rift; *in* Keller, G. R., and Cather, S. M. (eds.), Basins of the Rio Grande rift—structure, stratigraphy, and tectonic setting: Geological Society of America, Special Paper 21, pp. 5–25.

Chapin, C. E., and Seager, W. R., 1975, Evolution of the Rio Grande rift in the Socorro and Las Cruces areas; *in* Seager, W. R., Clemons, R. E., and Callender, J. (eds.), Guidebook of the Las Cruces country: New Mexico Geological Society, Guidebook 26, pp. 297–321.

Chapman-Fahey, J., 1996, Petrology of an Upper Cretaceous volcanic complex as recorded in clasts of the McRae and Love Ranch Formations, Jornada del Muerto Basin, southcentral New Mexico: Unpublished M.S. thesis, New Mexico State University, 106 pp.

Cheel, R. J., and Leckie, D. A., 1993, Hummocky cross-stratification, *in* Wright, V. P. (ed.), Sedimentology Review no. 1: Blackwell Scientific Publications, Oxford, pp. 103–122.

Clemons, R. E., 1975, Petrology of the Bell Top Formation; *in* Seager, W. R., Clemons, R. E., and Callender, J. (eds.), Guidebook of the Las Cruces country: New Mexico Geological Society, Guidebook 26, pp. 123–130.

Clemons, R. E., 1976, Sierra de las Uvas ash-flow field, south-central New Mexico; *in* Woodward, L. A., and Northrop, S. A. (eds.), Tectonics and mineral resources of southwestern United States: New Mexico Geological Society, Special Publication no. 6, pp. 115–121.

Clemons, R. E., 1979, Geology of Good Sight Mountains and Uvas Valley, southwest New Mexico: New Mexico Bureau of Mines and Mineral Resources, Circular 169, 32 pp.

Clemons, R. E., 1982, Geology of Massacre Peak quadrangle, Luna County, New Mexico: New Mexico Bureau of Mines and Mineral Resources, Geologic Map 51, scale 1:24,000.

Clemons, R. E., 1984, *Nuia siberica* Maslov—alias oolite (abs.): Geological Society of America, Abstracts with Programs, v. 16, pp. 473.

Clemons, R. E., 1991, Petrography and depositional environments of the lower Ordovician El Paso Formation: New Mexico Bureau of Mines and Mineral Resources, Bulletin 125, 68 pp.

Clemons, R. E., and Brown, G. A., 1983, Geology of Gym Peak quadrangle, Luna County New Mexico: New Mexico Bureau of Mines and Mineral Resources, Geologic map 58, scale 1:24,000.

Clemons, R. E., and Osburn, G. R., 1986, Geology of the Truth or Consequences area; *in* Clemons, R. E., King, W. E., Mack, G. H., and Zidek, J. (eds.), Guidebook of the Truth or Consequences region: New Mexico Geological Society, Guidebook 37, pp. 69–81.

Clemons, R. E., and Seager, W. R., 1973, Geology of Souse Springs quadrangle, New Mexico: New Mexico Bureau of Mines and Mineral Resources, Bulletin 100, 31 pp.

Clippenger, D. M., 1949, Barite of New Mexico: New Mexico Bureau of Mines and Mineral Resources, Circular 21, 28 pp.

Clopine, W. W., 1992, Lower and Middle Pennsylvanian fusulinid biostratigraphy of southern New Mexico and westernmost Texas: New Mexico Bureau of Mines and Mineral Resources, Bulletin 143, 67 pp.

Cloud, P. E., and Barnes, V. E., 1948, The Ellenberger Group of central Texas: University of Texas, Publication no. 4821, 473 pp.

Cobban, W. A., and Hook, S. C., 1989, Mid-Cretaceous molluscan record from west-central New Mexico; *in* Beaumont, E. C., Read, C. B., Love, D. W., and Cather, S. M. (eds.), Guidebook of the southeastern Colorado Plateau: New Mexico Geological Society, Guidebook 40, pp. 247–264.

Coleman, J. M., and Prior, D. B., 1980, Deltaic sand bodies: American Association of Petroleum Geologists, Education Course Note Series, no. 15, 171 pp.

Condie, K. C., 1982, Plate-tectonics model for Proterozoic continental accretion in the southwestern United States: Geology, v. 10, pp. 37–42.

Condie, K. C., and Budding, A. J., 1979, Geology and geochemistry of Precambrian rocks, central and south-central New Mexico: New Mexico Bureau of Mines and Mineral Resources, Memoir 35, 58 pp.

Coney, P. J., 1987, The regional tectonic setting and possible causes of Cenozoic extension in the North American Cordillera; *in* Coward, M. P., Dewey, J. F., and Hancock, P. L., (eds.), Continental Extensional Tectonics: Geological Society (London), Special Publication 28, pp. 177–186.

Coney, P. J., and Harms, T. A., 1984, Cordilleran metamorphic core complexes—Cenozoic extensional relicts of Mesozoic compression: Geology, v. 12, pp. 550–554.

Coney, P. J., and Reynolds, S., 1977, Cordilleran Benioff zones: Nature, v. 270, pp. 403–406.

Conover, C. S., 1954, Ground-water conditions in the Rincon and Mesilla valleys and adjacent areas of New Mexico: U.S. Geological Survey, Water-Supply Paper 1230, 200 pp.

Cope, E. D., 1881, Geology of the Lake Valley mining district: American Naturalist, v. 15, pp. 831–832.

Cope, E. D., 1882, Invertebrate fossils from the Lake Valley district of New Mexico: American Naturalist, v. 16, pp. 158–159.

Cross, W., 1899, Description of the Telluride quadrangle: U.S. Geological Survey, Geologic Atlas, Folio 57, 18 pp.

Crowell, J. C., 1978, Gondwanan glaciation, cyclothems, continental positioning, and climate change: American Journal of Science, v. 278, pp. 1345–1372.

Crowley, T. J., Hyde, W. T., and Short, D. A., 1989, Seasonal cycle variations on the supercontinent of Pangaea: Geology, v. 17, pp. 457–460.

Cruden, D. M., and Varnes, D. J., 1996, Landslide types and processes; *in* Turner, A. K., and Schuster, R. L (eds.), Landslides—investigation and mitigation: National Research Council, Transportation Research Board, Special Report 247, pp. 36–75.

Cumella, S. P., 1983, Relation of Upper Cretaceous regressive sandstone units of the San Juan Basin to source area tectonics; *in* Reynolds, M. W., and Dolly, E. D. (eds.), Mesozoic paleogeography of west-central United States: Society of Economic Paleontologists and Mineralogists, Rocky Mountain Section, pp. 189–199.

Dane, C. H., and Bachman, G. O., 1957, The Dakota Sandstone and Mancos Shale in the Gallup area; *in* Little, C. J., and Gill, J. J. (eds.), Geology of southwestern San Juan Basin: Four Corners Geological Society, Guidebook 2, pp. 95–98.

Darton, N. H., 1917, A comparison of Paleozoic sections in southern New Mexico country: U.S. Geological Survey Bulletin 108-C, pp. 31–55.

Darton, N. H., 1922, Geologic structure of parts of New Mexico: U.S. Geological Survey Bulletin 726-E, pp. 173–275.

DeCelles, P. G., and Currie, B. S., 1996, Long-term sediment accumulation in the Middle Jurassic early Eocene Cordilleran retroarc foreland-basin system: Geology, v. 24, pp. 591–594.

DeCelles, P. G., Lawton, T. F., and Mitra, G., 1995, Thrust timing, growth of structural culminations, and synorogenic sedimentation in the type Sevier orogenic belt, western United States: Geology, v. 23, pp. 699–702.

Deffeyes, K. S., Lucia, F. J., and Weyl, P. K., 1965, Dolomitization of recent and Plio-Pleistocene sediments by marine evaporite waters on Bonaire, Netherlands Antilles: Society of Economic Paleontologists and Mineralogists, Special Publication 13, pp. 71–88.

Demarest, J. M., and Kraft, J. J., 1987, Stratigraphic record of Quaternary sea levels—implications for more ancient strata: Society of Economic Paleontologists and Mineralogists, Special Publication 41, pp. 223–239.

Dewey, J. F., 1988, Extensional collapse of orogens: Tectonics, v. 7, pp. 1123–1139.

Dickinson, W. R., 1981, Plate tectonic evolution of the southern Cordillera; *in* Dickinson, W. R., and Payne, W. D. (eds.), Relations of tectonics to ore deposits: Arizona Geological Society Digest, v. 14, pp. 113–136.

Dickinson, W. R., and Snyder, W. S., 1978, Plate tectonics of the Laramide orogeny; *in* Mathews, V. (ed.), Laramide folding associated with basement block faulting in the western United States: Geological Society of America, Memoir 151, pp. 355–366.

Dickinson, W. R., Klute, M. A., and Swift, P. N., 1986, The Bisbee Basin and its bearing on Late Mesozoic paleogeographic and paleotectonic relations between the Cordillera and Caribbean regions; *in* Abbott, P. L. (ed.), Cretaceous stratigraphy of western North America: Society of Economic Paleontologists and Mineralogists, Pacific Section, Field Trip Guidebook, no. 46, pp. 51–62.

Dokka, R. K., and Ross, T. M., 1995, Collapse of southwestern North America and the evolution of early Miocene detachment faults, metamorphic core complexes, the Sierra Nevada orocline, and the San Andreas fault system: Geology, v. 23, pp. 1075–1078.

Dott, R. H., and Bourgeois, J., 1982, Hummocky stratification—significance of its variable bedding sequences: Geological Society of America Bulletin, v. 93, pp. 663–680.

Doyle, J. C., 1951, Geology of the northern Caballo Mountains, Sierra County, New Mexico: Unpublished M.S. thesis, New Mexico Institute of Mining and Technology, 51 pp.
Dunham, K. C., 1935, The geology of the Organ Mountains: New Mexico Bureau of Mines and Mineral Resources, Bulletin 11, 272 pp.
Eaton, G. P., 1984, The Miocene Great Basin as an extending back-arc region: Tectonophysics, v. 102, pp. 275–295.
Ebinger, C. J., 1989a, Geometric and kinematic development of border faults and accommodation zones, Kivu–Rusizi rift, Africa: Tectonics, v. 8, pp. 117–133.
Ebinger, C. J., 1989b, Tectonic development of the western branch of the East African rift system: Geological Society of America, Bulletin, v. 101, pp. 885–903.
Elston, W. E., 1957, Geology and mineral deposits of Dwyer quadrangle, Grant, Luna, and Sierra Counties, New Mexico: New Mexico Bureau of Mines and Mineral Resources, Bulletin 38, 86 pp.
Elston, W. E., 1984, Subduction of young oceanic lithosphere and extensional orogeny in southwestern North America during mid-Tertiary time: Tectonics, v. 3, pp. 229–250.
Elston, W. E., Seager, W. R., and Clemons, R. E., 1975, Emory cauldron, Black Range, New Mexico—source of the Kneeling Nun; *in* Seager, W. R., Clemons, R. E., and Callender, J. (eds.), Guidebook of the Las Cruces country: New Mexico Geological Society, Guidebook 26, pp. 283–292.
Endlich, F. M., 1883, The mining regions of southern New Mexico: American Naturalist, v. 17, pp. 149–157.
Engebretson, D. C., Cox, A., and Thompson, G. A., 1984, Correlation of plate motions with continental tectonics—Laramide to Basin-Range: Tectonics, v. 3, pp. 115–119.
Esser, R. P., 2003a, $^{40}Ar/^{39}Ar$ geochronology results from volcanic rocks, southern New Mexico: New Mexico Bureau of Geology and Mineral Resources, Argon open-file reports, OF-AR–18.
Esser, R. P., 2003b, $^{40}Ar/^{39}Ar$ geochronology results from clasts from Late Cretaceous/early Tertiary units of the Caballo Mountains, New Mexico: New Mexico Bureau of Geology and Mineral Resources, Argon open-file reports, OF-AR–16.
Evans, K. V., and Clemons, R. E., 1988, Cambrian–Ordovician (500 Ma) alkalic plutonism in southwestern New Mexico—U–Th–Pb isotopic data from the Florida Mountains: American Journal of Science, v. 288, pp. 735–755.
Eveleth, R. W., 1986, The Palomas Gap vanadium mines; *in* Clemons, R. E., King, W. E., and Mack, G. H. (eds.), 1986, Truth or Consequences region: New Mexico Geological Society Guidebook 37, pp. 297–300.
Faulds, J. E., and Varga, R. J., 1998, The role of accommodation zones and transfer zones in the regional segmentation of extended terranes; *in* Faulds, J. E., and Stewart, J. H. (eds.), Accommodation zones and transfer zone—the regional segmentation of the Basin and Range province: Geological Society of America, Special Paper 323, pp. 1–45.
Fine, M. M., and Kennedy, J. S., 1948, Investigation of ore-dressing methods for barite ores from New Mexico, Missouri, and Arkansas: U.S. Bureau of Mines, Report of Investigations 4280, 31 pp.
Flower, R. H., 1953, Age of the Bliss Sandstone, New Mexico: American Association of Petroleum Geologists, Bulletin, v. 37, pp. 2054–2055.
Flower, R. H., 1959, Cambrian-Devonian beds of southern New Mexico; *in* Joint field conference in the Sacramento Mountains: Roswell Geological Society and Society of Economic Paleontologists and Mineralogists, Permian Basin Section, Guidebook, pp. 154–171.
Flower, R. H., 1965, Early Paleozoic of New Mexico; *in* Fitzsimmons, J. P., and Lochman-Balk, C. (eds.), Guidebook of southwestern New Mexico II: New Mexico Geological Society, Guidebook 16, pp. 112–131.
Flower, R. H., 1969, Early Paleozoic of New Mexico and the El Paso region; *in* LeMone, D. V. (ed.), The Ordovician symposium: El Paso Geological Society and Permian Basin Society of Economic Paleontologists and Mineralogists, Guidebook 3, pp. 31–101.
Foley, L. L., LaForge, R. C., and Piety, L. A., 1988, Seismotectonic study for Elephant Butte and Caballo Dams, Rio Grande Project, New Mexico: U.S. Bureau of Reclamation, Seismotectonic Report 88-9, 97 pp.
Frakes, L. A., Francis, J. E., and Syktus, J. L., 1992, Climatic modes of the Phanerozoic: Cambridge University Press, 274 pp.
Frush, M. P., and Eicher, D. L., 1975, Cenomanian and Turonian foraminifera and palaeoenvironments in the Big Bend region of Texas and Mexico: Geological Association of Canada, Special Paper, no. 13, pp. 277–301.
Fryberger, S. G., and Schenk, C., 1981, Wind sedimentation tunnel experiments on the origins of eolian strata: Sedimentology, v. 28, pp. 805–821.
Fryberger, S. G., Ahlbrandt, T. S., and Andrews, S., 1979, Origin, sedimentary features and significance of low-angle eolian "sand sheet" deposits, Great Sand Dunes National Monument and vicinity, Colorado: Journal of Sedimentary Petrology, v. 49, pp. 733–746.
Gans, P. B., Mahood, G. A., and Schermer, E., 1989, Synextensional magmatism in the Basin and Range province—a case study in the eastern Great Basin: Geological Society of America, Special Paper 233, 53 pp.
Gehring, A. U., 1989, The formation of goethitic ooids in condensed Jurassic deposits in northern Switzerland; *in* Young, T. P., and Taylor, W. E. G. (eds.), Phanerozoic ironstones: Geological Society (London), Special Publication 46, pp. 133–139.
Gile, L. H., Hawley, J. W., and Grossman, R. B., 1981, Soils and geomorphology in the Basin and Range area of southern New Mexico—Guidebook to the Desert Project: New Mexico Bureau of Mines and Mineral Resources, Memoir 39, 222 pp.
Gile, L. H., Peterson, F. F., and Grossman, R. B., 1966, Morphological and genetic sequences of carbonate accumulation in desert soils: Soil Science, v. 101, pp. 347–360.
Gillette, D. D., Wolberg, D. L., and Hunt, A. P., 1986, *Tyrannosaurus rex* from McRae Formation (Lancian, Upper Cretaceous), Elephant Butte reservoir, Sierra County, New Mexico; *in* Clemons, R. E., King, W. E., Mack, G. H., and Zidek, J. (eds.), Guidebook of the Truth or Consequences region: New Mexico Geological Society, Guidebook 37, pp. 235–238.
Gilmer, A., Mauldin, R., and Keller, G., 1986, A gravity study of the Jornada del Muerto and Palomas Basins; *in* Clemons, R. E., King, W. E., Mack, G. H., and Zidek, J. (eds.), Guidebook of the Truth or Consequences region: New Mexico Geological Society, Guidebook 37, pp. 131–134.
Goldstein, A., 1984, Tectonic controls of Late Paleozoic subsidence in the south central United States: Journal of Geology, v. 92, pp. 217–222.
Gordon, C. H., 1907, Notes on the Pennsylvanian formations in the Rio Grande valley, New Mexico: Journal of Geology, v. 15, pp. 805–816.
Gordon, C. H., and Graton, L. C., 1906, Lower Paleozoic formations in New Mexico: Journal of Science, v. 21, pp. 590–591.
Gordon, C. H., and Graton, L. C., 1907, Lower Paleozoic formations in New Mexico (abs.): Journal of Geology, v. 15, pp. 91–92.
Graham, S. A., Tolson, R. B., DeCelles, P. G., Ingersoll, R. V., Bargar, E., Caldwell, M., Cavazza, W., Edwards, D. P., Follo, F. F., Handschy, J. F., Lemke, L., Moxon, I., Rice, R., Smith, G. A., and White, G. A., 1986, Provenance modeling as a technique for analyzing source terrane evolution and controls on foreland sedimentation: International Association of Sedimentologists, Special Publication 8, pp. 425–436.
Grambling, J. H., Williams, M. L., and Mawer, C. K., 1988, Proterozoic tectonic assembly in New Mexico: Geology, v. 16, pp. 724–727.
Greenwood, E., Kottlowski, F. E., and Thompson, S., III, 1977, Petroleum potential and stratigraphy of Pedregosa Basin—comparison with Permian and Orogrande Basins: American Association of Petroleum Geologists, Bulletin, v. 61, pp. 1448–1469.
Groves, J. R., 1986, Foraminiferal characterization of the Morrowan–Atokan (lower Middle Pennsylvanian) boundary: Geological Society of America, Bulletin, v. 97, pp. 346–353.
Gustavson, T. C., 1991, Arid basin depositional systems and paleosols: Fort Hancock and Camp Rice Formations (Pliocene–Pleistocene), Hueco Bolson, west Texas and adjacent Mexico: Texas Bureau of Economic Geology, Report of Investigations 198, 49 pp.
Hallam, A., and Bradshaw, M. J., 1979, Bituminous shales and oolitic ironstones as indicators of transgressions and regressions: Geological Society of London, Journal, v. 136, pp. 157–164.
Harbour, R. L., 1972, Geology of the northern Franklin Mountains, Texas and New Mexico: U.S. Geological Survey, Bulletin 1298, 129 pp.
Harder, S. H., Keller, G. R., Daggett, P. H., and Sinno, Y. A., 1986, Cenozoic-fill-thickness estimates from P-wave delays in the Jornada del Muerto and Palomas Basin; *in* Clemons, R. E., King, W. E., Mack, G. H., and Zidek, J. (eds.), Guidebook of the Truth or Consequences region: New Mexico Geological Society, Guidebook 37, pp. 135–138.
Harding, T. P., 1984, Graben hydrocarbon occurrences and structural style: American Association of Petroleum Geologists, Bulletin, v. 68, pp. 333–362.
Harley, G. T., 1934, The Geology and ore deposits of Sierra County, New Mexico: New Mexico Bureau of Mines and Mineral Resources, Bulletin 10, 220 pp.
Harms, J. C., Southard, J. B., Spearing, D. R., and Walker, R. G., 1975, Depositional environments as interpreted from primary sedimentary structures and stratification sequences: Society of Economic

Paleontologists and Mineralogists, Short Course no. 2, 161 pp.
Harrison, R. W. and Cather, S. M., in press, The Hot Springs fault system—evidence in south-central New Mexico for northward translation of the Colorado Plateau during the Laramide orogeny; *in* Cather, S. M., McIntosh, W. C., and Kelley, S. (eds.), Tectonics, volcanism, and geochronology in the southern Rocky Mountains and Rio Grande rift: New Mexico Bureau of Geology and Mineral Resources, Bulletin 160
Harrison, R. W., and Chapin, C. E., 1990, A NNE-trending dextral wrench fault zone of Laramide age in southern New Mexico (abs.): Geological Society of America, Abstracts with Programs, vol. 22, no. 7, p. 327.
Hawley, J. W., 1965, Geomorphic surfaces along the Rio Grande valley from El Paso, Texas, to Caballo reservoir; *in* Fitzsimmons, J. P., and Lochman-Balk, C. (eds.), Guidebook of southwestern New Mexico II: New Mexico Geological Society, Guidebook 16, pp. 188–198.
Hawley, J. W., and Kottlowski, F. E., 1969, Quaternary geology of the south-central New Mexico border region; *in* Kottlowski, F. E., and LeMone, D. V. (eds.), Border Stratigraphy Symposium: New Mexico Bureau of Mines and Minerals Resources, Circular 104, pp. 89–115.
Hawley, J. W., Kottlowski, F. E., Strain, W. S., Seager, W. R., King, W. E., and LeMone, D. V., 1969, The Santa Fe Group in the south-central New Mexico border region; *in* Kottlowski, F. E., and LeMone, D. V. (eds.), Border Stratigraphy Symposium: New Mexico Bureau of Mines and Mineral Resources, Circular 104, pp. 52–79.
Hayes, P. T., and Cone, G. C., 1975, Cambrian and Ordovician rocks of southern Arizona and New Mexico and westernmost Texas: U.S. Geological Survey, Professional Paper 873, 98 pp.
Heckel, P. H., 1980, Paleogeography of eustatic model for deposition of midcontinent Upper Pennsylvanian cyclothems; *in* Fouch, T. D., and Magathan, E. R. (eds.), Paleozoic paleogeography of west-central United States, Rocky Mountain paleogeography symposium 1: Society of Economic Paleontologists and Mineralogists, Rocky Mountain Section, pp. 197–215.
Hedlund, D. C., 1977, Geologic map of the Hillsboro and San Lorenzo quadrangles, Sierra and Doña Ana Counties, New Mexico: U.S. Geological Survey, Map MF–900A, scale 1:48,000.
Heller, P. L., Bowler, S. S., Chambers, H. P., Coogan, J. C., Hagen, E. S., Shuster, M. W., Winslow, N. S., and Lawton, T. F., 1986, Time of initial thrusting in the Sevier orogenic belt, Idaho, Wyoming, and Utah: Geology, v. 14, pp. 388–391.
Herrick, C. L., 1898, The occurrence of copper and lead in the San Andres and Caballo Mountains: Economic Geologist, vol. 22, pp. 285–291.
Herrick, C. L., 1900, Report of a geological reconnaissance in western Socorro and Valencia Counties, New Mexico: Economic Geology, v. 25, pp. 331–346.
Hess, F. L., 1913, Vanadium in the Sierra de los Caballos, New Mexico: U.S. Geological Survey, Bulletin 530, pp. 157–160.
Hills, J. M., 1970, Late Paleozoic directions in southern Permian Basin, west Texas and southeastern New Mexico: American Association of Petroleum Geologists Bulletin, v. 54, pp. 1809–1827.
Hoffman, J. H., 1976, Stratigraphy and sedimentology of the Bliss Sandstone (Cambro–Ordovician), southern Franklin Mountains, Texas: Unpublished M.S. thesis: Louisiana State University (Baton Rouge), 175 pp.
Hook, S. C., 1983, Stratigraphy, paleontology, depositional framework, and nomenclature of marine Upper Cretaceous rocks, Socorro County, New Mexico; *in* Chapin, C. E., and Callender, J. (eds.), Guidebook of the Socorro region: New Mexico Geological Society, Guidebook 34, pp. 165–172.
Hook, S. C., and Cobban, W. A., 1981, *Lopha Sannionis* (White)—common Upper Cretaceous guide fossil in New Mexico: New Mexico Bureau of Mines and Mineral Resources, Annual Report 1979–1980, pp. 52–56.
Hook, S. C., Molenaar, C. M., and Cobban, W. A., 1983, Stratigraphy and revision of upper Cenomanian to Turonian (Upper Cretaceous) rocks of west-central New Mexico: New Mexico Bureau of Mines and Mineral Resources, Circular 185, pp. 7–28.
Howard, J. D., and Reineck, H. E., 1981, Depositional facies of high-energy beach-to-offshore sequence—comparison with low-energy sequence: American Association of Petroleum Geologists, Bulletin, v. 65, pp. 807–830.
Hsu, K. J., 1975, Catastrophic debris streams (sturzstroms) generated by rockfalls: Geological Society of America, Bulletin, v. 86, pp. 129–140.
Humphreys, E. D., 1995, Post-Laramide removal of the Farallon slab, western United States: Geology, v. 23, pp. 987–990.
Hunt, A., 1983, Plant fossils and lithostratigraphy of the Abo Formation (Lower Permian) in the Socorro area and plant biostratigraphy of Abo red beds in New Mexico; *in* Chapin, C. E., and Callender, J. (eds.), Guidebook of the Socorro region: New Mexico Geological Society, Guidebook 34, pp. 157–163.
Hunter, J. C., 1986, Laramide synorogenic sedimentation in south-central New Mexico—petrologic evolution of the McRae Basin: Unpublished M.S. thesis, Colorado School of Mines, 75 pp.
Hunter, J. C., and Ingersoll, R. V., 1981, Canas Gypsum Member of Yeso Formation (Permian) in New Mexico: New Mexico Geology, v. 3, no. 4, pp. 49–53.
Hunter, R. E., 1977, Basic types of stratification in small eolian dunes: Sedimentology, v. 24, pp. 361–387.
Illing, R. V., Wells, A. J., and Taylor, J. C. M., 1965, Penecontemporary dolomite in the Persian Gulf: Society of Economic Paleontologists and Mineralogists, Special Publication 13, pp. 89–111.
James, N. P., 1984, Shallowing-upward sequences in carbonates: Geoscience Canada, Reprint Series 1, 2nd edition, pp. 213–228.
Jicha, H. L., Jr., 1954, Geology and mineral resources of Lake Valley quadrangle, Grant, Luna, and Sierra Counties, New Mexico: New Mexico Bureau of Mines and Mineral Resources, Bulletin 37, 93 pp.
Johnson, S. Y., 1989, Significance of loessite in the Maroon Formation (Middle Pennsylvanian to Lower Permian), Eagle Basin, northwest Colorado: Journal of Sedimentary Petrology, v. 59, pp. 782–791.
Johnston, W. D., Jr., 1928, Fluorspar in New Mexico: New Mexico Bureau of Mines and Mineral Resources, Bulletin 4, 128 pp.
Jordan, C. F., 1975, Lower Permian (Wolfcampian) sedimentation in the Orogrande Basin, New Mexico; *in* Seager, W. R., Clemons, R. E., and Callender, J. (eds.), Guidebook of the Las Cruces country: New Mexico Geological Society, Guidebook 26, pp. 109–117.
Jordan, T. E., 1981, Thrust loads and foreland basin evolution, Cretaceous western United States: American Association of Petroleum Geologists, Bulletin, v. 65, pp. 2506–2520.
Johansen, S. J., 1986, Provenance of the Mesaverde Group of west-central New Mexico: Unpublished Ph.D. dissertation, University of Texas (Austin), 310 pp.
Kalesky, J. F., 1988, Lithofacies, stratigraphy, and cyclic sedimentation in a mixed carbonate and siliciclastic system, Red House Formation (Atokan), Sierra County, New Mexico: Unpublished M.S. thesis, New Mexico State University, 202 pp.
Kauffman, E. G., 1975, Dispersal and biostratigraphic potential of Cretaceous benthonic bivalvia in the Western Interior: Geological Association of Canada, Special Paper 13, pp. 163–194.
Keller, G. R., and Cordell, L., 1983, Bouguer gravity anomaly map of New Mexico: National Oceanographic and Atmospheric Administration, Boulder, Colorado, Scientific Map Series, scale 1:500,000.
Kelley, S. A., and Chapin, C. E., 1997, Cooling histories of mountain ranges in the southern Rio Grande rift based on apatite fission-track analysis—a reconnaissance survey: New Mexico Geology, v. 19, no. 1, pp. 1–14.
Kelley, V. C., 1949, Geology and economics of New Mexico iron-ore deposits: University of New Mexico, Publications in Geology, no. 2, 246 pp.
Kelley, V. C., 1951, Oolitic iron deposits of New Mexico: American Association of Petroleum Geologists, Bulletin, v. 35, pp. 2199–2228.
Kelley, V. C., and Silver, C., 1952, Geology of the Caballo Mountains: University of New Mexico, Publications in Geology, no. 4, 286 pp.
Kelley, V. C., 1955, Geologic map of the Sierra County region, New Mexico; *in* Fitzsimmons, J. P. (ed.), South-central New Mexico: New Mexico Geological Society Guidebook 6, back pocket.
Kendall, C. G., and Skipwith, P. A. d'E., 1969, Holocene shallow-water carbonate and evaporite sediments of Khor al Bazam, Abu Dhabi, southwest Persian Gulf: American Association of Petroleum Geologists, Bulletin, v. 53, pp. 841–869.
Keyes, C. R., 1903, Geology of the Apache Canyon placers: Engineering and Mining Journal, v. 76, pp. 966–967.
Keyes, C. R., 1904, Unconformity of the Cretaceous on older rocks in central New Mexico: American Journal of Science, 4th series, v. 18, pp. 360–362.
Keyes, C. R., 1905, Ore deposits of the Sierra de los Caballos: Engineering and Mining Journal, v. 80, pp. 149–151.
Kieling, M. J., 1993, Depositional environments and petrography of the Thurman Formation (Oligocene) and their implications to evolution of the southern Rio Grande rift, New Mexico: Unpublished M.S. thesis, New Mexico State University, 80 pp.
Kieling, J. E., 1994, Sedimentology and provenance of the Hayner Ranch and Rincon Valley Formations (upper Oligocene(?)–Miocene) in the southern Rio Grande rift: Unpublished M.S. thesis, New Mexico State University, 105 pp.

Kietzke, K. K., and Lucas, S. G., 1995, Some microfissils from the Robledo Mountains Member of the Hueco Formation, Doña Ana County, New Mexico; *in* Lucas, S. G., and Heckert, A. B. (eds.), Early Permian footprints and facies: New Mexico Museum of Natural History and Science, Bulleton 6, pp. 57–62.

Kimberley, M. M., 1994, Debate about ironstone—has solute supply been surficial weathering, hydrothermal convection, or exhalation of deep fluids?: Terra Nova, v. 6, pp. 116–132.

King, W. E., 1973, Fusulinids *Millerella* and *Eostaffella* from the Pennsylvanian of New Mexico and Texas: New Mexico Bureau of Mines and Mineral Resources, Memoir 26, 34 pp.

King, W. E., Hawley, J. W., Taylor, A. M., and Wilson, R. P., 1971, Geology and ground-water resources of central and western Doña Ana County, New Mexico: New Mexico Bureau of Mines and Mineral Resources, Hydrologic Report 1, 64 pp.

Klappa, C. F., 1980, Rhizoliths in terrestrial carbonates—classification, recognition, genesis, and significance: Sedimentology, v. 27, pp. 613–629.

Kluth, C. F., 1986, Plate tectonics of the Ancestral Rocky Mountains: American Association of Petroleum Geologists, Memoir 41, pp. 353–369.

Kluth, C. F., and Coney, P. J., 1981, Plate tectonics of the Ancestral Rocky Mountains: Geology, v. 9, pp. 10–15.

Kortemier, C. P., 1982, Occurrence of Bishop Ash near Grama, New Mexico: New Mexico Geology, v. 4, pp. 22–24.

Kottlowski, F. E., 1953, Tertiary-Quaternary sediments of the Rio Grande valley in southern New Mexico; *in* Kottlowski, F. E. (ed.), Guidebook of southwestern New Mexico: New Mexico Geological Society, Guidebook 4, pp. 144–148.

Kottlowski, F. E., 1960, Summary of Pennsylvanian sections in southwestern New Mexico and southeastern Arizona: New Mexico Bureau of Mines and Mineral Resources, Bulletin 66, 187 pp.

Kottlowski, F. E., 1963, Paleozoic and Mesozoic strata of southwestern and south-central New Mexico: New Mexico Bureau of Mines and Mineral Resources, Bulletin 79, 100 pp.

Kottlowski, F. E., 1965, Sedimentary basins of south-central and southwestern New Mexico: American Association of Petroleum Geologists, Bulletin, v. 49, pp. 2120–2139.

Kottlowski, F. E., 1975, Stratigraphy of the San Andres Mountains in south-central New Mexico; *in* Seager, W. R., Clemons, R. E., and Callender, J. (eds.), Guidebook of the Las Cruces country: New Mexico Geological Society, Guidebook 26, pp. 95–104.

Kottlowski, F. E., and Pray, L. C., 1967, Silurian outcrops of south-central and southwestern New Mexico; *in* Symposium volume, Silurian-Devonian rocks of Oklahoma and environs: Tulsa Geological Society Digest, v. 35, pp. 209–230.

Kottlowski, F. E., LeMone, D.V., and Foster, R. W., 1973, Remnant mountains in Early Ordovician seas of the El Paso region, Texas and New Mexico: Geology, v. 1, no. 3, pp. 137–140.

Kottlowski, F. E., Weber, R. H., and Willard, M. E., 1969, Tertiary intrusive-volcanic mineralization episodes in the New Mexico region (abs.): Geological Society of America, Abstracts with Programs for Annual Meeting, v. 1, pt. 7, pp. 278–280.

Kottlowski, F. E., Flower, R. H., Thompson, M. L, and Foster, R. W., 1956, Stratigraphic studies of the San Andres Mountains, New Mexico: New Mexico Bureau of Mines and Mineral Resources, Memoir 1, 132 pp.

Kozur, H. W., and LeMone, D. V., 1995, The Shalem Colony section of the Abo and Upper Hueco Members of the Hueco Formation of the Rebledo Mountains, Doña Ana County, New Mexico—stratigraphy and new conodont-based age determinations; *in* Lucas, S. G., and Heckers, a. B. (eds.), Early Permian footprints and facies: New Mexico Museum of Natural History and Science, Bulletin 6, pp. 39–55.

Kucks, R. P., Hill, P. L., and Heywood, C. E., 2001, New Mexico aeromagnetic and gravity maps and data—a website for distribution of data: U.S. Geological Survey, Open-file Report 01-0061, version 1.0, available at http://greenwood.cr.usgs.gov/pub/open-file-reports/ofr-01-0061/, accessed 10/18/2002.

Kuellmer, F. J., 1954, Geologic section of the Black Range at Kingston, New Mexico: New Mexico Bureau of Mines and Mineral Resources, Bulletin 33, 100 pp.

Kues, B. S., 1986, Paleontology of the Caballero and Lake Valley Formations (Lower Mississippian) west of the Rio Grande, south-central New Mexico; *in* Clemons, R. E., King, W. E., Mack, G. H., and Zidek, J. (eds.), Guidebook of the Truth or Consequences region: New Mexico Geological Society, Guidebook 37, pp. 203–214.

Kues, B. S., 1995, Marine fauna of the Early Permian (Wolfcampian) Robledo Mountains Member, Hueco Formation, southern Robledo Mountains, New Mexico; *in* Lucas, S. G., and Heckert, A. B. (eds.), Early Permian footprints and facies: New Mexico Museum of Natural History and Science, Bulletin, no. 6, pp. 63–90.

Kues, B. S., 2001, The Pennsylvanian System in New Mexico—overview with suggestions for revision of stratigraphic nomenclature: New Mexico Geology, v. 23, no. 4, pp. 103–122.

Kutzbach, J. E., and Gallimore, R. G., 1989, Pangean climates—megamonsoons of the megacontinent: Journal of Geophysical Research, v. 94, pp. 3341–3357.

Laferriere, A. P., Hattin, D. E., and Archer, A. W., 1987, Effects of climate, tectonics, and sea-level changes on rhythmic bedding patterns in the Niobrara Formation (Upper Cretaceous), U.S., Western Interior: Geology, v. 15, pp. 233–236.

Lane, H. R., 1974, Mississippian of southeastern New Mexico and west Texas—a wedge-on-wedge relation: American Association of Petroleum Geologists, Bulletin, v. 58, pp. 269–282.

Lane, H. R., and DeKeyser, T. L., 1980, Paleogeography of the late Early Mississippian (Tournaisian 3) in the central and southwestern United States; *in* Fouch, T. D., and Magathan, E. R. (eds.), Paleozoic Paleogeography of west-central United States: Society of Economic Paleontologists and Mineralogists, Rocky Mountain Section, pp. 149–162.

Lane, H. R., and Ormiston, A. R., 1982, Waulsortian facies, Sacramento Mountains, New Mexico—guide for an international field seminar, March 2–6, 1982; *in* Bolton K., Lane, H. R., and LeMone, D. V. (eds.), Symposium on the Paleoenvironmental setting and distribution of the Waulsortian facies: El Paso Geological Society and University of Texas (El Paso), pp. 115–182.

Langston, W., 1953, Permian amphibians from New Mexico: University of California, Publications in the Geological Sciences, v. 29, pp. 349–416.

Larsh, P. A., 1911, Caballo Mountain vanadium mines: Engineering and Mining Journal, v. 92, p. 118.

Lasky, S. G., and Wootton, T. P., 1933, The metal resources of New Mexico and their economic features: New Mexico Bureau of Mines and Mineral Resources, Bulletin 7, 178 pp.

Lattman, L. H., 1973, Calcium carbonate cementation of alluvial fans in southern Nevada: Geological Society of America, Bulletin, v. 84, pp. 3013–3028.

Laudon, L. R., and Bowsher, A. L., 1949, Mississippian formations of southwestern New Mexico: Geological Society of America, Bulletin, v. 60, pp. 1–87.

Lawton, T. F., 1985, Style and timing of frontal structures, Thrust Belt, central Utah: American Association of Petroleum Geologists, Bulletin, v. 69, pp. 1145–1159.

Lawton, T. F., 1994, Tectonic setting of Mesozoic sedimentary basins, Rocky Mountain region, United States; *in* Caputo, M. V., Peterson, J. A., and Franczyk, K. J. (eds.), Mesozoic Systems of the Rocky Mountain Region, USA: Society for Sedimentary Geology, Rocky Mountain Section, pp. 1–25.

Lawton, T. F., 2000, Inversion of Late Jurassic–Early Cretaceous extensional faults of the Bisbee Basin, southeastern Arizona and southwestern New Mexico; *in* Lawton, McMillian, N. J., and McLemore, V. T. (eds.), Southwest passage—a trip through the Phanerozoic: New Mexico Geological Society, Guidebook 51, pp. 95–102.

Lawton, T. F., and Trexler, J. H., Jr., 1991, Piggyback basin in the Sevier orogenic belt, Utah—implications for development of the thrust wedge: Geology, v. 19, pp. 827–830.

Lawton, T. F., Roca, E., and Guimera, J., 1999, Kinematic-stratigraphic evolution of a growth syncline and its implication for tectonic development of the proximal foreland basin, southeastern Ebro Basin, Catalunya, Spain: Geological Society of America, Bulletin, vol. 111, pp. 412–431.

Lawton, T. F., Giles, K. A., Mack, G. H., Singleton, D. S., and Thompson, A. D., 2002, Lower Wolcampian conglomerate in the southern Caballo Mountains, Sierra County, New Mexico—stratigraphy, correlation, and implications for late Pennsylvanian–Early Permian tectonics; *in* Lueth, V. W., Giles, K. A., Lucas, S. G., Kues, B. S., Myers, R., and Ulmer-Scholle, D. S. (eds.), Geology of White Sands: New Mexico Geological Society, Guidebook 53, pp. 257–265.

Leatherbee, B., 1910, Sierra County, New Mexico, vanadium deposits: Mining World, v. 33, p. 799

Lee, W. T., 1905, The Engle coal field, New Mexico: U.S. Geological Survey, Bulletin 285, 240 pp.

Lee, W. T., and Girty, G. H., 1909, Stratigraphy of the Manzano Group of the Rio Grande valley, New Mexico: U.S. Geological Survey, Bulletin

389, 141 pp.
Leeder, M. R., and Gawthorpe, R. L., 1987, Sedimentary models for extensional tilt-block/half-graben basins: Geological Society (London), Special Publication 28, pp. 139–152.
Leeder, M. R., Mack, G. H., and Salyards, S. L., 1996a, Axial-transverse fluvial interactions in half-graben—Plio-Pleistocene Palomas Basin, southern Rio Grande rift, New Mexico, USA: Basin Research, v. 12, pp. 225–241.
Leeder, M. R., Mack, G. H., Peakall, J., and Salyards, S. L., 1996b, First quantitative test of alluvial stratigraphic models—southern Rio Grande rift, New Mexico: Geology, vol. 24, pp. 87–90.
LeMone, D. V., 1969, Lower Paleozoic rocks in the El Paso area; *in* Córdoba, D. A., Wengerd, S. A., and Shoemaker, J. (eds.), Guidebook of the border region: New Mexico Geological Society, Guidebook 20, pp. 68–79.
Levron, R. Z., 1995, Morphology and geochemistry of paleosols of the Jose Creek Member of the McRae Formation (Cretaceous: Maastrichtian), south-central New Mexico: Unpublished M.S. thesis, New Mexico State University, 104 pp.
Lewis, D. W., 1962, Glauconite in the Cambrian–Ordovician Bliss Formation near Silver City, New Mexico: New Mexico Bureau of Mines and Mineral Resources, Circular 59, 30 pp.
Lindgren, W., Graton, L. C., and Gordon, C. H., 1910, The ore deposits of New Mexico: U.S. Geological Survey, Professional Paper 68, 131 pp.
Lipman, P. W., 1980, Cenozoic volcanism in the western United States—implications for continental tectonics; *in* Continental Tectonics: National Research Council, Studies in Geophysics, pp. 161–174.
Logan, B. W., Rezak, R., and Ginsburg, R. N., 1964, Classification and environmental significance of algal stromatolites: Journal of Geology, v. 72, pp. 68–83.
Loring, A. K., and Armstrong, D. G., 1980, Cambrian–Ordovician syenites of New Mexico, part of a regional alkalic intrusive episode: Geology, v. 8, pp. 344–348.
Loring, A. K., and Loring, R. B., 1980, K/Ar ages of middle Tertiary igneous rocks from southern New Mexico: Isochron/West, no. 28, pp. 17–19.
Lozinsky, R. P., 1986, Geology and late Cenozoic history of the Elephant Butte area, Sierra County, New Mexico: New Mexico Bureau of Mines and Mineral Resources, Circular 187, 40 pp.
Lozinsky, R. P., and Hawley, J. W., 1986a, The Palomas Formation of south-central New Mexico—a formal definition: New Mexico Geology, v. 8, pp. 73–78, 82.
Lozinsky, R. P., and Hawley, J. W., 1986b, Upper Cenozoic Palomas Formation of south-central New Mexico; *in* Clemons, R. E., King, W. E., Mack, G. H., and Zidek, J. (eds.), Guidebook of the Truth or Consequences region: New Mexico Geological Society, Guidebook 37, pp. 239–247.
Lozinsky, R. P., Hunt, A. P., Wolberg, D. L., and Lucas, S. G., 1984, Late Cretaceous (Lancian) dinosaurs from the McRae Formation, Sierra County, New Mexico: New Mexico Geology, v. 6, pp. 72–77
Lucas, S. G., and Anderson, O. J., 1998, Corals from Upper Cretaceous of south-central New Mexico; *in* Mack, G. H, Austin, G. S., and Barker, J. M. (eds.), Guidebook of the Las Cruces country II: New Mexico Geological Society, Guidebook 49, pp. 205–207.
Lucas, S. G., and Oakes, W., 1986, Pliocene (Blancan) vertebrates from the Palomas Formation, south-central New Mexico; *in* Clemons, R. E., King, W. E., Mack, G. H., and Zidek, J. (eds.), Guidebook of the Truth or Consequences region: New Mexico Geological Society, Guidebook 37, pp. 249–255.
Lucas, S. G., Mack, G. H., and Estep, J. W., 1998, The ceratopsian dinosaur *Torosaurus* from the Upper Cretaceous McRae Formation, Sierra County, New Mexico; *in* Mack, G. H., Austin, G. S., and Barker, J. M. (eds.), Guidebook of the Las Cruces country II: New Mexico Geological Society, Guidebook 49, pp. 223–228.
Lucia, F. J., 1968, Sedimentation and paleogeography of El Paso Group: West Texas Geological Society, Publication 68-55, pp. 61–75.
Machette, M. N., 1987, Preliminary assessment of Quaternary faulting near Truth or Consequences, New Mexico: U.S. Geological Survey, Open-file Report 87–652, 40 pp.
Machette, M. N., Personius, S. F., Kelson, K. I., Haller, K. M., and Dart, R. L., 1998, Map and data for Quaternary faults and folds in New Mexico: U.S. Geological Survey, Open-file report, 443 pp.
Mack, G. H., 1987, Mid-Cretaceous (late Albian) change from rift to retroarc foreland basin in southwestern New Mexico: Geological Society of America, Bulletin, v. 98, pp. 507–514.
Mack, G. H., 1992, Paleosols as an indicator of climatic change at the Early–Late Cretaceous boundary, southwestern New Mexico: Journal of Sedimentary Petrology, v. 62, pp. 483–494.
Mack, G. H., and Dinterman, P. A., 2002, Depositional environments and paleogeography of the Lower Permian (Leonardian) Yeso and correlative formations in New Mexico: The Mountain Geologist, v.39, pp. 75–88.
Mack, G. H., and James, W. C., 1986, Cyclic sedimentation in the mixed siliciclastic-carbonate Abo–Hueco transitional zone (Lower Permian), southwestern New Mexico: Journal of Sedimentary Petrology, v. 56, pp. 635–647.
Mack, G. H., and James, W. C., 1992, Calcic paleosols of the Plio–Pleistocene Camp Rice and Palomas Formations, southern Rio Grande rift: Sedimentary Geology, v. 77, pp. 89–109.
Mack, G. H., and James, W. C., 1993, Control of basin symmetry on fluvial lithofacies, Camp Rice and Palomas Formations (Plio–Pleistocene), southern Rio Grande rift, USA: International Association of Sedimentologists, Special Publication 17, pp. 439–449.
Mack, G. H., and Leeder, M. R., 1999, Climatic and tectonic controls on alluvial-fan and axial-fluvial sedimentation in the Plio–Pleistocene Palomas half graben, southern Rio Grande rift: Journal of Sedimentary Research, v. 69, pp. 635–652.
Mack, G. H., and Seager, W. R., 1990, Tectonic control on facies distribution of the Camp Rice and Palomas Formations (Plio–Pleistocene) in the southern Rio Grande rift: Geological Society of America Bulletin, v. 102, pp. 45–53.
Mack, G. H., and Seager, W. R., 1995, Transfer zones in the southern Rio Grande rift: Geological Society (London), Journal, v. 152, pp. 551–560.
Mack, G. H., and Seager, W. R., in press, Geology of the Engle quadrangle, Sierra County, New Mexcio: New Mexico Bureau of Mines and Mineral Resources, Geologic Map.
Mack, G. H., and Suguio, K., 1991, Depositional environments of the Yeso Formation (Lower Permian), southern Caballo Mountains, New Mexico: New Mexico Geology, v. 13, pp. 45–49, 59.
Mack, G. H., Cole, D. R., and Trevino, L., 2000, The distribution and discrimination of shallow, authigenic carbonate in the Plio–Pleistocene Palomas Basin, southern Rio Grande rift, USA: Geological Society of America, Bulletin, v. 112, pp. 643–656.
Mack, G. H., James, W. C., and Salyards, S. L., 1994c, Late Pliocene and early Pleistocene sedimentation as influenced by intrabasinal faulting, southern Rio Grande rift: Geological Society of America, Special Paper 291, pp. 257–264.
Mack, G. H., Kottlowski, F. E., and Seager, W. R., 1998a, The stratigraphy of south-central New Mexico; *in* Mack, G. H., Austin, G. S., and Barker, J. M. (eds.), Guidebook of the Las Cruces country II: New Mexico Geological Society, Guidebook 49, pp. 135–154.
Mack, G. H., Lawton, T. F., and Giles, K. A., 1998b, First-day road log from Las Cruces to Derry Hills and Mescal Canyon in the Caballo Mountains; *in* Mack, G. H., Austin, G. S., and Barker, J. M. (eds.), Guidebook of the Las Cruces country II: New Mexico Geological Society, Guidebook 49, pp. 1–21.
Mack, G. H., Lawton, T. F., and Sherry, C. R., 1995, Fluvial and estuarine depositional environments of the Abo Formation (Early Permian), Caballo Mountains, south-central New Mexico: New Mexico Museum of Natural History and Science, Bulletin 6, pp. 181–187.
Mack, G. H., Leeder, M., and Salyards, S. L., 2002, Temoporal and spatial varibility of alluvial-fan and axial-fluvial sedimentation in the Plio–Pleistocene Palomas half graben, southern Rio Grande rift, New Mexico, USA; *in* Sedimentation in Continental rifts: SEPM, Special Publication, no. 73, pp. 165–177.
Mack, G. H., Love, D. W., and Seager, W. R., 1997, Spillover models for axial rivers in regions of continental extension—the Rio Mimbres and Rio Grande in the southern Rio Grande rift, USA: Sedimentology, v. 44, pp. 637–652.
Mack, G. H., Salyards, S. L., and James, W. C., 1993, Magnetostratigraphy of the Plio–Pleistocene Camp Rice and Palomas Formations in the Rio Grande rift of southern New Mexico: American Journal of Science, v. 293, pp. 49–77.
Mack, G. H., Seager, W. R., and Kieling, J., 1994b, Late Oligocene and Miocene faulting and sedimentation, and evolution of the southern Rio Grande rift, New Mexico, USA: Sedimentary Geology, v. 92, pp. 79–96.
Mack, G. H., Leeder, M., Perez-Arlucea, M., and Bailey, B. D. J., in press, Early Permian silt-bed fluvial sedimentation in the Orogrande Basin of the Ancestral Rocky Mountains, New Mexico, USA: Sendimentary Geology.
Mack, G. H., Salyards, S. L., Cole, D. R., James, W. C., and Giordano, T. H., 1994d, Stable oxygen and carbon isotopes of pedogenic carbonate

as indicators of Plio–Pleistocene paleoclimate in the southern Rio Grande rift, south-central New Mexico: American Journal of Science, v. 294, pp. 621–640.

Mack, G. H., McIntosh, W. C., Leeder, M. R., and Monger, H. C., 1996, Plio–Pleistocene pumice floods in the ancestral Rio Grande, southern Rio Grande rift, USA: Sedimentary Geology, v. 103, pp. 1–8.

Mack, G. H., Nightengale, A. L., Seager, W. R., and Clemons, R. E., 1994a, The Oligocene Goodsight-Cedar Hills half graben near Las Cruces and its implications to the evolution of the Mogollon–Datil volcanic field and to the southern Rio Grande rift; *in* Chamberlin, R. M., Kues, B. S., Cather, S. M., Barker, J. M., and McIntosh, W. C. (eds.), Guidebook of the Mogollon slope, west-central New Mexico and east-central Arizona: New Mexico Geological Society, Guidebook 45, pp. 135–142.

Mack, G. H., Salyards, S. L., McIntosh, W. C., and Leeder, M. R., 1998c, Reversal magnetostratigraphy and radioisotopic geochronology of the Plio–Pleistocene Camp Rice and Palomas Formations, southern Rio Grande rift; *in* Mack, G. H., Austin, G. S., and Barker, J. M. (eds.), Guidebook of the Las Cruces country II: New Mexico Geological Society, Guidebook 49, pp. 229–336.

Mason, J. T., 1976, The geology of the Caballo Peak quadrangle, Sierra County, New Mexico: Unpublished M.S. thesis, University of New Mexico, 131 pp.

Maxwell, C. H., and Oakman, M. R., 1990, Geologic map of the Cuchillo quadrangle, Sierra County, New Mexico: U.S. Geological Survey, Geologic Quadrangle Map, GQ–1686, scale 1:24,000.

McAnulty, W. N., 1978, Fluorspar in New Mexico: New Mexico Bureau of Mines and Mineral Resources, Memoir 34, 61 pp.

McCleary, J. T., 1960, Geology of the northern part of the Fra Cristobal range, Sierra and Socorro Counties, New Mexico: Unpublished M.S. Thesis, University of New Mexico, 59 pp.

McGookey, D. P., Haun, J. D., Hale, L. A., Goodell, H. G., McCubbin, D. G., Weimer, R. J., and Wulf, G. R., 1972, The Cretaceous System; *in* Mallory, W. E. (ed.), Geologic Atlas of Rocky Mountain Region: Rocky Mountain Association of Geologists, pp. 190–228.

McIntosh, W. C., Kedzie, L. L., and Sutter, J. F., 1991, Paleomagnetism and $^{40}Ar/^{39}Ar$ ages of ignimbrites, Mogollon–Datil volcanic field, southwestern New Mexico: New Mexico Bureau of Mines and Mineral Resources, Bulletin 135, 79 pp.

McIntosh, W. C., Chapin, C. E., Ratté, J. C., and Sutter, J. F., 1992, Time-stratigraphic framework for the Eocene–Oligocene Mogollon–Datil volcanic field, southwest New Mexico: Geological Society of America, Bulletin, v. 104, pp. 851–871.

McIntosh, W. C., Sutter, J. F., Chapin, C. E., Osburn, G. R., and Ratté, J. C., 1986, A stratigraphic framework for the eastern Mogollon-Datil volcanic field based on paleomagnetism and high-precision $^{40}Ar/^{39}Ar$ dating of ignimbrites—a progress report; *in* Clemons, R. E., King, W. E., Mack, G. H., and Zidek, J. (eds.), Guidebook of the Truth or Consequences region: New Mexico Geological Society, Guidebook 37, pp. 183–195.

McIntosh, W. C., Sutter, J. F., Chapin, C. E., and Kedzie, L. L., 1990, High-precision $^{40}Ar/^{39}Ar$ sanidine geochronology of ignimbrites in the Mogollon–Datil volcanic field, southwestern New Mexico: Volcanology, v. 52, pp. 584–601.

McLemore, V. T., 1986, Geology, geochemistry, and mineralization of syenites in the Red Hills, southern Caballo Mountains, Sierra County, New Mexico—preliminary observations; *in* Clemons, R. E., King, W. E., Mack, G. H., and Zidek, J. (eds.), Guidebook of the Truth or Consequences region: New Mexico Geological Society, Guidebook 37, pp. 151–159.

McLemore, V. T., 1987a, Geology and regional implications of carbonatites in the Lemitar Mountains, central New Mexico: Journal of Geology, v. 95, pp. 255–270.

McLemore, V. T., 1987b, Petrologic, paleomagnetic, and structural evidence of a Paleozoic rift system in Oklahoma, New Mexico, Colorado, and Utah—discussion and reply: Geological Society of America, Bulletin, v. 99, pp. 315–318.

McLemore, V. T., McMillan, N. J., Heizler, M. T., and McKee, C., 1999, Cambrian alkaline rocks at Lobo Hill, Torrance County, New Mexico—more evidence for a Cambrian–Ordovician aulacogen; *in* Pazzaglia, F. V., and Lucas, S. G. (eds.), Guidebook of the Albuquerque country: NMGS, Guidebook 50, pp. 247–253.

McMillan, N. J., 1998, Temporal and spatial magmatic evolution of the Rio Grande rift; *in* Mack, G. H., Austin, G. S., and Barker, J. M. (eds.), Guidebook of the Las Cruces country II: New Mexico Geological Society, Guidebook 49, pp. 107–115.

McMillan, N. J., and Mc Lemore, V. T., 1999, The Lobo Hill alkalic complex, Torrance County, New Mexico; Cambrian magmatism in the New Mexico aulacogen (abs.): New Mexico Geology, v. 21, p. 36.

Meek, F. B., and Hayden, F. V., 1861, Descriptions of new Lower Silurian (Primordial), Jurassic, Cretaceous, and Tertiary fossils collected in Nebraska by the exploring expeditions: Proceedings of the Academy of Natural Sciences, Philadelphia, vol. 13, pp. 414–447.

Melancon, P. E., 1952, Uranium occurrences in the Caballo Mountains, Sierra County, New Mexico: U.S. Atomic Energy Commission, Technical Memorandum 213, 7 pp.

Melvin, J. W., 1963, Cretaceous stratigraphy in the Jornada del Muerto region, including geology of the Mescal Creek area, Sierra County, New Mexico: Unpublished M.S. thesis, University of New Mexico, 121 pp.

Meyers, W. J., 1974, Carbonate cement stratigraphy of the Lake Valley Formation (Mississippian), Sacramento Mountains, New Mexico: Journal of Sedimentary Petrology, v. 44, pp. 837–861.

Meyers, W. J., 1977, Chertification in the Mississippian Lake Valley Formation, Sacramento Mountains, New Mexico: Sedimentology, v. 24, pp. 75–105.

Meyers, W. J., 1978, Carbonate cements—their regional distribution and interpretation in Mississippian limestones of southwestern New Mexico: Sedimentology, v. 25, pp. 371–397.

Meyers, W. J., 1980, Compaction in Mississippian skeletal limestones, southwestern New Mexico: Journal of Sedimentary Petrology, v. 50, pp. 457–474.

Meyers, W. J., and Hill, B. E., 1983, Quantitative studies of compaction in Mississippian skeletal limestones, New Mexico: Journal of Sedimentary Petrology, v. 53, pp. 231–242.

Meyers, W. J., and James, A. T., 1978, Stable isotopes of cherts and carbonate cements in the Lake Valley Formation (Mississippian), Sacramento Mountains, New Mexico: Sedimentology, v. 25, pp. 105–124.

Meyers, W. J., and Lohman, K. C., 1978, Microdolomite-rich syntaxial cements—proposed meteoritic-mixing zone phreatic cements from Mississippian limestones, New Mexico: Journal of Sedimentary Petrology, v. 48, pp. 475–488.

Middleton, G. V., 1972, Albite of secondary origin in Charny Sandstones, Quebec: Journal of Sedimentary Petrology, v. 42, pp. 341–349.

Mitra, S., 1993, Geometry and kinematic evolution of inversion structures: American Association of Petroleum Geologists, Bulletin, v. 77, pp. 1159–1191.

Molenaar, C. M., 1983a, Major depositional cycles and regional correlations of Upper Cretaceous rocks, southern Colorado Plateau and adjacent areas; *in* Reynolds, M. W., and Dolly, E. D. (eds.), Mesozoic paleogeography of the west-central United States, Rocky Mountain Paleogeography Symposium 2: Society of Economic Paleontologists and Mineralogists, Rocky Mountain Section, Denver, Colorado, pp. 201–224.

Molenaar, C. M., 1983b, Principal reference sections and correlation of Gallup Sandstone, northwestern New Mexico: New Mexico Bureau of Mines and Mineral Resources, Circular 185, pp. 29–40.

Morgan, G. S., Lucas, S. G., and Estep, J. W., 1998, Pliocene (Blancan) vertebrate fossils from the Camp Rice Formation near Tonuco Mountain, Doña Ana County, southern New Mexico; *in* Mack, G. H., Austin, G. S., and Barker, J. M. (eds.), Guidebook of the Las Cruces country II: New Mexico Geological Society, Guidebook 49, pp. 237–250.

Morgan, P., Seager, W. R., and Golombek, M. P., 1986, Cenozoic thermal, mechanical and tectonic evolution of the Rio Grande rift: Journal of Geophysical Research, v. 91, pp. 6263–6276.

Muehlberger, W. R., Hedge, C. E., Denison, R. E., and Marvin, R. R., 1966, Geochronology of the mid-continent region, United States, part 3—southern areas: Journal of Geophysical Research, v. 71, pp. 5409–5426.

Nelson, M.A., 1974, Geology of Fluorspar deposits of the southern Caballo Mountains, Sierra and Doña Ana Counties, New Mexico: Unpublished M.S. thesis, University of Texas (El Paso), 55 pp.

Nightengale, A., 1993, Stratigraphy, sedimentology, and provenance of the Bell Top Formation, Doña Ana and Sierra Counties, New Mexico: Unpublished M.S. thesis, New Mexico State University, 54 pp.

Northrop, S.A., 1959, Minerals of New Mexico: University of New Mexico Press, 665 pp.

Olsen, K. H., Baldridge, W. W., and Callender, J. F., 1987, Rio Grande rift—an overview: Techtonophysics, vol. 143, pp. 119–139.

Osburn, G. R., and Chapin, C. E., 1983, Nomenclature for Cenozoic rocks of northeast Mogollon–Datil volcanic field, New Mexico: New Mexico Bureau of Mines and Mineral Resources, Stratigraphic Chart 1.

Otte, C., Jr., 1959, Late Pennsylvanian and Early Permian stratigraphy of the northern Sacramento Mountains, Otero County, New Mexico: New Mexico Bureau of Mines and Mineral Resources, Bulletin 50, 111 pp.

Ottensman, D. C., 1982, A paleoenvironmental and lithofacies analysis of part of the Bliss Formation (Cambro–Ordovician), southwestern New Mexico and west Texas: Unpublished M.S. thesis, University of Texas (Dallas), 208 pp.

Palmer, A. R., and Geissman, J., 1999, Geologic time scale: Geological Society of America.

Parrish, J. T., Ziegler, A. M., and Scotese, C. R., 1982, Rainfall patterns and the distribution of coals and evaporites in the Mesozoic and Cenozoic: Palaeogeography, Palaeoclimatology, Palaeoecology, v. 40, pp. 67–101.

Pimentel, N. L., Wright, V. P., and Azevedo, T. M., 1996, Distinguishing early groundwater alteration effects from pedogenesis in ancient alluvial basins—examples from the Palaeogene of southern Portugal: Sedimentary Geology, v. 105, pp. 1–10.

Pope, M. C., 2002, Cherty facies of the Late Ordovician Montoya Group, southern New Mexico and western Texas—implications for Laurentia oceanography and duration of Gondwana glaciation; *in* Lueth, V. W., Giles, K. A., Lucas, S. G., Kues, B. S., Myers, R., and Ulmer-Scholle, D. S. (eds.), Geology of White Sands: New Mexico Geological Society, Guidebook 53, pp. 159–165.

Pratt, L. M., 1984, Influence of paleoenvironmental factors on preservation of organic matter in middle Cretaceous Greenhorn Formation, Pueblo, Colorado: American Association of Petroleum Geologists Bulletin, v. 68, pp. 1146–1159.

Pray, L. C., 1959, Stratigraphic and structural features of the Sacramento Mountain escarpment, New Mexico; *in* Guidebook for joint field conference in the Sacramento Mountains of Otero County, New Mexico: Roswell Geological Society and Society of Economic Paleontologists and Mineralogists , Permian Basin Section, Guidebook, pp. 86–130.

Pray, L. C., 1961, Geology of the Sacramento Mountains escarpment, Otero County, New Mexico: New Mexico Bureau of Mines and Mineral Resources, Bulletin 35, 1444 pp.

Pysklywec, R. N., and Mitrovica, J. X., 1998, Mantle flow mechanisms for the large-scale subsidence of continental interiors: Geology, v. 26, pp. 687–690.

Raatz, W. S., 2002, A stratigraphic history of the Tularosa Basin area, south-central New Mexico; *in* Lueth, V. W., Giles, K. A., Lucas, S. G., Kues, B. S., Myers, R., and Ulmer-Scholle, D. S. (eds.), Geology of White Sands: New Mexico Geological Society, Guidebook 53, pp. 141–157.

Ramberg, I. B., and Smithson, S. B., 1975, Gridded fault patterns in a late Ceonzoic and a Paleozoic continental rift: Geology, v. 2, pp. 201–205.

Read, C. B., and Mamay, S. H., 1964, Upper Paleozoic floral zones and floral provinces of the United States: U.S. Geological Survey, Professional Paper 454–K, 25 pp.

Repenning, C. A., and May, S. R., 1986, New evidence for the age of the lower part of the Palomas Formation, Truth or Consequences, New Mexico; *in* Clemons, R. E., King, W. E., Mack, G. H., and Zidek, J. (eds.), Guidebook of the Truth or Consequences region: New Mexico Geological Society, Guidebook 37, pp. 257–260.

Reynolds, R. L., and Larson, E. E., 1972, Paleomagnetism of pearlette-like air-fall ash in the midwestern and western United States—a means of correlating Pleistocene deposits (abs): Geological Society of America, Rocky Mountain Section, 25th Annual Meeting, Abstracts with Programs, v. 4, p. 405.

Riba, O., 1976, Syntectonic unconformities of the Alto Cardener, Spanish Pyrenees—a genetic interpretation: Sedimentary Geology, v. 15, pp. 213–233.

Richardson, G. B., 1904, Report of a reconnaissance in Trans-Pecos Texas north of the Texas and Pacific railway: University of Texas Mineral Survey, Bulletin 9, 119 pp.

Richardson, G. B., 1908, Paleozoic formations in Trans-Pecos Texas: American Journal of Science, v. 25, pp. 474–484.

Richardson, G. B., 1909, Description of the El Paso district: U.S. Geological Survey, Geologic Atlas, El Paso folio, no. 166, 11 pp.

Robson, D. A., 1971, The structure of the Gulf of Suez (Clysmic) rift with special reference to the eastern side: Geological Society (London) Journal, v. 127, pp. 247–276.

Romer, A. S., 1960, The vertebrate fauna of the New Mexico Permian; *in* Beaumont, E. C., and Read, C. B. (eds.), Guidebook of the Rio Chama country: New Mexico Geological Society, Guidebook 11, pp. 48–54.

Ross, R. J., 1976, Ordovician sedimentation in the western United States: *in* Bassett, M.G. (ed.), The Ordovician System—proceedings of a Paleontological Association Symposium, Birmingham, Sept. 1974: University of Wales Press and National Museum of Wales, Cardiff, pp. 73–105.

Ross, C. A., 1986, Paleozoic evolution of southern margin of Permian Basin: Geological Society of America, Bulletin, v. 97, pp. 536–554.

Rothrock, H. E., Johnson, C. H., and Hahn, A. D., 1946, Fluorspar resources of New Mexico: New Mexico Bureau of Mines and Mineral Resources, Bulletin 21, 239 pp.

Ruhe, R. V., 1964, Landscape morphology and alluvial deposits in southern New Mexico—annals of the Association of American Geographers, v. 54, pp. 147–159.

Ruhe, R. V., 1967, Geomorphic surfaces and surficial deposits in southern New Mexico: New Mexico Bureau of Mines and Mineral Resources, Memoir 18, 66 pp.

Sahagian, D., 1987, Epeirogeny and eustatic sea level changes as inferred from Cretaceous shoreline deposits—applications to the central and western United States: Journal of Geophysical Research, v. 92, pp. 4895–4904.

Schlanger, S. O., and Jenkyns, H. C., 1976, Cretaceous oceanic anoxic events—causes and consequences: Geologie en Mijinbouw, v. 55, pp. 179–184.

Schlische, R. W., 1995, Geometry and origin of fault-related folds in extensional settings: American Association of Petroleum Geologists, Bulletin, v. 79, pp. 1661–1678.

Schlische, R. W., Withjack, M. O., and Eisenstadt, G., 2002, An experimental study of the secondary deformation pproduced by oblique-slip normal faulting: American Association of Petroleum Geologists, Bulletin, v. 86, pp. 885–906.

Scotese, C. R., 1997, Continental drift (0–750 million years), a quicktime computer animation: University of Texas (Arlington), Paleomap project.

Seager, W. R., 1975, Cenozoic tectonic evolution of the Las Cruces area, New Mexico; *in* Seager, W. R., Clemons, R. E., and Callender, J. (eds.), Guidebook of the Las Cruces country: New Mexico Geological Society, Guidebook 26, pp. 241–250.

Seager, W. R., 1981, Geology of Organ Mountains and southern San Andres Mountains, New Mexico: New Mexico Bureau of Mines and Mineral Resources, Memoir 36, 97 pp.

Seager, W. R., 1983, Laramide wrench faults, basement-cored uplifts, and complementary basins in southern New Mexico: New Mexico Geology, v. 5, pp. 69–76.

Seager, W. R., in press, Geology of Alivio quadrangle, New Mexico: New Mexico Bureau of Mines and Mineral Resources, Bulletin.

Seager, W. R., and Clemons, R. E., 1975, Middle to late Tertiary geology of the Cedar Hills–Selden Hills area, New Mexico: New Mexico Bureau of Mines and Mineral Resources, Circular 133, 24 pp.

Seager, W. R., and Hawley, J. W., 1973, Geology of Rincon quadrangle, New Mexico: New Mexico Bureau of Mines and Mineral Resources, Bulletin 101, 42 pp.

Seager, W. R., and Mack, G. H., 1986, Laramide paleotectonics of southern New Mexico: American Association of Petroleum Geologists, Memoir 41, pp. 660–685.

Seager, W. R., and Mack, G. H., 1991, Geology of Garfield quadrangle, Sierra and Doña Ana Counties, New Mexico: New Mexico Bureau of Mines and Mineral Resources, Bulletin 128, 24 pp.

Seager, W. R., and Mack, G. H., 1995, Jornada Draw fault—a major Pliocene–Pleistocene normal fault in the southern Jornada Del Muerto: New Mexico Geology, v. 17, pp. 37–43.

Seager, W. R., and Mack, G. H., 1998, Geology of the McLeod Tank quadrangle, Sierra and Doña Ana Counties, New Mexico: New Mexico Bureau of Mines and Mineral Resources, Geologic Map 77, scale 1:24,000.

Seager, W. R., and Mack, G. H., in press a, Geologic map and sections of Apache Gap and Caballo quadrangles, Sierra County, New Mexico: New Mexico Bureau of Mines and Mineral Resources, Geologic Map, scale 1:24,000.

Seager, W. R., and Mack, G. H., in press b, Geologic map of Cutter and Upham quadrangles: New Mexico Bureau of Mines and Mineral Resources, Geologic Map, scale 1:24,000.

Seager, W. R., and Mayer, A. B., 1988, Uplift, erosion, and burial of Laramide fault blocks, Salado Mountains, Sierra County, New Mexico: New Mexico Geology, v. 10, pp. 49–53, 60.

Seager, W. R., Clemons, R. E., and Hawley, J. W., 1975, Geology of Sierra Alta quadrangle, Doña Ana County, New Mexico: New Mexico Bureau of Mines and Mineral Resources, Bulletin 102, 56 pp.

Seager, W. R., Hawley, J. W., and Clemons, R. E., 1971, Geology of San Diego Mountain area, Doña Ana County, New Mexico: New Mexico

Bureau of Mines and Mineral Resources, Bulletin 97, 38 pp.
Seager, W. R., Kottlowski, F. E., and Hawley, J. W., 1976, Geology of Doña Ana Mountains, New Mexico: New Mexico Bureau of Mines and Mineral Resources, Circular 147, 36 pp.
Seager, W. R., Mack, G. H., and Hawley, J. W., in press, Geologic map of Hatch quadrangle, Doña Ana County, New Mexico: New Mexico Bureau of Mines and Mineral Resources, Geologic Map, scale 1:24,000.
Seager, W. R., Mack, G. H., and Lawton, T. F., 1997, Structural kinematics and depositional history of a Laramide uplift-basin pair in southern New Mexico—implications for development of intraforeland basins: Geological Society of America, Bulletin, v. 109, pp. 1389–1401.
Seager, W. R., Clemons, R. E., Hawley, S. W., and Kelley, R. E., 1982, Geology of northwest part of Las Cruces 1° x 2° sheet, New Mexico: New Mexico Bureau of Mines and Mineral Resources, Geologic Map 53, scale 1:125,000.
Seager, W. R., Hawley, J. W., Kottlowski, F. E., and Kelley, S. A., 1987, Geology of east half of Las Cruces and northeast El Paso 1° x 2° sheet, New Mexico: New Mexico Bureau of Mines and Mineral Resources, Geologic Map 57, scale 1:125,000.
Seager, W. R., Mack, G. H., Raimonde, M. S., and Ryan, R. G., 1986, Laramide basement-cored uplift and basins in south-central New Mexico; *in* Clemons, R. E., King, W. E., Mack, G. H., and Zidek, J. (eds.), Guidebook of the Truth or Consequences region: New Mexico Geological Society, Guidebook 37, pp. 123–130.
Seager, W. R., Shafiqullah, M., Hawley, J. W., and Marvin, R. F., 1984, New K–Ar dates from basalts and the evolution of the southern Rio Grande rift: Geological Society of America Bulletin, v. 95, pp. 87–99.
Sears, J. D., 1925, Geology and coal resources of the Gallup–Zuni Basin: U.S. Geological Survey, Bulletin, 53 pp.
Sherry, C. R., 1990, Fluvial sedimentology and paleosols of the Abo formation (Wolfcampian) in central New Mexico: Unpublished M.S. thesis, New Mexico State University, 120 pp.
Shinn, E. A., 1968, Practical significance of birdseye structures in carbonate rocks: Journal of Sedimentary Petrology, v. 38, pp. 215–223.
Shinn, E. A., Ginsberg, R. N., and Lloyd, R. M., 1965, Recent supratidal dolomite from Andros Island, Bahamas: Society of Economic Paleontologists and Mineralogists, Special Publication 13, pp. 12–123.
Shumard, G. G., 1859, The geological structure of the "Jornada del Muerto," New Mexico: Transactions of the Academy of Science of St. Louis, vol. 1, pp. 341–355.
Siehl, A., and Thein, J., 1989, Minette-type ironstones; *in* Young, T. P., and Taylor, W. E. G. (eds.), Phanerozoic ironstones: Geological Society (London), Special Publication 46, pp. 175–193.
Singleton, D., 1990, Depositional environments and tectonic significance of the Bar B Formation (Virgilian), Sierra County, New Mexico: Unpublished M.S. thesis, New Mexico State University, 132 pp.
Sinno, Y. A., Daggett, P. H., Keller, G. R., Morgan, P., and Harder, S. H., 1986, Crustal structure of the southern Rio Grande rift determined from seismic refraction profiling: Journal of Geophysical Research, v. 91, pp. 6143–6156.
Sleep, N., 1976, Platform subsidence mechanisms and "eustatic" sea-level changes: Tectonophysics, v. 36, pp. 45–56.
Sloss, L. L., 1963, Sequences in the cratonic interior of North America: Geological Society of America, Bulletin, v. 74, pp. 93–113
Sloss, L. L., and Speed, R. C., 1974, Relationships of cratonic and continental-margin tectonic episodes; *in* Dickinson, W. R. (ed.), Tectonics and sedimentation: Society of Economic Paleontologists and Mineralogists, Special Publication 22, pp. 98–119.
Smith, G. A., 1991, Facies sequences and geometries in continental volcaniclastic sediments: Society of Economic Paleontologists and Mineralogists, Special Publication 45, pp. 109–121.
Soegaard, K., and Caldwell, K. R., 1990, Depositional history and tectonic significance of alluvial sedimentation in the Permo–Pennsylvanian Sangre de Cristo Formation, Taos Trough, New Mexico; *in* Bauer, P. W., Lucas, S. G., Mawer, C. K., and McIntosh, W. C. (eds.), Guidebook of the tectonic development of the southern Sangre de Cristo Mountains: New Mexico Geological Society, Guidebook 41, pp. 227–289.
Soreghan, G. S., 1992a, Sedimentology and process stratigraphy of the Upper Pennsylvanian, Pedregosa (Arizona) and Orogrande (New Mexico) Basins: Unpublished Ph.D. dissertation, University of Arizona (Tucson), 278 pp.
Soreghan, G. S., 1992b, Preservation and paleoclimatic significance of eolian dust in the Ancestral Rocky Mountains province: Geology, v. 20, pp. 1111–1114.
Soreghan, G. S., 1994, Stratigraphic responses to geologic processes—Late Pennsylvanian eustasy and tectonics in the Pedregosa and Orogrande Basins, Ancestral Rocky Mountains: Geological Society of America, Bulletin, v. 106, pp. 1195–1211.
Speer, S. W., 1983, Abo Formation (Early Permian), Sacramento Mountains, New Mexico—a dry alluvial fan and associated basin-fill: Unpublished M.S. thesis, University of Texas (Austin), 129 pp.
Stageman, C. J., 1987, Depositional facies and provenance of Lower Paleozoic sandstones of the Bliss, El Paso, and Montoya Formations, southern New Mexico and west Texas: Unpublished M.S. thesis, New Mexico State University, 101 pp.
Staatz, M. H., Adams, J. W., and Conklin, N. M., 1965, Thorium-bearing microcline-rich rocks in the southern Caballo Mountains, Sierra County, New Mexico: U.S. Geological Survey Professional Paper 525-D, pp. d48–d51.
Stearns, D. W., 1978, Faulting and forced folding in the Rocky Mountains foreland; *in* Matthews, V., III (ed.), Laramide folding associated with basement block faulting in the western United States: Geological Society of America, Memoir 151, pp. 1–37.
Stevenson, G. M., and Baars, D. L., 1996, The Paradox—a pull-apart basin of Pennsylvanian age; *in* Peterson, J. A. (ed.), Paleotectonics and sedimentation in the Rocky Mountain region: American Association of Petroleum Geologists, Memoir 41, pp. 513–539.
Strain, W. S., 1966, Blancan mammalian fauna and Pleistocene formations, Hudspeth County, Texas: Texas Memorial Museum, Austin, Bulletin 10, 55 pp.
Sutherland, P. K., and Manger, W. L., 1984, Morrowan brachiopods in the type "Derryan" Series (Pennsylvanian), New Mexico (abs): Geological Society of America, Abstracts with Programs, v. 16, p. 115.
Swift, D. J. P., 1968, Coastal erosion and transgressive stratigraphy: Journal of Geology, v. 76, pp. 444–456.
Swift, D. J. P., and Field, M., 1981, Evolution of a classic sand ridge field—Maryland sector, North American inner shelf: Sedimentology, v. 28, pp. 461–482.
Tabet, D. E., 1980, Summary of the geology of the Engle coal field: New Mexico Bureau of Mines and Mineral Resources, Open-File Report OF-115, 9 pp.
Tabet, D. E., and Frost, S. J., 1978, Coal fields and mines of New Mexico: New Mexico Bureau of Mines and Mineral Resources, Resource Map 10, scale 1:1,000,000
Talmadge, S. B., and Wootton, T. P., 1937, The nonmetallic mineral resources of New Mexico and their economic features (exclusive of fuels): New Mexico Bureau of Mines and Mineral Resources, Bulletin 12, 159 pp.
Taylor, J. F., and Reptski, J. E., 1995, High-resolution trilobite and conodont biostratigraphy across the Cambrian–Ordovician boundary in south-central New Mexico: *in* Cooper, J. D., Droser, M. L., and Finney, S. C. (eds.), Ordovician odyssey—short papers for the Seventy International Symposium on the Ordovician System: Society for Sedimentary Geology (SEPM), Pacific Section, Book 77, pp. 133–136.
Tedford, R. H., 1981, Mammalian biochronology of late Cenozoic basins of New Mexico: Geological Society of America, Bulletin, v. 92, pp. I1008–I1022.
Thompson, A. D., 1991, Fusulinid biostratigraphy of the Bar B Formation (Desmoinesian–Wolfcampian), southern Caballo Mountains, New Mexico: Unpublished M.S. thesis, New Mexico State University, 100 p.
Thompson, M. L., 1942, Pennsylvanian System in New Mexico: New Mexico Bureau of Mines and Mineral Resources, Bulletin 17, 90 pp.
Thompson, M. L., 1948, Early Pennsylvanian fusulinids of New Mexico and western Texas: University of Kansas, Paleontology Contributions 4, Article 1, part 3, pp. 68–97.
Thompson, M. L., 1954, American Wolfcampian fusulinids: University of Kansas, Paleontology Contribution 14, article 5, 226 pp.
Thompson, S., III, 1955, Geology of the southern part of the Fra Cristobal Range; Unpublished M.S. thesis, University of New Mexico, 75 pp. (Revised version dated 1961).
Thompson, S., III, 1982, Oil and gas exploration wells in southwestern New Mexico; *in* Powers, R. B. (ed.), Geologic Studies of the Cordilleran Thrust Belt: Rocky Mountain Association of Geologists, pp. 521–536.
Thompson, S., III, and Potter, P. E., 1981, Paleocurrents of the Bliss Sandstone (Cambrian–Ordovician), southwestern New Mexico and western Texas: New Mexico Bureau of Mines and Mineral Resources, Annual Report, pp. 36–51.
Tonking, W. H., 1957, Geology of Puertocito quadrangle, Socorro County, New Mexico: New Mexico Bureau of Mines and Mineral Resources, Bulletin 41, 67 pp.
Upchurch, G. R., Jr., and Mack, G. H., 1998, Latest Cretaceous leaf megafloras from the Jose Creek Member, McRae Formation of New

Mexico; *in* Mack, G. H., Austin, G. S., and Barker, J. M. (eds.), Guidebook of the Las Cruces country II: New Mexico Geological Society, Guidebook 49, pp. 209–222.

Vail, P. R., Mitchum, R. M., Jr., and Thompson, S., III, 1977, Seismic stratigraphy and global changes of sea level, part 4—global cycles of relative changes of sea level: American Association of Petroleum Geologists, Memoir 26, pp. 83–97.

Vanderhill, J. B., 1986, Lithostratigraphy, vertebrate paleontology, and magnetostratigraphy of Plio–Pleistocene sediments in the Mesilla Basin, New Mexico: Unpublished Ph.D. dissertation, University of Texas (Austin), 330 pp.

Van Houten, F. B., and Purucker, M. E., 1984, Glauconitic peloids and chamositic ooids—favorable features, constraints, and problems: Earth Science Reviews, v. 20, pp. 211–243.

Van Wagoner, J. C., Mitchum, R. M., Campion, K. M., and Rahmanian, V. D., 1990, Siliciclastic sequence stratigraphy in well logs, cores, and outcrops—concepts for high resolution correlation of time and facies: American Association of Petroleum Geologists, Methods in Exploration Series, no. 7, 55 pp.

Varnes, D. J., 1978, Slope movement types and processes; *in* Schuster, R. L., and Krizek, R. J. (eds.), Landslides—analysis and control: Transportation Research Board, National Research Council, Washington, DC, Special Report 176, pp. 11–33.

Wallin, E. T., 1983, Stratigraphy and paleoenvironments of the Engle coal field, Sierra County, New Mexico: Unpublished M.S. thesis, New Mexico Institute of Mining and Technology, 127 pp.

Walton, A. W., 1979, Volcanic sediment apron in the Tascotal Formation (Oligocene?), Trans-Pecos, Texas: Journal of Sedimentary Petrology, v. 49, pp. 303–314.

Walton, A. W., 1986, Effect of Oligocene volcanism on sedimentation in the Trans-Pecos volcanic field of Texas: Geological Society of America, Bulletin, v. 97, pp. 1192–1207.

Warren, R. G., 1978, Characterization of the lower crust-upper mantle of the Engle Basin, Rio Grande rift, from a petro-chemical and field geological study of basalts and their inclusions: Unpublished M.S. thesis, University of New Mexico, 156 pp.

Wells, E. H., 1918, Manganese in New Mexico: New Mexico Bureau of Mines and Mineral Resources, Bulletin 2, 85 pp.

Wernicke, B. P., Christiansen, R. L., England, P. C., and Sonder, L. J., 1987, Tectonomagmatic evolution of Cenozoic extension in North American Cordillera; *in* Coward, M. P., Dewey, J. F., and Hancock, P. L. (eds.), Continental extensional tectonics: Geological Society (London), Special Publication 28, pp. 203–221.

Williams, F. E., 1966, Fluorspar deposits of New Mexico: U.S. Bureau of Mines, Information Circular 8307, 143 pp.

Williams, F. E., Fillo, P. V., and Bloom, P. A., 1964, Barite deposits of New Mexico: New Mexico Bureau of Mines and Mineral Resources, Circular 76, 46 pp.

Williams, G. D., Powell, C. M., and Cooper, M. A., 1989, Geometry and kinematics of inversion tectonics; *in* Cooper, M. A. and Williams, G. D. (eds.), Inversion Tectonics: Geological Society (London), Special Publication, no. 44, pp. 3–15.

Wilpolt, R. H., and Wanek, A. A., 1951, Geology of the region from Socorro and San Antonio east to Chupadera Mesa, Socorro County, New Mexico: U.S. Geological Survey, Oil and Gas Investigations Preliminary Map, OM–121, scale 1:63,360.

Wilson, J. L., and Jordan, C. F., Jr., 1988, Late Paleozoic–Early Mesozoic rifting in southern New Mexico and northern Mexico—controls on subsequent platform development; *in* Robichaud, S. R., and Gallick, C. M. (eds.), Basin to shelf facies transition of the Wolfcampian stratigraphy of the Orogrande Basin: Society of Economic Paleontologists and Mineralogists, Permian Basin Section, Publication 88-28, pp. 79–87.

Winchester, J. A., and Floyd, P. A., 1977, Geochemical discrimination of different magma series and their differentiation products using immobile elements: Chemical Geology, v. 20, pp. 325–343.

Withjack, M. O., Olson, J., and Peterson, E., 1990, Experimental models of extensional forced folds: American Association of Petroleum Geologists, Bulletin, v. 74, pp. 1038–1054.

Wolberg, D. L., Lozinsky, R. P., and Hunt, A. P., 1986, Late Cretaceous (Maastrichtian–Lancian) vertebrate paleontology of the McRae Formation, Elephant Butte area, Sierra County, New Mexico; *in* Clemons, R. E., King, W. E., Mack, G. H., and Zidek, J. (eds.), Guidebook of the Truth or Consequences region: New Mexico Geological Society, Guidebook 37, pp. 227–234.

Woodward, L. A., Callender, J. F., Seager, W. R., Chapin, C. E., Gries, J. C., Shaffer, W. L., and Zilinski, R. E., 1978, Tectonic map of the Rio Grande rift; *in* J. W. Hawley, compiler, Guidebook to the Rio Grande rift in New Mexico and Colorado: New Mexico Bureau of Mines and Mineral Resources, Circular 163, scale 1:1,000,000.

Ye, H., Royden, L., Burchfiel, C., and Schuepbach, M., 1996, Late Paleozoic deformation of interior North America—the greater Ancestral Rocky Mountains: American Association of Petroleum Geologists, Bulletin, v. 80, pp. 1397–1432.

Young, T. P., 1989, Phanerozoic ironstones: an introduction and review; *in* Young, T. P., and Taylor, W. E. G. (eds.), Phanerozoic ironstones: Geological Society (London), Special Publication, no. 46, pp. ix–xxv.

Zoback, M. L., and Thompson, G. A., 1978, Basin and Range rifting in northern Nevada—clues from a mid-Miocene rift and its subsequent offsets: Geology, v. 6, pp. 111–116.

Glossary of geologic terms

Most definitions are modified from the Glossary of Geology (Bates and Jackson, 1987)

Accommodation zone—As used in this paper, the term refers to an area between the tips of two or more parallel but offset faults where strain is transferred from one fault to the other without involving strike slip. Also referred to as a transfer zone.

Alkalic—Pertains to rocks carrying unusual quantities of potassium and/or sodium.

Allochems—A collective term for various types of carbonate grains or aggregates of grains, such as oolites and fossil fragments, found in limestone.

Amphibolite facies—Refers to rocks produced by medium- to high-grade regional metamorphism.

Anorogenic granite—A granitic body emplaced within the earth's crust during a time of no mountain-building activity.

Antithetic fault(ing)—A fault whose sense of displacement is opposite to the major fault with which it is associated. The term is also applied to faults that dip and are downthrown in the opposite direction than the dip of the rocks displaced.

Aplitic texture—A term used to describe the fine-grained, sugary texture found in some dikes of granitic composition, i.e., aplite dikes.

Argillic—Pertaining to clay or clay minerals. **Argillic horizon**—The clay-rich part of the B horizon of a soil profile.

Aulacogen—An elongate rift basin that extends into a craton either from a passive continental margin or from a fold mountain belt that represents the deformation of a passive continental margin.

Authigenic—Usually refers to minerals such as quartz or calcite that formed after deposition of the original sediment.

Avulsion—A sudden cutting off or separation of land by a flood or by an abrupt change in the course of a stream, as by a stream cutting through a meander, or by a sudden change in flow whereby a stream deserts its old course in favor of a new one at a lower elevation.

Basement—In New Mexico, the term refers to the Precambrian granitic and metamorphic rocks found beneath sedimentary and igneous rocks of Phanerozoic age. Granitic rocks of possible Late Cambrian and Ordovician age may also be part of the basement in a few areas.

Bench, structural bench—A fault block at an intermediate structural level between higher and lower blocks, the collective blocks forming a stair-step geometry.

Bimodal volcanism—Generally refers to approximately coeval basaltic and rhyolitic volcanism, which is characteristic of extensional terranes in parts of the North American Cordillera.

Bioturbation—The churning and stirring of sediment by burrowing organisms.

Boudinage—A structure in deformed sedimentary and metamorphic rocks in which strong layers or beds between weaker layers are stretched, thinned, and broken at regular intervals into pillow-shaped fragments resembling sausages (called boudins).

Boundstone—Term for a type of limestone whose original components were bound together during deposition, and remained in the position of growth, as shown by intergrown skeletal fossil fragments in the limestone rock.

Calcrete—Term for thick caliche, or for sand and gravel cemented into hard rock by calcium carbonate that accumulated during the soil-building process in an arid climate.

Caldera/Cauldron—A term for volcanic subsidence structures, regardless of shape, size, depth of erosion or connection to the surface; includes calderas.

Clastic dike—A sedimentary dike consisting of a variety of clastic materials derived either from soft, unconsolidated underlying beds or from loose overlying sediment.

Crevasse splay—A stream channel on the floodplain of a river.

Cyclothem—A sequence of rocks that is repeated in the sedimentary record one after another. They may contain paleosols and be caused by cyclical climate changes.

Distal—Refers to a sedimentary deposit consisting of fine-grained or chemically precipitated material and formed far from the source.

Drape fold—Type of fault propagation fold in which unfaulted, relatively ductile strata are draped over the faulted edge of an underlying, more rigid rock mass.

Eolian—Applied to deposits that are due to the transporting action of the wind.

Epeirogenic—Refers to broad uplift or subsidence of a continent or the seafloor.

Epiclast—A grain or fragment of a pre-existing rock.

Epiclastic (rock)—A sedimentary rock formed of fragments of pre-existing rocks.

Epicontinental—Situated on the continental shelf or on the continent.

Epicratonal—Refers to locations upon a continental craton; i.e., in the interior of a continent.

Epizonal—Shallow level of the earth's crust characterized by low to moderate pressures and temperatures and low to high shearing stresses.

Eustatic—Pertains to worldwide sea level changes affecting all oceans, caused either by changes in the volume of sea water or changes in the volume of the ocean basins.

Fan-head trench—A linear gully or channel that is incised considerably below the surface of an alluvial fan.

Farallon plate—A broad, eastern Pacific ocean plate that subducted beneath the western United States during the Cretaceous and Tertiary periods. Now largely consumed, remnants of the plate are the Juan de Fuca plate off the coast of Oregon and Washington and the Rivera plate off the western coast of Mexico.

Fault-propagation fold—Fold produced by movement on a fault.

Footwall—The rock mass beneath an inclined fault or vein. The footwall is relatively uplifted by movement on normal faults, forming mountain ranges or lower ridges **(footwall uplifts).** Reverse or thrust fault movements relatively lower the footwall, creating basins.

Foreland basin—A sedimentary basin lying adjacent to and on the continent side of a large fold-thrust mountain range, and filled with the sedimentary detritus eroded from the range.

Ga—Billions of years before the present.

Geostrophic current—A wind or ocean current in which the horizontal pressure force is exactly balanced by the equal but opposite Coriolis force.

Glacial-eustatic—Refers to worldwide sea-level changes resulting from melting or growing of continental ice sheets.

Grainstone—Term for a type of limestone consisting almost entirely of carbonate grains that are in contact and self supporting.

Hanging wall—The rock mass above an inclined fault or vein. Hanging walls are relatively uplifted by movement on thrust or reverse faults, creating mountains or lower ridges **(hanging-wall uplifts).** Normal fault movements relatively lower the hanging wall, creating basins.

Harzburgite—A peridotite composed chiefly of olivine and orthopyroxene.

Highstand systems tract—The package of sediment, tens to hundreds of meters thick, deposited in a marine or mixed marine and non-marine basin during slow sea level rise and the beginning of sea-level fall.

Hypabyssal—Refers to igneous intrusions that have been emplaced at relatively shallow levels of the Earth's crust; i.e., above the deeper plutonic levels.

Imbrication—A sedimentary fabric characterized by tabular or elongate fragments dipping in a preferred direction at an angle to bedding. It is produced on a stream bed by running water, which tilts the pebbles so that their flat surfaces dip and face upstream.

Isoclinal fold(ing)—A fold whose limbs are parallel, or nearly so.

Jasperoid—A dense, usually gray chertlike siliceous rock that has replaced host rock, usually limestone or dolomite, and typically is the gangue for sulfide, flourspar, barite, and other types of ore deposits. Jasperoid is often referred to as " **silicified limestone or silicified dolomite.**"

Karst—A type of topography that is developed on limestone and other soluble rocks by solution and is characterized by sinkholes, caves, and underground drainage.

Kinematic—Refers to the physics of motion. **Kinematic evolution of a geologic structure** involves a description of the motion that rocks progress through to achieve the structural geometry seen today.

Lateral accretion sets—Sets of crossbeds created when streams meander sideways, eroding their outer banks and depositing crossbedded sand on the point bars at their inner banks.

Lherzolite—A peridotite composed chiefly of olivine with lesser amounts of orthopyroxene and clinopyroxene.

Lithosome—A rock body having essentially a homogenous or uniformly heterogeneous character that has intertonguing relationships in all directions with adjacent rock masses of different lithologic character.

Lowstand systems tract—The package of sediment, tens to hundreds of meters thick, deposited in the seaward side of a basin during rapid sea-level fall.

Ma—Millions of years before the present.

Magnetostratigraphy—All parts of stratigraphy that is based on paleomagnetic signatures in the rocks, i.e., remnant magnetism in the rocks. **Reversal magnetostratigraphy** utilizes the pattern of normal and reversed polarity of the earth's magnetic field recorded in the rocks to date and correlate rock units.

Megacryst—A crystal or mineral grain in an igneous rock that is much larger than it's surrounding mineral grains.

Metasomatism—The process by which gases and fluids within a rock body can cause the replacement of original minerals by new ones of partly or wholly different composition. The process involves simultaneous solution and deposition, and the gases and fluids may be either introduced from external sources or be an original part of the rock body.

Meteoric (water)—Water recently derived from and belonging to the earth's atmosphere.

Milankovitch cycle—Theory proposed by Milutin Milankovitch (1879–1958) in which cyclic climatic changes result from the seasonal and geographic distribution of solar energy, determined by cyclical variations in tilt of Earth's axis, eccentricity of Earth's orbit, and longitude of perihelion. Climatic cycles can reliably be related to glacial and interglacial cycles.

Morphometric study—As used in this book, the term applies to the study of the shape of piedmont fault scarps, especially the ratio of their height and slope angle, to help estimate the age of the scarp.

Morphostratigraphic unit—A body of rock or sediment that is identified primarily by the surface form it displays and/or by the position of the surface form in the landscape, e.g., an alluvial fan surface and the underlying gravel or an inset terrace and it's associated deposit. Like formations, morphostratigraphic units may be named after a locale where they were first identified or are well exposed.

Nonconformity—A buried erosion surface (unconformity) that separates plutonic rocks below from sedimentary or volcanic rocks above.

Onlap—Refers to the deposition of stratigraphic units beyond the limit of their predecessors onto older rocks, as in the deposits of a transgressing sea.

Packstone—Term for a type of limestone whose grains are arranged in a self-supporting framework, yet contains some matrix of carbonate mud.

Paleosol—a buried or exhumed soil formed in the geologic past

Pangea—A supercontinent that existed between approximately 300 to 200 m.y. ago from which the present continents were derived by fragmentation and continental displacement. During an intermediate stage of the fragmentation, Pangea consisted of a northern landmass, called Laurasia, and a large southern fragment, called Gondwana.

Paralic—Adjective used to describe environments near the sea, yet nonmarine, such as lagoons and swamps.

Parasequence—A relatively thin (up to 5 m) sequence of marine or mixed-marine and non-marine sedimentary rocks that, from bottom to top, indicate progressively shallower depths of water during deposition.

Ped—A naturally formed unit of soil structure, e.g., granule, block, crumb, aggregate.

Pediment—Gently sloping erosion surface cut in bedrock at the base of a mountain front.

Pedogenic—Pertaining to soil formation.

Petrocalcic paleosol—An ancient soil characterized by a B horizon that is impregnated with or indurated by calcium carbonate.

Phanerozoic—That part of geologic time during which evidence of life is abundant, that is Cambrian and later time.

Phreatic (water)—A synonym for ground water.

Piedmont scarp—A low cliff or steep slope occurring in alluvium on a piedmont slope at the foot of, and essentially parallel to, a steep mountain front, resulting from displacement of the surface by faulting.

Pilotaxitic texture—Texture of a crystalline igneous rock in which small, lath-shaped plagioclase crystals in the matrix are interwoven in a random, unoriented fashion.

Pisoid—Small, approximately spherical, accretionary grain produced in soils.

Planar crossbeds—Crossbedding in which the lower bounding surface is planar; it results from erosional beveling and subsequent deposition.

Plateau basalt—A term applied to those basaltic lavas which at times have flooded vast areas of the earth's surface and accumulated to modest or often great thickness. Erupted in rapid succession as horizontal flows, they are generally believed to be the product of fissure eruptions.

Plinian eruption—An explosive eruption in which a steady, turbulent stream of fragmented magma and magmatic gas is released at high velocity from a vent. Large volumes of tephra and tall eruption columns are characteristic.

Plume—A localized, cylindrical body of hot rock rising through the mantle to the base of the lithoshere or into the crust, and thought to be the cause of "hot spots."

Plutonic—Pertains to igneous rocks formed at great depth.

Prograde—To build forward or outward by deposition of sediments, as in a delta or alluvial fan.

Protolith—The original rock from which a given metamorphic rock was formed by metamorphism.

Proximal—Refers to a sedimentary deposit consisting of coarse clastics and formed close to the source.

Ptygmatic(ally)—Refers to complexly folded granitic veins in metamorphic or other host rocks.

Ramp—As used in this report, a series of tilted strata that help accommodate the transfer of strain from one fault to another in an accommodation zone. Approximately perpendicular to the strike of the faults, dips on the ramp carry strata from the footwall of one fault down into the hanging wall of the other, or vice versa.

Rhizolith—Stoney or concretionary, downward-tapering, tube-shaped body in some sedimentary beds, that formed around the root of a living plant.

Rip-up clasts—A sedimentary structure formed of tabular shale clasts that have been "ripped up" by currents from a semiconsolidated mud deposit and transported to a new depositional site. Rip-up-clast conglomerate may form by this process.

Roof pendant—A downward projection of country rock into an igneous intrusion.

Sauk sequence—An informal stratigraphic sequence on the North American craton that overlies an unconformity on Precambrian rocks and underlies an unconformity covered by strata of the Tippecanoe sequence.

Schlieren—Wispy, tabular-shaped concentrations of minerals within an igneous intrusion due to flowage of magma. Dark schlieren formed by mafic minerals are most conspicuous.

Septa—Wall-like partitions of country rock that separate different plutons.

Sequence boundary—An unconfomity cut in the landward side of a basin during rapid sea level fall. May be coeval to a lowstand systems tract.

Siliciclastic—Refers to clastic, noncarbonate rocks consisting mostly of quartz or, to a lesser extent, other silicate minerals.

Slab—Down-going plate in a subduction zone.

Stage I–IV paleosols—Refers to maturity of paleosols, with stage I being the least developed and stage IV the most mature. The stage is usual-

ly determined by the extent to which soil carbonate or and/or clay have accumulated in the soil.

Stratiform (stratabound) ore deposit—An ore deposit that is essentially coextensive with a sedimentary, metamorphic, or igneous layer. Sedimentary strataform (stratabound) layers usually form as a result of replacement of the sedimentary rocks by ore minerals and gangue.

Stratigraphic separation—The thickness of the strata that originally separated two beds brought into contact at a fault.

Stromatolite—An organic-sedimentary structure produced by the trapping, binding and/or precipitation of sediment by algae. The structure is usually layered, and may be domal, columnar, or approximately spherical in shape.

Structural inversion—Refers to the different relative displacement on a single fault from one episode of movement to another. Positive structural inversion results when a down-dropped block is subsequently raised (relatively) by reactivation of the same fault. Negative structural inversion occurs when an originally uplifted block subsequently subsides (relatively) by movement on the same fault.

Subaerial—Formed, existing, or taking place on the earth's surface.

Subcrop map—A geologic map that shows the distribution of formations that have been preserved and remain buried beneath a given stratigraphic unit or beneath an unconformity.

Subcrop—An area in which a formation occurs directly beneath an unconformity.

Syn-, syneruption, syndepositional etc.—Refers to events or deposits that took place or were formed simultaneously with volcanic eruptions, deposition of sediments, etc.

Tephra—A general term for all solid or near-solid particles (pyroclastics) erupted from a volcano.

Ternary eutectic—Temperature at which a rock consisting of three essential compositional components just begins to melt upon heating, or wholly freezes from a liquid upon cooling.

Transgressive system tract—The package of sediment, from tens to hundreds of meters thick, deposited in a marine or mixed-marine and non-marine basin during rapid sea-level rise.

Trough crossbeds—Crossbedding in which the lower bounding surfaces are curved surfaces of erosion; it results from local scour by some current, such as water, and subsequent deposition.

Vergence, verging—The direction of overturning or asymmetry of a fold. A northeast-verging anticline would have its overturned or steeper limb on it's northeastern side; i.e., "facing northeast."

Volcaniclastic—Refers to clastic rocks containing volcanic fragments of whatever origin.

Wackestone—Term used for a type of limestone consisting of more than 10% grains supported by a mud matrix.

Websterite—A pyroxenite composed chiefly of ortho- and clinopyroxene.

Xenolith—A fragment of wallrock or other foreign rock carried in an igneous intrusion.

Index

Selected conversion factors*

TO CONVERT	MULTIPLY BY	TO OBTAIN	TO CONVERT	MULTIPLY BY	TO OBTAIN
Length			**Pressure, stress**		
inches, in	2.540	centimeters, cm	lb in^{-2} (=lb/in^2), psi	7.03 x 10^{-2}	kg cm^{-2} (kg/cm^2)
feet, ft	3.048 x 10^{-1}	meters, m	lb in^{-2}	6.804 x 10^{-2}	atmospheres, atm
yards, yds	9.144 x 10^{-1}	m	lb in^{-2}	6.895 x 10^{3}	newtons (N)/m^2, N m^{-2}
statute miles, mi	1.609	kilometers, km	atm	1.0333	kg cm^{-2}
fathoms	1.829	m	atm	7.6 x 10^{-2}	mm of Hg (at 0°C)
angstroms, Å	1.0 x 10^{-8}	cm	inches of Hg (at 0°C)	3.453 x 10^{-2}	kg cm^{-2}
Å	1.0 x 10^{-4}	micrometers, µm	bars, b	1.020	kg cm^{-2}
Area			b	1.0 x 10^{6}	dynes cm^{-2}
in^2	6.452	cm^2	b	9.869 x 10^{-1}	atm
ft^2	9.29 x 10^{-2}	m^2	b	1.0 x 10^{-1}	megapascals, MPa
yds^2	8.361 x 10^{-1}	m^2	**Density**		
mi^2	2.590	km^2	lb in^{-3} (= lb/in^3)	2.768 x 10^{1}	gr cm^{-3} (= gr/cm^3)
acres	4.047 x 10^{3}	m^2	**Viscosity**		
acres	4.047 x 10^{-1}	hectares, ha	poises	1.0	gr cm^{-1} sec^{-1} *or* dynes cm^{-2}
Volume (wet and dry)			**Discharge**		
in^3	1.639 x 10^{-1}	cm^3	U.S. gal min^{-1}, gpm	6.308 x 10^{-2}	1 sec^{-1}
ft^3	2.832 x 10^{-2}	m^3	gpm	6.308 x 10^{-5}	m^3 sec^{-1}
yds^3	7.646 x 10^{-1}	m^3	ft^3 sec^{-1}	2.832 x 10^{-2}	m^3 sec^{-1}
fluid ounces	2.957 x 10^{-2}	liters, l *or* L	**Hydraulic conductivity**		
quarts	9.463 x 10^{-1}	l	U.S. gal day^{-1} ft^{-2}	4.720 x 10^{-7}	m sec^{-1}
U.S. gallons, gal	3.785	l	**Permeability**		
U.S. gal	3.785 x 10^{-3}	m^3	darcies	9.870 x 10^{-13}	m^2
acre-ft	1.234 x 10^{-3}	m^3	**Transmissivity**		
barrels (oil), bbl	1.589 x 10^{-1}	m^3	U.S. gal day^{-1} ft^{-1}	1.438 x 10^{-7}	m^2sec^{-1}
Weight, mass			U.S. gal min^{-1} ft^{-1}	2.072 x 10^{-1}	1 sec^{-1} m^{-1}
ounces avoirdupois, avdp	2.8349 x 10^{1}	grams, gr	**Magnetic field intensity**		
troy ounces, oz	3.1103 x 10^{1}	gr	gausses	1.0 x 10^{5}	gammas
pounds, lb	4.536 x 10^{-1}	kilograms, kg	**Energy, heat**		
long tons	1.016	metric tons, mt	British thermal units BTU	2.52 x 10^{-1}	calories, cal
short tons	9.078 x 10^{-1}	mt	BTU	1.0758 x 10^{2}	kilogram-meters, kgm
oz mt[1]	3.43 x 10^{1}	parts per million, ppm	BTU lb^{-1}	5.56 x 10^{-1}	cal kg^{-1}
Velocity			**Temperature**		
ft sec^{-1} (= ft/sec)	3.048 x 10^{-1}	m sec^{-1} (= m/sec)	°C + 273	1.0	°K (Kelvin)
mi hr^{-1}	1.6093	km hr^{-1}	°C + 17.78	1.8	°F (Fahrenheit)
mi hr^{-1}	4.470 x 10^{-1}	m sec^{-1}	°F - 32	5/9	°C (Celsius)

**Divide by* the factor number to reverse conversions.
Exponents: for example 4.047 x 10^{3} (see acres) = 4,047; 9.29 x 10^{-2} (see ft^2) = 0.0929

Colophon

Typeface: Palatino
Presswork: Cottonwood Printing Company, Inc.
Binding: Perfect bound with softbound cover
Paper: Cover on Kivar®3–17 Linenweave. Text on 70-lb white matte -
Ink: Cover—PMS 320, four color process. Text—black
Print run: 1000

Seager and Mack

Geology of the Caballo Mountains, New Mexico

New Mexico Bureau of Geology and Mineral Resources

Memoir 49

ISBN 1-883905-15-X

9 781883 905156 90000

New Mexico Bureau of Geology and Mineral Resources
New Mexico Tech
Earth Science for the 21st Century